

DEVELOPMENT AND VALIDATION OF A PORTABLE fNIRS DEVICE TO AID IN POST-STROKE MOTOR RECOVERY

by

Christopher Lee Friesen

Submitted in partial fulfilment of the requirements

for the degree of Doctor of Philosophy

at

Dalhousie University

Halifax, Nova Scotia

March 2021

© Copyright by Christopher Lee Friesen, 2021

# TABLE OF CONTENTS

LIST OF TABLES.....	V
LIST OF FIGURES.....	VI
LIST OF ABBREVIATIONS USED.....	XIII
ABSTRACT.....	XIV
ACKNOWLEDGEMENTS.....	XV
CHAPTER 1 - INTRODUCTION.....	1
1.1 THE PROBLEM OF PHYSICAL REHABILITATION POST-STROKE AND THE SOLUTION SPACE.....	1
1.1.1 <i>The Problem</i> .....	1
1.1.2 <i>The Solution Space</i> .....	4
1.2 MECHANISMS OF DISRUPTION AND REPAIR IN THE BRAIN POST-STROKE.....	6
1.2.1 <i>Mechanisms of disruption to the cortical motor system</i> .....	6
1.2.2 <i>The Brain’s Regenerative Response to Stroke and the Motor System</i> .....	8
1.3 NEURAL BIOMARKERS OF STROKE RECOVERY.....	9
1.3.1 <i>Potential role for neural biomarkers in stroke recovery</i> .....	9
1.3.2 <i>MI Laterality (MI-LAT)</i> .....	13
1.3.3 <i>Resting State MI Functional Connectivity (MI-rsFC)</i> .....	17
1.3.4 <i>MI Neurofeedback (MI-NFB)</i> .....	19
1.4 AXEM HOME.....	23
1.4.1 <i>Axem Home Overview</i> .....	23
1.4.2 <i>On the suitability of Functional Near-Infrared Spectroscopy (fNIRS) for use in the Axem Home</i> .....	24
1.4.3 <i>Axem Home Rehabilitation Software</i> .....	30
1.5 DISSERTATION SCOPE.....	33
1.6 – CONTRIBUTIONS TO STUDY CHAPTERS.....	34
1.7 - REFERENCES.....	36
CHAPTER 2 - AXEM HOME PROTOTYPE DATA QUALITY STUDY.....	57
2.0 ABSTRACT.....	57
2.1 INTRODUCTION.....	58
2.1.1 <i>Study Purpose and Design</i> .....	58
2.1.2 <i>fNIRS Signal Quality Deconstructed</i> .....	59
2.1.3 <i>On the Suitability of Existing fNIRS Systems for Rehabilitation-based Brain-Computer-Interface (BCI)</i> .....	64
2.2 METHODS.....	66
2.2.1 <i>Participants</i> .....	66
2.2.2 <i>fNIRS Prototypes</i> .....	67
2.2.3 <i>Experimental Task</i> .....	73
2.2.4 <i>fNIRS Measurement</i> .....	74
2.2.5 <i>fNIRS Pre-processing</i> .....	75
2.2.6 <i>Dynamic Time Warping Classification</i> .....	76
2.3 RESULTS.....	78
2.3.1 AP-1 RESULTS.....	78
2.3.2 AP-2 RESULTS.....	81
2.4 DISCUSSION.....	84

2.5 REFERENCES.....	87
<b>CHAPTER 3 - PORTABLE WIRELESS AND FIBRELESS FNIRS HEADBAND COMPARES FAVOURABLY TO A STATIONARY HEADCAP-BASED SYSTEM .....</b>	<b>90</b>
3.0 ABSTRACT.....	90
3.1 INTRODUCTION.....	91
3.2 METHODS.....	94
3.2.1 <i>Participants</i> .....	94
3.2.2 <i>fNIRS Devices and Sensor Configuration</i> .....	94
3.2.3 <i>Experimental Procedure</i> .....	96
3.2.4 <i>fNIRS Acquisition and Pre-processing</i> .....	97
3.3 RESULTS.....	99
3.3.1 <i>Comfort Questionnaire Results</i> .....	99
3.3.2 <i>fNIRS Analysis &amp; Results</i> .....	99
3.4 DISCUSSION.....	103
3.5 REFERENCES.....	108
<b>CHAPTER 4 – AXEM HOME FORMATIVE USABILITY STUDY.....</b>	<b>111</b>
4.0 ABSTRACT.....	111
4.1 INTRODUCTION.....	112
4.1.1 <i>Background</i> .....	112
4.1.2 <i>Axem Home Use Specification</i> .....	113
4.1.3 <i>Research Questions</i> .....	115
4.1.4 <i>Axem Home prototypes used in present study</i> .....	116
4.1.4 <i>Study Design Overview and Rationale</i> .....	121
4.2 METHODS.....	123
4.2.1 <i>Note on COVID-19’s impact on the present study</i> .....	123
4.2.2 <i>Participants &amp; Inclusion Criteria</i> .....	124
4.2.3 <i>Measures</i> .....	124
4.2.4 <i>Experimental Protocol</i> .....	127
4.2.5 <i>fNIRS Analysis and Feedback Signal</i> .....	129
4.3- RESULTS.....	129
4.3.1 – <i>Participant Characteristics</i> .....	129
4.3.2 – <i>General Study Feasibility</i> .....	130
4.3.3 – <i>AP-LL Testing</i> .....	130
4.3.4 – <i>AP-S/AP-2 Testing</i> .....	131
4.3.5 – <i>Assessment of Perceived Usefulness</i> .....	133
4.4- DISCUSSION.....	134
4.5 REFERENCES.....	141
<b>CHAPTER 5 - MEASUREMENT OF SENSORIMOTOR BRAIN ACTIVITY IN STROKE SURVIVORS DURING AT-HOME UPPER-EXTREMITY REHABILITATION: A MOBILE FNIRS PILOT STUDY..</b>	<b>144</b>
5.0 ABSTRACT:.....	144
5.1 INTRODUCTION.....	145
5.2 METHODS.....	150
5.2.1 <i>Participants – inclusion and exclusion criteria</i> .....	150
5.2.2 – <i>Cognitive Testing</i> .....	150
5.2.3 – <i>Fugl-Meyer short form upper extremity section</i> .....	150
5.2.4 <i>SIS-Hand</i> .....	151
5.2.5 – <i>Motor Task</i> .....	151
5.2.6 <i>Prototype fNIRS Headband</i> .....	152
5.2.7 <i>fNIRS Acquisition and Pre-processing</i> .....	154
5.2.8 <i>fNIRS Analysis</i> .....	155

5.2.9 <i>fNIRS M1-LAT Analysis</i> .....	156
5.3 RESULTS .....	160
5.4 DISCUSSION .....	164
5.5 REFERENCES.....	168
<b>CHAPTER 6 - DISCUSSION</b> .....	<b>176</b>
6.1 – SUMMARY OF FINDINGS BY CHAPTER .....	176
6.1.1 <i>Axem Home Prototype Data Quality Study</i> .....	176
6.1.2 <i>Portable Wireless and Fibreless fNIRS Headband Compares Favourably to a Stationary Headcap-based system</i> .....	177
6.1.3 <i>Axem Home Formative Usability Study</i> .....	178
6.1.4 <i>Measurement of Sensorimotor Brain Activity in Stroke Survivors during At-home Upper-extremity Rehabilitation: a mobile fNIRS pilot study</i> .....	179
6.2 – LESSONS LEARNED DURING THE DEVELOPMENT OF AN <i>fNIRS</i> SYSTEM FOR USE BY STROKE SURVIVORS, AND THE FUTURE DIRECTION FOR ERGONOMIC <i>fNIRS</i> .....	180
6.2.1 <i>Coupling</i> .....	181
6.2.2 <i>Notes on Emission</i> .....	185
6.2.3 <i>Notes on Detection</i> .....	189
6.3 – HUMAN FACTORS LESSONS LEARNED AND THOUGHTS ON FUTURE DIRECTIONS: DEVELOPMENT OF AN AT-HOME <i>fNIRS</i> BRAIN-COMPUTER-INTERFACE SYSTEM FOR STROKE REHABILITATION .....	192
6.3.1 – <i>fNIRS Hardware User Experience: Limitations, Lessons Learned, and Future Directions</i> .....	192
6.3.2 – <i>Axem Home Software User Experience: Limitations, Lessons Learned, and Future Directions</i> ...	195
6.4 – THE POTENTIAL OF <i>fNIRS</i> BIOMARKERS IN STROKE RECOVERY: PROGRESS, LIMITATIONS, AND FUTURE DIRECTIONS .....	202
6.5 – CONCLUSION.....	205
6.6 – REFERENCES.....	206
APPENDIX A – CHAPTER 2 SUPPLEMENTAL MATERIAL .....	215
APPENDIX B – CHAPTER 2 SUPPLEMENTAL PRELIMINARY ANALYSES.....	216
APPENDIX C – AXEM HOME USER NEEDS.....	220
APPENDIX D – USABILITY QUESTIONNAIRE AND INTERVIEW.....	222
APPENDIX E – AP-LL PLACEMENT INSTRUCTIONS .....	225
APPENDIX F - DECLARATION OF INTERESTS .....	227
BIBLIOGRAPHY .....	228

## LIST OF TABLES

TABLE 2-1. PARTICIPANT CHARACTERISTICS FOR THE SESSIONS CONDUCTED WITH AP-1 AND AP-2 FNIRS SYSTEMS.....	66
TABLE 2-2. DESCRIPTIVE STATISTICS FOR THE SUB-SEGMENT OF PARTICIPANTS IN THE AP-1 GROUP WHO WERE UNDER 50 YEARS OF AGE (TOP ROW) AND OVER 50 YEARS OF AGE (BOTTOM ROW). .....	79
TABLE 4-1. USER NEEDS ADDRESSED IN SOME CAPACITY IN THE PRESENT STUDY.....	122
TABLE 4-2. DISTRIBUTION OF ANSWERS TO THE QUESTION “HOW DIFFICULT WAS IT TO PLACE THE AXEM HOME SURFACE MODEL ON YOUR HEAD?” .....	130
TABLE 4-3. DISTRIBUTION OF ANSWERS TO THE QUESTION “HOW COMFORTABLE DID YOU FIND THE AXEM HOME PROTOTYPE?” .....	132
TABLE 4-4. DISTRIBUTION OF ANSWERS TO THE QUESTIONS RELATING TO THE USABILITY OF THE AP-S SOFTWARE PROTOTYPE.....	132
TABLE 4-5. DISTRIBUTION OF ANSWERS TO THE QUESTIONS RELATING TO THE PERCEIVED USEFULNESS OF THE AXEM HOME SYSTEM. ....	133

# LIST OF FIGURES

FIGURE 1-1. FACTORS CONTRIBUTING TO POST-STROKE FUNCTIONAL IMPAIRMENT. ILLUSTRATION (TAKEN FROM<sup>32</sup>) OF THE DIFFERENT CAUSES OF CORTICAL DYSFUNCTION DUE TO STROKE. .... 7

FIGURE 1-2. ILLUSTRATION OF HOW THE LEFT M1 FACILITATES MOVEMENT MOTOR CONTROL IN THE RIGHT SIDE OF THE BODY. FOLLOWING STROKE THIS PATTERN GETS DISRUPTED, WITH THE UNDAMAGED M1 PLAYING AN OUTSIZED ROLE IN INITIATING MOVEMENT FOR BOTH SIDES OF THE BODY..... 14

FIGURE 1-3. ILLUSTRATION OF FUNCTIONAL CONNECTIVITY BETWEEN BRAIN AREAS, AND HOW IT PROVIDES DIFFERENT INFORMATION THAN THE LATERALITY BETWEEN BRAIN AREAS (DISCUSSED IN SECTION 1.3.2). FOR ILLUSTRATIVE PURPOSES A TYPICAL PATTERN OF LATERALITY UPON SIMPLE UNILATERAL MOVEMENT IS DEPICTED; WHEREAS CONNECTIVITY CAN BE, AND IS MOST OFTEN, MEASURED AT REST. IT IS IMPORTANT TO NOTE THAT FUNCTIONAL CONNECTIVITY CAN BE MEASURED IN MANY WAYS — DEPICTED HERE IS A SIMPLE CORRELATION IN BRAIN ACTIVITY ACROSS TIME. STROKE CAN CAUSE DISRUPTION OF M1 CONNECTIVITY..... 18

FIGURE 1-4. ILLUSTRATION OF THE PROCESS OF PRESENTING NFB FROM CEREBRAL HEMODYNAMIC SOURCES (NOTE THAT THESE STEPS ARE MIRRORED IN THE PRESENTATION OF NFB FROM ELECTROMAGNETIC SOURCES (ADAPTED FROM<sup>150</sup>). ..... 21

FIGURE 1-5. (LEFT) ILLUSTRATION OF THE NFB SETUP USED BY MIHARA ET AL.<sup>154</sup> (RIGHT) ILLUSTRATION OF THE RELATIONSHIP BETWEEN GROUP (NFB OR SHAM), INCREASES IN IPSILESIONAL M1 ACTIVITY DURING PARETIC LIMB MOVEMENT, AND IMPROVEMENTS IN FINGER MOVEMENT ABILITY AS MEASURED BY THE FUGL-MEYER ASSESSMENT..... 22

FIGURE 1-6. ILLUSTRATION OF THE AXEM HOME BEING WORN BY A PATIENT DURING A REHABILITATION SESSION. THE MODEL USED IN THIS PHOTO IS A PRELIMINARY MODEL BASED ON IDEALIZED INDUSTRIAL DESIGN. .... 24

FIGURE 1-7. ILLUSTRATION OF THE LIGHT PATHS FROM BOTH 3CM (D1) AND 1CM (D2) PATHS. OF PARTICULAR NOTE IS THAT ONLY THE LONGER LIGHT PATH PASSES THROUGH THE GRAY MATTER AT THE CORTICAL SURFACE. TAKEN FROM<sup>173</sup> ..... 26

FIGURE 1-8. ABSORPTION COEFFICIENTS FOR OXY- (HbO<sub>2</sub>) AND DEOXYHEMOGLOBIN (Hb) TAKEN FROM<sup>176</sup> ..... 27

FIGURE 1-9. REPRESENTATIVE fNIRS DATA DURING LOCAL NEURAL ACTIVITY. RED REPRESENTS  $\Delta$ HbO,  $\Delta$ Hb, AND GREEN RELATIVE TOTAL HEMOGLOBIN (TAKEN FROM<sup>175</sup>). ..... 28

FIGURE 1-10. IDEALIZED TIME COURSE OF THE CANONICAL RELATIVE OXYHEMOGLOBIN AT THE M1 DURING MOVEMENT. .... 30

FIGURE 1-11. PROTOTYPE USER HOME SCREEN. THE USER HOME SCREEN DISPLAYS REPRESENTATIONS OF THE PATIENT’S PAST USAGE OF THE APP, IN TERMS OF THE AMOUNT OF REHABILITATION COMPLETED, AS WELL AS METRICS BASED ON THE BRAIN ACTIVITY DATA COLLECTED DURING REHABILITATION SESSIONS. ....	31
FIGURE 1-12. PROTOTYPE EXERCISE SELECTION SCREEN. DISPLAYS THE REHABILITATION EXERCISES AVAILABLE, AND INCLUDES BASIC INFORMATION ABOUT EACH MOVEMENT, AND THE ABILITY TO PREVIEW EACH MOVEMENT’S VIDEO. ....	32
FIGURE 1-13. DISPLAYED ABOVE IS (A) THE ACTIVE PERIOD SCREEN, DURING WHICH THE USER IS INSTRUCTED TO MOVE IN SYNCH WITH (I.E., IMITATE) THE VIDEO, AS WELL AS (B) THE REST SCREEN, WHICH SHOWS FEEDBACK TO THE USER BASED ON THEIR BRAIN ACTIVITY DURING THE PRECEDING ACTIVE PERIOD. ....	33
FIGURE 2-1 – SCHEMATIC OF THE MAJOR ASPECTS CONTRIBUTING TO AN FNIRS SYSTEM’S ABILITY TO MEASURE CEREBRAL HEMODYNAMICS. ....	60
FIGURE 2-2. EXAMPLE OF REMOVABLE OPTODE ASSEMBLY THAT ENABLES A THIRD PARTY TO MOVE HAIR AWAY FROM THE CENTER OF THE OPTODE ASSEMBLY (IN THIS CASE WITH A SCREWDRIVER TOOL). ....	61
FIGURE 2-3. ILLUSTRATION OF HIGHLY COLLIMATED LIGHT (LEFT) CONTRASTED WITH LESS COLLIMATED LIGHT (RIGHT). <sup>10</sup> ....	63
FIGURE 2-4. EXAMPLE PHOTOGRAPHS TAKEN IN THE STUDY, USED TO THEN CODE CHARACTERISTICS OF THE PARTICIPANTS HAIR AND SKIN CHARACTERISTICS (A CONSISTENT COLOUR SCALE WAS INCLUDED IN THESE PHOTOGRAPHS TO ALLOW FOR RELATIVE CALIBRATION TO COMPENSATE FOR DIFFERENCES IN PHOTO QUALITY, LIGHTING ETC.). ....	67
FIGURE 2-5. ENGINEERING SCHEMATIC OF THE LAYOUT OF ELECTRICAL COMPONENTS AND MEASUREMENT LOCATIONS FOR AP-1 AND AP-2. SCHEMATIC HAS A TOP-DOWN VIEW ON THE FNIRS DEVICE, ASSUMING THAT THE LEFT-MOST COMPONENTS ARE AT THE LEFT SIDE OF THE HEAD, AND THE RIGHT-MOST COMPONENTS ARE AT THE RIGHT SIDE OF THE HEAD. CIRCLES LABELED D1-D4 REPRESENT THE LOCATION OF PHOTO DIODES. CIRCLES MARKED S1-4 REPRESENT THE LOCATION OF SHORT-PATH LEDs, ENABLING A MEASUREMENT LOCATION AT THE MID-POINT BETWEEN EACH SHORT-PATH LED AND ITS ASSOCIATED DETECTOR (E.G., BETWEEN S1 AND D1). CIRCLES MARKED F1-4 AND R1-4 REPRESENT LONG-PATH LEDs, ENABLING THE MEASUREMENT LOCATIONS MARKED BY WHITE CIRCLES LABELED 1-12. ....	68
FIGURE 2-6. PROTOTYPE OF THE CENTRAL BAND OF THE DEVICE HEADBAND, DEMONSTRATING ITS ABILITY TO ACCOMMODATE FLEXION IN THE CORONAL PLANE. ....	69
FIGURE 2-7. PICTURE OF AP-1 AS WORN IN THE PRESENT STUDY. ....	69
FIGURE 2-8. A) SIMPLIFIED ILLUSTRATION OF THE LIGHT GUIDES BUTT COUPLED TO THE OPTICAL COMPONENTS OF THE DEVICE HEADBAND. (B-C) INITIAL (IDEALIZED) AXEM HOME	

HEADBAND INDUSTRIAL DESIGN CONCEPT, ILLUSTRATING THIS BUTT COUPLED-BASED DESIGN IMPLEMENTED IN A FULL FNIRS HEADBAND. THE PROPOSED RIDGES SURROUNDING THE LIGHT PIPES ARE CONCEIVED AS BOTH INTENDED TO ACT AS COMBS FOR HAIR, AS WELL AS TO CREATE A ‘BED OF NAILS’ EFFECT WHEREBY THE PRESSURE OF THE LIGHT GUIDES ON THE HEAD IS DIMINISHED, RESULTING IN IMPROVED COMFORT; WHILE IDEALLY THESE RIDGE FEATURES WOULD BE MADE OF A MATERIAL WITH A LOWER DUROMETER, PRELIMINARY VERSIONS OF THESE FEATURES MADE OUT OF PLASTIC WERE IMPLEMENTED IN BOTH AP-1 AND AP-2. .... 71

FIGURE 2-9. ILLUSTRATION OF THE SPRING ATTACHMENT DESIGN, ALLOWING THE INDIVIDUAL LED PODS (EXAMPLE OF THESE PODS ARE POINTED TO WITH RED ARROW IN FIGURE) TO ARTICULATE IN THE SAGITTAL PLANE, INDEPENDENT FROM THE CENTRAL HEADBAND. .... 72

*FIGURE 2-10. PICTURE OF AP-2 AS WORN IN THE PRESENT STUDY. .... 73*

FIGURE 2-11. LEFT PANE - ILLUSTRATION OF THE REVISED LIGHT GUIDE DESIGN IMPLEMENTED IN AP-2. RIGHT PANE – ILLUSTRATION OF THESE LIGHT GUIDES AS BUTT COUPLED TO BOTH THE INDIVIDUALLY ARTICULATING LONG-CHANNEL LED PODS (SEE ITEMS LABELED 106) AS WELL AS THE SiPDs (E.G., SEE ITEM LABELLED 104) AND SHORT-CHANNEL LEDs (E.G., SEE ITEM LABELLED 104). .... 73

FIGURE 2-12. EXERCISE BALL USED IN THE UNILATERAL HAND SQUEEZE. .... 74

FIGURE 2-13. POSITION OF THE AP-1 AND AP-2 MEASUREMENT LOCATION GRIDS AT BOTH MEASUREMENT LOCATIONS TO BE EMPLOYED IN THE PRESENT STUDY, RELATIVE TO THE 10-20 EEG PLACEMENT SYSTEM. LOCATIONS MARKED IN GREEN ARE GAINED WHEN D0 IS POSITIONED AT CZ; LOCATIONS MARKED IN BLUE ARE GAINED WHEN D0 IS POSITIONED AT 1CM ANTERIOR TO CZ. .... 75

FIGURE 2-14. AN ILLUSTRATION OF THE WAY IN WHICH SHAPE COMPARISON IN DTW ITERATIVELY WARPS THE PATH OF ONE SHAPE IN ORDER TO COMPARE IT WITH ANOTHER IN A MANNER UNAFFECTED BY DIFFERENCES IN PHASE. TAKEN FROM<sup>19</sup> ..... 78

FIGURE 2-15. TOPOGRAPHICAL HEAT MAP OF ALL MEASUREMENT LOCATIONS USED IN THE PRESENT STUDY, FOR (A) LEFT AND (B) RIGHT-HANDED FIST SQUEEZING. HEAT VALUES REPRESENT THE AVERAGE ΔHbO CHANGES ACROSS ALL PARTICIPANTS DURING THE 10S OF A FIRST SQUEEZING TASK DURING THE 10 SECOND TASK PERIOD. MEASUREMENT LOCATIONS LABELED C3/C4 WERE APPROXIMATELY IN THESE LOCATIONS AS DEFINED BY THE INTERNATIONAL 10-20 SYSTEM. .... 79

FIGURE 2-16. REPRESENTATIVE EXAMPLES OF THE DIFFERENCES IN HAIR DENSITY BETWEEN YOUNGER (LEFT) AND OLDER (RIGHT) PARTICIPANTS. .... 80

FIGURE 2-17. PLOTTED NEGATIVE RELATIONSHIP (PEARSON R = -0.664) BETWEEN HAIR DENSITY AND AGE IN THE PARTICIPANTS IN THE AP-1 GROUP. .... 80



FIGURE 2-18. DTW-NN CLASSIFICATION ACCURACY BETWEEN TASK AND REST  $\Delta$ HbO DATA FOR PARTICIPANTS  $<50$  (LEFT PANE) AND  $\geq 50$  YEARS OF AGE (RIGHT PANE) FOR THE LEFT-HANDED (TOP PANES) AND RIGHT-HANDED (BOTTOM PANES) FIST SQUEEZING TASK ..... 81

FIGURE 2-19. DATA PRESENTED COMES FROM THE CONTRALATERAL MEASUREMENT LOCATION THAT DEMONSTRATED THE LARGEST MEAN INCREASE IN  $\Delta$ HbO DURING THE TASK PERIOD. BOTH PARTICIPANTS WERE  $<40$  YEARS OF AGE. .... 83

FIGURE 2-20. TOPOGRAPHICAL HEAT MAP OF ALL MEASUREMENT LOCATIONS USED IN THE PRESENT STUDY, FOR (A) LEFT AND (B) RIGHT-HANDED FIST SQUEEZING. HEAT VALUES REPRESENT THE AVERAGE  $\Delta$ HbO CHANGES ACROSS ALL PARTICIPANTS DURING THE 10S OF A FIRST SQUEEZING TASK DURING THE 10 SECOND TASK PERIOD. .... 84

FIGURE 3-1. A: PROTOTYPE FNIRS DEVICE. B: ARRAY OF OPTICAL COMPONENTS INCLUDED IN THE FNIRS PROTOTYPE. THE CENTRAL THREE DETECTORS (BEING 3CM FROM 4 LONG-PATH LEDs) ENABLED 4 MEASUREMENT LOCATIONS EACH, WITH THE TWO DETECTORS ON EITHER END (BEING 3CM FROM 2 LONG-PATH LEDs) ENABLING TWO, RESULTING IN A TOTAL OF 16 MEASUREMENT LOCATIONS. C: NIRSCOUT DEVICE. D: THE NIRSCOUT'S ARRAY OF OPTICAL COMPONENTS SUPPORTING 28 MEASUREMENT LOCATIONS. .... 95

FIGURE 3-2.  $\Delta$ HbO TIMESERIES (95% CONFIDENCE RIBBONS) PLOTTED AT ALL MEASUREMENT LOCATIONS WITHIN EACH SYSTEM (FACET ROWS) AND FOR EACH TASK (FACET COLUMNS). PLOTS AT EACH LOCATION ARE SCALED TO HAVE COMMON AXES, THE GREY BAND MARKS THE TASK PERIOD AND THE BLACK LINE MARKS THE MEAN OF THE PERIOD PRECEDING THE TASK. .... 100

FIGURE 3-3. TOPOGRAPHIC MAPS OF GROUP MEAN SLOPE (IN UNITS OF  $\text{MMOL}/\text{MM}^3$ ) DURING TASK. COLORS INDICATE POSTERIOR MEDIAN; LOCATIONS WITH POSTERIOR DISTRIBUTIONS IN WHICH ZERO FALLS OUTSIDE THE 95% CREDIBLE INTERVAL ARE MARKED WITH AN ASTERISK. .... 102

FIGURE 3-4. POSTERIOR DISTRIBUTIONS FOR SNR IN EACH TASK FOR EACH FNIRS SYSTEM AS WELL AS THE SNR DIFFERENCE RATIO BETWEEN FNIRS SYSTEMS (RIGHT-MOST PANE)—I.E., THE SNR OF AN FNIRS PROTOTYPE SYSTEM DIVIDED BY THE SNR OF THE NIRSCOUT SYSTEM (WITH 1 MEANING NO DIFFERENCES). GREY VIOLINS DEPICT THE MIRRORED DENSITY-SMOOTHED DISTRIBUTIONS, BLACK DOTS DEPICT THE POSTERIOR MEDIAN, THICK WHITE RECTANGLES DEPICT THE 50% CREDIBLE INTERVAL AND THIN WHITE LINES DEPICT THE 95% CREDIBLE INTERVAL. RED BANDS IN THE RATIO PLOT DEPICT THE RANGE OF RATIOS FROM 0.95 TO 1.05. .... 103

FIGURE 4-1. (A) AP-LL PROTOTYPE USED IN THE PRESENT STUDY, TOGETHER WITH THE VISUAL CUE (RED LINE) USED AS AN OVERLAY FOR THE INSTRUCTIONS THAT WERE PRESENTED TO PARTICIPANTS IN THE PRESENT STUDY. (B) A REVISED VERSION OF THE VISUAL USED FOR THE INSTRUCTIONS FOR AP-LL PLACEMENT USED FOR LATTER PARTICIPANTS. .... 116

FIGURE 4-2. FINAL ITERATION OF THE 'EXERCISE SELECT' SCREEN OF AP-S. .... 119

FIGURE 4-3. REPRESENTATIVE STILLS FROM VIDEOS THAT PLAY DURING REHABILITATION EXERCISES. WHILE THESE VIDEOS PLAYED PARTICIPANTS WERE INSTRUCTED TO FOLLOW ALONG WITH THE MOVEMENTS IN THE VIDEO (OR IMAGINE MOVEMENT IF THEY WERE NOT ABLE TO APPROXIMATE THE MOVEMENT AT ALL)..... 119

FIGURE 4-4. **LEFT PANE (A)** - REPRESENTATIVE ILLUSTRATION OF THE ‘REST PERIOD’ FEEDBACK THAT WOULD DISPLAY IN BETWEEN ACTIVE PERIODS OF REHABILITATION EXERCISE. A ‘BRAIN ACTIVITY SCORE’ (SEE SECTION 4.2.4) WAS DISPLAYED TO THE PARTICIPANTS WHILE A COUNTDOWN TO THE NEXT ACTIVE PERIOD COUNTED DOWN. **RIGHT PANE (B)** - REPRESENTATIVE ILLUSTRATION OF THE ‘EXERCISE SUMMARY’ SCREEN THAT WOULD DISPLAY FOLLOWING THE COMPLETION OF ALL TRIALS FOR A PARTICULAR EXERCISE THE PARTICIPANT HAD SELECTED. PARTICIPANTS WERE ALSO ABLE TO RATE THEIR PERCEIVED CHALLENGE AND ENJOYMENT ASSOCIATED WITH THAT PARTICULAR EXERCISE, USING A VISUALIZED LIKERT SCALE. .... 120

FIGURE 4-5. LEFT – PARTICIPANTS MMSE SCORES; RIGHT – PARTICIPANT SCORES ON THE SIS-HAND AND FM-12. .... 129

FIGURE 4-6. LOCATIONS WHERE INDIVIDUALS PLACED THE AP-LL MODEL IN THE CURRENT STUDY. THE LOCATION MARKED REPRESENTS THE POSITION OF THE CENTER OF THE AP-LL MODEL IN THE SAGITTAL PLANE. THE GREEN LOCATIONS REPRESENT THOSE MEASUREMENT LOCATIONS VERIFIED AS VALID PLACEMENT LOCATIONS IN THE DATA QUALITY STUDY (CHAPTER 2). . 131

FIGURE 4-7. IMAGES WHERE THE ‘COMFORT FEATURES’ (I.E., RIDGES ON THE VENTRAL SIDE OF THE HEADBAND, MEANT TO REDUCE THE PRESSURE FELT AT THE TIP OF THE LIGHT GUIDE) ARE ILLUSTRATED IN BOTH THE AP-2 (LEFT PANE; BLACK BUMPS ON THE VENTRAL SIDE OF THE PODS DENOTED WITH THE RED ARROWS) AND IN IDEALIZED INDUSTRIAL DESIGN OF THE AXEM HOME (RIGHT PANE; SEE THE RIDGE IN WHITE LINING THE VENTRAL PORTION OF THE HEADBAND). .... 137

FIGURE 5-1. ILLUSTRATION OF THE EXPERIMENTAL SET UP FOR THE PRESENT STUDY. PARTICIPANTS WORE THE fNIRS PROTOTYPE HEADBAND WHILE A MOVEMENT VIDEO PLAYED A FIST SQUEEZING TASK ON A TABLET. PARTICIPANTS WERE ASKED TO FOLLOW ALONG WITH THE MOVEMENTS IN THE VIDEO AS BEST THEY COULD. .... 152

FIGURE 5-2. (A) PROTOTYPE fNIRS HEADBAND AP-2 USED IN THE PRESENT STUDY. (B) ARRAY OF OPTICAL COMPONENTS INCLUDED IN THE fNIRS PROTOTYPE. THE CENTRAL THREE DETECTORS (BEING 3CM FROM 4 LONG-PATH LEDs) ENABLED 4 MEASUREMENT LOCATIONS EACH, WITH THE TWO DETECTORS ON EITHER END (BEING 3CM FROM 2 LONG-PATH LEDs) ENABLED TWO, RESULTING IN A TOTAL OF 16 MEASUREMENT LOCATIONS..... 154

FIGURE 5-3. ESTIMATED 95% CONFIDENCE RIBBONS FOR  $\Delta\text{HbO}$  TIMESERIES FOR ALL PARTICIPANTS. TIME SERIES WINDOWS HIGHLIGHTED IN RED ARE CONTRALATERAL TO THE HAND BEING USED IN THE TASK. THE PORTION OF THE TIME SERIES SHADED IN GREY REPRESENTS THE 10S BLOCK OF  $\sim 1\text{HZ}$  FIST SQUEEZING OR ATTEMPTED FIST SQUEEZING. VISUALIZED RIBBONS WERE OBTAINED FROM A GAM FIT SEPARATELY TO EACH PARTICIPANT

AND MEASUREMENT, AND SPECIFICALLY REPRESENT  $\pm 2$  STANDARD ERROR OF THE MEAN, RESULTING IN A 95% CONFIDENCE INTERVAL. .... 161

FIGURE 5-4. TOPOGRAPHIC MAPS (TOP-DOWN VIEW, WITH THE TOP ROW REPRESENTING THE ANTERIOR ROW OF MEASUREMENT LOCATIONS, AND VICE VERSA; LOCATIONS ON THE LEFT OF THE GRID REPRESENTING THE LEFT HEMISPHERE, AND VICE VERSA) OF GROUP MEAN SLOPE (IN UNITS OF  $\text{mMOL}/\text{MM}^3$ ) DURING TASK FOR AP-2'S 16 MEASUREMENT LOCATIONS. BECAUSE NOT ALL PARTICIPANTS USED THE SAME HAND IN THE TASK, THE HEMISPHERES FOR SOME OF THE PARTICIPANTS' DATA WERE FLIPPED SUCH THAT THE LEFT SIDE REPRESENTS THE HEMISPHERE CONTRALATERAL TO THE PARTICIPANTS' PARETIC HAND. COLORS INDICATE POSTERIOR MEDIAN OF  $\Delta\text{HbO}$  VALUES; LOCATIONS WITH POSTERIOR DISTRIBUTIONS IN WHICH ZERO FALLS OUTSIDE THE 95% CREDIBLE INTERVAL ARE MARKED WITH CROSSES. .... 161

FIGURE 5-5. CORRELATION COEFFICIENTS (AND 95%ILE CREDIBLE INTERVALS THEREOF) BETWEEN M1-LAT AND BOTH FM-12 AND SIS-HAND RESPECTIVELY. M1-LAT IS CALCULATED SUCH THAT HIGHER VALUES REPRESENTS HIGHER  $\Delta\text{HbO}$  LATERALIZATION TOWARDS THE CONTRALESIONAL HEMISPHERE (I.E., THE HEMISPHERE IPSILATERAL). THESE PRELIMINARY ANALYSES WERE CONDUCTED USING THE PRE-PROCESSING PIPELINE DESCRIBED IN CHAPTER 2. .... 163

FIGURE 5-6. POSTERIOR DISTRIBUTIONS FOR CORE MODEL PARAMETERS. WHITE DOTS CONVEY THE POSTERIOR MEDIAN WHILE THE THICK AND THIN BARS CONVEY 50% CREDIBLE INTERVALS (I.E., BOUNDED BY THE 25%ILE AND 75%ILE) AND THE 95% CREDIBLE INTERVAL (I.E., BOUNDED BY THE 2.5%ILE AND 97.5%ILE). .... 164

FIGURE 6-1. SCHEMATIC OF THE MAJOR ASPECTS CONTRIBUTING TO AN FNIRS SYSTEM'S ABILITY TO MEASURE CEREBRAL HEMODYNAMICS. .... 181

FIGURE 6-2. LIGHT GUIDES FROM AP-1 (LEFT; BUTT COUPLED TO THE LIGHT GUIDES USED IN AP-1) AND AP-2 (RIGHT; BUTT COUPLED TO THE LIGHT GUIDES USED IN AP-2) FNIRS SYSTEMS SHOWN; DOTTED LIGHT REPRESENTS HYPOTHETICAL LIGHT RAY EMITTED FROM THE SAME LOCATION WITHIN THE LED LENS, AND AT THE SAME ANGLE. .... 187

FIGURE 6-3. FIGURE 6 FROM TESSNOW ET AL. (2007).<sup>8</sup> THEORETICAL FRESNEL LOSSES AT AN AIR GAP, COMPARING STANDARD SURFACE LAMBERTIAN (I.E., FLAT LENSED) LED (LED ONLY) VERSUS A FULLY COLLIMATED SOURCE (LED + CPC, OR COMPOUND PARABOLIC CONCENTRATOR). .... 189

FIGURE 6-4. EXAMPLE OF A MOBILE FNIRS SYSTEM UTILIZING APDs. <sup>18</sup> .... 191

FIGURE 6-5. AXEM HOME HEADBAND PROTOTYPE AS OF JANUARY 2021. THIS PROTOTYPE INCLUDES A ONE-TIME ADJUSTABLE FOREHEAD STRAP THAT IS SIZED DEPENDING ON THE HEAD SIZE OF THE WEARER (I.E., THIS STRAP WOULD ONLY NEED TO BE SIZED BY THE WEARER UPON FIRST USE), AS WELL AS AN ADJUSTABLE BAND BACK THAT ALLOWS FOR A SNUG FIT TO BE ACHIEVED EACH TIME THEY DON THE DEVICE. .... 195

FIGURE 6-6. ILLUSTRATION OF BOTH TYPES OF NEUROFEEDBACK USED IN A STUDY TESTING THE EFFICACY OF INTERMITTENT VERSUS ‘REAL-TIME’ MOTOR IMAGERY NEUROFEEDBACK. .... 200

FIGURE 6-7. LEFT PANE - ILLUSTRATION OF THE NEUROFEEDBACK SCORE DISPLAY UTILIZED IN KOBER ET AL.<sup>40</sup> GREEN AREAS REPRESENTED TASK PERIODS WHILE GREY AREAS REPRESENTED REST PERIODS. THE LINE GRAPH WOULD ONLY DISPLAY THE RELATIVE OXYHEMOGLOBIN VALUE DURING TASK PERIODS, AND FOLLOWING EACH TASK PERIOD THE USER WAS GIVEN A SCORE BASED ON THE SLOPE OF THE OXYHEMOGLOBIN VALUE DURING THAT TASK PERIOD (I.E., THE “+6” IN THIS SCREEN) WHICH WOULD BE ADDED TO THEIR CUMULATIVE SCORE (I.E., THE “4” IN THIS SCREEN). RIGHT PANE – ILLUSTRATION OF DIGITAL MIRROR BOX TASK USED IN<sup>43</sup>. ..... 201

## LIST OF ABBREVIATIONS USED

**AP-1** — Axem Neurotechnology’s first fNIRS prototype  
**AP-2** — Axem Neurotechnology’s second fNIRS prototype  
**AP-LL** — Axem Neurotechnology’s ‘Axem Home looks-like’ prototype  
**AP-S** — Axem Neurotechnology’s Axem Home software prototype  
**APD** — Avalanche photo diode  
**BCI** — brain computer interface  
**BDNF** — brain-derived neurotrophic factor  
**BOLD** — blood oxygen level dependent  
**CASP** — cognitive assessment for stroke patients  
**CBSI** — correlation-based signal improvement  
**CST** — corticospinal tract  
**EEG** — electroencephalography  
**DTI** — diffusion tensor imaging  
**DTW** — dynamic time warping  
**FM-12** — short-form fugl-meyer assessment  
**fMRI** — functional magnetic resonance imaging  
**fNIRS** — functional near-infrared spectroscopy  
**GAM** — general additive model  
**HbO** — oxyhemoglobin  
**Hb** — deoxyhemoglobin  
**IHI** — interhemispheric inhibition  
**KNN** — k nearest neighbors  
**LAST** — language screen test  
**LI** — laterality index  
**LED** — light emitting diode  
**M1** — motor cortex  
**M1-LAT** — motor cortex laterality  
**M1-NFB** — motor cortex neurofeedback  
**M1-rsFC** — motor cortex resting state functional connectivity  
**MCMC** — Markov chain Monte Carlo  
**MI** — motor imagery  
**MMSE** — mini mental state examination  
**MRI** — magnetic resonance imaging  
**NFB** — neurofeedback  
**PCA** — principal component analysis  
**PCB** — printed circuit boards  
**PREP** — predict recovery potential algorithm  
**SEM** — structural equation model  
**SiPD** — silicon photodiode  
**SIS** — stroke impact scale  
**SIS-Hand** — hand domain of stroke impact scale  
**SNR** — signal-to-noise ratio  
**TDDR** — temporal derivative distribution repair  
**TMS** — transcranial magnetic stimulation

## ABSTRACT

Post-stroke physical rehabilitation has been shown to be beneficial in helping to completely or partially reduce stroke survivors' impairment and increase their functional abilities, as well as in helping stroke survivors maintain their current level of function and mitigate the risk of further impairment. However, the high costs of rehabilitation, together with the scientific and medical communities' inability to understand the relationship between the particulars of an individual's stroke, their rehabilitation, and their motor recovery, results in suboptimal post-stroke motor recovery at a population level. This dissertation outlines the initial steps in the development and validation of a product which endeavours to positively impact these problems: the Axem Home. The Axem Home is a brain-computer-interface system designed to independently guide stroke survivors through rehabilitation exercises while collecting neurophysiological data (via functional near-infrared spectroscopy or fNIRS) relating to their motor recovery. In particular, the chapters of this dissertation outline work: investigating the viability of early fNIRS prototypes (Chapter 2), comparing the performance of an early fNIRS prototype to an established research system (Chapter 3), conducting an initial formative usability study (Chapter 4), and examining preliminary fNIRS data collected on stroke survivors in their homes (Chapter 5). While the steps described herein are only preliminary, the creation of such a product (which has the capacity to both provide cost-effective rehabilitation and improve our collective understanding of post-stroke motor recovery) represents a noteworthy attempt to innovate in an important and challenging clinical and scientific domain.

## ACKNOWLEDGEMENTS

I'm grateful to a lot of people for helping me get to this point—but let's face it, this thing is long(!)—so I'll be brief. To Shaun Boe, a great mentor and friend. I learned many things from you, both directly through our work, and indirectly through the example you set as you ran your lab both pragmatically and humanely. In particular I'll always remember how you emphasized treating those you worked with well over superficial achievements. Only a flexible, pragmatic, and trustworthy supervisor like you could have helped me stick the landing on this degree.

Thanks to Heather Neyedli for her ever-insightful guidance, and for being a fantastic, generous collaborator over my time at Dal. Thanks to Aaron Newman, for putting Dal on my radar in the first place with the RADIANT program; I'm very grateful for the work you (as well as Shaun and others) put into that program, and I'm very pleased this important work (training science students in how to think about contributing to technological innovation) continues to this day.

I owe a lot to everyone who ever helped Axem Neurotechnology get to where it is today, especially our team (past and current), and most obviously my co-founders Mike Lawrence—whose assistance and guidance on the statistically-dense portions of this document are very much appreciated—and Tony Ingram, who has been and continues the best business partner I could have asked for.

Finally, to my entire awesome family. In particular my loving and supportive parents, who trusted I knew what I was doing (more or less!), weaving academia in-and-out of my life throughout my twenties. And most of all to my wife Zoë—thank you so much for supporting me through many months of travel for work, for your deeply humane nature I can always count on to temper my judgment, and now for being an exceptional mum to our Seamus, whose cries (surprisingly loud for 1 week old!) and coos I can hear as I write this. You are an amazing woman who I'm deeply grateful to share my life with.

# Chapter 1 - INTRODUCTION

## 1.1 THE PROBLEM OF PHYSICAL REHABILITATION POST-STROKE AND THE SOLUTION SPACE

### 1.1.1 The Problem

Neurological disorders are one of the greatest threats to public health. For instance, stroke alone has a worldwide incidence of over 17 million annually.<sup>1</sup> Of all the challenges faced by stroke survivors, one of the most common is hemiparesis (i.e., weakness or spasticity in one side of the body), resulting in nearly 80% of stroke survivors continuing to experience upper-extremity deficits three months following their stroke.<sup>2</sup> The presence of hemiparesis contributes to stroke's ranking as the leading cause of adult disability worldwide.<sup>3,4</sup> In the United States there are six million stroke survivors and over 800,000 new strokes each year,<sup>1</sup> resulting in a cumulative cost of over \$70 billion a year, with the majority of expenses related to living with stroke in the subacute and chronic phases of the disease.<sup>1</sup> This cumulative cost for Canada is estimated to be over \$3.6 billion annually.<sup>5</sup>

Post-stroke physical rehabilitation has been shown to be beneficial in helping to completely or partially reduce stroke survivors' impairment and increase their functional abilities, as well as in helping stroke survivors maintain their current level of function and mitigate the risk of further impairment.<sup>6,7</sup> The standard of care for physical rehabilitation following a stroke is for a healthcare professional to assess the functional status of a patient while they are an inpatient in the acute stage of stroke recovery (i.e., in the first days and weeks following stroke), and use this estimation of their current function (usually an established, standardized assessment—e.g., Fugl Meyer, Barthel Index, Functional Independence Measure), together with other relevant variables, such as comorbidities, to create a rehabilitation plan



consisting of personalized one-on-one therapy sessions. This plan is updated based on monitoring the progress of the patient, generally achieved by directly observing their progress (both informally and/or formally through repeated use of standard assessments of impairment and/or function). Unfortunately, because of the high costs of housing and treating stroke survivors in an inpatient setting, patients across the western world often don't get access to adequate rehabilitation in the acute stage.<sup>8,9</sup> The U.S. for example has seen a decrease in the standard length of stay at inpatient rehabilitation facilities<sup>10</sup>, a troubling sign considering that rehabilitation at inpatient facilities has been associated with better outcomes than alternative facilities.<sup>11</sup> Meanwhile countries with single payer healthcare systems have related problems, with long wait times delaying the initiation of inpatient<sup>12</sup> stroke rehabilitation, and limited resources putting pressure on a system that often fails to deliver an adequate volume of rehabilitation to the patients it has the capacity to take in.<sup>13,14</sup> Canada is a good example of this situation, with one report showing that inpatient rehabilitation is delayed in its onset, and fails to deliver the appropriate intensity and duration of therapy needed best suited to individual patients.<sup>15</sup>

When the patient leaves the inpatient rehabilitation setting, they are able to pursue outpatient rehabilitation services. In lieu of this, some stroke survivors may use a home care service that includes 1-on-1 rehabilitation as part of their offering. In either case, this results in patients engaging in periodic 1-on-1 rehabilitation sessions, with a home exercise program outlining rehabilitation exercises the patient is to complete independently on the days they do not have these sessions. However outpatient rehabilitation is not accessible to the majority of patients, due to high costs<sup>16</sup> and long wait times,<sup>17</sup> as well as the challenge associated with travelling to appointments—an issue that is exacerbated in rural areas where there may not be an

outpatient rehabilitation clinic nearby.<sup>18,19</sup> This is a particular challenge for geographically large countries like Canada, where the problem of access to outpatient rehabilitation is being exacerbated by the downsizing and/or closure of outpatient rehabilitation centers.<sup>20</sup> Moreover, while clinician-assigned home rehabilitation programs may be seen as a work-around to the problem of outpatient rehabilitation's limited access (due to cost and transportation challenges), patients typically demonstrate poor compliance with their assigned home rehabilitation program,<sup>21</sup> likely simply comprised of pieces of paper which vaguely instruct the stroke survivor on which exercises to complete. These traditional home programs do not motivate stroke survivors to comply, nor do they provide any accountability or sense of achievement for completing them.

The problems of access are also tethered to problems of effectiveness, with some studies showing as many as 47% of inpatient stroke survivors who receive rehabilitation fail to meaningfully benefit from it over the recovery that might have been expected through mechanisms of spontaneous recovery.<sup>22</sup> While the efficacy of post-stroke rehabilitation is evidence-based (as mentioned above), the murky status of the relationship between inputs (i.e., resources spent) and outputs (clinical benefits) casts a pall over the issue, with some academics continuing to call into question the effectiveness of rehabilitation.<sup>23</sup>

Meanwhile alongside these disturbing clinical trends and academic controversy, the costs of post-stroke rehabilitation are increasing worldwide. The United States spends approximately \$47 billion dollars on stroke rehabilitation currently,<sup>24</sup> and the worldwide incidence of stroke survivors is estimated to continue increasing at a rate of 3% compounding annual growth<sup>3</sup>, due to an aging global population, increasing incidence of stroke in young adults,<sup>25</sup> and continual improvements in acute stroke care (which continues to prevent more deaths from stroke).

For all these reasons, there is an undeniable need for innovation in the world of post-stroke physical rehabilitation.

### **1.1.2 The Solution Space**

From the lens of scientific and commercial innovation there are several broad classes of solutions to the problems of post-stroke physical rehabilitation outlined above, the two most apparent being, (1) augmenting the functioning of the nervous systems of stroke survivors to promote recovery via drugs that might enhance neurological recovery, and/or stimulating either the central or peripheral nervous system directly via the application of electrical or magnetic fields; and (2) the use of new therapeutic tools that enhance one-on-one therapy, and/or enable effective therapy that does not require one-on-one interaction with a health care professional (e.g., robotic or virtual reality therapy). While there is rightfully much work being done in both of these areas, the heterogeneity of strokes (which contributes to the heterogeneity of stroke recovery treatment-response relationships) makes it difficult to be certain about how effective any such innovative intervention may be for an individual stroke survivor. The uncertainty associated with physical stroke rehabilitation also represents a challenge for determining a treatment plan during both inpatient and outpatient therapy, discharge planning, as well as chronic care management. All this points to a third potential class of solutions to the problem of physical stroke rehabilitation; (3) tools that enable a better optimization of resource allocation, through a better (i.e., more personalized) understanding of the effectiveness of stroke rehabilitation. This could be accomplished by either enabling a better understanding of the data currently being generated in the course of stroke recovery or enabling the collection of novel data on stroke survivors, which might then be used to improve predictions of how specific interventions will impact specific patients' outcomes. An idealized example of this can be found

in pre-clinical work where researchers developed a predictive model for rehabilitation volume prescriptions that was found to increase the likelihood rats would benefit from post-stroke upper-extremity rehabilitation by 13 times.<sup>26</sup> Importantly, both post-stroke function and information on the central nervous system damage sustained by the animals was necessary to enable this predictive model.

To date the only notable effort to deploy such an innovation clinically is the predict recovery potential (PREP) algorithm,<sup>27</sup> where stroke patients (in addition to functional assessment) undergo both structural and diffusion tensor imaging (DTI), magnetic resonance imaging (MRI) and transcranial magnetic stimulation (TMS) in order to quantify their degree of motor-function-specific brain damage. This quantification of neural damage is then used to determine whether rehabilitation of a given patient should focus exclusively on basic functions which might enable eventual discharge (e.g., sit-to-stand and posture), or whether it should also include a focus on areas of therapy that might enable an overall fuller recovery (e.g., upper-extremity function). The use of PREP has been shown to result in shorter discharge times with no reduction in patients' level of function at discharge.<sup>27</sup> While these results are encouraging, and there are in fact other methods of predicting treatment response that were not used by the PREP system (discussed more in section 1.3.1), to date this system has not been able to scale, given that the methods employed (MRI and TMS) require expertise to operate, are costly and time/space-intensive. The fundamental scientific challenges associated with developing these types of solutions, together with the logistical challenges associated with scalability, has resulted in an absence of private sector interest in this third class of solutions compared to the first two mentioned above. This situation is dissimilar to the advances in treatment management that have been made across several other health problems, such as cancer diagnosis, where the use of

technology to better understand the data already being collected as part of the standard of care has resulted in significant improvements in the standard of care<sup>1</sup>. This discrepancy is likely due to the fact that insufficient physiological data are collected as a part of the standard of care for stroke recovery—meaning that for a product to deliver value with respect to treatment management, it may need to enable the collection of *more* physiological data than what is currently being realized. This challenge to using physiological data to improve treatment management in recovery of physical function post-stroke is unfortunate, as there are surely synergistic effects to be had by applying solutions from each solution class in concert: for example, a pharmacological intervention aimed at increasing the response to therapy could be made more effective by tailoring it to a patient with particular characteristics (e.g., lesion location/size, physical deficits, time post-stroke, the presence of comorbidities), made possible through a solution that generates data allowing for a personalization of the standard of care.

One way around such a conundrum is to develop a product that enables the collection of novel physiological data *while also* enhancing and/or reducing the therapist time needed to provide rehabilitation therapy. This dissertation discusses the development of a product that seeks to benefit stroke survivors in recovering physical function by collecting physiological data that may (as a long-term goal) be used to better understand and thereby optimize stroke rehabilitation dosage and delivery, whilst also (as a more immediate goal) delivering engaging automated physical therapy in the comfort of a stroke survivor's home.

## **1.2 MECHANISMS OF DISRUPTION AND REPAIR IN THE BRAIN POST-STROKE**

### **1.2.1 Mechanisms of disruption to the cortical motor system**

Stroke results in tissue damage due to a lack of blood flow—with some regions experiencing complete cell death (the focal center of the lesioned region), and adjacent regions

(i.e., the penumbra) experiencing various types and degrees of structural degeneration and associated dysfunction<sup>28-30</sup> but not total cell death.<sup>31</sup>

Of course, the cellular damage that occurs as a result of stroke has downstream effects on other brain regions as well. The three major types of downstream dysfunction that result (visualized in Figure 1.1) are: (1) structural connectivity damage, or damage to white matter projections of the lesion brain area, (2) diaschisis, or the dysfunction of brain regions which were functionally connected with the dead region, or (3) an alteration of the typical pattern of interhemispheric inhibition (IHI) and excitation

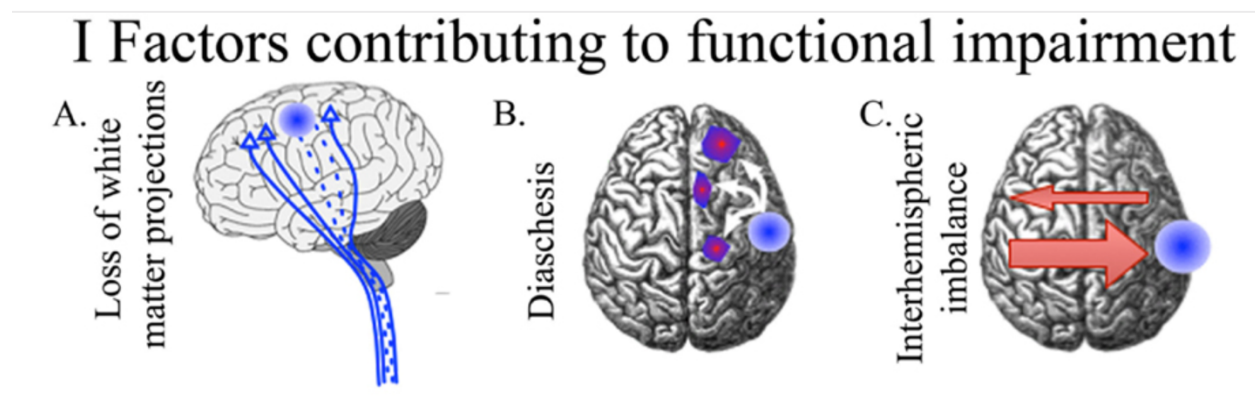


*Figure 1-1.* Factors contributing to post-stroke functional impairment. Illustration (taken from<sup>32</sup>) of the different causes of cortical dysfunction due to stroke.

All three classes of neural dysfunction illustrated in Figure 1.1 contribute to the atypical pattern of functional activation during movement, as well as at rest, that has been observed within the cortical motor system post-stroke. Primary motor cortex (M1) is the point of origin for the majority of corticospinal tract fibers.<sup>33,34</sup> While diaschisis affects a large swath of the brain, M1 is especially well connected to many cortical and subcortical regions,<sup>35,36</sup> and thus especially susceptible to dysfunction via the loss of white matter tracts. And finally, the typical pattern of mutual inhibition between the primary motor cortices (facilitated by the presence of the transcallosal fibers connecting them<sup>37</sup>), during movement has also been shown to be disrupted

post-stroke;<sup>38,39</sup> this is often described as a pattern of maladaptive IHI, where a disinhibited contralesional M1 becomes hyperexcitable, leading to an increasingly hypoexcitable ipsilesional M1; however, there is controversy about the meaning of these findings since it has been shown that motor function can improve alongside an increase in ipsilesional M1 excitability in the first three months post-stroke, without a change in IHI or a reduction in the excitability of contralesional M1<sup>40</sup> (a topic further discussed in section 1.3.2).

### **1.2.2 The Brain's Regenerative Response to Stroke and the Motor System**

In the wake of stroke, several molecules that spur cell survival and growth are up-regulated,<sup>41,42</sup> and likewise several factors which normally inhibit plasticity in the adult brain are down-regulated.<sup>41,42</sup> This adaptive response leads to a period immediately post-stroke where there are many changes to neurons in and connected to damaged neural regions, including changes to glial and epidural cells,<sup>43,44</sup> as well as the extracellular matrix.<sup>41,45</sup> In addition, during this period the growth of new axon collaterals is up-regulated, which contributes to the reinnervation of neural regions that are damaged but not completely devoid of surviving neurons; indeed, animal models have shown that post-stroke axonal sprouting occurs within ipsilesional motor areas.

And finally, this period of increased neural pliability slowly decreases over time, which has caused the first months post-stroke to be referred to as the post-stroke 'critical period'.<sup>51</sup> Thus, the timing of any rehabilitation intervention is an important factor to consider, since the ability to use the experience-dependent plasticity of rehabilitation to catalyze increases in function are not time-constant.

The presence of spontaneous biological recovery mechanisms, and their steep decline in the subacute period of stroke, has resulted in many researchers demonstrating the ability to

predict where a stroke survivors' functional status will plateau based on their initial function—known as the 'proportional recovery rule'. This rule holds that stroke patients are expected to gain roughly 70% of the difference between their baseline post-stroke function and the maximum possible function. This rule has led many to even question whether post-stroke rehabilitation “matters” at all in the midst of these spontaneous mechanisms.<sup>23</sup> While the proportional recovery rule has received many caveats<sup>52</sup> and technical critiques questioning strength of its predictive power,<sup>53,54</sup> its place in the dialogue around post-stroke recovery is important to acknowledge. Viewed in a certain light, the proportional recovery rule is an evidence-based account for why stroke rehabilitation may not be worth doing at all. In opposition to this view, the following section discusses several promising leads that may enable clinical practice to move past the proportional recovery rule, to understand post-stroke motor recovery at a higher resolution which might enable an improvement to the standard of care's optimization of clinical resources.

### **1.3 NEURAL BIOMARKERS OF STROKE RECOVERY**

#### **1.3.1 Potential role for neural biomarkers in stroke recovery**

Pre-clinical work has shown that quantifying the size of a rat's infarct can enable a predictive model from which one can derive an estimated threshold of rehabilitation dose in order to achieve an optimal motor outcome, wherein after deriving this model the authors then used it to prescribe rehabilitation dosage, resulting in a 13 times better chance of recovery than using a standard 'one dosage fits all' model.<sup>26</sup> A potential mechanism that could be responsible for the existence of a 'minimum effective dose' of rehabilitation may involve the release of brain-derived neurotrophic factor, given the extensive pre-clinical work demonstrating that its release is correlated with post-stroke motor recovery,<sup>55-58</sup> and limited but encouraging human work that has found analogous results<sup>59</sup>. Moreover, one recent study interested in the origin of



this increase in the post-stroke brain suggested the role of brain-derived neurotrophic factor (BDNF) may have particular relevance for the M1, finding that motor recovery (induced by rehabilitation combined with a centrally-delivered GABA-A antagonist) was precipitated by an increase in BDNF at the ipsi-lesional (but not contra-lesional) M1. Other studies have shown that BDNF delivered through the blood-brain barrier has a beneficial impact that enhances this recovery,<sup>60,61</sup> and moreover that the inhibition of BDNF in a pre-clinical model has been shown to nearly completely negate the possibility of post-stroke motor recovery.<sup>57</sup> The role of BDNF in post-stroke generally, and being critical to the response associated with hitting a dosage threshold, may also be contingent on the genetics of an individual, with one study in chronic stroke survivors showing a relationship between the BDNF-Val66Met polymorphism and response to rehabilitation.<sup>62</sup> Support for the idea of a dose threshold in post-stroke rehabilitation that is sensitive to the timing of rehabilitation (relative to the time of stroke) is also supported by several reviews of stroke rehabilitation studies in humans, which have found that more rehabilitation results in better outcomes,<sup>63,64</sup> and moreover that the timing of that therapy matters.<sup>64</sup> Further theoretical support for the idea is found in biologically-plausible simulation studies of upper-extremity rehabilitation and motor recovery, which support the idea of a non-linear relationship between rehabilitation and recovery, in that a particular threshold must be crossed to begin the processes which facilitate motor recovery.

The possibility that, for some segment of stroke survivors, gains from rehabilitation may only be triggered by hitting a dose-dependent ‘threshold’ of rehabilitation, makes it comprehensible that a study may find that, for instance, 47% of inpatients fail to benefit from upper-extremity rehabilitation,<sup>22</sup> and moreover, it provides a potential mechanism for stroke rehabilitation’s ability to improve function at the chronic stage—a view supported by a large

recent study that demonstrated positive findings by utilizing a particularly intense dosage of upper-extremity rehabilitation.<sup>65</sup> Indeed, it seems plausible that the failure to hit this individualized “threshold” for a minimally effective dose of rehabilitation may be hindering our efforts to maximize the value of costly and laborious one-on-one therapy. This depressing potentiality is made even more so by the stark contrast between the pre-clinical literature, which demonstrates the number of repetitions required to drive neuroplasticity for optimal motor recovery to be in the thousands,<sup>66</sup> and observational human studies that have repeatedly shown stroke survivors receive significantly less volume, even when given access to care.<sup>13,14</sup>

Amid these realities, it’s clear that a more individualized approach (i.e., beyond tailoring the rehabilitation approach to a patient based on their presenting motor function), whereby one could better predict the likelihood treatment response for a particular stroke survivor being given a specific rehabilitation regimen (which, as discussed earlier, was achieved pre-clinically by Jeffers et al.<sup>26</sup>) would be remarkably beneficial. Luckily, while preliminary, some strides towards this goal have been made in human stroke survivors. The laterality of M1 activity during paretic upper-extremity movement (M1-LAT; discussed more in the next section) as measured by functional magnetic resonance imaging (fMRI),<sup>67,68</sup> the presence or absence of motor-evoked-potentials as measured by TMS,<sup>69</sup> and corticospinal tract (CST) integrity (as measured by DTI),<sup>52</sup> have all been shown to add unique information in helping researchers predict treatment response, over-and-above what is possible using functional status alone. One of these studies that used M1-LAT<sup>67</sup> even found that M1-LAT outperformed functional status as an independent predictor of treatment response. Other findings which suggest that performing functional motor assessments are not sufficient to enable truly personalized rehabilitation show that initial motor function did not have an effect on the dose-response relationship,<sup>70</sup> that stroke survivors who are ‘non-fitters’

of the proportionate recovery rule respond the best to rehabilitation,<sup>71</sup> and that particular functional outcomes have low predictive power<sup>72</sup> for moderately severe strokes (typically considered the best candidates for rehabilitation). These findings help contextualize the desire by researchers to further the development of biomarkers of recovery which might help us better understand, and therefore optimize, stroke rehabilitation response and motor outcomes;<sup>73</sup> furthermore these findings also make more comprehensible the finding that rehabilitation intervention trials which have a biological-based rationale perform better than those that do not.<sup>74</sup>

It is important to point out that none of the work above calls into question the notion that an increase in the volume of rehabilitation for all stroke survivors would be beneficial in helping stroke survivors, in aggregate, achieve greater functional motor outcomes. However, for a variety of reasons, the lever of prescribing “more rehabilitation for all” is inaccessible to health care professionals and policy-makers; it is for this reason that the above findings ought to be translated into actionable public health change as soon as possible, given the high costs and the unclear return on investment post-stroke rehabilitation has demonstrated over time.<sup>23</sup> If technology could, for example, aid us in identifying a probabilistic, personalized minimum “threshold” of rehabilitation volume for stroke survivors, then we may be able to provide a tangible, hypothesis-driven method for increasing the amount of rehabilitation performed by stroke survivors. As the studies outlined above suggest, the literature is inching us in that direction; and recently the first of these systems used in humans was shown to increase the efficiency of rehabilitation: in this study, 192 inpatients who had experienced stroke were randomized to either an intervention group or a control group who received the standard of care. While all patients performed the assessments included in the PREP algorithm (discussed in section 1.1.2 above), the rehabilitation team were only provided with the PREP algorithm’s

predictions (of either ‘Excellent’, ‘Good’, ‘Limited’, or ‘No’ recovery potential) and asked to follow its guidelines (to focus more on compensation and pain reduction for patients with lower recovery potentials) for patients in the intervention group. The study’s results showed a one week decrease in the length of stay for patients in the intervention group, with no differences between the groups with respect to clinical outcomes.<sup>75</sup> While this study only improved efficiency and not overall clinical outcomes, and there is considerable work to be done before this type of value can become scalable, this study could be a harbinger of a brighter future to come, where rehabilitation resources are more intelligently employed. The ability to measure the brain at scale may yet aid in this mission, and therefore the remainder of this section will introduce and discuss the potential utility of two candidate biomarkers of stroke recovery that may be measurable by the Axem Home system.

### **1.3.2 M1 Laterality (M1-LAT)**

The M1 actuates movement via the CST, a signal chain which terminates with alpha motor neurons causing muscle fibers to contract, leading to movement of the body. Approximately 90% of the fibres of the corticospinal tract decussate at the medulla<sup>76</sup>, such that activity in the left M1 is primarily responsible for initiating movement in the right side of the body, and vice versa. Given this cross-over pattern of connection between the M1 and the body, in a typical case, when a person moves their right arm, their left M1 is more active than their right, and vice versa.

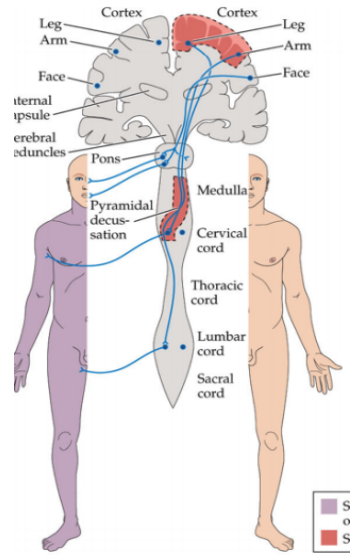


*Figure 1-2.* Illustration of how the left M1 facilitates movement motor control in the right side of the body. Following stroke this pattern gets disrupted, with the undamaged M1 playing an outsized role in initiating movement for both sides of the body.

Multiple meta-analyses have found that atypical functional activation patterns in stroke survivors with motor deficits are consistently found in both the ipsilesional and contralesional hemisphere—specifically a hypoactivation of the ipsilesional hemisphere, and a hyperactivation of the contralateral hemisphere.<sup>77,78</sup> As mentioned previously, in the typical case unilateral upper-extremity movements elicit a pattern of M1 activity that is lateralized to the contralateral hemisphere—a finding that has been demonstrated in humans via fMRI<sup>79</sup>, functional near-infrared spectroscopy (fNIRS),<sup>80</sup> electroencephalography (EEG)<sup>81</sup> and magnetoencephalography.<sup>82</sup> However, following a stroke this pattern of M1 laterality changes during movements of their paretic upper-extremity—it either becomes symmetrical or reverses, such that, for example, the undamaged right side of the M1 is more active when moving the right side of the body.

Repeated studies have also shown that successful recovery of one’s movement ability is reflected in a return to a typical pattern of M1 laterality. This has been demonstrated in both

cross-sectional data on acute<sup>83</sup> and chronic patients,<sup>84</sup> as well as in longitudinal data where patients are tracked from the acute through to the chronic phase.<sup>85–88</sup> Moreover, clinical studies have shown this shift towards the typical pattern of laterality during paretic limb movement is associated with functional gains, as opposed to simply being associated with the amount of time that has elapsed since stroke.<sup>89,90</sup> This work is further supported by pre-clinical studies which have shown that forced-use of the paretic limb leads to the growth of new intracortical axons in the ipsilesional M1,<sup>91</sup> as well as re-modelling of the ipsi-lesional corticospinal tract more generally;<sup>92</sup> whereas training of the non-paretic limb leads to dendritic plasticity at the contralesional cortex,<sup>93</sup> as well as a deleterious effect on motor recovery of the paretic limb.<sup>46,94,95</sup> Similar findings have also been demonstrated in humans, via several TMS<sup>96–99</sup> and neuroimaging<sup>68,100–102</sup> studies that show that a failure to reduce the hyperactivity seen during paretic arm movement in contralesional M1 leads to worse functional outcomes.

While the mechanism underlying this phenomenon is not fully elucidated, there is support for the theory that it relates to altered patterns of transcallosal inhibition between the motor cortices. In the typical case, while at rest the motor cortices send inhibitory signals to each other in a pattern of mutual IHI;<sup>103,104</sup> moreover, during unilateral movement there's a pattern of IHI whereby contralateral M1 inhibits ipsilateral M1. This inhibition is thought to be cortically controlled through neural pathways that run along the corpus callosum<sup>104,105</sup>, with the IHI controlled by local neurons in M1 that cross over the corpus callosum and directly innervate inhibitory interneurons located at the opposite M1,<sup>106</sup> as well as subcortical regions (though these mechanisms are less well-defined).<sup>107</sup>

In both cortical and subcortical stroke there is a reduction in IHI from the ipsilesional to the contralesional hemisphere, while levels of IHI from the contralesional to the ipsilesional

hemisphere remained unchanged;<sup>108</sup> and moreover, it has been demonstrated this change is not solely due to increased excitability in contralesional M1.<sup>40</sup> Disinhibition of contralesional M1 has also been demonstrated during paretic limb movement—with the contralesional (i.e., ipsilateral) M1 inhibiting the ipsilesional (i.e., contralesional) M1 during movements of the paretic arm, leading to contralesional M1 hyperactivity during movement of the paretic side.<sup>39,40,77,109–111</sup> Moreover, this pattern of dysfunctional IHI has also been shown during movement preparation in chronic stroke patients.<sup>39</sup>

While this disruption to the typical pattern of IHI post-stroke may be a cause of the pattern of hyper- and hypoactivation seen at contra- and ipsilesional M1, it should be noted that stroke survivors' ipsilesional M1 activity during paretic limb movements can increase without any change in IHI, or any reduction in contralesional excitability.<sup>41</sup> And while IHI is thought to be associated with post-stroke motor recovery, one study found that IHI only becomes abnormal in the chronic phase of stroke, and that its change from normal to abnormal over time was associated with gains in finger dexterity.<sup>112</sup> These findings, showing that abnormal M1 IHI can be unrelated the level of M1 ipsilesional activity during paretic limb movement, as well as upper-limb function itself, suggests that a disruption in M1 IHI is either not the cause—or at least not the only cause—of the dysfunctional patterns of functional hyper- and hypo-activation seen in the contra- and ipsilesional M1 post-stroke, as well as the inability of stroke survivors to benefit from rehabilitation.

While these data all suggest it is via a shift of functional activity back to the ipsilesional M1 that stroke survivors make upper-extremity functional gains, it is important to note that there have been contradictory findings which show that higher levels of *contralesional* activation correlate positively to functional recovery.<sup>113–116</sup> This finding has been demonstrated to apply

specifically to patients with very large lesions,<sup>117</sup> those who are especially weak,<sup>118</sup> or those who have sustained either direct M1<sup>119</sup> or a high degree of CST damage.<sup>113</sup> While still a matter of active investigation, the preliminary consensus is that if a patient sustains a sufficiently large amount of brain damage, the ipsilesional adaptations that would otherwise promote optimal recovery are simply not possible, meaning patients must rely primarily on contralesional reorganization (specifically resulting in increased levels of activity during paretic arm movement at contralesional M1) for the recovery of movement ability. Taken together, these findings suggest that a functional reorganization (and subsequent increase in functional brain activity) in the ipsilesional cortical motor network is an important aspect of optimal stroke recovery in the majority of cases; and that in a minority of cases, where stroke causes a large amount of cortical cell death and/or a large amount of corticospinal tract damage, an analogous functional reorganization at the contralesional hemisphere can instead play a similar role in bolstering the function of the paretic limb.

In addition to reflecting the functional status of stroke survivors, measures of M1-LAT have repeatedly been found to be prognostic, successfully predicting stroke survivors' response to rehabilitation intervention.<sup>68,120,121</sup> In fact, one study suggested these metrics can provide a better prediction of functional outcomes than the functional assessments currently used.<sup>121</sup>

And finally, while these studies all focused on the recovery of upper-extremity function, similar data acquired with fNIRS have shown that this pattern also holds for discrete lower-limb movements,<sup>122,123</sup> where an improvement in walking ability leads to the return of a typical pattern of M1 laterality during walking tasks (which is a symmetrical pattern, the inverse of the pattern seen in unilateral upper-extremity movement).<sup>124,125</sup>

### **1.3.3 Resting State M1 Functional Connectivity (M1-rsFC)**



M1-rsFC reflects the correlation of blood oxygen level dependent (BOLD) activity between the primary motor cortices while at rest. Decreased M1-rsFC compared with typical controls is a common finding for stroke survivors with movement deficits, and decreased levels of M1-rsFC have repeatedly been shown to correlate with functional status post-stroke, in the acute,<sup>126,127</sup> subacute<sup>128</sup> and chronic<sup>129,130</sup> phases of stroke recovery. As with M1-LAT (discussed in the preceding section), these findings have often been thought to relate directly to the literature on interrupted IHI (discussed in the previous section),<sup>131</sup> however the connection between these phenomena has not been definitely established.

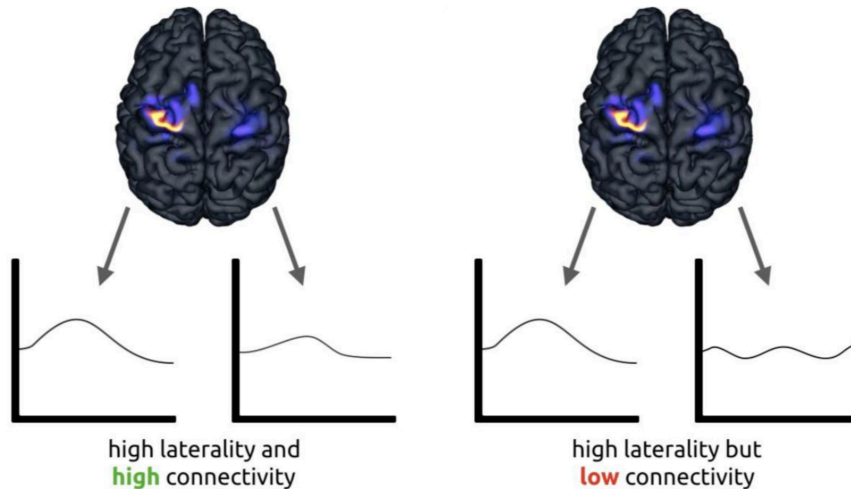


*Figure 1-3.* Illustration of functional connectivity between brain areas, and how it provides different information than the laterality between brain areas (discussed in section 1.3.2). For illustrative purposes a typical pattern of laterality upon simple unilateral movement is depicted; whereas connectivity can be, and is most often, measured at rest. It is important to note that functional connectivity can be measured in many ways — depicted here is a simple correlation in brain activity across time. Stroke can cause disruption of M1 connectivity.

Longitudinal studies have also found that receiving treatment, and the associated increases in functional status over time (both from the acute to early chronic phase,<sup>132–135</sup> as well as throughout the chronic phase<sup>136,137</sup>) are associated with an increase in M1-rsFC. Moreover M1-rsFC measures have been shown to predict treatment response in stroke survivors in the acute,<sup>126</sup>

subacute<sup>138 139 140</sup> and chronic<sup>136 89 141</sup> phase of recovery. However there has also been a longitudinal study, where M1-rsFC measurements were taken throughout the first year post-stroke, showing no change in M1-rsFC over time despite substantial motor recovery having taken place.<sup>142</sup>

Some of the inconsistencies in these findings may be due to the changing nature of M1-rsFC across the continuum of stroke recovery. For example, one study found M1-rsFC correlates positively with corticospinal tract damage, but only in the first month post-stroke, and that after the first month post-stroke, M1-rsFC was correlated with motor function, but only for stroke survivors who had not suffered significant corticospinal tract damage.<sup>143</sup> The authors suggested that once the brain's spontaneous biological recovery tapers off, M1-rsFC diverges from corticospinal tract damage, such that in the acute phase, corticospinal tract damage will determine the extent of M1-rsFC disruption, but as endogenous plasticity occurs M1-rsFC continues to change in ways that contribute to increased motor function.

While the majority of studies documenting these post-stroke changes in M1-rsFC utilize fMRI, similar disruptions in post-stroke M1-rsFC related to movement deficits have been documented using fNIRS<sup>144</sup> and EEG.<sup>145</sup>

#### **1.3.4 M1 Neurofeedback (M1-NFB)**

In addition to the use of metrics derived from functional neuroimaging at M1 (i.e., M1 laterality and M1-rsFC) for tracking and predicting the recovery of movement abilities post-stroke, there is also accumulating evidence that the provision of data from M1 as immediate feedback—often termed ‘neurofeedback’—during rehabilitation may enhance its efficacy. Neurofeedback simply refers to the process of taking measurements from the brain, then communicating a metric back to the individual on whom the measurements are being taken; this

metric is usually a simple, univariate metric, like power in a particular frequency band, or the level of a BOLD response, and moreover the metric is usually presented in such a way that it is easily legible whether modulations of this metric represent movements towards or away from the win-state of the NFB system (e.g., the metric may be represented by a bar graph, with previous instructions informing the user that they should try to keep the height of the bar as high as possible). This process of constant feedback helps individuals optimize the aspect of brain activity being fed back to them, through a process akin to operant conditioning.<sup>146</sup> This feedback might be provided simultaneously with the task—so called “real-time” feedback—or during rest periods—so called “intermittent feedback”. While the majority of the literature has utilized real-time feedback, three studies have compared the two methods, with two single-session studies finding that intermittent feedback is superior at enabling individuals to modulate the particular NFB being used—activity at the M1 during motor imagery (the mental rehearsal of movement) in one,<sup>147</sup> and amygdala activity during a self-guided emotion induction task in another;<sup>148</sup> while one longitudinal study found intermittent feedback superior to this end in the first session, but that over repeated session continuous was the better performing type of NFB.<sup>149</sup>

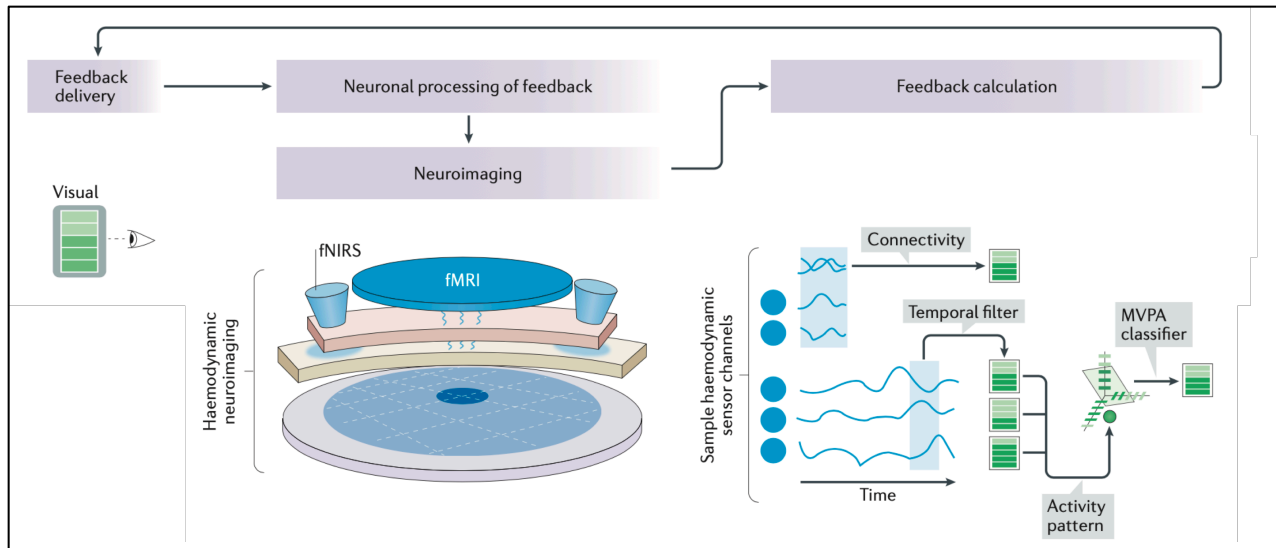


Figure 1-4. Illustration of the process of presenting NFB from cerebral hemodynamic sources (note that these steps are mirrored in the presentation of NFB from electromagnetic sources (adapted from<sup>150</sup>).

Through a careful choice of what is being fed back and how it is being fed back, it has been shown that NFB can have beneficial effects in a variety of domains. In the case of M1-NFB for use in movement rehabilitation, data about M1 activity can be provided to the individual engaging in a movement rehabilitation task in a manner which encourages them to achieve brain activity patterns seen in individuals who are successfully regaining their movement abilities. For example, this could mean either promoting an increase in contralateral (i.e., ipsilesional) brain activity, an inhibition of ipsilateral (i.e., contralesional) brain activity, or both (i.e., M1 laterality) during movement of the paretic limb. And indeed, many studies have characterized the feasibility of allowing individuals to modulate their M1 activity during a variety of movement related tasks, such as the execution of movement, as well as during motor imagery.<sup>151–153</sup>

In addition to a wide range of studies in healthy individuals, M1-NFB has also been used to promote M1 modulation during rehabilitation interventions. In one case, a patient group that received real-time M1 laterality NFB during motor imagery of upper-limb movement showed

greater functional improvements compared to a control group which conducted motor imagery without the provision of M1 laterality NFB<sup>154</sup> (see Figure 1.5).

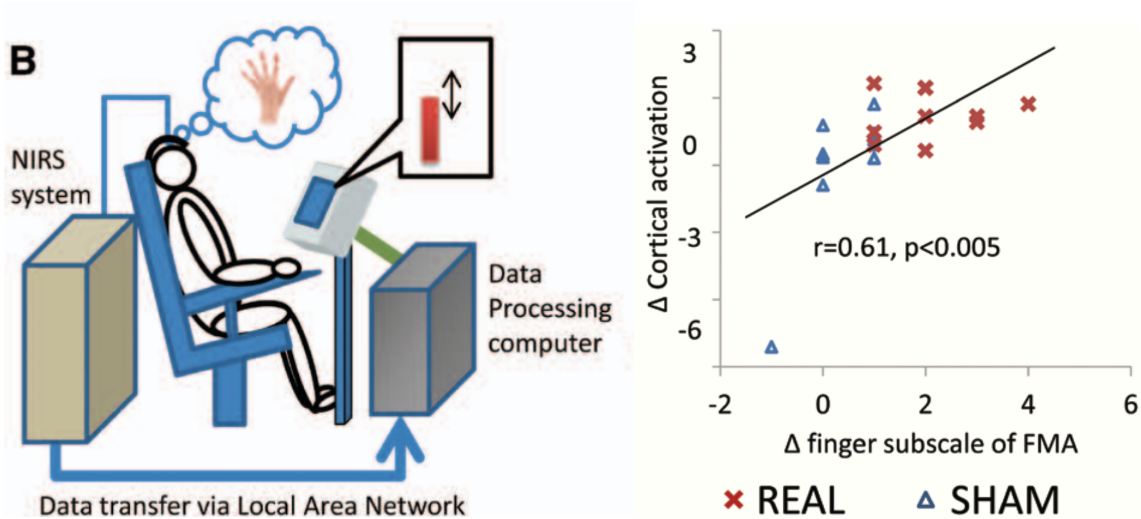


Figure 1-5. (Left) Illustration of the NFB setup used by Mihara et al.<sup>154</sup> (Right) Illustration of the relationship between group (NFB or sham), increases in ipsilesional M1 activity during paretic limb movement, and improvements in finger movement ability as measured by the Fugl-Meyer assessment.

Despite relatively small effect sizes, positive clinical benefits have been shown for many M1-NFB studies, including those using M1-NFB during motor imagery,<sup>155 154 156</sup> as well as in conjunction with functional electrical stimulation<sup>157</sup>, an assistive exoskeleton or orthosis,<sup>158,159</sup> mirror therapy,<sup>160 161 162 163</sup> mirror therapy,<sup>160 155,164</sup> and robotic therapy.<sup>165</sup> In all these studies, the up-regulation of ipsilesional M1 was found to correlate with functional gains made from the intervention.

While in yet another type of approach, it has been shown that patients engaged in M1-rsFC NFB (where the patients were simply told to increase the amount of M1-connectivity while resting) showed enhanced outcomes compared with a group that received feedback about the connectivity levels of a control brain region.<sup>166</sup>

While these studies all use disparate neuroimaging and rehabilitation modalities, feedback signals and user experience and user interface approaches, the positive findings suggest

that further work in this area could render tools to increase the efficacy of various types of post-stroke rehabilitation therapies. However, a significant barrier to translating these findings to scalable clinical impact is the fact that all these studies utilized neuroimaging devices designed for laboratory use only (i.e., devices that are expensive and require set up by an experimenter); the next section will introduce and provide an overview of a neuroimaging device designed to leverage this clinical potential at scale.

## **1.4 AXEM HOME**

### **1.4.1 Axem Home Overview**

Axem Neurotechnology is in the process of developing what is projected to be their first product, the Axem Home—rehabilitation system that provides guidance, feedback, and support for post-stroke upper-extremity rehabilitation. The Axem Home is intended to be usable either within a clinical setting overseen by a healthcare professional, or independently by a stroke survivor in the comfort of their own home. The Axem Home consists of (1) an fNIRS headband (the “Axem Home band”) designed to measure the hemodynamic response from the portion of M1 associated with upper-extremity movement, (2) a tablet containing software which guides stroke survivors through rehabilitation exercises during which they receive NFB based on the relative oxygenation ( $\Delta\text{HbO}$ ) detected during movement by the Axem Home band, and lastly (3) a web-based software enabling healthcare professionals (HCP) to remotely monitor usage of the Axem Home by the stroke survivor. Future releases of the Axem Home (or future products from Axem Neurotechnology that are built to work together with the Axem Home) may focus on using insights from the fNIRS data collected from the Axem Home, together with other sources (be it those accessed from a stroke survivor’s health record, or generated by the Axem Home itself—e.g., movement tracking metrics derived from the camera on the tablet being used for

rehabilitation) to provide actionable insights to health care professionals and/or policy makers that might help them determine what an optimal personalized treatment plan (be it overall dose, timing, or type of rehabilitation intervention) might be for a particular stroke survivor.

While chapter 2 will describe the particulars of Axem Home headband, as well as discuss some of the challenges associated with its development, the following section will be used to provide context around the selection of fNIRS as the functional neuroimaging modality chosen for the Axem Home. Furthermore, while section 4.3 will provide an overview of the software meant to guide rehabilitation for stroke survivors, the software for healthcare professionals will not be specifically discussed (see section 5 for a comment on the scope of this dissertation).



*Figure 1-6.* Illustration of the Axem Home being worn by a patient during a rehabilitation session. The model used in this photo is a preliminary model based on idealized industrial design.

#### **1.4.2 On the suitability of Functional Near-Infrared Spectroscopy (fNIRS) for use in the Axem Home**

Functional near-infrared spectroscopy<sup>167</sup> was invented as a modality of functional neuroimaging in the late 1970s and it has been gaining in prominence steadily since that time. In

particular, recent advances in light emitting diode (LED) and silicon photodiode (SiPD) technology has accelerated its popularity as a research tool in the past decade.

Broadly, fNIRS relies on the same principles of neurovascular coupling which enable measurements from many neuroimaging modalities, including fMRI and transcranial doppler. Neurovascular coupling broadly refers to the relationship between neural activity and cerebral blood flow, enabling the measurement of a BOLD signal that reflects local neural activity. There are three distinct methods of performing fNIRS—continuous wave, frequency domain, and time domain. Continuous wave fNIRS measurements are derived strictly by measuring changes in light intensity of continuously emitted light, while both frequency and time domain techniques measure this in addition to the time of flight of photons, allowing for greater temporal resolution. Because extremely sophisticated components are required to enable both the frequency domain and time domain measurements, continuous wave fNIRS is the most common modality used. Given that Axem Neurotechnology is striving not to push the cutting edge of neuroimaging resolution, but rather to push the cutting edge of neuroimaging accessibility (and real-world clinical utility), only the continuous wave technique is relevant, and for the purposes of this document, fNIRS will be used interchangeably with continuous wave fNIRS.

The fundamental principle of fNIRS is, firstly, given that light waves in the infrared range (i.e., 700-1000nm) are both non-ionizing and permeable to human tissue, bone, and related mediums, they can be safely emitted into the body; the amount of light that returns to the surface of the body can then be measured, allowing one to make inferences about its absorption pattern as it passed through the biological medium. Secondly, by emitting infrared light at the scalp (using a path of emission orthogonal to the cerebral cortex) and positioning a photodetector an appropriate distance from the location of the emitter (~2-5cm can be used, with 3cm being the



most commonly used distance<sup>168</sup>), a portion of the light that was emitted can be assumed to have passed through the cerebral cortex.

In addition to this ~3cm light path, recently it has been shown that by including measurements of these same near-infrared wavelengths taken at shorter emitter-detector separations, it is possible to capture the influence of hemodynamic changes occurring superficial to the brain from those occurring at the level of the cortex so that they might be removed from those associated with cerebral hemodynamics.<sup>169,170</sup> In particular it has been shown that emitter-detector separations  $\leq 1$ cm are optimal for this purpose, since they are not significantly affected by cerebral hemodynamic changes.<sup>171</sup> This process has been shown to reduce physiological noise, and to further improve the correspondence between fNIRS and fMRI.<sup>172</sup>

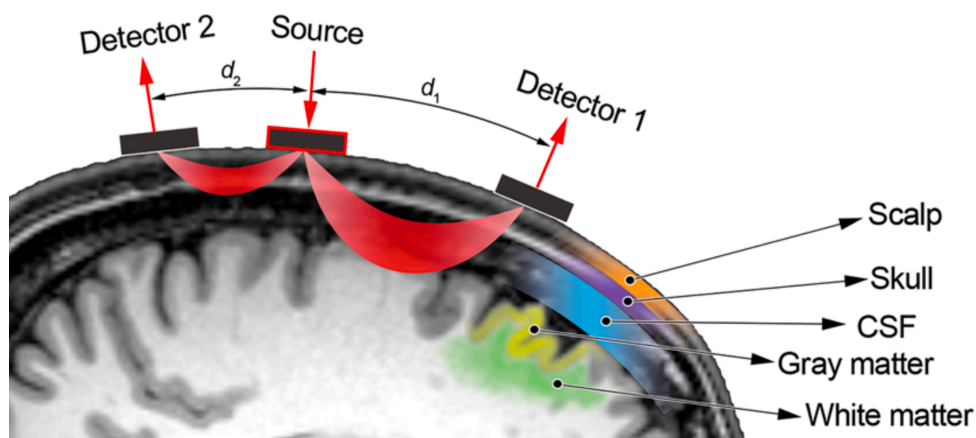


*Figure 1-7.* Illustration of the light paths from both 3cm ( $d_1$ ) and 1cm ( $d_2$ ) paths. Of particular note is that only the longer light path passes through the gray matter at the cortical surface. Taken from<sup>173</sup>

Thirdly, if at least two wavelengths are used, and these wavelengths are differentially absorbed by the chromophores oxyhemoglobin (HbO) and deoxyhemoglobin (Hb; see Figure 1.8), inferences about the hemodynamic response can be made by using a modified version of the Beer-Lambert law.<sup>174</sup> This allows fNIRS to quantify relative levels of oxyhemoglobin and deoxyhemoglobin.

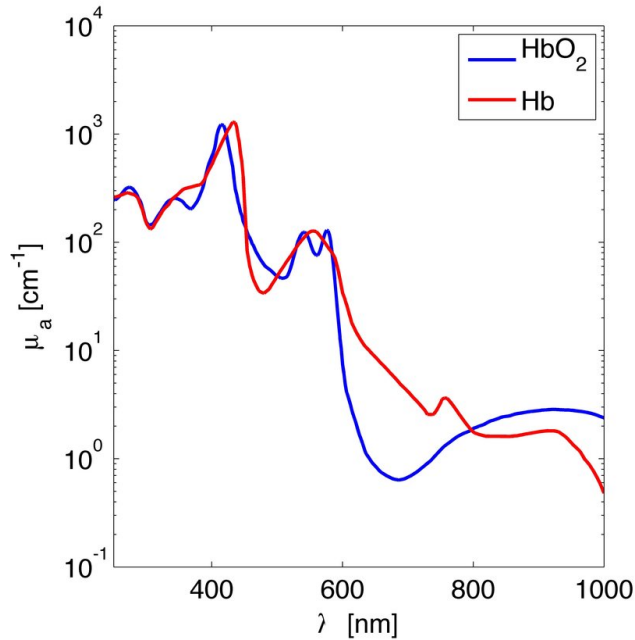


Figure 1-8. Absorption coefficients for oxy- (HbO<sub>2</sub>) and deoxyhemoglobin (Hb) taken from<sup>176</sup>.

Oxyhemoglobin and deoxyhemoglobin are altered in response to neural activity in a canonical manner—with a near instantaneous initial decrease in oxyhemoglobin (as oxyhemoglobin is converted to deoxyhemoglobin to provide the energy required for cellular activity), followed by an increase in oxyhemoglobin starting at approximately five seconds following the onset of neural activity, with a slow return to equilibrium following the cessation of local neural activity (see Figure 1.9). Meanwhile, an inverse pattern is seen in deoxyhemoglobin, however the magnitude of chromophore change is smaller. This means that fNIRS is not taking absolute measurements, which is not possible without resolving the light scattering and absorption coefficients (requiring time of flight measurements), but instead relative changes in the presence of these chromophores.

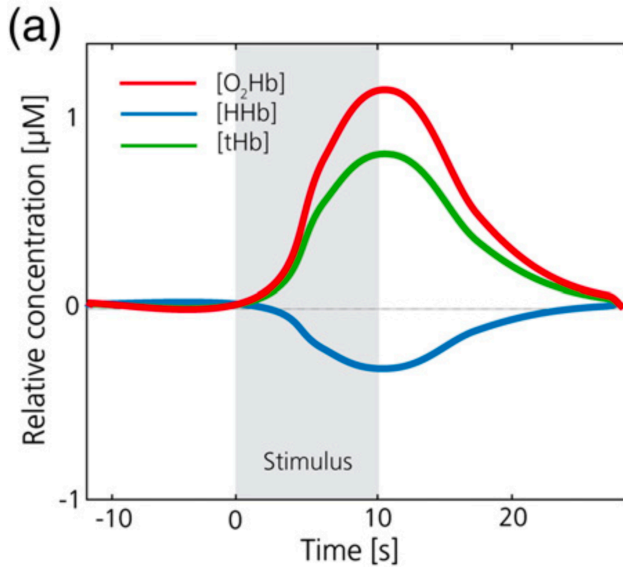


Figure 1-9. Representative fNIRS data during local neural activity. Red represents  $\Delta HbO$ ,  $\Delta Hb$ , and green relative total hemoglobin (taken from<sup>175</sup>).

A restriction to relative measures is also the case in fMRI data, which also relies on the principles of neurovascular coupling to quantify the BOLD response. Accordingly, studies have shown good correspondence between simultaneously acquired fMRI and fNIRS.<sup>177,178</sup> However, there are three primary differences between the capabilities of fNIRS versus fMRI that warrant outlining.

The first is that while fMRI is able to quantify neuronal activity throughout the brain, fNIRS is constrained to measurements at the cortical surface. While this limitation of fNIRS is suboptimal, as discussed in section 1.3.2 and 1.3.3, many subcortical changes associated with motor deficits post-stroke manifest at the level of the cortex, specifically the primary M1. The second difference between fNIRS and fMRI is that fMRI has a higher spatial resolution than fNIRS (millimeter<sup>179</sup> and centimeter scale,<sup>180</sup> respectively); and while this does somewhat limit the types of data one might glean from fNIRS versus fMRI measurements of the primary motor cortices, the neural biomarkers of recovery the Axem Home endeavors to measure in stroke

patients (M1-LAT and M1-rsFC) are measures relying on differences in brain activity between hemispheres, meaning centimeter scale spatial specificity is sufficient.

The third important difference between fNIRS and fMRI is that fNIRS can be implemented in a portable/wireless device; thus fNIRS devices can be made to be ergonomic—i.e., ergonomics here meaning “designed to minimize physical effort and discomfort, and hence maximize efficiency<sup>181</sup>”—, or to be made to suit a variety of different tasks, settings, or types of users. This relates specifically to the field of neuroergonomics, which includes the development of brain measurement devices for use in novel, real-world settings.<sup>182,183</sup> This difference between fMRI and fNIRS, together with the considerable difference in the cost of an MRI versus an fNIRS system (which is somewhere between one and two orders of magnitude, even for research grade fNIRS devices), is critical for the present discussion, as it precludes fMRI from being used as a routine measurement device throughout the course of care in stroke rehabilitation.

Thus, from the perspective of what form factors may or may not be within its possibility space, fNIRS has more in common with EEG (which has been utilized in several commercial products<sup>184</sup>) than fMRI. However, compared with EEG, fNIRS has many advantages which resulted in it being chosen for use in the Axem Home—most importantly, a vastly superior spatial specificity (i.e., the ability to discern where in the brain measured activity is coming from) due to the spatial smearing that occurs, for example, when measuring electrical signals from the scalp with EEG.<sup>185</sup> While EEG can gain centimeter scale spatial specificity, it can only do so reliably by use of a large array of wet electrodes<sup>186,187</sup>, thus compromising its ability to deliver measurements with a user-friendly form-factor. The ability to measure the brain with spatial specificity is of critical importance in the design of a clinical tool to enhance and monitor

stroke rehabilitation by measuring the cerebral cortex, given that the primary area of interest is the M1 specifically—a 1cm strip across the brain (approximately in-line with the ears). Measurements from this region have been demonstrated using a limited number of fNIRS sensors.<sup>188</sup> Another reason fNIRS is preferable to EEG for this application is the higher signal-to-noise ratio of fNIRS compared with that of dry EEG (which would be required for a clinical application, given the long setup time associated with wet EEG). This translates to a smaller number of trials being required to gain interpretable data: in other words, patients will not have to perform large numbers of trials of rehabilitation exercises in order for the data measured from their M1 to be interpretable—see Figure 1.9 for representative fNIRS data from the M1.

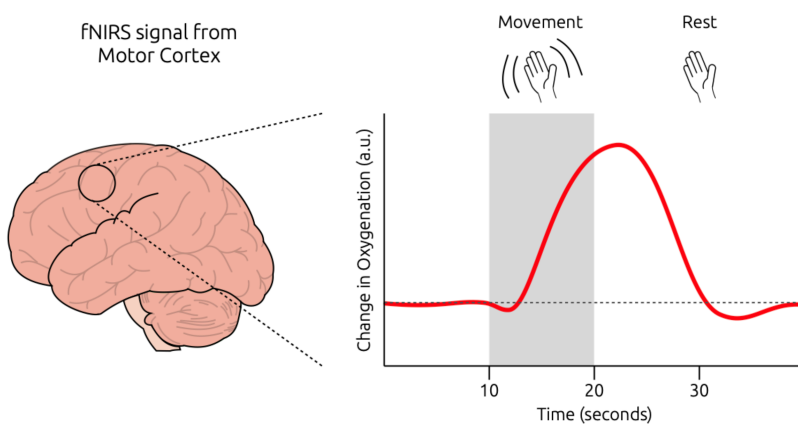


*Figure 1-10.* Idealized time course of the canonical relative oxyhemoglobin at the M1 during movement.

### **1.4.3 Axem Home Rehabilitation Software**

The Axem Home app is a tablet-based software application designed to work together with the Axem Home headband to allow stroke survivors to engage in upper-extremity rehabilitation exercises in an easy and enjoyable way. To support this, the Axem Home app connects with and receives data from the Axem Home headband and provides instructions to users on how to correctly place the headband to enable valid measurements. Using the data

collected from the Axem Home headband, the app presents feedback to the user during rehabilitation exercises, providing motivating reinforcement throughout what can otherwise be a dull and demotivating activity. The Axem Home app also tracks the rehabilitation activity of the user over time, meaning the app can explicitly encourage the user to comply with their home rehabilitation goals.

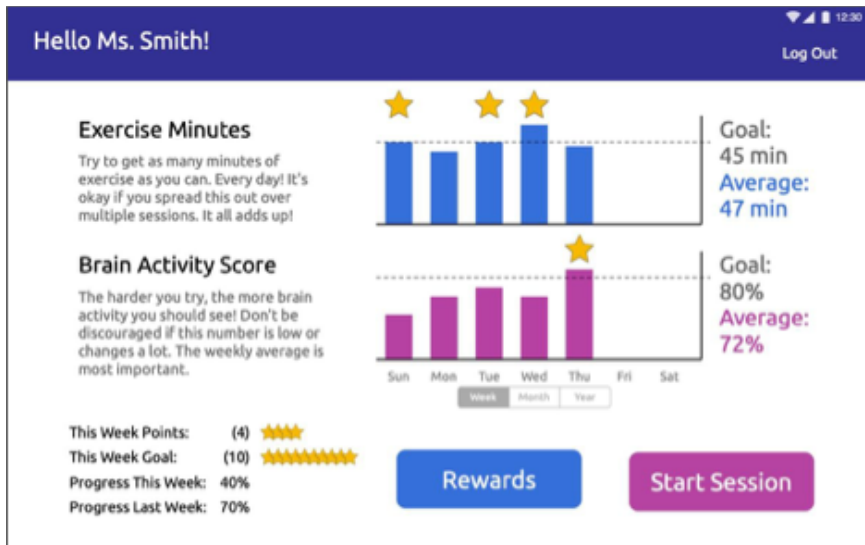
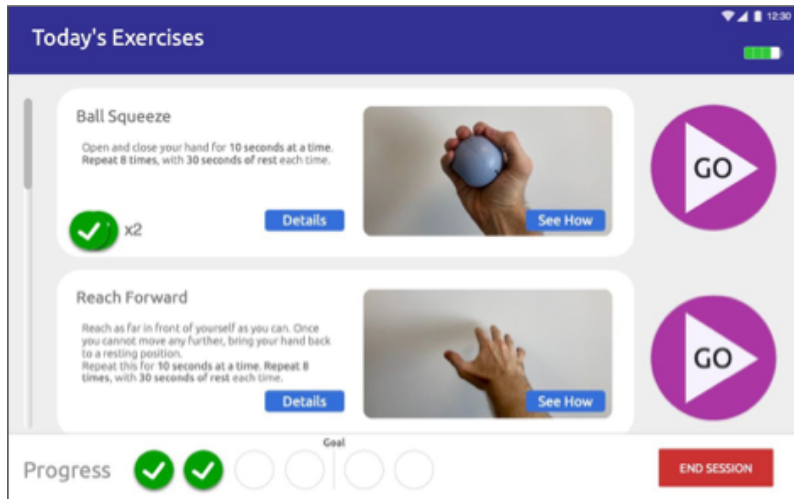


Figure 1-11. Prototype user home screen. The user home screen displays representations of the patient’s past usage of the app, in terms of the amount of rehabilitation completed, as well as metrics based on the brain activity data collected during rehabilitation sessions.

While the Axem Home app will allow health care providers to remotely determine some aspects of a patient’s home exercise program (i.e., what rehabilitation exercises the patient has access to, the timing parameters of a rehabilitation exercise, and goals for compliance), the app will allow patients to choose which exercises they would like to perform (see Figure 1.12).



*Figure 1-12.* Prototype Exercise Selection screen. Displays the rehabilitation exercises available, and includes basic information about each movement, and the ability to preview each movement’s video.

During rehabilitation exercises, users will be encouraged to follow along with a video demonstrating the exercise, performing it themselves as shown in the video (Figure 1.12, left pane). After a specified time performing the exercise, users will be asked to rest for some time. During rest, the user is presented with feedback about their brain activity as measured by the device, akin to the “intermittent feedback” discussed in section 1.3.4 (Figure 1.12, right pane); this feedback is meant to allow the user to modulate their brain activity during the rehabilitation exercise. This feedback might be used, for example, to encourage stroke survivors to achieve a more typical pattern of M1 laterality during paretic upper-limb movement, or it may use some criteria to personalize the feedback for the individual user. As discussed in subsequent sections, in preliminary studies the feedback presented is based solely on activity in the patient’s ipsilesional M1 during paretic arm movement. However, due to the fact that, as mentioned in section 1.3.2, there are likely a portion of stroke survivors for whom contralesional sensorimotor activity will be more beneficial, in the future the Axem Home should include features that allow the software to determine which type of feedback will be most beneficial. However, for the first

manifestation of the Axem Home, it will be assumed that all patients will benefit from increasing ipsilesional M1 activity. This assumption, while flawed, rests on the fact that (A) this is the case for the majority of all stroke patients with upper-extremity deficits, (B) that, over and above this fact, the subset of all stroke survivors with upper-extremity deficits *who will become Axem Home users* is likely to consist *even more disproportionately* of those for whom a return to a normal pattern of M1 laterality will be beneficial, given that those patients for whom a further inversion of the typical pattern of M1 laterality will be beneficial will be patients with to patients with very large lesions<sup>117</sup> (and thus more likely to have contraindications such as cognitive impairment), and those who are especially weak.<sup>118</sup>

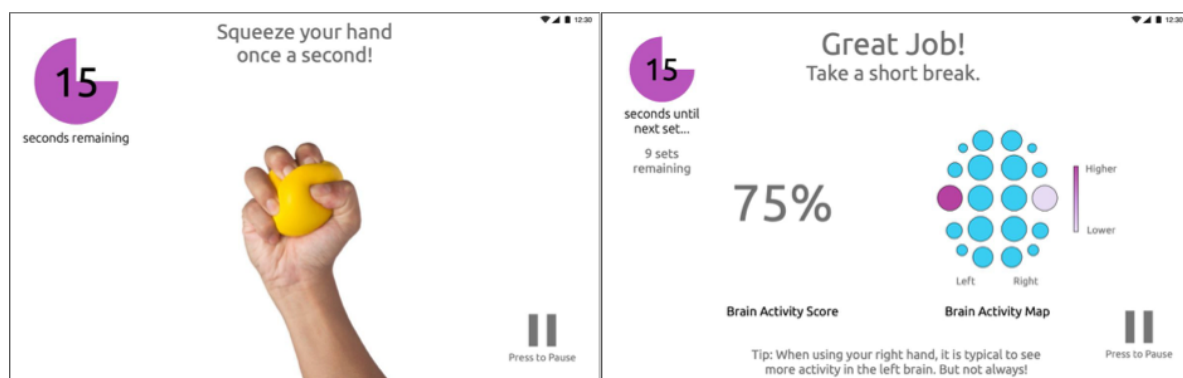


*Figure 1-13.* Displayed above is (A) the active period screen, during which the user is instructed to move in synchrony with (i.e., imitate) the video, as well as (B) the rest screen, which shows feedback to the user based on their brain activity during the preceding active period.

## 1.5 DISSERTATION SCOPE

The vision for the Axem Home is two-fold: firstly, to provide stroke survivors with an engaging and accessible way to engage in upper-extremity rehabilitation in the comfort of their own homes, therefore helping them better comply with a home rehabilitation program, all while enhancing the effectiveness of that rehabilitation through the provision of M1 NFB; and secondly, to use the data generated by the Axem Home to better optimize the deployment of rehabilitation interventions.



The scope of this dissertation is more modest. It is to (1) provide scientific and clinical context for the Axem Home as a potentially useful tool, as well as to (2) document the initial experiments associated with design verification (i.e., determining if the Axem Home performs as intended) and usability (i.e., determining if the device can be used as intended, by representative users, in the intended use environment). Also, since these activities do not directly involve the health care professional-facing aspect of the Axem Home software, that aspect of the Axem Home product vision is beyond the scope of this dissertation as well.

## **1.6 – CONTRIBUTIONS TO STUDY CHAPTERS**

Chapter 3 is based on work conducted by Christopher Friesen (CF), Michael Lawrence (ML), Tony Ingram (TI), Megan Smith (MS), Eric Hamilton (EH), Chris Holland (CH), Heather Neyedli (HN), and Shaun Boe (SB). CF conceived the study with assistance from SB and HN. EH and MS contributed to the changes made to the study devices. CH was responsible for data collection with supervision by HN, CF, and ML. ML was responsible for data analyses, with assistance from CF. CF and ML were responsible for data interpretation, with assistance from TI, HN, and SB. CF wrote and revised manuscript in consultation with SB; all other study authors also contributed to the revision process in some way.

Chapter 4 is based on work conducted by CF, ML, TI, and SB. CF and TI conceived the study with assistance from SB. ML, TI, and CF were responsible for data collection. CF was responsible for data analyses. CF was responsible for data interpretation, with assistance from ML and TI. CF wrote and revised the manuscript in consultation with SB.

Chapter 5 is based on work conducted by CF, ML, TI, and SB. CF and TI conceived the study with assistance from SB. ML, TI, and CF were responsible for data collection. ML was responsible for data analyses, with assistance from CF. ML and CF were responsible for data

interpretation, with assistance from TI. CF wrote and revised the manuscript in consultation with SB.

## 1.7 - REFERENCES

1. Ma, V. Y., Chan, L. & Carruthers, K. J. Incidence, prevalence, costs, and impact on disability of common conditions requiring rehabilitation in the United States: stroke, spinal cord injury, traumatic brain injury, multiple sclerosis, osteoarthritis, rheumatoid arthritis, limb loss, and back pain. *Arch. Phys. Med. Rehabil.* **95**, 986-995.e1 (2014).
2. Lawrence, E. S. *et al.* Estimates of the Prevalence of Acute Stroke Impairments and Disability in a Multiethnic Population. *Stroke* (2001).
3. Feigin, V. L. *et al.* Global and regional burden of stroke during 1990-2010: findings from the Global Burden of Disease Study 2010. *Lancet Lond. Engl.* **383**, 245–254 (2014).
4. Adamson, J., Beswick, A. & Ebrahim, S. Is stroke the most common cause of disability? *J. Stroke Cerebrovasc. Dis. Off. J. Natl. Stroke Assoc.* **13**, 171–177 (2004).
5. 2019 Report on Heart, Stroke and Vascular Cognitive Impairment. (2019).
6. Winstein, C. J. *et al.* Guidelines for Adult Stroke Rehabilitation and Recovery: A Guideline for Healthcare Professionals From the American Heart Association/American Stroke Association. *Stroke* **47**, e98–e169 (2016).
7. French, B. *et al.* Repetitive task training for improving functional ability after stroke. *Cochrane Database Syst. Rev.* **11**, CD006073 (2016).
8. Conroy, B. E., DeJong, G. & Horn, S. D. Hospital-Based Stroke Rehabilitation in the United States. *Top. Stroke Rehabil.* **16**, 34–43 (2009).
9. Buntin, M. B. Access to Postacute Rehabilitation. *Arch. Phys. Med. Rehabil.* **88**, 1488–1493 (2007).
10. NCHS Data Brief No. 95, May 2012. 8 (2012).

11. Hong, I. *et al.* Comparison of Functional Status Improvements Among Patients With Stroke Receiving Postacute Care in Inpatient Rehabilitation vs Skilled Nursing Facilities. *JAMA Netw. Open* **2**, e1916646–e1916646 (2019).
12. Institute for Clinical Evaluative Services. Ontario Stroke Evaluation Report 2012.
13. Bernhardt Julie, Dewey Helen, Thrift Amanda, & Donnan Geoffrey. Inactive and Alone. *Stroke* **35**, 1005–1009 (2004).
14. UK Sentinel Stroke National Audit Programme (SSNAP), July-Sept 2015 report.
15. Joint Stroke Strategy Working Group. Towards an Integrated Stroke Strategy for Ontario: Report. (2000).
16. Ayala, C. *et al.* Use of Outpatient Rehabilitation Among Adult Stroke Survivors — 20 States and the District of Columbia, 2013, and Four States, 2015. *Morb. Mortal. Wkly. Rep.* **67**, 575–578 (2018).
17. Passalent, L. A., Landry, M. D. & Cott, C. A. Wait Times for Publicly Funded Outpatient and Community Physiotherapy and Occupational Therapy Services: Implications for the Increasing Number of Persons with Chronic Conditions in Ontario, Canada. *Physiother. Can.* **61**, 5–14 (2009).
18. Jia, H., Cowper, D. C., Tang, Y., Litt, E. & Wilson, L. Postacute stroke rehabilitation utilization: are there differences between rural-urban patients and taxonomies? *J. Rural Health Off. J. Am. Rural Health Assoc. Natl. Rural Health Care Assoc.* **28**, 242–247 (2012).
19. Bellinger, J. D. *et al.* Post-discharge Rehabilitation Care Delivery for Rural Medicare Beneficiaries with Stroke. *S. C. Rural Health Res. Cent.*
20. Teasell, R., Meyer, M. J., Foley, N., Salter, K. & Willems, D. Stroke Rehabilitation in Canada: A Work in Progress. *Top. Stroke Rehabil.* **16**, 11–19 (2009).

21. Miller, K. K., Porter, R. E., DeBaun-Sprague, E., Van Puymbroeck, M. & Schmid, A. A. Exercise after Stroke: Patient Adherence and Beliefs after Discharge from Rehabilitation. *Top. Stroke Rehabil.* **24**, 142–148 (2017).
22. A, H., Rh, N., Ac, G. & G, K. Functional recovery of the paretic upper limb after stroke: who regains hand capacity? *Archives of physical medicine and rehabilitation* vol. 94 <https://pubmed.ncbi.nlm.nih.gov/23201317/> (2013).
23. The proportional recovery rule for stroke revisited - Krakauer - 2015 - *Annals of Neurology* - Wiley Online Library. <https://onlinelibrary.wiley.com/doi/abs/10.1002/ana.24537>.
24. Ovbiagele, B. *et al.* Forecasting the Future of Stroke in the United States: A Policy Statement From the American Heart Association and American Stroke Association. *Stroke* **44**, 2361–2375 (2013).
25. Rising Stroke Incidence in Young Adults: More Epidemiological Evidence, More Questions to Be Answered | Journal of the American Heart Association. <https://www.ahajournals.org/doi/full/10.1161/jaha.116.003661>.
26. Jeffers, M. S. *et al.* Does Stroke Rehabilitation Really Matter? Part B: An Algorithm for Prescribing an Effective Intensity of Rehabilitation. *Neurorehabil. Neural Repair* **32**, 73–83 (2018).
27. Stinear, C. M., Byblow, W. D., Ackerley, S. J., Barber, P. A. & Smith, M.-C. Predicting Recovery Potential for Individual Stroke Patients Increases Rehabilitation Efficiency. *Stroke* **48**, 1011–1019 (2017).
28. Lisboa, P. J. & Taktak, A. F. G. The use of artificial neural networks in decision support in cancer: A systematic review. *Neural Netw.* **19**, 408–415 (2006).

29. Doyle, K. P., Simon, R. P. & Stenzel-Poore, M. P. Mechanisms of ischemic brain damage. *Neuropharmacology* **55**, 310–318 (2008).
30. Hinman, J. D. The back and forth of axonal injury and repair after stroke. *Curr. Opin. Neurol.* **27**, 615–623 (2014).
31. Baron, J.-C., Yamauchi, H., Fujioka, M. & Endres, M. Selective Neuronal Loss in Ischemic Stroke and Cerebrovascular Disease. *J. Cereb. Blood Flow Metab.* **34**, 2–18 (2014).
32. Heiss, W.-D. The ischemic penumbra: how does tissue injury evolve? *Ann. N. Y. Acad. Sci.* **1268**, 26–34 (2012).
33. Frontiers | A Review of Transcranial Magnetic Stimulation and Multimodal Neuroimaging to Characterize Post-Stroke Neuroplasticity | Neurology.  
<https://www.frontiersin.org/articles/10.3389/fneur.2015.00226/full>.
34. Chapter 2 Comparative anatomy and physiology of the corticospinal system. - Abstract - Europe PMC. <https://europepmc.org/abstract/med/18808887>.
35. Nathan, P. W., Smith, M. C. & Deacon, P. THE CORTICOSPINAL TRACTS IN MANCOURSE AND LOCATION OF FIBRES AT DIFFERENT SEGMENTAL LEVELS. *Brain* **113**, 303–324 (1990).
36. Rizzolatti, G. & Luppino, G. The Cortical Motor System. *Neuron* **31**, 889–901 (2001).
37. Kaas, J. H. Evolution of somatosensory and motor cortex in primates. *Anat. Rec. A. Discov. Mol. Cell. Evol. Biol.* **281A**, 1148–1156 (2004).
38. Ferbert, A. *et al.* Interhemispheric inhibition of the human motor cortex. *J. Physiol.* **453**, 525–546 (1992).
39. Murase, N., Duque, J., Mazzocchio, R. & Cohen, L. G. Influence of interhemispheric interactions on motor function in chronic stroke. *Ann. Neurol.* **55**, 400–409 (2004).

40. Bütefisch, C. M., Weßling, M., Netz, J., Seitz, R. J. & Hömberg, V. Relationship Between Interhemispheric Inhibition and Motor Cortex Excitability in Subacute Stroke Patients. *Neurorehabil. Neural Repair* **22**, 4–21 (2008).
41. Stinear, C. M., Petoe, M. A. & Byblow, W. D. Primary Motor Cortex Excitability During Recovery After Stroke: Implications for Neuromodulation. *Brain Stimulat.* **8**, 1183–1190 (2015).
42. Phillips, L. L., Chan, J. L., Doperalski, A. E. & Reeves, T. M. Time dependent integration of matrix metalloproteinases and their targeted substrates directs axonal sprouting and synaptogenesis following central nervous system injury. *Neural Regen. Res.* **9**, 362–376 (2014).
43. Plautz, E. J. *et al.* Post-infarct cortical plasticity and behavioral recovery using concurrent cortical stimulation and rehabilitative training: A feasibility study in primates. *Neurol. Res.* **25**, 801–810 (2003).
44. Allred, R. P., Kim, S. Y. & Jones, T. A. Use it and/or lose it—experience effects on brain remodeling across time after stroke. *Front. Hum. Neurosci.* **8**, (2014).
45. Hermann, D. M., Buga, A.-M. & Popa-Wagner, A. Neurovascular remodeling in the aged ischemic brain. *J. Neural Transm.* **122**, 25–33 (2015).
46. Allred, R. P., Maldonado, M. A., Hsu and, J. E. & Jones, T. A. Training the “less-affected” forelimb after unilateral cortical infarcts interferes with functional recovery of the impaired forelimb in rats. *Restor. Neurol. Neurosci.* **23**, 297–302 (2005).
47. Mascaro, A. L. A. *et al.* In vivo single branch axotomy induces GAP-43–dependent sprouting and synaptic remodeling in cerebellar cortex. *Proc. Natl. Acad. Sci.* **110**, 10824–10829 (2013).

48. Perederiy, J. V. & Westbrook, G. L. Structural plasticity in the dentate gyrus- revisiting a classic injury model. *Front. Neural Circuits* **7**, (2013).
49. Overman, J. J. *et al.* A role for ephrin-A5 in axonal sprouting, recovery, and activity-dependent plasticity after stroke. *Proc. Natl. Acad. Sci.* **109**, E2230–E2239 (2012).
50. Li, S. *et al.* GDF10 is a signal for axonal sprouting and functional recovery after stroke. *Nat. Neurosci.* **18**, 1737–1745 (2015).
51. Cramer, S. C. & Riley, J. D. Neuroplasticity and brain repair after stroke. *Curr. Opin. Neurol.* **21**, 76–82 (2008).
52. Byblow, W. D., Stinear, C. M., Barber, P. A., Petoe, M. A. & Ackerley, S. J. Proportional recovery after stroke depends on corticomotor integrity. *Ann. Neurol.* **78**, 848–859 (2015).
53. Bonkhoff, A. K. *et al.* Bringing proportional recovery into proportion: Bayesian modelling of post-stroke motor impairment. *Brain* **143**, 2189–2206 (2020).
54. Hope, T. M. H. *et al.* Recovery after stroke: not so proportional after all? *Brain J. Neurol.* **142**, 15–22 (2019).
55. MacLellan, C. L. *et al.* A critical threshold of rehabilitation involving brain-derived neurotrophic factor is required for poststroke recovery. *Neurorehabil. Neural Repair* **25**, 740–748 (2011).
56. Sun, J. *et al.* Gradually Increased Training Intensity Benefits Rehabilitation Outcome after Stroke by BDNF Upregulation and Stress Suppression. *BioMed Research International* vol. 2014 e925762 <https://www.hindawi.com/journals/bmri/2014/925762/> (2014).
57. Brain-Derived Neurotrophic Factor Contributes to Recovery of Skilled Reaching After Focal Ischemia in Rats | Stroke. <https://www.ahajournals.org/doi/full/10.1161/STROKEAHA.108.531806>.



58. Ishida, A. *et al.* Early constraint-induced movement therapy promotes functional recovery and neuronal plasticity in a subcortical hemorrhage model rat. *Behav. Brain Res.* **284**, 158–166 (2015).
59. Niimi, M. *et al.* Role of Brain-Derived Neurotrophic Factor in Beneficial Effects of Repetitive Transcranial Magnetic Stimulation for Upper Limb Hemiparesis after Stroke. *PLOS ONE* **11**, e0152241 (2016).
60. Zhang, Y. & Pardridge, W. M. Blood–brain barrier targeting of BDNF improves motor function in rats with middle cerebral artery occlusion. *Brain Res.* **1111**, 227–229 (2006).
61. Effect of Brain-Derived Neurotrophic Factor Treatment and Forced Arm Use on Functional Motor Recovery After Small Cortical Ischemia | Stroke.  
<https://www.ahajournals.org/doi/full/10.1161/01.STR.0000119754.85848.0D>.
62. Shiner, C. T. *et al.* BDNF Genotype Interacts with Motor Function to Influence Rehabilitation Responsiveness Poststroke. *Front. Neurol.* **7**, (2016).
63. Lohse Keith R., Lang Catherine E., & Boyd Lara A. Is More Better? Using Metadata to Explore Dose–Response Relationships in Stroke Rehabilitation. *Stroke* **45**, 2053–2058 (2014).
64. Lang, C. E., Lohse, K. R. & Birkenmeier, R. L. Dose and timing in neurorehabilitation: Prescribing motor therapy after stroke. *Curr. Opin. Neurol.* **28**, 549–555 (2015).
65. Ward, N. S., Brander, F. & Kelly, K. Intensive upper limb neurorehabilitation in chronic stroke: outcomes from the Queen Square programme. *J. Neurol. Neurosurg. Psychiatry* **90**, 498–506 (2019).
66. Nudo, R. J. & Milliken, G. W. Reorganization of movement representations in primary motor cortex following focal ischemic infarcts in adult squirrel monkeys. *J. Neurophysiol.* **75**, 2144–2149 (1996).

67. Rehme, A. K. *et al.* Individual prediction of chronic motor outcome in the acute post-stroke stage: Behavioral parameters versus functional imaging. *Hum. Brain Mapp.* **36**, 4553–4565 (2015).
68. Quinlan, E. B. *et al.* Neural function, injury, and stroke subtype predict treatment gains after stroke. *Ann. Neurol.* **77**, 132–145 (2015).
69. Corticospinal tract lesion load: An imaging biomarker for stroke motor outcomes - Feng - 2015 - Annals of Neurology - Wiley Online Library.  
<https://onlinelibrary.wiley.com/doi/abs/10.1002/ana.24510>.
70. Lang, C. E. *et al.* Dose-response of task-specific upper limb training in people at least 6 months post stroke: A Phase II, single-blind, randomized, controlled trial. *Ann. Neurol.* **80**, 342–354 (2016).
71. Senesh, M. R. & Reinkensmeyer, D. J. Breaking Proportional Recovery After Stroke. *Neurorehabil. Neural Repair* **33**, 888–901 (2019).
72. Langhorne, P., Baylan, S., & Early Supported Discharge Trialists. Early supported discharge services for people with acute stroke. *Cochrane Database Syst. Rev.* **7**, CD000443 (2017).
73. Boyd, L. A. *et al.* Biomarkers of stroke recovery: Consensus-based core recommendations from the Stroke Recovery and Rehabilitation Roundtable. *Int. J. Stroke Off. J. Int. Stroke Soc.* **12**, 480–493 (2017).
74. Borschmann, K. *et al.* Rationale for Intervention and Dose Is Lacking in Stroke Recovery Trials: A Systematic Review. *Stroke Res. Treat.* **2018**, 8087372 (2018).

75. Stinear, C. M., Barber, P. A., Petoe, M., Anwar, S. & Byblow, W. D. The PREP algorithm predicts potential for upper limb recovery after stroke. *Brain J. Neurol.* **135**, 2527–2535 (2012).
76. Welniarz, Q., Dusart, I. & Roze, E. The corticospinal tract: Evolution, development, and human disorders: Corticospinal Tract Human Disorders. *Dev. Neurobiol.* **77**, 810–829 (2017).
77. Tang, Q. *et al.* Modulation of interhemispheric activation balance in motor-related areas of stroke patients with motor recovery: Systematic review and meta-analysis of fMRI studies. *Neurosci. Biobehav. Rev.* **57**, 392–400 (2015).
78. Rehme, A. K., Eickhoff, S. B., Rottschy, C., Fink, G. R. & Grefkes, C. Activation likelihood estimation meta-analysis of motor-related neural activity after stroke. *NeuroImage* **59**, 2771–2782 (2012).
79. Activation of Cortical and Cerebellar Motor Areas during Executed and Imagined Hand Movements: An fMRI Study | Journal of Cognitive Neuroscience | MIT Press Journals. <https://www.mitpressjournals.org/doi/abs/10.1162/089892999563553>.
80. Holper, L., Biallas, M. & Wolf, M. Task complexity relates to activation of cortical motor areas during uni- and bimanual performance: A functional NIRS study. *NeuroImage* **46**, 1105–1113 (2009).
81. McFarland, D. J., Miner, L. A., Vaughan, T. M. & Wolpaw, J. R. Mu and Beta Rhythm Topographies During Motor Imagery and Actual Movements. *Brain Topogr.* **12**, 177–186 (2000).
82. Stippich, C. *et al.* Motor, somatosensory and auditory cortex localization by fMRI and MEG. *NeuroReport* **9**, 1953 (1998).

83. Nhan, H. *et al.* Brain Function Early after Stroke in Relation to Subsequent Recovery. *J. Cereb. Blood Flow Metab.* **24**, 756–763 (2004).
84. Daly, J. J., Hrovat, K., Holcomb, J. & Pundik, S. Brain control of functional reach in healthy adults and stroke survivors. *Restor. Neurol. Neurosci.* **32**, 559–573 (2014).
85. Marshall, R. S. *et al.* Evolution of Cortical Activation During Recovery From Corticospinal Tract Infarction. *Stroke* **31**, 656–661 (2000).
86. The relationship between motor deficit and primary motor cortex hemispheric activation balance after stroke: longitudinal fMRI study | Journal of Neurology, Neurosurgery & Psychiatry. <https://jnnp.bmj.com/content/81/7/788.short>.
87. Tombari, D. *et al.* A longitudinal fMRI study: in recovering and then in clinically stable sub-cortical stroke patients. *NeuroImage* **23**, 827–839 (2004).
88. Takeda, K. *et al.* Shift of motor activation areas during recovery from hemiparesis after cerebral infarction: A longitudinal study with near-infrared spectroscopy. *Neurosci. Res.* **59**, 136–144 (2007).
89. Carey, J. R. *et al.* Analysis of fMRI and finger tracking training in subjects with chronic stroke. *Brain* **125**, 773–788 (2002).
90. Young, B. M. *et al.* Changes in functional brain organization and behavioral correlations after rehabilitative therapy using a brain-computer interface. *Front. Neuroengineering* **7**, (2014).
91. Plasticity in the Injured Brain: More than Molecules Matter - Justine J. Overman, S. Thomas Carmichael, 2014. <https://journals.sagepub.com/doi/abs/10.1177/1073858413491146>.

92. Hu, J. *et al.* Constrained-induced movement therapy promotes motor function recovery by enhancing the remodeling of ipsilesional corticospinal tract in rats after stroke. *Brain Res.* **1708**, 27–35 (2019).
93. Jones, T. A. *et al.* Remodeling the Brain With Behavioral Experience After Stroke. *Stroke* **40**, S136–S138 (2009).
94. Allred, R. P., Cappellini, C. H. & Jones, T. A. The “good” limb makes the “bad” limb worse: Experience-dependent interhemispheric disruption of functional outcome after cortical infarcts in rats. *Behav. Neurosci.* **124**, 124–132 (2010).
95. Allred, R. P. & Jones, T. A. Maladaptive effects of learning with the less-affected forelimb after focal cortical infarcts in rats. *Exp. Neurol.* **210**, 172–181 (2008).
96. Nowak, D. A., Grefkes, C., Ameli, M. & Fink, G. R. Interhemispheric Competition After Stroke: Brain Stimulation to Enhance Recovery of Function of the Affected Hand. *Neurorehabil. Neural Repair* **23**, 641–656 (2009).
97. Turton, A., Wroe, S., Trepte, N., Fraser, C. & Lemon, R. N. Contralateral and ipsilateral EMG responses to transcranial magnetic stimulation during recovery of arm and hand function after stroke. *Electroencephalogr. Clin. Neurophysiol. Mot. Control* **101**, 316–328 (1996).
98. Feydy, A. *et al.* Longitudinal Study of Motor Recovery After Stroke: Recruitment and Focusing of Brain Activation. *Stroke* **33**, 1610–1617 (2002).
99. Johansen-Berg, H. *et al.* The role of ipsilateral premotor cortex in hand movement after stroke. *Proc. Natl. Acad. Sci.* **99**, 14518–14523 (2002).
100. Loubinoux, I. *et al.* Correlation between cerebral reorganization and motor recovery after subcortical infarcts. *NeuroImage* **20**, 2166–2180 (2003).

101. Christensen, H. *et al.* Neuroimaging in Stroke Recovery: A Position Paper from the First International Workshop on Neuroimaging and Stroke Recovery. *Cerebrovasc. Dis.* **18**, 260–267 (2004).
102. Ward, N. S., Brown, M. M., Thompson, A. J. & Frackowiak, R. S. J. Neural correlates of motor recovery after stroke: a longitudinal fMRI study. *Brain* **126**, 2476–2496 (2003).
103. Hübers, A., Orekhov, Y. & Ziemann, U. Interhemispheric motor inhibition: its role in controlling electromyographic mirror activity. *Eur. J. Neurosci.* **28**, 364–371 (2008).
104. Beaulé, V., Tremblay, S. & Théoret, H. Interhemispheric Control of Unilateral Movement. *Neural Plast.* **2012**, 1–11 (2012).
105. Meyer, B.-U., Rörich, S., von Einsiedel, H. G., Kruggel, F. & Weindl, A. Inhibitory and excitatory interhemispheric transfers between motor cortical areas in normal humans and patients with abnormalities of the corpus callosum. *Brain* **118**, 429–440 (1995).
106. Di Lazzaro, V. *et al.* Direct demonstration of interhemispheric inhibition of the human motor cortex produced by transcranial magnetic stimulation. *Exp. Brain Res.* **124**, 520–524 (1999).
107. Inhibitory influence of the ipsilateral motor cortex on responses to stimulation of the human cortex and pyramidal tract - Gerloff - 1998 - The Journal of Physiology - Wiley Online Library. <https://physoc.onlinelibrary.wiley.com/doi/full/10.1111/j.1469-7793.1998.249bz.x>.
108. Frontiers | Role of the Contralesional Hemisphere in Post-Stroke Recovery of Upper Extremity Motor Function | Neurology. <https://www.frontiersin.org/articles/10.3389/fneur.2015.00214/full>.
109. Chollet, F. *et al.* The functional anatomy of motor recovery after stroke in humans: A study with positron emission tomography. *Ann. Neurol.* **29**, 63–71 (1991).

110. Shimizu, T. *et al.* Motor cortical disinhibition in the unaffected hemisphere after unilateral cortical stroke. *Brain* **125**, 1896–1907 (2002).
111. Bütefisch, C. M., Netz, J., Weßling, M., Seitz, R. J. & Hömberg, V. Remote changes in cortical excitability after stroke. *Brain* **126**, 470–481 (2003).
112. Rethinking interhemispheric imbalance as a target for stroke neurorehabilitation - Xu - 2019 - *Annals of Neurology* - Wiley Online Library.  
<https://onlinelibrary.wiley.com/doi/abs/10.1002/ana.25452>.
113. Schaechter, J. D. & Perdue, K. L. Enhanced Cortical Activation in the Contralesional Hemisphere of Chronic Stroke Patients in Response to Motor Skill Challenge. *Cereb. Cortex* **18**, 638–647 (2008).
114. Bütefisch, C. M. *et al.* Recruitment of contralesional motor cortex in stroke patients with recovery of hand function. *Neurology* **64**, 1067–1069 (2005).
115. Lotze, M. *et al.* The Role of Multiple Contralesional Motor Areas for Complex Hand Movements after Internal Capsular Lesion. *J. Neurosci.* **26**, 6096–6102 (2006).
116. Riecker, A. *et al.* The role of the unaffected hemisphere in motor recovery after stroke. *Hum. Brain Mapp.* **31**, 1017–1029 (2010).
117. The Effect of Lesion Size on the Organization of the Ipsilesional and Contralesional Motor Cortex - Boris Touvykine, Babak K. Mansoori, Loyda Jean-Charles, Joan Deffeyes, Stephan Quessy, Numa Dancause, 2016.  
<https://journals.sagepub.com/doi/abs/10.1177/1545968315585356>.
118. Schaechter, J. D. *et al.* Motor Recovery and Cortical Reorganization after Constraint-Induced Movement Therapy in Stroke Patients: A Preliminary Study. *Neurorehabil. Neural Repair* **16**, 326–338 (2002).

119. Park, W., Kwon, G. H., Kim, Y.-H., Lee, J.-H. & Kim, L. EEG response varies with lesion location in patients with chronic stroke. *J. NeuroEngineering Rehabil.* **13**, 21 (2016).
120. Prognostic Value of fMRI in Recovery of Hand Function in Subcortical Stroke Patients | Cerebral Cortex | Oxford Academic.  
<https://academic.oup.com/cercor/article/17/12/2980/383649>.
121. Individual prediction of chronic motor outcome in the acute post-stroke stage: Behavioral parameters versus functional imaging - Rehme - 2015 - Human Brain Mapping - Wiley Online Library. <https://onlinelibrary.wiley.com/doi/abs/10.1002/hbm.22936>.
122. Cho, S.-H. *et al.* Cortical activation changes induced by visual biofeedback tracking training in chronic stroke patients. *NeuroRehabilitation* **22**, 77–84 (2007).
123. Kim, Y. H. & Jang, S. H. Longitudinal fMRI study for locomotor recovery in patients with stroke. *Neurology* **67**,.
124. Miyai, I. *et al.* Longitudinal Optical Imaging Study for Locomotor Recovery After Stroke. *Stroke* **34**, 2866–2870 (2003).
125. Miyai, I., Suzuki, M., Hatakenaka, M. & Kubota, K. Effect of body weight support on cortical activation during gait in patients with stroke. *Exp. Brain Res.* **169**, 85–91 (2006).
126. Carter, A. R. *et al.* Resting Inter-hemispheric fMRI Connectivity Predicts Performance after Stroke. *Ann. Neurol.* **67**, 365–375 (2010).
127. Baldassarre, A. *et al.* Dissociated functional connectivity profiles for motor and attention deficits in acute right-hemisphere stroke. *Brain* **139**, 2024–2038 (2016).
128. Upstream Dysfunction of Somatomotor Functional Connectivity After Corticospinal Damage in Stroke - Alex R. Carter, Kevin R. Patel, Serguei V. Astafiev, Abraham Z. Snyder, Jennifer Rengachary, Michael J. Strube, Anna Pope, Joshua S. Shimony, Catherine E. Lang,



Gordon L. Shulman, Maurizio Corbetta, 2012.

<https://journals.sagepub.com/doi/abs/10.1177/1545968311411054>.

129. Chen, J. L. & Schlaug, G. Resting State Interhemispheric Motor Connectivity and White Matter Integrity Correlate with Motor Impairment in Chronic Stroke. *Front. Neurol.* **4**, (2013).
130. Resting-State Functional Connectivity and Its Association With Multiple Domains of Upper-Extremity Function in Chronic Stroke - M. A. Urbin, Xin Hong, Catherine E. Lang, Alex R. Carter, 2014. <https://journals.sagepub.com/doi/abs/10.1177/1545968314522349>.
131. Westlake, K. P. & Nagarajan, S. S. Functional Connectivity in Relation to Motor Performance and Recovery After Stroke. *Front. Syst. Neurosci.* **5**, (2011).
132. Golestani, A.-M., Tymchuk, S., Demchuk, A. & Goodyear, B. G. Longitudinal Evaluation of Resting-State fMRI After Acute Stroke With Hemiparesis. *Neurorehabil. Neural Repair* **27**, 153–163 (2013).
133. Contribution of the Resting-State Functional Connectivity of the Contralesional Primary Sensorimotor Cortex to Motor Recovery after Subcortical Stroke. <https://journals.plos.org/plosone/article?id=10.1371/journal.pone.0084729>.
134. The plasticity of intrinsic functional connectivity patterns associated with rehabilitation intervention in chronic stroke patients | SpringerLink. <https://link.springer.com/article/10.1007/s00234-016-1647-4>.
135. Fan, Y. *et al.* Neuroplastic changes in resting-state functional connectivity after stroke rehabilitation. *Front. Hum. Neurosci.* **9**, (2015).
136. Predicting efficacy of robot-aided rehabilitation in chronic stroke patients using an MRI-compatible robotic device - IEEE Conference Publication. <https://ieeexplore.ieee.org/abstract/document/6091843>.

137. Ueda, R., Yamada, N., Abo, M., Ruwan, P. W. & Senoo, A. MRI evaluation of motor function recovery by rTMS and intensive occupational therapy and changes in the activity of motor cortex. *Int. J. Neurosci.* **130**, 309–317 (2020).
138. Different Brain Connectivity between Responders and Nonresponders to Dual-Mode Noninvasive Brain Stimulation over Bilateral Primary Motor Cortices in Stroke Patients. <https://www.hindawi.com/journals/np/2019/3826495/>.
139. Dong Yun, Dobkin Bruce H., Cen Steven Y., Wu Allan D., & Winstein Carolee J. Motor Cortex Activation During Treatment May Predict Therapeutic Gains in Paretic Hand Function After Stroke. *Stroke* **37**, 1552–1555 (2006).
140. Várkuti, B. *et al.* Resting State Changes in Functional Connectivity Correlate With Movement Recovery for BCI and Robot-Assisted Upper-Extremity Training After Stroke. *Neurorehabil. Neural Repair* **27**, 53–62 (2013).
141. Lam, T. K. *et al.* Variability in stroke motor outcome is explained by structural and functional integrity of the motor system. *Sci. Rep.* **8**, 9480 (2018).
142. No evidence for motor recovery-related cortical reorganization after stroke using resting-state fMRI | bioRxiv. <https://www.biorxiv.org/content/10.1101/681320v1.abstract>.
143. Carter, A. R. *et al.* Upstream dysfunction of somatomotor functional connectivity after corticospinal damage in stroke. *Neurorehabil. Neural Repair* **26**, 7–19 (2012).
144. Arun, K. M., Smitha, K. A., Sylaja, P. N. & Kesavadas, C. Identifying Resting-State Functional Connectivity Changes in the Motor Cortex Using fNIRS During Recovery from Stroke. *Brain Topogr.* (2020) doi:10.1007/s10548-020-00785-2.
145. Dubovik, S. *et al.* EEG Alpha Band Synchrony Predicts Cognitive and Motor Performance in Patients with Ischemic Stroke. *Behav. Neurol.* **26**, 187–189 (2013).

146. Increasing Patient Engagement in Rehabilitation Exercises Using Computer-Based Citizen Science. <https://journals.plos.org/plosone/article?id=10.1371/journal.pone.0117013>.
147. Johnson, K. A. *et al.* Intermittent “Real-time” fMRI Feedback Is Superior to Continuous Presentation for a Motor Imagery Task: A Pilot Study. *J. Neuroimaging* **22**, 58–66 (2012).
148. Hellrung, L. *et al.* Intermittent compared to continuous real-time fMRI neurofeedback boosts control over amygdala activation. *NeuroImage* **166**, 198–208 (2018).
149. Emmert, K. *et al.* Continuous vs. intermittent neurofeedback to regulate auditory cortex activity of tinnitus patients using real-time fMRI - A pilot study. *NeuroImage Clin.* **14**, 97–104 (2017).
150. Sitaram, R. *et al.* Closed-loop brain training: the science of neurofeedback. *Nat. Rev. Neurosci.* **18**, 86–100 (2017).
151. Kober, S. E. *et al.* Near-infrared spectroscopy based neurofeedback training increases specific motor imagery related cortical activation compared to sham feedback. *Biol. Psychol.* **95**, 21–30 (2014).
152. Mihara, M. *et al.* Neurofeedback Using Real-Time Near-Infrared Spectroscopy Enhances Motor Imagery Related Cortical Activation. *PLOS ONE* **7**, e32234 (2012).
153. Boe, S. *et al.* Laterality of brain activity during motor imagery is modulated by the provision of source level neurofeedback. *NeuroImage* **101**, 159–167 (2014).
154. Mihara, M. *et al.* Near-infrared Spectroscopy-mediated Neurofeedback Enhances Efficacy of Motor Imagery-based Training in Poststroke Victims. *Stroke* (2013).
155. Pichiorri, F. *et al.* Brain-computer interface boosts motor imagery practice during stroke recovery. *Ann. Neurol.* **77**, 851–865 (2015).

156. Rieke, J. D. *et al.* Development of a combined, sequential real-time fMRI and fNIRS neurofeedback system to enhance motor learning after stroke. *J. Neurosci. Methods* **341**, 108719 (2020).
157. Tsuchimoto, S. *et al.* Sensorimotor Connectivity after Motor Exercise with Neurofeedback in Post-Stroke Patients with Hemiplegia. *Neuroscience* **416**, 109–125 (2019).
158. Frolov, A. A. *et al.* Post-stroke Rehabilitation Training with a Motor-Imagery-Based Brain-Computer Interface (BCI)-Controlled Hand Exoskeleton: A Randomized Controlled Multicenter Trial. *Front. Neurosci.* **11**, (2017).
159. Bundy David T. *et al.* Contralesional Brain–Computer Interface Control of a Powered Exoskeleton for Motor Recovery in Chronic Stroke Survivors. *Stroke* **48**, 1908–1915 (2017).
160. Ono, Y. *et al.* Hand Motor Rehabilitation of Patients with Stroke Using Physiologically Congruent Neurofeedback. in *2018 IEEE International Conference on Systems, Man, and Cybernetics (SMC)* 39–44 (2018). doi:10.1109/SMC.2018.00016.
161. Ramos-Murguialday, A. *et al.* Brain–machine interface in chronic stroke rehabilitation: A controlled study. *Ann. Neurol.* **74**, 100–108 (2013).
162. 齊田和哉. Biofeedback Effect of Hybrid Assistive Limb in Stroke Rehabilitation: A Proof of Concept Study Using Functional Near Infrared Spectroscopy. (福岡大学, 2018).
163. Wada, K. *et al.* Development of a Brain-machine Interface for Stroke Rehabilitation Using Event-related Desynchronization and Proprioceptive Feedback. *Adv. Biomed. Eng.* **8**, 53–59 (2019).
164. Effects of Neurofeedback Training with an Electroencephalogram-Ba...: Ingenta Connect. <https://www.ingentaconnect.com/content/mjl/sreh/2011/00000043/00000010/art00012>.

165. A Randomized Controlled Trial of EEG-Based Motor Imagery Brain-Computer Interface Robotic Rehabilitation for Stroke - Kai Keng Ang, Karen Sui Geok Chua, Kok Soon Phua, Chuanchu Wang, Zheng Yang Chin, Christopher Wee Keong Kuah, Wilson Low, Cuntai Guan, 2015. <https://journals.sagepub.com/doi/10.1177/1550059414522229>.
166. Mottaz, A. *et al.* Modulating functional connectivity after stroke with neurofeedback: Effect on motor deficits in a controlled cross-over study. *NeuroImage Clin.* **20**, 336–346 (2018).
167. Newman, A. *Research methods for cognitive neuroscience.* (Sage, 2019).
168. Germon, T. J. *et al.* Sensitivity of Near Infrared Spectroscopy to Cerebral and Extra-Cerebral Oxygenation Changes is Determined by Emitter-Detector Separation. *J. Clin. Monit. Comput.* **14**, 353–360 (1998).
169. Sato, T. *et al.* Reduction of global interference of scalp-hemodynamics in functional near-infrared spectroscopy using short distance probes. *NeuroImage* **141**, 120–132 (2016).
170. Funane, T. *et al.* Quantitative evaluation of deep and shallow tissue layers' contribution to fNIRS signal using multi-distance optodes and independent component analysis. *NeuroImage* **85**, 150–165 (2014).
171. Brigadoi, S. & Cooper, R. J. How short is short? Optimum source–detector distance for short-separation channels in functional near-infrared spectroscopy. *Neurophotonics* **2**, 025005 (2015).
172. Funane, T. *et al.* Concurrent fNIRS-fMRI measurement to validate a method for separating deep and shallow fNIRS signals by using multidistance optodes. *Neurophotonics* **2**, 015003 (2015).

173. Pinti, P. *et al.* The present and future use of functional near-infrared spectroscopy (fNIRS) for cognitive neuroscience. *Ann. N. Y. Acad. Sci.* **0**,
174. Delpy, D. T. *et al.* Estimation of optical pathlength through tissue from direct time of flight measurement. *Phys. Med. Biol.* **33**, 1433–1442 (1988).
175. Scholkmann, F. *et al.* A review on continuous wave functional near-infrared spectroscopy and imaging instrumentation and methodology. *NeuroImage* **85**, 6–27 (2014).
176. Rossi, V. M. Digital Fourier Holographic Microscopy and Potential Applications Towards the Design of Photodynamic Therapy of Osteosarcoma.
177. Wijekumar, S., Huppert, T. J., Magnotta, V. A., Buss, A. T. & Spencer, J. P. Validating an image-based fNIRS approach with fMRI and a working memory task. *NeuroImage* **147**, 204–218 (2017).
178. Cui, X., Bray, S., Bryant, D. M., Glover, G. H. & Reiss, A. L. A quantitative comparison of NIRS and fMRI across multiple cognitive tasks. *NeuroImage* **54**, 2808–2821 (2011).
179. Thulborn, K. R., Chang, S. Y., Shen, G. X. & Voyvodic, J. T. High-resolution echo-planar fMRI of human visual cortex at 3.0 tesla. *NMR Biomed.* **10**, 183–190 (1997).
180. Combining energy and Laplacian regularization to accurately retrieve the depth of brain activity of diffuse optical tomographic data.  
<https://www.spiedigitallibrary.org/journals/journal-of-biomedical-optics/volume-21/issue-3/036008/Combining-energy-and-Laplacian-regularization-to-accurately-retrieve-the-depth/10.1117/1.JBO.21.3.036008.full>.
181. ‘Ergonomic’; adjective.

182. Ayaz, H. *et al.* Continuous monitoring of brain dynamics with functional near infrared spectroscopy as a tool for neuroergonomic research: empirical examples and a technological development. *Front. Hum. Neurosci.* **7**, (2013).
183. Gramann, K., Fairclough, S. H., Zander, T. O. & Ayaz, H. Editorial: Trends in Neuroergonomics. *Front. Hum. Neurosci.* **11**, (2017).
184. Krigolson, O. E., Williams, C. C., Norton, A., Hassall, C. D. & Colino, F. L. Choosing MUSE: Validation of a Low-Cost, Portable EEG System for ERP Research. *Front. Neurosci.* **11**, (2017).
185. Müller-Gerking, J., Pfurtscheller, G. & Flyvbjerg, H. Designing optimal spatial filters for single-trial EEG classification in a movement task. *Clin. Neurophysiol.* **110**, 787–798 (1999).
186. Michel, C. M. & Murray, M. M. Towards the utilization of EEG as a brain imaging tool. *NeuroImage* **61**, 371–385 (2012).
187. Malmivuo, J. Comparison of the Properties of EEG and MEG in Detecting the Electric Activity of the Brain. *Brain Topogr.* **25**, 1–19 (2012).
188. Estimating the spatial resolution of fNIRS sensors for BCI purposes.  
<https://www.spiedigitallibrary.org/conference-proceedings-of-spie/8945/894504/Estimating-the-spatial-resolution-of-fNIRS-sensors-for-BCI-purposes/10.1117/12.2037351.short?SSO=1>.

# Chapter 2 - AXEM HOME PROTOTYPE DATA QUALITY STUDY

## 2.0 ABSTRACT

This study's purpose was to determine whether preliminary wireless fNIRS prototypes were capable of taking neurophysiological measurements from the M1 during upper-extremity movements. First a convenience sample of 57 healthy adults ( $m = 43.9$ ,  $sd = 16.6$  years) were recruited to perform a simple upper-extremity motor task using Axem Neurotechnology's first prototype (AP-1); information on the head size, hair density and colour, as well as skin colour, were all recorded given their potential relevance to fNIRS signal quality. While analyses on the data obtained via AP-1 demonstrated the expected contra-lateralization of increased oxyhemoglobin, 8 participants were excluded due to the obvious unviability of the fNIRS measurements (i.e., raw data from the device's analog-digital converter was not above the noise floor<sup>1</sup>); and moreover, dynamic time warping (DTW) classification analysis indicated that fNIRS data collected from participants >50 years of age (who had less dense hair than their younger counterparts) was of lower quality than from their younger counterparts. These results motivated substantial improvements to AP-1, and data from a new prototype (AP-2) was then tested on 17 participants ( $m = 39.06$ ,  $sd = 13.1$  years). While a quantitative comparison between the data from AP-1 and AP-2 was not performed, aggregate data analysis from AP-2 demonstrated the expected contra-lateralization of increased oxyhemoglobin, with no participants excluded due to poor data quality; this together with a qualitative comparison of data collected with AP-1 and AP-2 on the same individuals (all of whom had dense hair), suggested the improvements made

---

<sup>1</sup> In this case specifically meaning there was no visible difference in the raw time series of ADC values being collected when comparing time periods when the device's emitters were shining light versus time periods when they were not.



from AP-1 and AP-2 had substantially improved its ability to measure M1 activity during an upper-extremity task.

## **2.1 INTRODUCTION**

### **2.1.1 Study Purpose and Design**

The purpose of this study was to examine the ability of an fNIRS prototype developed by Axem Neurotechnology to take neurophysiological measurements from M1 during a simple upper-extremity task in a group of healthy adults (ideally representing the population at large), with the study design allowing for iteration on the fNIRS prototypes used. Towards this end, an experimental paradigm employing both a left- and right-handed unilateral fist squeezing task was used, allowing the results to be evaluated with respect to their conformity to the expected pattern of increased  $\Delta\text{HbO}$  in the hemisphere contralateral to the limb used in each task. In addition, information on the hair density and colour, as well as skin colour of the participants was recorded, due to their potential relevance to the ability to take neurophysiological measurements from M1 via fNIRS (with denser hair, and darker hair and skin leading to more near-infrared light absorption, thus diminishing the amount of light being emitted through the scalp and eventually to be potentially measured by the detector)—specifically, recording these covariates of fNIRS signal quality allowed for post-hoc analyses on sub-segments of our recruited sample to be performed, to help further contextualize the performance of this fNIRS prototype and thus better understand the generalization of any findings to the population at large.

Moreover, the study protocol allowed for iteration to the fNIRS prototypes (i.e., the actual electrical/mechanical permutation of the prototype itself) as needed. However, in reality the first 57 participants completed the experimental protocol using Axem's first wireless fNIRS prototype (AP-1; described in section 2.2.2.1), while the subsequent 17 participants completed

the protocol using a distinct prototype (AP-2; described in section 2.2.2.2)—a prototype that was made in response to the specific shortcomings of AP-1 uncovered in the course of this study (discussed in section 2.3.1). Prior to the collection of these 17 participants using AP-2, the data quality between AP-1 and AP-2 was compared on individuals with dense hair who were easily available to Axem Neurotechnology (i.e., Axem Neurotechnology’s personnel) by visual inspection of fNIRS raw data as well as processed  $\Delta\text{HbO}$  following completion of the paradigm described in the present study. Following this, to further determine whether AP-2 was capable of obtaining a neurophysiological signal from M1, a sample of 17 subsequent participants were collected, at which point the COVID-19 pandemic halted data collection. The study was discontinued at this point, since it had not been intended to be a two-arm study and thus was deemed unnecessary to the study’s purpose to match the sample size collected with AP-1.

### **2.1.2 fNIRS Signal Quality Deconstructed**

At the most basic level, the ability for an fNIRS device to successfully measure a motor evoked signal is dependent on its ability to get sufficient light (specifically light of appropriate wavelengths, as discussed below and highlighted in item 4 of Figure 1) from its emitters through to the scalp, and the ability to bring a portion of this light that emerges back out of the scalp to its light-measuring optical components. However, this process can be further broken up into sub-components, which—while all interconnected—can be considered in isolation.

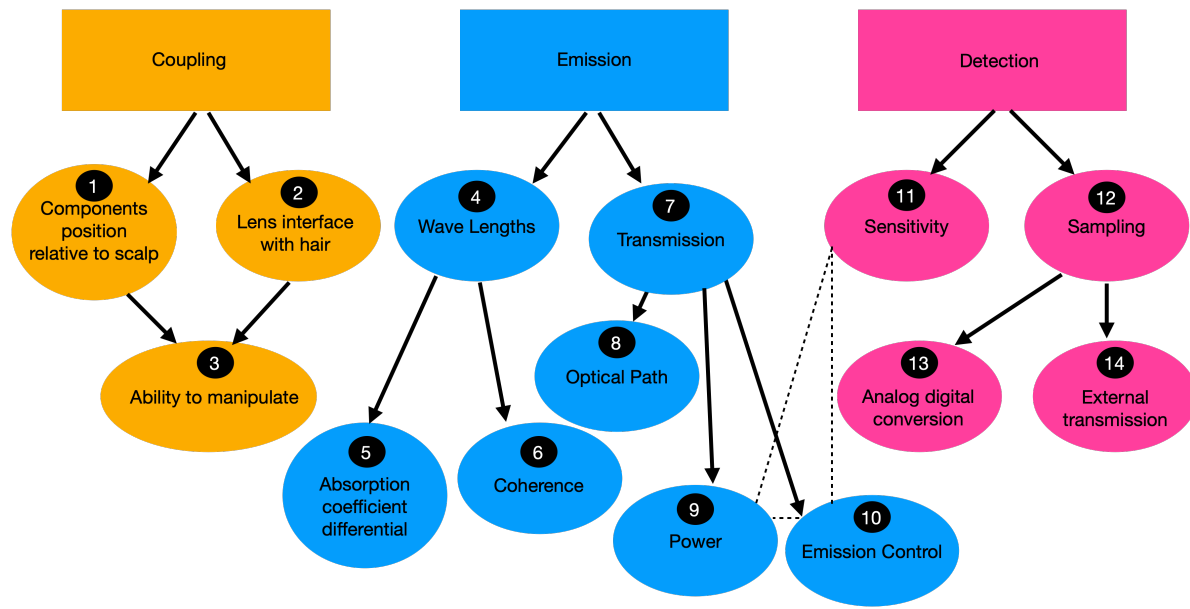


*Figure 2-1 – Schematic of the major aspects contributing to an fNIRS system’s ability to measure cerebral hemodynamics.*

The first, most basic pre-requisite, is that the device must enable all optical components to make sufficiently good contact with the participant’s scalp. This requires the device to be designed such that the optical components can be positioned with sufficient proximity to the scalp (Figure 2.1 item 1), and moreover, that whatever medium or mediums acting as light guides (both from the emitter to the scalp, and from the scalp to the detector) have an interface with any hair that may be present such that the hair does not block all the light from being transmitted to or from the scalp (Figure 2.1 item 2). One aspect related to both of these sub-components of gaining good contact between the optical components and the scalp is the ability for this interface (i.e., between the apparatus, its optical components, and the scalp) to be manually improved through manipulation—either by the user or a third party (Figure 2.1 item 3). The most common example of this is in the design of fNIRS systems designed for research, where the optodes are designed to be removable, whereupon a thin hair-combing tool is to be used to dislodge hairs that might otherwise obstruct the path of the light (see Figure 2.2).<sup>1</sup>

However this might also be accomplished without any disassembly, by designing the device such that the light transmitting components can be ‘worked through’ hair, by simply moving them in such a way that they are more likely to gain good coupling with the scalp, while the device is on the head, until the light transmission components are making better contact with the scalp; however, this requires the components responsible for light transmission to be neither rigid (to prevent discomfort or pain) nor fragile (to prevent damage to the system).

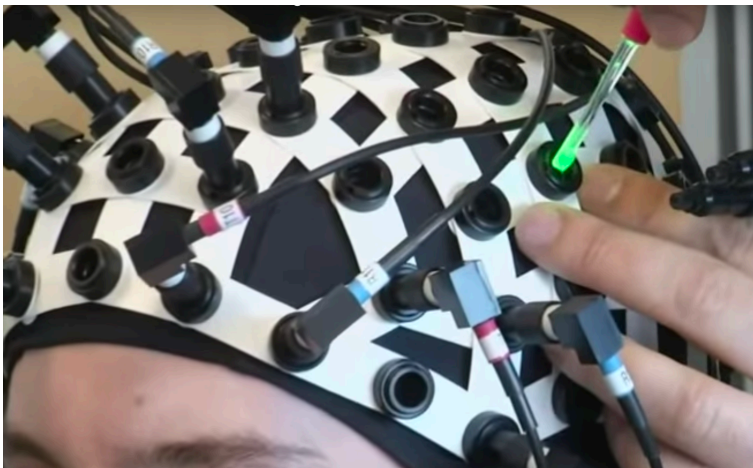


*Figure 2-2. Example of removable optode assembly that enables a third party to move hair away from the center of the optode assembly (in this case with a screwdriver tool).*

The particulars of light emission are another major component, which can itself be broken down to three sub-components: the wavelengths of emitted light (Figure 2.1 item 4), the transmission of the emitted light (Figure 2.1 item 7), and the control of the light emission (Figure 2.1 item 10). The two sub-components comprising the factor of emission wavelength are: what pair of wavelengths are being used for the modified Beer-Lambert calculation (Figure 2.1 item 5; with the larger the difference between each wavelength’s absorption coefficients for oxy- and deoxyhemoglobin the more sensitive the results will be to true changes in these chromophores; see Chapter 1 Figure 1.7 for an illustration of the absorption coefficients for both oxy- and deoxyhemoglobin), and the coherence of emission spectrum for these wavelengths (Figure 2.1

item 6), where the greater the coherence (i.e., a lack of variability in the emitted light across the frequency spectrum) the larger the signal-to-noise ratio will be.<sup>2</sup> Light transmission simply refers to the necessity of getting an appropriate amount of light going along an optical path whereby it will travel through the brain and then arrive at the light detector; too little light and the measurements will have too low a signal-to-noise ratio to detect hemodynamic changes; too much and the detector will become saturated, with the boundaries of ‘too little’ and ‘too much’ light being a function of detector sensitivity (Figure 2.1 item 11). The factor ‘light transmission’ depends on two sub-components: emission power (Figure 2.1 item 9) and optical path (Figure 2.1 item 8). Emission power referring to the number of photons being generated by light source; and connected to this aspect is the ability for the firmware of the fNIRS device to alter the level of emission at different times (e.g., less emission for bald individuals, and more emission for individuals with dense, long dark hair; see Figure 2.1 item 10); this dependency, together with the influence of detector sensitivity, is reflected in the dotted lines connecting items 9-11 in Figure 2.1. The optical path that describes the path those photons take is a function of both the light source and light guide used,<sup>3</sup> with the greatest performance coming from fully collimated light (i.e., from a source emitting a focused beam of parallel rays, as opposed to a divergent beam of scattered rays<sup>4</sup>, see Figure 2.3) being emitting tangential to the scalp.<sup>5</sup> The two different types of light sources used in fNIRS systems are lasers and LEDs.<sup>6</sup> While lasers emit more collimated light than LEDs,<sup>7</sup> the fact that lasers require significantly more support electronics (given that they require more power supply and temperature monitoring than LEDs<sup>7</sup>), means that fNIRS systems using lasers are not a suitable choice for ergonomic fNIRS systems.<sup>8,9</sup>

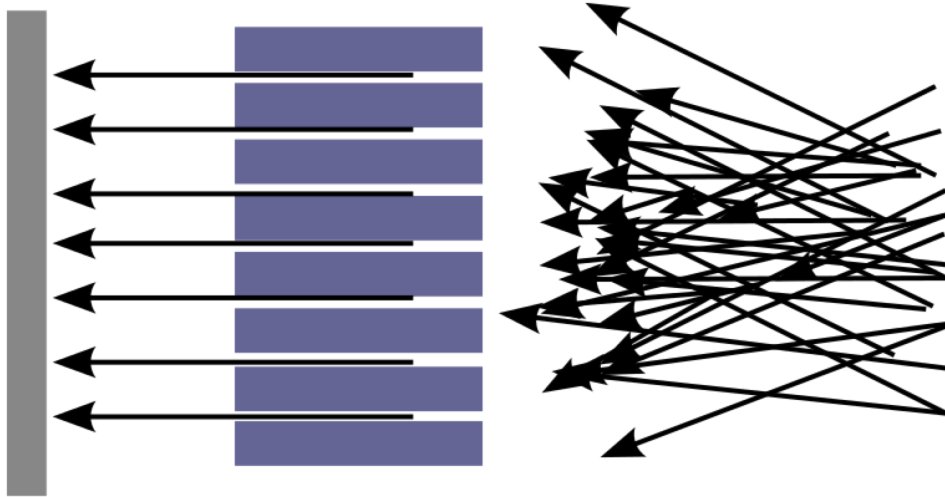


*Figure 2-3. Illustration of highly collimated light (left) contrasted with less collimated light (right).<sup>10</sup>*

The next major factor in determining the functionality of an fNIRS system is the specifics of how the system detects light. While it is true that the more sensitive the light detector used the lower the noise floor, and thus the greater potential ability of an fNIRS system to detect hemodynamic changes (Figure 2.1 item 11), as previously mentioned, it is also critical that the detector be calibrated to work with the amount of light provided by the emitter portion of the fNIRS system (hence the inclusion of item 11 in the relationship illustrated between items 9-11 in Figure 2.1). And finally, another sub-component of an fNIRS system's light detection is the ability of the system to take measurements from its light detectors—this relates to actual sampling itself, accomplished by the device's microprocessor accessing the system's analog-digital converter (Figure 2.1 item 13), their suitability for sampling from the light detectors used, as well as the method of transmitting these samples to an external device (e.g., a computer or phone; Figure 2.1 item 14).

The above factors all play a part in an fNIRS system's ability to detect changes in cortical hemodynamics, and thus provide a broad context through which to understand the current

study—the purpose of which is to determine the ability of preliminary fNIRS prototypes to take these measurements, in addition to iterating on these prototypes (with respect to these factors listed in Figure 2.1).

### **2.1.3 On the Suitability of Existing fNIRS Systems for Rehabilitation-based Brain-Computer-Interface (BCI)**

As discussed in the previous chapter (in section 1.3.4), all research using fNIRS for the purposes of rehabilitation BCI and/or measuring neural biomarkers of stroke were done with fNIRS systems designed for use in the laboratory, requiring a lengthy set-up to be carried out by a trained experimenter. Because the focus of this dissertation overall, and this study in particular, is the use and development of fNIRS technology (for reasons discussed in section 1.4.2 of the preceding chapter), this section will focus on evaluating existing fNIRS technology in its ability to be used in a scalable (i.e., widely deployed and easily repeatable) rehabilitation BCI. Specifically, the requirements of an fNIRS system for use in a scalable rehabilitation BCI are that it be (1) portable and easy to transport; (2) wireless, so that the user is not encumbered in how they might move while fNIRS measurements are being taken, and also so that it is able to be used in a wide variety of environments; (3) capable of taking measurements from the sensorimotor regions of the brain (see section 1.3 for a discussion of relevant functional neuroimaging biomarkers of physical recovery from stroke, all of which are derived from this region of the brain); and finally, while perhaps not a requirement, an fNIRS system aiming to be used in a scalable (stroke or neuro-) rehabilitation BCI application would also ideally (4) be capable of being set-up by the wearer of the fNIRS device themselves.

While the established fNIRS systems used in the research discussed in Chapter 1 are the ideal tools to use for taking fNIRS measurements from sensorimotor regions of the brain if all that is prioritized is signal quality, they are not portable, wireless, or capable of being set-up by

the individual on whom measurements are being taken; therefore, they are not ideal for scalable clinical use cases. However, recently several groups have developed fNIRS systems that seek to deliver novel value over and above the established laboratory-based fNIRS systems in the measurement of cerebral hemodynamics from regions surrounding M1. One study<sup>11</sup> designed a novel brush optode design (that was added onto an existing fNIRS system's optodes) whereby instead of using a single light guide, a bundle of several small flexible fibres (akin to the individual fibres of a brush) were used to transmit light through hair to the scalp. Despite providing better penetration through hair compared to the original manufacturers design, the fragility of the brush optodes compared to the use of a single light guide, as well as the need to have an experimenter carefully set up such a system (lest the wearer of the device manipulate the interface between the brush optodes and the scalp too roughly, causing damage to the brush optodes) mean that this concept is far from ready for implementation in a scalable fNIRS system.<sup>2</sup> Another recently developed system<sup>12</sup> provided high density measurements from the region surrounding M1, with relatively little setup required (i.e., no adjustment of the optodes were required by an experimenter)—however, this system was not portable or wireless, nor capable of being set up by the wearer of the device (still utilizing a form of headcap), and thus, while impressive, its value is not markedly differentiated from those of established fNIRS systems. Likewise, a novel system was previously shown to enable M1 measurement during an outdoor bike riding task;<sup>13</sup> and while this device is also impressive, it does not provide significant value over the NIRSport by NirX (<https://nirx.net/nirsport>), since both require experimenter set-up and for a full backpack (containing the power supply and control

---

<sup>2</sup> As an aside, and in the pursuit of full transparency, this study's design was replicated (as per the information provided in this publication) by Axem Neurotechnology in fNIRS prototypes developed prior to those presented herein, and the same performance through hair (compared with a single light guide design) was not replicated. Moreover these small fibers were found to be very fragile and thus difficult to use.



electronics) to be worn. And finally, another recent novel fNIRS system was designed to take M1 measurements in a portable form factor<sup>14</sup>—however, this system did not use wireless data transmission and thus was not fully wireless; and while the system did not use any fiber optic cable, it nevertheless required significant intervention by the experimenter—to both set up its strapping system affixing the device to the head, as well as to adjust the springs that were used to provide flexibility to its optodes (which enabled conformity to a variety of head sizes and shapes).

## 2.2 METHODS

### 2.2.1 Participants

Participants provided written informed consent to participate in this single-session, non-interventional study that was approved by the Ethics Review Board of the National Research Council of Canada. All participants were over 17 years of age and had not been diagnosed with any musculoskeletal conditions as determined via self-report.

For the first 57 participants, AP-1 was the fNIRS measurement device utilized, while for the subsequent 17 participants AP-2 was utilized (Table 2.1). Participants’ hair (length/density/curl/pigmentation) and skin (pigmentation) characteristics were rated by the experimenter on a 5 point scale; this rating was determined by the experimenter, utilizing the previous ratings as an anchor for their judgments to ensure relative consistency between measurements, a photograph of the top of the participants’ heads, as well as a close-up of their skin at the wrist area (see Figure 2.4 for example) were taken in order to enable more rigorous follow-up analyses if required.

*Table 2-1. Participant characteristics for the sessions conducted with AP-1 and AP-2 fNIRS systems.*

	<b>AP-1</b>	<b>AP-2</b>
--	-------------	-------------

	<b>M</b>	<b>SD</b>	<b>M</b>	<b>SD</b>
<b>Age</b>	43.92	16.6	39.06	13.1
<b>Head circumference</b>	57.56	2.12	57.83	2.4
<b>Nasion to inion</b>	34.39	1.9	34.69	2.3
<b>Tragus to tragus</b>	39.46	1.8	38.69	2.2
	<b>Male</b>	<b>Female</b>	<b>Male</b>	<b>Female</b>
<b>Sex</b>	33	24	12	6
	<b>Left</b>	<b>Right</b>	<b>Left</b>	<b>Right</b>
<b>Handedness</b>	5	52	2	16

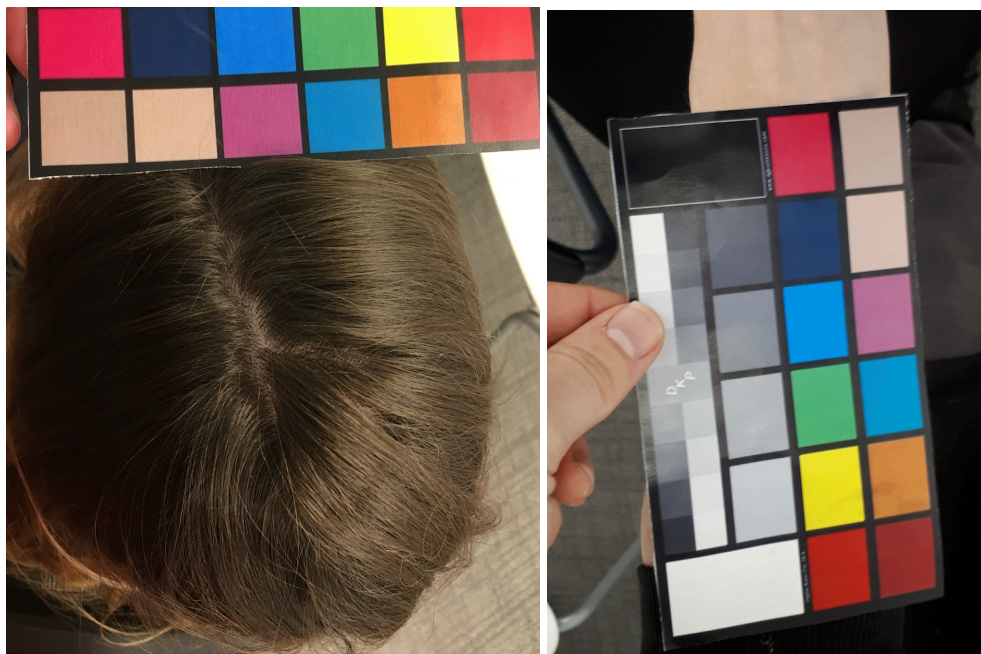


Figure 2-4. Example photographs taken in the study, used to then code characteristics of the participants hair and skin characteristics (a consistent colour scale was included in these photographs to allow for relative calibration to compensate for differences in photo quality, lighting etc.).

## **2.2.2 fNIRS Prototypes**

### *2.2.2.1 AP-1*

As illustrated in Figure 2.5, AP-1 is an fNIRS device consisting of two 2 x 3 measurement grids that overly (approximately) locations C3 and C4 of the international 10-20 system.<sup>15,16</sup>

These two by three measurement location grids each consist of two photodiodes, four emitters

positioned 3cm from one or two of these photodiodes, as well as two emitters positioned 8mm from each photodiode to capture and removal hemodynamic changes superficial to the cortex, as discussed in section 1.4.2 (see Figure 2.5).

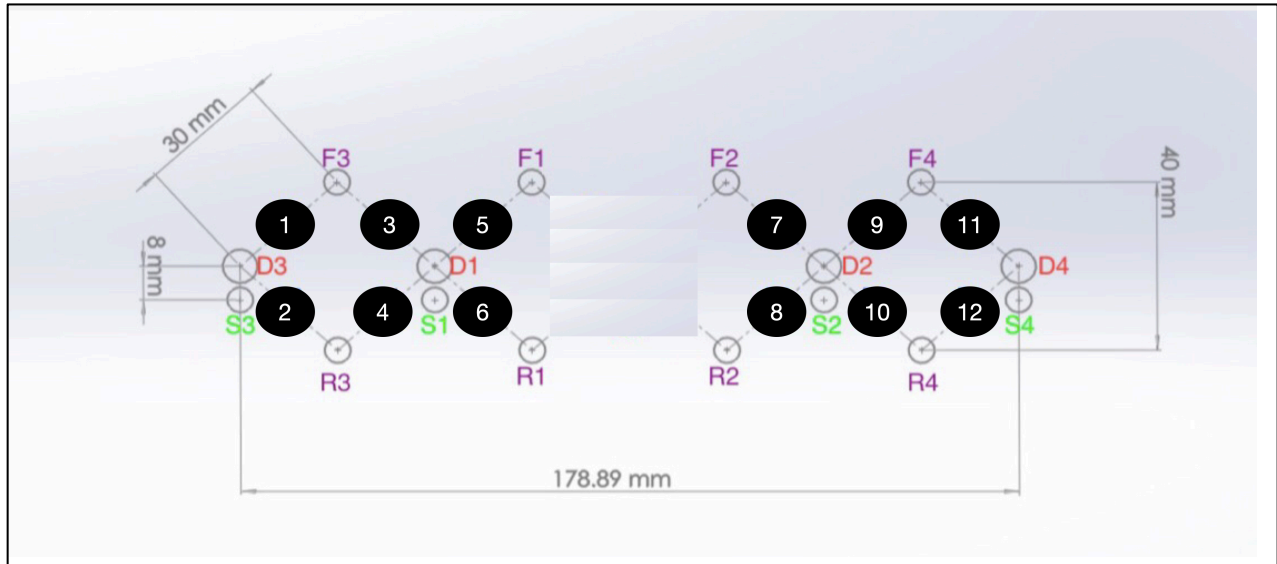


*Figure 2-5. Engineering schematic of the layout of electrical components and measurement locations for AP-1 and AP-2. Schematic has a top-down view on the fNIRS device, assuming that the left-most components are at the left side of the head, and the right-most components are at the right side of the head. Circles labeled D1-D4 represent the location of photo diodes. Circles marked S1-4 represent the location of short-path LEDs, enabling a measurement location at the mid-point between each short-path LED and its associated detector (e.g., between S1 and D1). Circles marked F1-4 and R1-4 represent long-path LEDs, enabling the measurement locations marked by white circles labeled 1-12.*

Furthermore, in order to accommodate a variety of head sizes, the AP-1 headband is flexible in the coronal plane, akin to the design employed in all over-ear headphones, allowing it to flex and contract based on the dimensions of an individual’s head, in a manner that does not require manual adjustment by the person placing the headband in position.

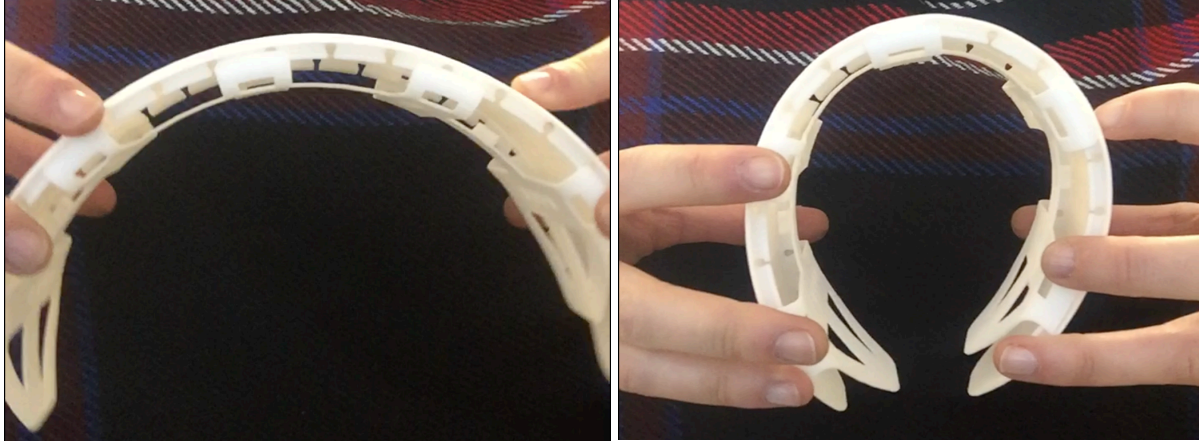


*Figure 2-6. Prototype of the central band of the device headband, demonstrating its ability to accommodate flexion in the coronal plane.*

AP-1 is powered by a lithium-ion battery that is housed (via velcro straps) atop the medial portion of the headband. AP-1 also includes two elastic, adjustable straps to help keep it in position in the presence of movement; one runs along the back of the head, and one is positioned under the jaw (see Figure 2.7, left pane). These straps were designed to hold the headband in place on the user's head during gross movements, or in the case where a user's hair is quite dense or long, necessitating as tight coupling as possible between the light guides and the scalp.

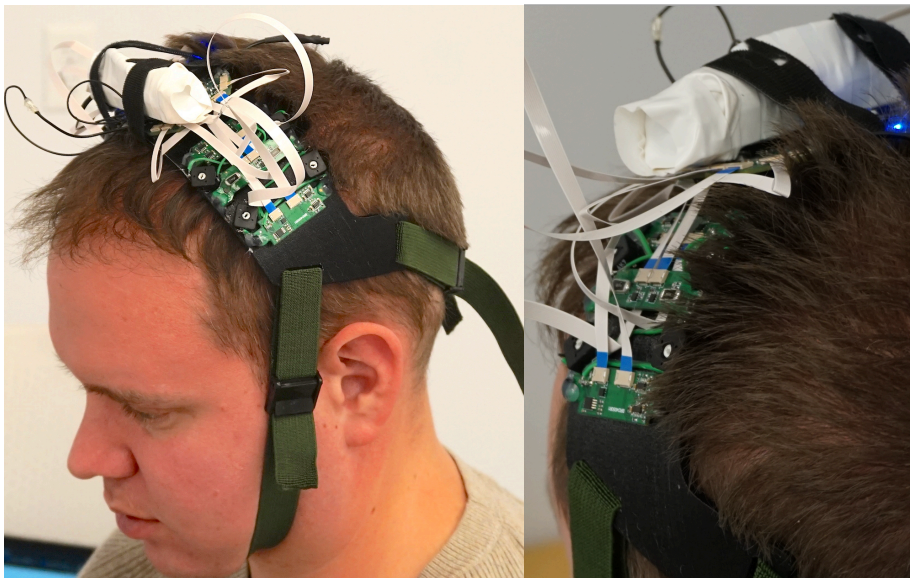


*Figure 2-7. Picture of AP-1 as worn in the present study.*

The optodes of AP-1 were comprised of class 1M LEDs (emitting wavelengths 745 and 850nm) and SiPDs, with light guides (i.e., small tube-shaped structures made of an optically transparent silicon designed to transmit light with minimal attenuation; see Figure 2.8) coupled to each of these components. The purpose of coupling the LEDs and SIPDs to light guides is to permit the transmission of light past hair in a manner that does not require (1) the assistance of a third party to remove hair from the components (a technique common among many modern research-grade fNIRS devices, as illustrated in Figure 2.2 and discussed above), (2) is not uncomfortable, or (3) fragile. These requirements come from the Axem Home design inputs which state that (1) a stroke survivor should be able to place the device, in the correct position, using a single hand, and (2) that the device not be uncomfortable for use when worn for at least 30 minutes (these as well as other design inputs of the Axem Home are further discussed in Chapter 4). These requirements precluded the use of fiber optical cable in the design (often employed in modern research-grade fNIRS systems), due to their rigidity, fragility, and bulk. And given the need to utilize some medium to transmit light from the LED to the scalp, and from the scalp to the SIPD, in the presence of hair (which absorbs light in the infrared range), light guides composed of optically transparent silicon were chosen since they were found to provide good light transmission in the presence of hair, while being composed of material that is slightly more pliable than, for example, acrylic, which provides slightly better transmission as a material, but which, due to its rigidity, is uncomfortable or painful when pressed against the scalp.

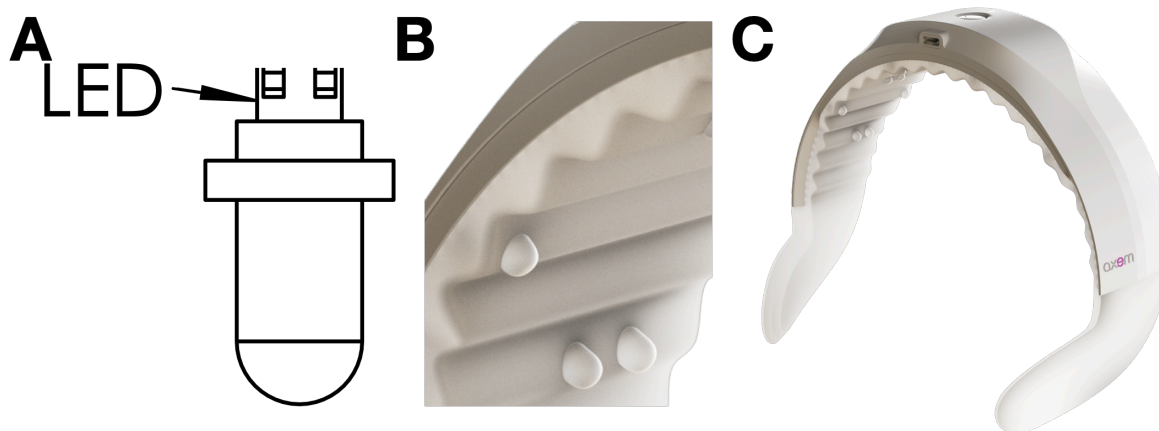


*Figure 2-8. A) Simplified illustration of the light guides butt coupled to the optical components of the device headband. (B-C) Initial (idealized) Axem Home headband industrial design concept, illustrating this butt coupled-based design implemented in a full fNIRS headband. The proposed ridges surrounding the light pipes are conceived as both intended to act as combs for hair, as well as to create a ‘bed of nails’ effect whereby the pressure of the light guides on the head is diminished, resulting in improved comfort; while ideally these ridge features would be made of a material with a lower durometer, preliminary versions of these features made out of plastic were implemented in both AP-1 and AP-2.*

#### 2.2.2.2 AP-2

To improve upon the performance of AP-1 (see section 2.3.1 for an in-depth discussion of the results from the AP-1 participant group), in particular to improve its ability to get the light emitted past the user’s hair, two major changes were made, resulting in a distinct fNIRS prototype headband (i.e., AP-2). Firstly, for AP-2 there was a desire to alter the design such that the optical components would be better able to move in a flexible manner, so as to make better contact with the scalp across a wider range of head sizes and shapes (this relates to item 1 in Figure 2.1). Thus, for AP-2, the emitters supporting the 3cm optical path were not fixed to the headband, but rather embedded in separate ‘pods’, attached to the headband by individually articulating springs (See Figure 2.9). This allows the device to flex in response to the size of the users’ head, in not only the coronal plane (as AP-1 was able to do, given the flexibility illustrated in Figure 2.6) but in the sagittal plane as well. These individually articulating LED pods were

designed so that the light guide coupled to the LED, as in AP-1, would be ~3cm from the photodiodes (which remained housed in the main headband itself). Moreover, similar to AP-1, 8mm adjacent each photo diode is another (lower power) LED (unchanged from AP-1).



*Figure 2-9. Illustration of the spring attachment design, allowing the individual LED pods (example of these pods are pointed to with red arrow in figure) to articulate in the sagittal plane, independent from the central headband.*

Secondly, the LEDs used to emit light supporting the 3cm optical path (which, in AP-1, were the same LEDs used to emit light supporting the 8mm optical path) were replaced by higher power LEDs capable of emitting more optical radiation (this relates to item 9 in Figure 2.1). The primary wavelengths emitted by these LEDs is 740 and 850nm respectively. This change meant that AP-2 required a significantly larger current draw than AP-1, and as a result a larger lithium-ion battery was used; given the increased size of the battery in AP-2, the battery was moved to the backstrap portion of the device. This battery pack is connected to the other device electronics via flexible printed-circuit-boards (PCB), which provide some flexibility to accommodate a range of head sizes, while also providing some structure to the device as a whole (as this flexible PCB is somewhere between a hard plastic and a fabric strap with respect to rigidity).

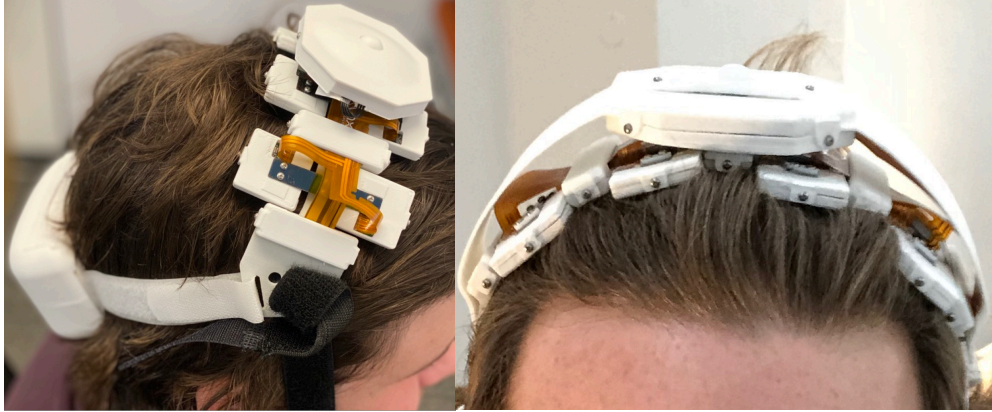


Figure 2-10. Picture of AP-2 as worn in the present study.

And lastly, after consultation with an expert in biomedical optics, the design of the light guides were updated in AP-2 to improve their ability to collimate the light from the flat lens of both the long- and short-path LEDs.

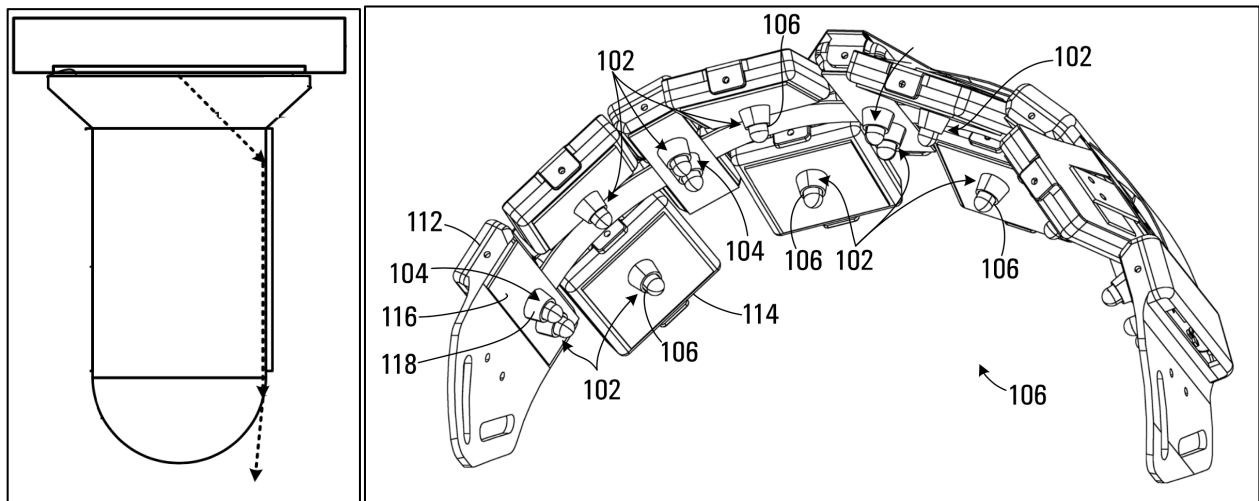


Figure 2-11. Left pane - Illustration of the revised light guide design implemented in AP-2. Right pane – illustration of these light guides as butt coupled to both the individually articulating long-channel LED pods (see items labeled 106) as well as the SiPDs (e.g., see item labelled 104) and short-channel LEDs (e.g., see item labelled 104).

### **2.2.3 Experimental Task**

All participants were seated in a chair with the fingers of both hands in finger holes affixed to an exercise ball (see Figure 2.12). Auditory cues instructed them to either squeeze the



left or right ball approximately once a second (i.e., 1 Hz), and when to rest. They were instructed to use moderate force—enough so that the ball deforms, but not so much that they experience muscle strain or fatigue. They were asked to refrain from squeezing and rest with their hands on their lap when they hear ‘rest’. Each trial of squeezing lasted 10 seconds, while each rest period lasted 30 seconds. Participants completed 24 trials of alternating right- and left-hand squeezing respectively (i.e., 12 left- and 12 right-hand squeezing blocks), for a total task time of 16 minutes.

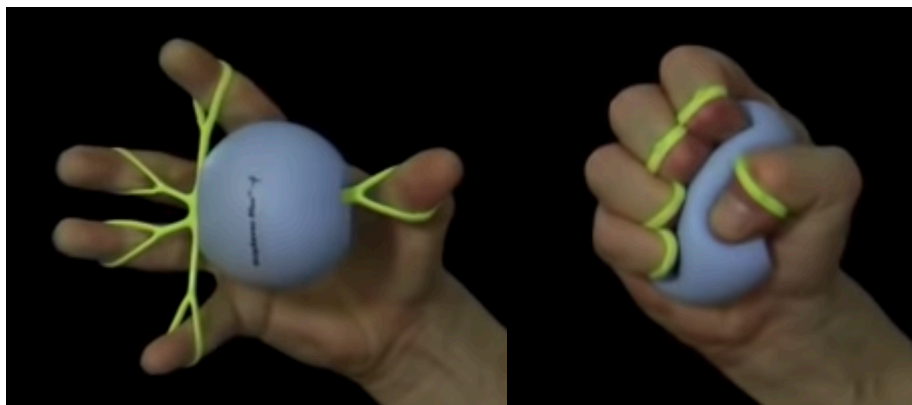


*Figure 2-12. Exercise ball used in the unilateral hand squeeze.*

#### **2.2.4 fNIRS Measurement**

As discussed in section 2.2.2, AP-1 and AP-2 contain a 3 x 2 grid of measurement locations in either hemisphere (with 2 ‘rows’ in the sagittal plane, and 3 ‘columns’ in the coronal plane; see Figure 2.4). Based on existing literature<sup>16</sup>, the hypothesized location of the motor evoked response for the motor tasks used in the present study are C3 and C4 for the left- and right-handed squeezing respectively.

Given individual variability and the exploratory nature of the study, measurements from both AP-1 and AP-2 were taken at two measurement locations. Given that the two measurement locations in the coronal plane are 2cm apart, and given the present study’s purpose (i.e., to characterize the ability of these prototypes to measure the motor evoked response associated with

upper-extremity motor tasks), participants performed 24 trials of unilateral fist squeezing twice, with the AP-1 or AP-2 headband located with the detector D0 at CZ according to the 10-20 system (the green marks in Figure 2.13), or with the detector D0 positioned 1cm anterior to this location (the blue marks in Figure 2.13). Using two measurement locations in this way thus both expands the range over which measurements were taken, as well as increases the spatial resolution over the C3 and C4 regions.

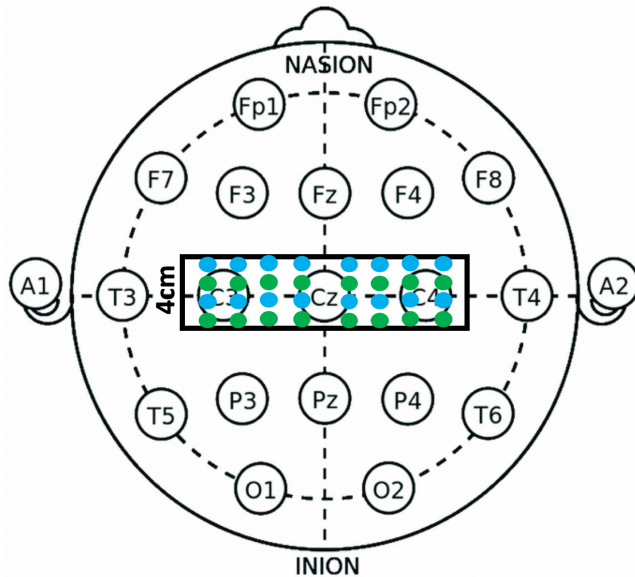


*Figure 2-13. Position of the AP-1 and AP-2 measurement location grids at both measurement locations to be employed in the present study, relative to the 10-20 EEG placement system. Locations marked in green are gained when D0 is positioned at CZ; locations marked in blue are gained when D0 is positioned at 1cm anterior to CZ.*

### **2.2.5 fNIRS Pre-processing**

Data from AP-1 and AP-2 were both sampled at a system-wide sampling rate of 5.4 Hz. For all data analysis for both AP-1 and AP-2, first the raw signals (i.e., light levels measured at each system's analog digital converter) were temporally aligned to the peaks of the pulse waveform of a single (arbitrarily selected) reference channel. Next, a modified Beer-Lambert law<sup>2</sup> was applied to generate  $\Delta\text{HbO}$ ; the first derivative of the  $\Delta\text{HbO}$  time series was then calculated. A principal component analysis (PCA) was then performed on all short-path channels

three times: first on the unfiltered time series, second following a low-pass (0.2 Hz) filter, and finally following a high-pass (0.2 Hz) filter. The first component from all 3 PCAs were then removed from all long-path channels via linear regression, whereupon each long-path channel had its adjacent short-path channel subtracted via linear regression. And finally, a bandpass filter (0.01 - 0.1 Hz) was then applied to isolate the frequency band containing hemodynamic changes.

### **2.2.6 Dynamic Time Warping Classification**

A classification method based on K Nearest Neighbors (KNN)<sup>17</sup> and Dynamic Time Warping (DTW)<sup>18</sup> were used to characterize the motor evoked response. The use of classification for inference in functional neuroimaging analysis is based on the idea that for data measured at a location in the brain which experiences increased cellular activity during a particular task, a naïve algorithm should be capable of differentiating rest data from task data to the extent that the rest and task time series differ (i.e., to the extent the data contains a task-evoked response). In particular, given an expected increase in oxyhemoglobin during the task period at M1, changes in  $\Delta\text{HbO}$  during the task period compared to during the rest period were compared.

The use of KNN and DTW together is a method of time series analysis used to quantify the difference between shapes<sup>19</sup>. This method iteratively warps the position of one time series over the other (see Figure 2.14 for illustration), computing difference values between the two series at each point and storing them in a matrix of differences; a search algorithm is then used to iterate the shortest path from one corner of the matrix to the other. Dynamic time warping is well-suited for classification in this study because it is robust to differences in phase (due to the fact that it warps over the temporal dimension)<sup>18</sup>; and unlike many other frequently used classification techniques, it is not a deep, powerful machine learning algorithm capable of

revealing patterns between data that are not apparent to the human eye (see <sup>20,21</sup> for overviews).

Given the strong expectation of an increase in oxyhemoglobin and a decrease in deoxyhemoglobin during task at the region of the brain being measured in the present study, such a shallow method is preferable, since it reduces the possibility of false-positive classification findings where some confounding factor in the data, learned by the algorithm through training across participants, contributes to the ability of the algorithm to classify data correctly (see<sup>22</sup> for an example of false-positive findings occurring under conditions of high noise when using deep learning in structural neuroimaging).

Each participant's time series data representing task-specific changes in relative oxy- and deoxyhemoglobin respectively was used. For each location, the difference between the shapes of all epochs was quantified using DTW, from which KNN classification was used to derive a classification accuracy—i.e., a percentage of correct predictions, with higher percentages corresponding to larger and more consistent differences between the  $\Delta\text{HbO}$  data collected at rest versus during the task period.

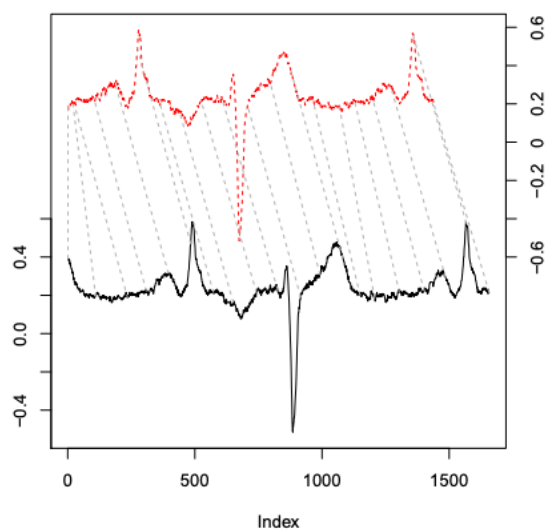


*Figure 2-14. An illustration of the way in which shape comparison in DTW iteratively warps the path of one shape in order to compare it with another in a manner unaffected by differences in phase. Taken from<sup>19</sup>*

## **2.3 RESULTS**

### **2.3.1 AP-1 Results**

For eight participants, data was not collected due to a lack of signal at any of the long-path channels (further discussed below). Also, throughout the course of data collection with AP-1 there were several sessions where not all of the measurement locations were operational (see Appendix A for a summary of the number of sessions gained from each measurement location).

Both the right- and left-handed fist squeezing tasks demonstrated the expected contralateralized pattern of  $\Delta\text{HbO}$  (Figure 2.15). However, throughout the course of data collection a clear trend emerged: whilst data from younger adults varied greatly in quality, data from older adults was uniformly good (see Appendix B for supplementary materials containing a brief summary of a preliminary analysis). This trend was observed first by the experimenters through examination of the raw data prior to data collection, which was required to determine if data collection could commence (i.e., to ensure that there was light getting to the long-path detectors; where poor raw data was characterized broadly as low light levels at the detectors during long-path measurements, with constant noise being observed on a visualizer of the raw data); the most obvious example of this, was that all individuals for whom data collection could not commence were not only young, but were rated as having very dense hair. These observations spurred a series of ad hoc analyses.

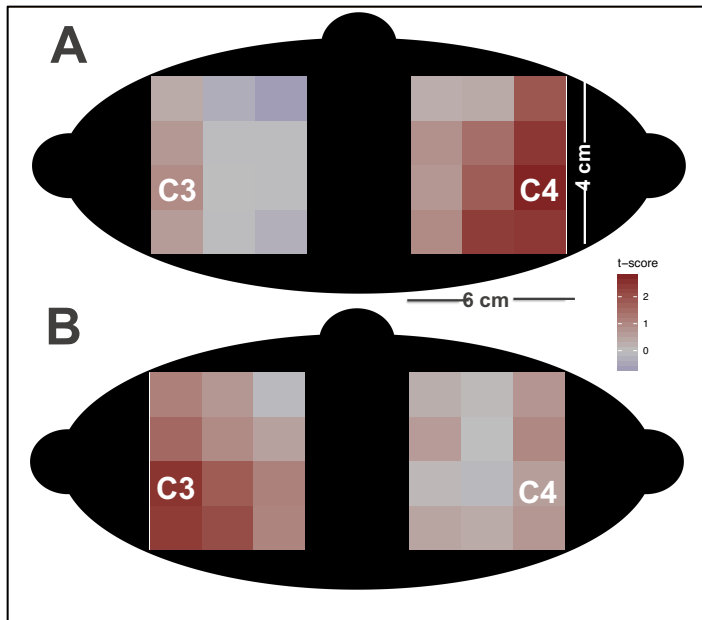


Figure 2-15. Topographical heat map of all measurement locations used in the present study, for (A) left and (B) right-handed fist squeezing. Heat values represent the average  $\Delta\text{HbO}$  changes across all participants during the 10s of a first squeezing task during the 10 second task period. Measurement locations labeled C3/C4 were approximately in these locations as defined by the international 10-20 system.

Indeed, the descriptive statistics for participants younger and older than 50 in Table 2.1 reveals a large striking difference in hair density between groups, and research looking at the effects of age on hair quality suggest these effects generalize to the population at large<sup>23-25</sup>, while the lower pane of Figure 2.17 plots the negative correlation (Pearson's  $r = -0.664$ ) between hair density and age in the AP-1 participant group.

Table 2-2. Descriptive statistics for the sub-segment of participants in the AP-1 group who were under 50 years of age (top row) and over 50 years of age (bottom row).

Age	Hair length	Hair density	Hair curl	Hair Shade
32.27 (8.1)	3.09 (1.08)	3.52 (0.77)	2.98 (0.99)	1.93 (0.34)
61.33 (7.77)	2.76 (0.97)	2.19 (0.68)	2.38 (1.21)	1.71 (0.87)



Figure 2-16. Representative examples of the differences in hair density between younger (left) and older (right) participants.

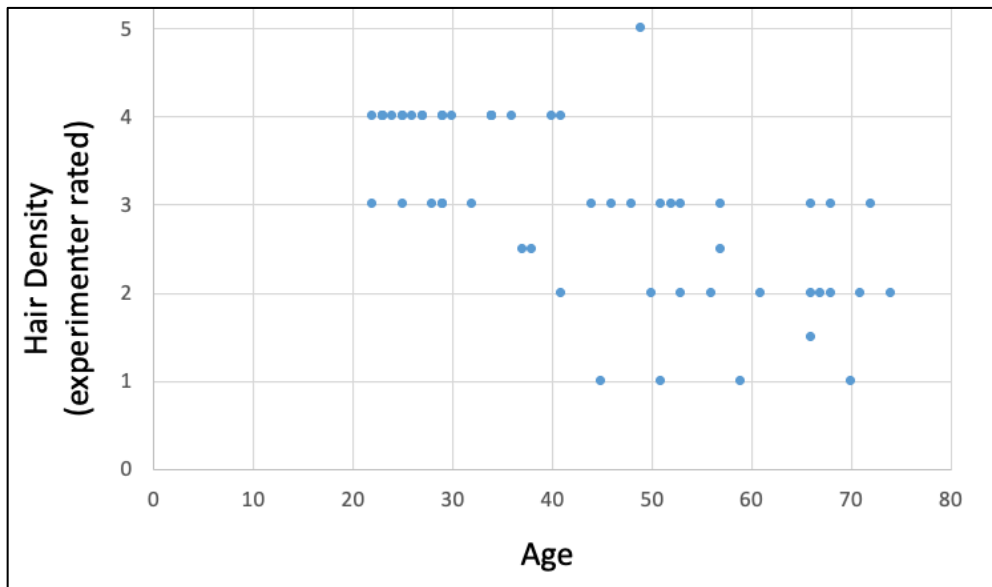


Figure 2-17. Plotted negative relationship (Pearson  $r = -0.664$ ) between hair density and age in the participants in the AP-1 group.

In order to examine whether these perceived differences in signal quality between younger and older participants manifested in quantifiable detriments in fNIRS signal quality, we performed KNN + DTW classification on data from each sub-segment separately.  $\Delta\text{HbO}$  values were used to classify a 10 second data segment as coming from either task or rest. This resulted in a clear difference in classification accuracy between the two groups: with the maximum sensor location for the right- and left-handed squeezing tasks garnering values that were 8% and 13%

better in the older sub-segment than in the younger sub-segment (Figure 2.18). Together, these observations and analyses led to the creation of the AP-2 prototype.

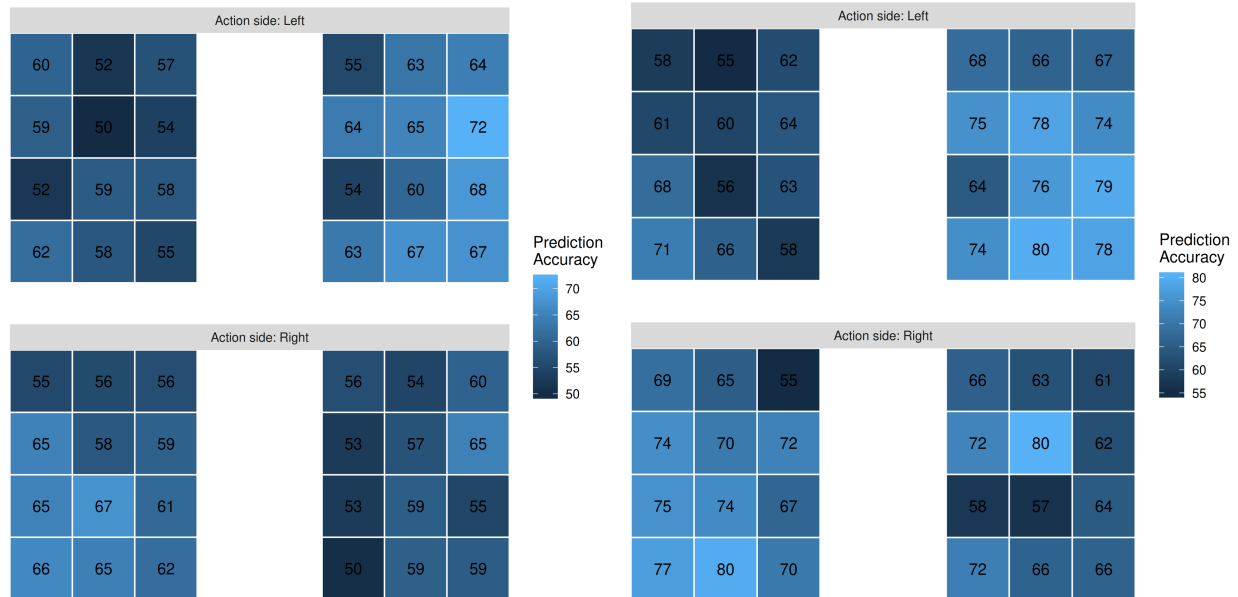


Figure 2-18. DTW-NN Classification accuracy between task and rest  $\Delta$ HbO data for participants <50 (left pane) and  $\geq$ 50 years of age (right pane) for the left-handed (top panes) and right-handed (bottom panes) fist squeezing task. \

In addition to this strong trend of decreased signal quality resulting from denser hair, another observation that was repeatedly noted by the experimenter is that the AP-1 device would often ‘tip’ in the sagittal plane (with the posterior portion of the headband lifting off of the head) in response to individuals who did not have sufficiently flat heads; while this phenomenon occurred to some degree in a large number of participants (nearly half; although this wasn’t formally noted during the study), it was formally noted in the experimenters notes as having an obvious detrimental effect on data quality in 5 of the 49 completed sessions.

### **2.3.2 AP-2 Results**

Following the collection of 57 participants with AP-1, Axem Neurotechnology had access to a new, revised prototype, AP-2. In order to quickly determine the effect of the improvements made over-and-above AP-1, as referenced in section 2.1.1, several individuals



with dense hair who were easily available to Axem Neurotechnology (i.e., Axem Neurotechnology personnel) were spot tested with both the AP-1 then the AP-2, with visual inspections of the data revealing that a clear improvement had been made from the AP-1 (whereon the raw data—i.e., the raw light levels from the device’s analog-digital-converter—obviously represented noise alone) to the AP-2 (where the presence of cardiac pulse and Mayer waves were distinguishable on nearly all channels). Moreover, in order to further inspect the difference between the ability of AP-2 with AP-1, task-related  $\Delta\text{HbO}$  data from this same unilateral fist-squeezing task, from these select individuals with dense hair, were compared by visual inspection. These comparisons (two representative examples are presented at Figure 2.19), in addition to the visual inspection of the raw data from each device, resulted in Axem Neurotechnology determining that the AP-2 had a significantly improved ability to take fNIRS measurements on individuals with dense hair.

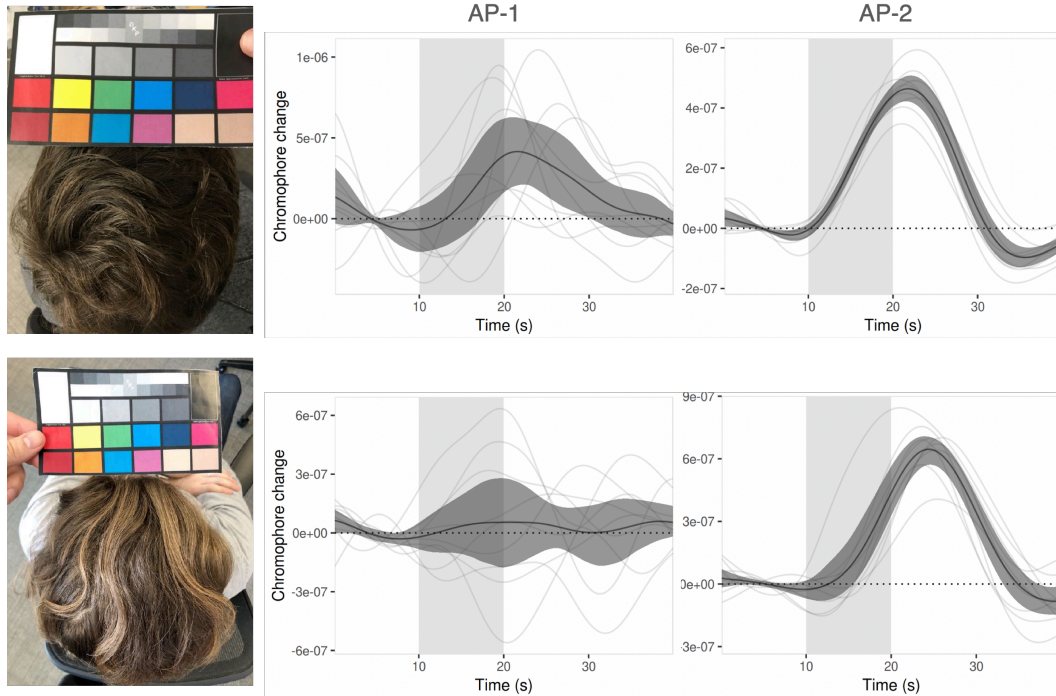


*Figure 2-19. Data presented comes from the contralateral measurement location that demonstrated the largest mean increase in  $\Delta\text{HbO}$  during the task period. Both participants were <40 years of age.*

In order to further validate the performance of AP-2 to obtain a neurophysiological signal from M1 during a simple upper-extremity task, a subsequent 17 participants completed the same unilateral fist-squeezing task protocol while measurements were taken with the AP-2. As with the AP-1, the aggregate data across these 17 participants showed the expected contra-lateralized pattern of increased  $\Delta\text{HbO}$  (Figure 2.20).

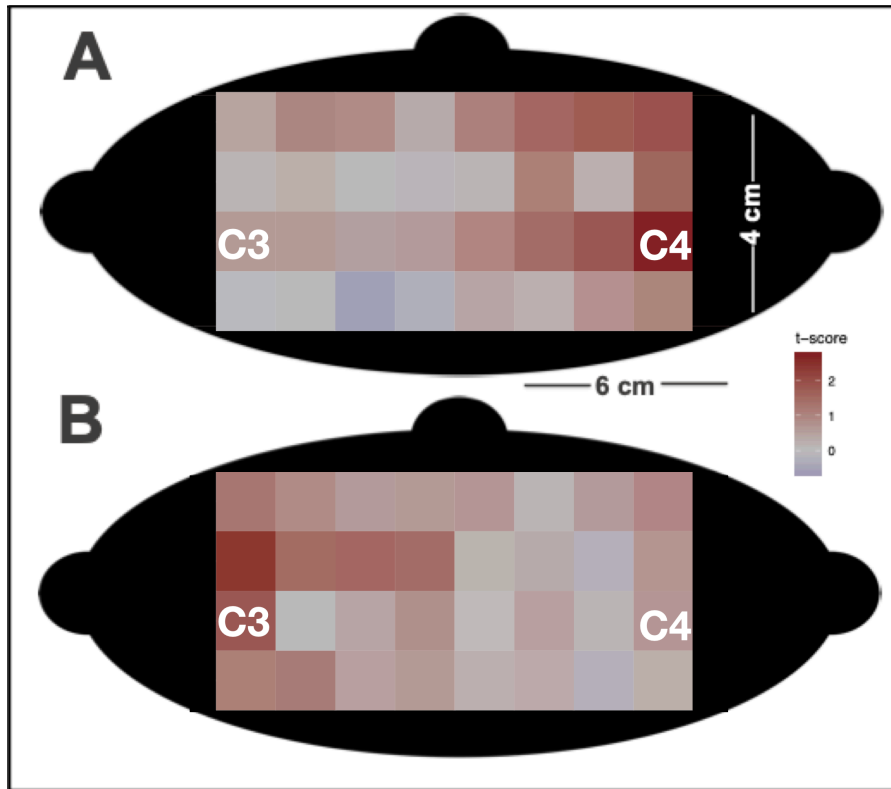


Figure 2-20. Topographical heat map of all measurement locations used in the present study, for (A) left and (B) right-handed fist squeezing. Heat values represent the average  $\Delta\text{HbO}$  changes across all participants during the 10s of a first squeezing task during the 10 second task period.

## 2.4 DISCUSSION

The aim of this study was to examine an fNIRS prototype's ability to obtain a neurophysiological signal from M1 across a broad range of healthy adults, including the possibility of iterating on the fNIRS hardware used in response to the data collected in order to achieve this aim. A simple unilateral upper-extremity task was used, enabling the evaluation of any results in reference to the expected contralateral increase in  $\Delta\text{HbO}$  for both right- and left-handed versions of this task; furthermore, the use of a classification algorithm was used, wherein the ability to successfully characterize  $\Delta\text{HbO}$  data collected during the motor task window as opposed to during a rest period was used as a proxy for data quality. Results showed that AP-1 showed contra-lateralized increases in  $\Delta\text{HbO}$  in both the left- and right-handed fist squeezing

tasks, a double dissociation indicating that AP-1 is in fact capable of measuring cerebral hemodynamics during upper-extremity movement. However, follow-up classification analysis were then performed to determine the ability of a classifier to differentiate task from rest  $\Delta\text{HbO}$  data in participants above and under 50 years of age. These analyses were instigated by observations during data collection that individuals with thick hair demonstrated worse data quality; as well as by an observed correlation between hair density and age in these participants (see Figure 2.17). And indeed, classification of  $\Delta\text{HbO}$  data between task and rest for individuals younger and older than 50 revealed significantly higher classification accuracies for the older subset of participants (see Figure 2.17). While the intended users of the Axem Home are stroke survivors (who tend to be older), the risk of the Axem Home headband being incapable of providing measurements of any kind on a significant portion of the population was deemed unacceptable, and thus these results spurred the development of AP-2. Given that the major deficiency with AP-1 seemed to be its inability to get sufficient photons from its long-path emitters to its detectors, two significant innovations were made for AP-2: (1) higher-power emitters were utilized, and (2) additional flexibility was built in, such that long-path emitters gained flexible in the sagittal plane (in order to maximize the likelihood of good coupling between the long-path emitters' light guides and the scalp).

Qualitative comparisons between the same young, dense-haired individuals both using AP-1 and AP-2 (i.e., visual examination both of the raw data during resting state, as well as processed task-evoked  $\Delta\text{HbO}$  data, see Figure 2.19) suggested a significant improvement upon AP-1 in this device's ability to take neurophysiological measurements via fNIRS in the presence of dense hair. Subsequently 17 participants were recruited to perform the same experimental protocol with AP-2. No participants needed to be removed from the study for poor data quality;

and the resulting  $\Delta\text{HbO}$  data (while not powered towards a between-participants comparison with that from AP-1) also showed contra-lateralized pattern of increased  $\Delta\text{HbO}$  in both the left- and right-handed fist squeezing. This suggests that the improvements made to AP-2 were significant.

The most relevant limitation of this present study is the lack of a between-participants comparison directly testing the differences between the data from the AP-1 and AP-2 systems, which raises the possibility that the improvements in signal quality (evidenced by the fact that none of the 17 participants who utilized the AP-2 device had unusable data, as well as via the qualitative comparisons of the data from the same individuals being measured both fNIRS prototypes) may not generalize. Relatedly, the limited sample size collected with the AP-2 device adds to the uncertainty regarding the generalizability of ability of the AP-2 device to obtain a neurophysiological signal from M1 across a broad range of healthy adults.

However, while this suggests further verification of the ability of AP-2 to measure M1 activity during upper-extremity movement is still required, the present study presents promising data from two preliminary fNIRS prototypes; results suggest that both the AP-1 and AP-2 fNIRS devices are able to obtain a neurophysiological signal from M1 in ideal conditions, and that significant improvements were made in the progression from AP-1 to AP-2 in the ability to gain measurement in non-ideal conditions (seemingly most importantly, in the presence of dense hair). Work to validate the ability of the AP-2 device to take neurophysiological measurements from M1, compared to an established fNIRS system, is presented in chapter 3, while preliminary human factors work examining the limited use of AP-2 by representative users is presented in chapters 4 and 5, and the implications of these findings for fNIRS design more broadly are discussed in Chapter 6, section 2.

## 2.5 REFERENCES

1. Kassab, A., Lan, J. L., Vannasing, P. & Sawan, M. Functional near-infrared spectroscopy caps for brain activity monitoring: a review. *Appl. Opt.* **54**, 576–586 (2015).
2. Baker, W. B. *et al.* Modified Beer-Lambert law for blood flow. *Biomed. Opt. Express* **5**, 4053–4075 (2014).
3. Funane, T. *et al.* Quantitative evaluation of deep and shallow tissue layers' contribution to fNIRS signal using multi-distance optodes and independent component analysis. *NeuroImage* **85**, 150–165 (2014).
4. Wang, L. V. & Wu, H. *Biomedical Optics: Principles and Imaging*. (John Wiley & Sons, 2012).
5. Mirbagheri, M., Hakimi, N., Ebrahimzadeh, E., Pourrezaei, K. & Setarehdan, S. K. Enhancement of optical penetration depth of LED-based NIRS systems by comparing different beam profiles. *Biomed. Phys. Eng. Express* **5**, 065004 (2019).
6. Scholkmann, F. *et al.* A review on continuous wave functional near-infrared spectroscopy and imaging instrumentation and methodology. *NeuroImage* **85**, 6–27 (2014).
7. Ott, M. & Aerospace, S. Capabilities and Reliability of LEDs and Laser Diodes. 7.
8. Pinti, P. *et al.* The present and future use of functional near-infrared spectroscopy (fNIRS) for cognitive neuroscience. *Ann. N. Y. Acad. Sci.* **0**,.
9. Ayaz, H. *et al.* Continuous monitoring of brain dynamics with functional near infrared spectroscopy as a tool for neuroergonomic research: empirical examples and a technological development. *Front. Hum. Neurosci.* **7**, (2013).
10. *Collimator.jpg*.

11. Khan, B. *et al.* Improving optical contact for functional near-infrared brain spectroscopy and imaging with brush optodes. *Biomed. Opt. Express* **3**, 878 (2012).
12. OSA | A wide field-of-view, modular, high-density diffuse optical tomography system for minimally constrained three-dimensional functional neuroimaging.  
<https://www.osapublishing.org/boe/fulltext.cfm?uri=boe-11-8-4110&id=433351>.
13. Piper, S. K. *et al.* A wearable multi-channel fNIRS system for brain imaging in freely moving subjects. *NeuroImage* **85 Pt 1**, 64–71 (2014).
14. Yamada, T., Ohashi, M. & Umeyama, S. Development of a fiber-less fNIRS system and its application to hair-covered head. in *Optical Techniques in Neurosurgery, Neurophotonics, and Optogenetics* vol. 8928 89280R (International Society for Optics and Photonics, 2015).
15. Homan, R. W. The 10-20 Electrode System and Cerebral Location. *Am. J. EEG Technol.* **28**, 269–279 (1988).
16. Homan, R. W., Herman, J. & Purdy, P. Cerebral location of international 10–20 system electrode placement. *Electroencephalogr. Clin. Neurophysiol.* **66**, 376–382 (1987).
17. Lkozma, L. K. k Nearest Neighbors algorithm (kNN). 33.
18. Folgado, D. *et al.* Time Alignment Measurement for Time Series. *Pattern Recognit.* **81**, 268–279 (2018).
19. Giorgino, T. Computing and Visualizing Dynamic Time Warping Alignments in R : The **dtw** Package. *J. Stat. Softw.* **31**, (2009).
20. Shrestha, A. & Mahmood, A. Review of Deep Learning Algorithms and Architectures. *IEEE Access* **7**, 53040–53065 (2019).
21. Deep learning for time series classification: a review | SpringerLink.  
<https://link.springer.com/article/10.1007/s10618-019-00619-1>.

22. Tanno, R. *et al.* Uncertainty Quantification in Deep Learning for Safer Neuroimage Enhancement. *ArXiv190713418 Cs Eess Stat* (2019).
23. Birch, M. P., Messenger, J. F. & Messenger, A. G. Hair density, hair diameter and the prevalence of female pattern hair loss. *Br. J. Dermatol.* **144**, 297–304 (2001).
24. Courtois, M., Loussouarn, G., Hourseau, C. & Grollier, J. F. Ageing and hair cycles. *Br. J. Dermatol.* **132**, 86–93 (1995).
25. Messenger, A. G. Hair through the female life cycle. *Br. J. Dermatol.* **165**, 2–6 (2011).



## Chapter 3 - PORTABLE WIRELESS AND FIBRELESS fNIRS HEADBAND COMPARES FAVOURABLY TO A STATIONARY HEADCAP-BASED SYSTEM

A version of this chapter has been submitted to PLOS ONE as: *C., Friesen, Lawrence, M., Ingram, T., Smith, M., Hamilton, E., Holland, C., Neyedli, H., Boe, S. "Wireless, fibreless, and user-friendly fNIRS headband compared with headcap fNIRS system for sensorimotor measurement of upper- and lower-extremity movement."*

Data from this study were utilized as the basis for the following Master's Thesis: *Holland, C. (2020). The Use of NIRS in Monitoring Lower-Limb Motor Activation: A Study Comparing a Mobile and Research-Grade System.* The analyses conducted herein are mutually exclusive with this work.

### 3.0 ABSTRACT

This study's purpose is to characterize the performance of a prototype fNIRS headband meant to enable quick and easy measurements from the sensorimotor cortices. The fact that fNIRS is well-suited to ergonomic designs (i.e., their ability to be made wireless, their relative robustness to movement artifacts among other characteristics) has resulted in many recent examples of novel ergonomic fNIRS systems; however, the optical nature of fNIRS measurement presents an inherent challenge to measurement at areas of the brain underlying haired parts of the head. It is for this reason that the majority of ergonomic fNIRS systems that have been developed to date target the prefrontal cortex. In the present study we compared the performance of a novel, portable fNIRS headband compared with a stationary full headcap fNIRS system to measure sensorimotor activity during simple upper- and lower-extremity tasks, in healthy individuals >50 years of age. Both fNIRS systems demonstrated the expected pattern of hemodynamic activity in both upper- and lower-extremity tasks, and a comparison of the signal-to-noise ratio between the two systems suggests the prototype fNIRS headband is non-inferior to an established, full head

fNIRS system in the measurement of motor cortex activation during these tasks. Conclusions:  
The use of a wireless and fibreless fNIRS design is feasible for measurement at the motor cortex.

### **3.1 INTRODUCTION**

Functional near-infrared spectroscopy is gaining popularity as a modality of functional neuroimaging. While less temporally precise than methods measuring the electromagnetic properties associated with neural activity (i.e., electro- and magnetoencephalography; due to the relatively slow nature of the hemodynamic response), and less spatially precise than fMRI (which, like fNIRS, measures cerebral hemodynamics<sup>1</sup>), fNIRS is more spatially precise than most electromagnetic methods, and more temporally precise than fMRI (not being limited by the need to serially measure slices of the brain). In addition to this balanced performance across these two dimensions (temporal and spatial precision), recent innovations in LED, SiPD, and lithium battery technologies have together opened up the possibility space for fNIRS systems to be built in ergonomic ways that enable new research, clinical, or consumer BCI applications. All this positions fNIRS well to contribute to the goal of using functional neuroimaging to provide value in contexts outside the laboratory (the so-called ‘neuroergonomics’ movement<sup>2,3</sup>).

However, while there have been many published articles demonstrating the ability to easily take fNIRS measurements from the prefrontal cortex in a naturalistic setting<sup>4-7</sup>, as well as the ability to take measurements from the whole head with intricate and bespoke headcap set-ups<sup>8</sup>, one aspect holding back fNIRS from contributing to future neuroergonomics work is the fact that it is much more difficult to take measurements from parts of the head that tend to be covered by hair. This limitation precludes fNIRS from the significant portion of neuroergonomic applications where sensorimotor, parietal, and/or occipital measurement locations are relevant—for example, physical rehabilitation following brain injury, applications involving motor learning

for skill acquisition, or the use of steady state visual stimulation for diagnostic purposes in concussion.

Taking fNIRS measurements requires the fNIRS system to get light from its source to the scalp, as well as from the scalp to its detectors at the other end of the measurement path. When taking measurements from areas other than the prefrontal cortex, this requires an fNIRS system to (1) ensure the system's light-transmitting parts (usually a light guide of some type) are in a properly oriented position, tangential and sufficiently proximate to the scalp (ideally abutting it); (2) ensure that the interface between its light-transmitting-parts and the scalp are such that a sufficient amount of light is not occluded and/or absorbed by hair; and (3) to accomplish this across a variety of head shapes and sizes, (4) while remaining comfortable. In traditional fNIRS devices that utilize an elastic full headcap, the headcap's elasticity serves as a robust solution to the first and third challenges. The ability to allow the experimenter to quickly attach and detach optodes (attached by fiber optic cable) from their location on the headcap, then manually dislodge and comb hair away from the area underneath the optodes' intended position, has emerged as a simple and effective solution to the second problem. Moreover, varying sizes of elastic headcaps, coupled with the ability to set the pressure with which a cap's individual optodes press against on the scalp (using springs), allows these systems to optimize the trade-off between optical coupling and comfort for all measurement locations, across a range of varying head shapes and sizes.

Unfortunately, the use of these solutions (headcaps and experimenter intervention) precludes these fNIRS systems from being used independently and/or quickly (i.e., enabling a <1 minute set up time), limiting the types of applications they might be used for. Thus, there is a need to develop fNIRS systems that can take valid measurements through hair that do not use

these solutions optimized for experimenter intervention. In the present study we tested the validity of data collected at the motor cortex from a prototype fNIRS system that is wireless and completely head-mounted; this system does not employ fiber optic cable or a headcap to take measurements, instead employing an ergonomic design that might enable fNIRS measurements of the sensorimotor cortices to be taken quickly and independently in the future. This fNIRS prototype device is a preliminary iteration of a device meant to enable (among other things) independent, at-home sensorimotor BCI applications such as stroke rehabilitation<sup>9</sup>.

In this study we specifically tested the validity of the fNIRS data from this prototype fNIRS system during a simple unilateral upper-extremity and bilateral lower-extremity movement task in healthy participants >50 years of age. Individuals >50 years of age were selected to age-match this sample to patients in need of post-stroke rehabilitation, potential future users of a neuroergonomic system. Moreover, in a within-subjects design we also collected data on these tasks with an established headcap-based fNIRS system. The validity of the data from this prototype fNIRS system can then be assessed by examining the topographic distribution of brain activity across the different tasks (with contra-lateralized increases in brain activity expected in the unilateral upper-extremity tasks, and more medially located increases in brain activity expected for the bilateral lower-extremity task) in comparison with the distribution seen in the established fNIRS system. Finally, a quantitative comparison of each system's signal-to-noise ratio can be used to examine whether this prototype fNIRS system might be considered non-inferior to an established fNIRS system.

## **3.2 METHODS**

### **3.2.1 Participants**

Twenty healthy participants over the age of 50 ( $M = 61.1$ ;  $SD = 10.1$ ; 10 female, 10 right-handed as per the Edinburgh handedness inventory<sup>10</sup>) who were not experiencing any physical disability, and had no history of neurological disease or insult were recruited.

Recruitment of older individuals was chosen to be representative of the end user of the fNIRS device being developed (i.e., stroke survivors).

### **3.2.2 fNIRS Devices and Sensor Configuration**

The fNIRS prototype used in the present study was powered by a lithium battery attached to a headband of optical components; the device utilized Bluetooth low energy and supports an 8 x 2 grid of 16 unique cerebral hemodynamic measurement locations (see Figure 1-A). The device is meant to be worn at the apex of the head (i.e., approximately where over-the-ear headphones sit) to enable measurement over the brain's sensorimotor region bilaterally. Given the preliminary nature of this study, we chose to utilize this fNIRS prototype in two locations: with the device's center detector positioned at Cz (according to the International 10-20 System), as well as 1cm anterior to this location. Given the two rows of 8 measurement locations are separated by 2cm, this allows for analysis to be conducted on a continuous grid of 4 x 8 locations.

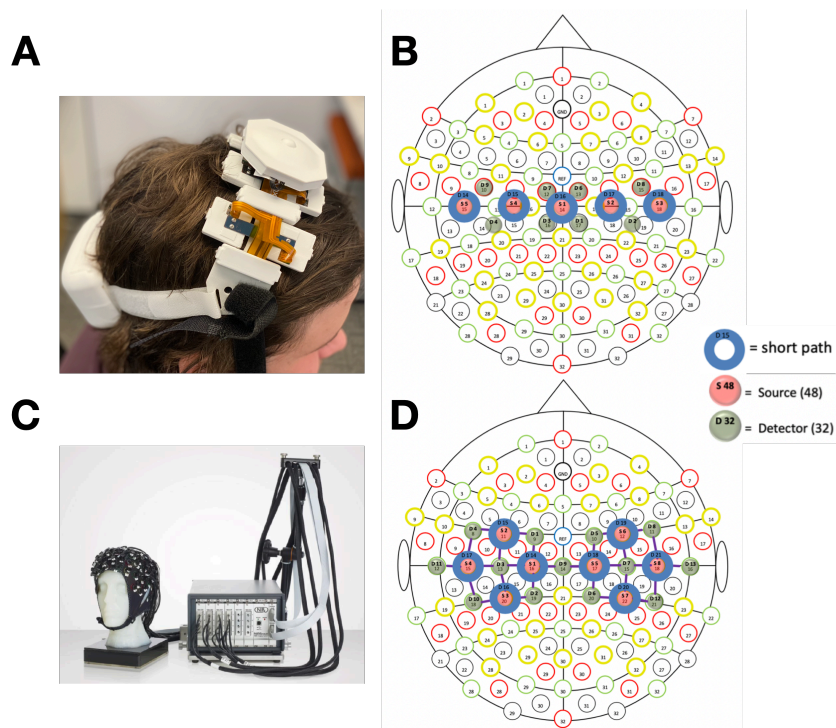


Figure 3-1. A: prototype fNIRS device. B: Array of optical components included in the fNIRS prototype. The central three detectors (being 3cm from 4 long-path LEDs) enabled 4 measurement locations each, with the two detectors on either end (being 3cm from 2 long-path LEDs) enabling two, resulting in a total of 16 measurement locations. C: NIRScout device. D: the NIRScout's array of optical components supporting 28 measurement locations.

The prototype fNIRS device contained both long-path (3cm from the detector; 745 and 850nm), as well as short-path (8mm from the detector; 735 and 850nm) channels. The collection of short-path readings has been shown to improve fNIRS measurement of cerebral hemodynamics by allowing for the removal of information reflecting hemodynamic activity superficial to the brain (i.e., within the scalp)<sup>11</sup>. The long-path LEDs were attached to the headband by individually articulating springs (Figure 1-A), allowing the device to adjust to the shape of users' heads in the sagittal plane, while the use of a flexible central band (which contained the SiPDs and short-path LEDs) allowed for adjustment in the coronal plane. Importantly, all optical components (i.e., LEDs and SiPDs) were butt coupled to light pipes which enabled light transmission to and from the scalp. These light pipes were of a relatively low

durometer compared to traditional fiber optic cable, allowing them to be “worked through hair” by simply shuffling the device back and forth on the head, whilst remaining comfortable despite making secure contact with the scalp. This combination of parts that are fixed in place and one-size-fits-all, yet flexible, and “softer” light transmitting parts than is typically utilized in fNIRS systems, serve to solve the challenges to gaining fNIRS measurements through hair (discussed in the Introduction) in a way that may enable measurements to be taken without experimenter intervention.

The NIRScout system contains 8 LED sources and 16 avalanche photodiodes which can be placed in customized configurations to measure from different regions of the brain, including the ability to take short-path measurements at all detector locations. In the present study the ‘motor montage’ specified by the manufacturer was used (see Figure 1-d), as this montage includes 28 measurements across the same sensorimotor areas the fNIRS prototype’s measurement grid spanned.

### **3.2.3 Experimental Procedure**

In a single experimental session, participants completed a demographic questionnaire, the Edinburgh handedness inventory, and three simple motor tasks: (1) left- and (2) right-handed ball-squeezing tasks, and (3) a seated marching task. Participants completed 10 trials of each task, completing a total of 30 trials in a randomized order. Each trial consisted of a 10 second active period and a 30 second rest period. During all tasks, participants were seated in a chair with their fingers affixed into the finger holes of a pliable, foam-like exercise ball. Auditory and visual cues instructed them to either squeeze the left or right ball at approximately 1 Hz, or to raise and lower their heels off the ground at approximately the speed of a typical walking pattern, alternating their left and right heels. For the ball-squeezing task they were instructed to use

moderate force—enough so that the ball deforms, but not so much that they experience muscle strain or fatigue. Given a requirement of an ergonomic fNIRS system to be comfortable for the user, participants were asked to quantify, on a 10-point Likert scale, the level of discomfort/pain felt while wearing the prototype fNIRS system (approximately one hour across both measurement locations the fNIRS prototype was used at). The scale was anchored by the descriptors ‘No pain/discomfort at all’ (1) and ‘Almost too painful to continue’ (10). The continuum of responses also included the descriptors ‘moderately uncomfortable’ (3), ‘quite uncomfortable and/or slightly painful’ (5), and ‘moderately painful’ (8).

Participants completed these blocks of 30 trials under three conditions where the fNIRS measurements being taken differed: two while fNIRS measurements were taken with a prototype fNIRS device (at two measurement locations) and one while measurements were taken with the NIRScout fNIRS system (NirX, <https://nirx.net/nirscout>). While both measurement conditions utilizing the prototype fNIRS device were completed sequentially, the order of which system was used first was counterbalanced across participants. The order of the two measurement conditions using the prototype fNIRS system was also counterbalanced.

### **3.2.4 fNIRS Acquisition and Pre-processing**

Both devices had short-path emitters co-located with all detectors, thus acquiring one short-path measurement for every long-path measurement taken. The system-wide sample rate was 5.4 Hz for the fNIRS prototype, and 7.8 Hz for the NIRScout.

The Temporal Derivative Distribution Repair<sup>12</sup> (TDDR) algorithm for removal of motion artifacts was applied to all signals. Where the TDDR algorithm has been observed to perform best when high-frequency instrument noise is first removed, we applied a 2Hz low-pass filter to all data before performing TDDR. Data were then bandpassed to the cardiac pulse band (0.5Hz



to 1.5Hz), and delays in the manifestation of the pulse were computed across paths (arbitrarily selecting a reference path, which was treated as having no delay). This procedure was repeated (starting with the TDDR output each time) to measure delays in the bands associated with respiration (0.15Hz to 0.30Hz) and Meyer waves (0.05Hz to 0.15Hz). Only the data from the 850nm signal on a given path was used to calculate these delays, as it can be assumed that while delays vary from path to path, they should be the same for each wavelength on a given path.

Next the data were converted from received light levels to relative concentrations of  $\Delta\text{HbO}$  and  $\Delta\text{Hb}$  using the modified Beer Lambert equations<sup>13</sup> (with the mean of the 10s preceding task onset used as the reference necessitated by these equations). Data from the short-paths (for  $\Delta\text{HbO}$  and  $\Delta\text{Hb}$  separately) was then submitted to a structural equation model to estimate latent common influences (similar in spirit to the use of Canonical Correlation, which has previously been used to similar effect<sup>14</sup>). This was performed four times, first on the unfiltered  $\Delta\text{HbO}$  and  $\Delta\text{Hb}$ , then on the same data after filtering to each of the three ranges of expected frequency content (cardiac pulse, respiration, Meyer waves); for the data in each of these three distinct, physiological-signal-approximating bands, the previously estimated delays were removed by interpolation prior to estimation of the latent common signal. The resulting four latent common signals were then regressed out of all long-path and short-path  $\Delta\text{HbO}$  and  $\Delta\text{Hb}$  channels, thereby removing influence of these common signals of any magnitude.

Next (again, for  $\Delta\text{HbO}$  and  $\Delta\text{Hb}$  separately) the short-path data were again filtered to the frequency bands of expected noise signals (cardiac pulse, respiration, Meyer waves), whereupon the previously estimated delays were again removed by linear interpolation; these delay-corrected short-path signals, together with the unfiltered short-path data, were then regressed out of the data from their associated long-path channel.

Each long-path channel was then bandpassed to the expected frequency range of the BOLD response (0.01Hz to 0.1Hz) and Correlation-Based Signal Improvement (CBSI)<sup>15</sup> was used to subtract any residual noise from the  $\Delta\text{HbO}$  data. After this the CBSI-corrected  $\Delta\text{HbO}$  was again bandpassed to the BOLD frequency range, and finally baselined to the mean of the 5s period preceding the onset of the task.

It should be noted that prior to filtering throughout these procedures, the signal was padded at both the beginning and end with a time-reversed copy of itself that was in turn linearly attenuated to zero at the new beginning and end. A first order Butterworth filter was then applied to both the padded signal and a time-reversed copy of the padded signal, and after un-reversing the output of the latter application, the two outputs were averaged and padding removed.

### **3.3 RESULTS**

#### **3.3.1 Comfort Questionnaire Results**

Overall, participants indicated a low level of discomfort with the prototype fNIRS device, evidenced by an average response of 2.07 (SD – 1.01). This value indicates responses fell squarely between ‘No pain/discomfort at all’ (1) and ‘moderately uncomfortable’ (3).

#### **3.3.2 fNIRS Analysis & Results**

After pre-processing, the data consisted of multiple trials of timeseries for each task condition at each location for each system and each participant. To visualize a representation related to an average timeseries across participants in each task, location and system, we first collapsed across trials (within each task, location, system and participant) to a mean timeseries using a Generalized Additive Model (GAM), where GAMs are a powerful tool to characterize timeseries data in a manner that flexibly accommodates non-linearity in a data-driven manner. Specifically, we fit the GAMs by generalized cross-validation, yielding a single timeseries per fit

(i.e., for each task, location, system and participant), whereupon GAM is again employed to obtain a timeseries that reflects a mean across participants, and specifically the 95% confidence ribbons of a mean time course across participants (see Figure 2). For all three tasks and both fNIRS systems, the expected increase in  $\Delta\text{HbO}$  at the onset of the task period was observed: i.e., a lateralized  $\Delta\text{HbO}$  increase in both unilateral hand squeezing tasks (towards the hemisphere contralateral to the hand being used), and an increase at medial locations in the marching task. These distributions of  $\Delta\text{HbO}$  values conform to our neuroanatomically informed priors—of contra-lateralized data in the unilateral upper-extremity tasks, and bilateral lower-extremity tasks.



*Figure 3-2.  $\Delta\text{HbO}$  timeseries (95% confidence ribbons) plotted at all measurement locations within each system (facet rows) and for each task (facet columns). Plots at each location are scaled to have common axes, the grey band marks the task period and the black line marks the mean of the period preceding the task.*

We next proceeded to a full Bayesian characterization wherein we trimmed the data to only the task period and sought to model a linear slope (given the expectation of a monotonic increase in  $\Delta\text{HbO}$  during the task period) during this period on each trial. We opted to model each location, system and task independently with a 3-level hierarchical model in which the mean slope for a given subject ( $\mu_{\text{subject}}$ ) was a random normal deviate from a group mean slope

( $\mu_{\text{group}}$ ):  $\mu_{\text{subject}} \sim \text{normal}(\mu_{\text{group}}, \sigma_{\text{subjs}})$ , the slope for a given trial ( $\mu_{\text{trial}}$ ) was a random normal deviate from the participant's mean slope:  $\mu_{\text{trial}} \sim \text{normal}(\mu_{\text{subject}}, \sigma_{\text{trials}})$ , and finally, the observations through time on a given trial were random normal deviates from that expected given the trial slope:  $\text{obs} \sim \text{normal}(\text{time} \times \mu_{\text{trial}}, \sigma_{\text{obs}})$ . Weakly-informed priors for all parameters were employed such that the gross variability observed in the data (quantified by computing the standard deviation across all datapoints,  $SD_{\text{obs}}$ ) informed on the general scale of the parameters. Specifically,  $\mu_{\text{group}} \sim \text{normal}(0, SD_{\text{obs}})$ ,  $\sigma_{\text{subjs}} \sim \text{weibull}(2, SD_{\text{obs}})$ ,  $\sigma_{\text{trials}} \sim \text{weibull}(2, SD_{\text{obs}})$ ,  $\sigma_{\text{obs}} \sim \text{weibull}(2, SD_{\text{obs}})$ . The model and priors were expressed in Stan<sup>16</sup>, permitting use of the cmdstan Markov chain Monte Carlo (MCMC) sampler to generate posterior samples reflecting the posterior probability distributions on the model parameters given the model structure, priors and observed data. Diagnostics for all sampling runs were evaluated to ensure that no samples encountered divergent transitions, all chains showed exhibited convergence ( $\text{rhat} < 1.01$ ) for all parameters, and no parameters exhibited low effective sample size for tail quantities.

Posterior samples for the group mean slope were obtained for each task (Figure 3). Consistent with the previous figure, we see the expected contralateral activation during the squeezing tasks and medial activation during the marching task, again with rather more spatial selectivity in the NIRScout system compared to the fNIRS prototype system.

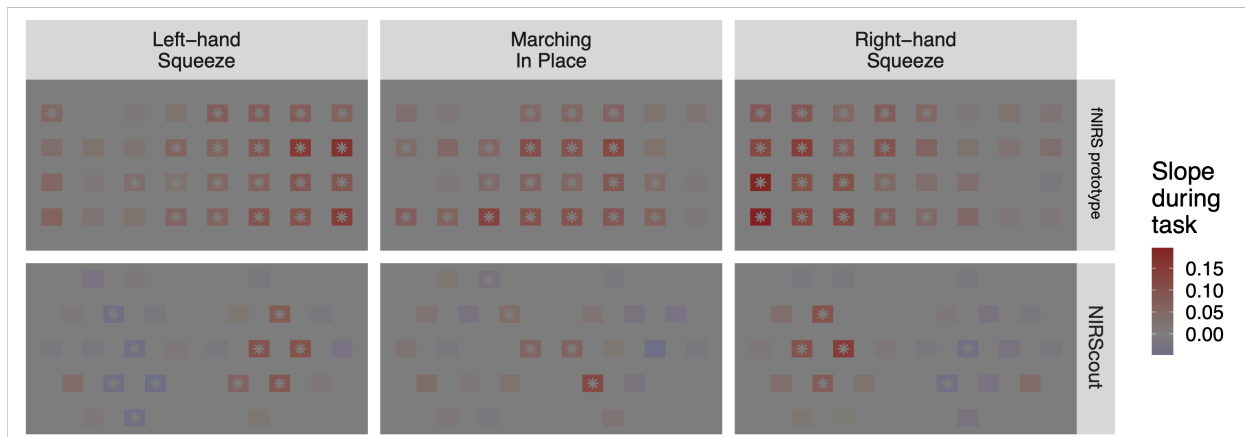


*Figure 3-3. Topographic maps of group mean slope (in units of mMol/mm<sup>3</sup>) during task. Colors indicate posterior median; locations with posterior distributions in which zero falls outside the 95% credible interval are marked with an asterisk.*

Next we sought to compare the measurement performance of the fNIRS prototype system and NIRScout system by comparing their respective Signal-to-Noise Ratios (SNRs). Using the slope during the task period as the numerator and  $\sigma_{\text{trials}}$  (variability in slope across trials) as the denominator. Such an SNR calculation is analogous to the various ‘contrast-to-noise’ approaches often employed in fMRI analysis<sup>17</sup>. Moreover, since the topography of a given subject might not reflect the same patterns as the group topography shown in Figures 2-3, the computation of posteriors for all SNR values was achieved by first finding the location (in each task and system) that had the maximum median posterior slope for that participant. Then, for each sample in the posterior from that location, that participant’s slope was divided by that sample’s value for  $\sigma_{\text{trials}}$ , yielding a value for SNR, for each sample in the posterior for that participant. These participant SNRs were then collapsed to a mean in each sample in the posterior for each task and system (see Figure 4, three left-most figures). With these SNR values (reflecting the size of the measured response proportionate to the variability of that response across trials) generated, a difference ratio was then calculated between the SNR values for each fNIRS system within each motor task (see Figure 4, right-most figure), by dividing the SNR of the fNIRS prototype system from that of the NIRScout system; a value of 1 therefore indicated no difference between the two SNR values. The 95% credible interval for the SNR difference ratios between fNIRS systems for all tasks were found to include a ratio of one, suggesting no evidence of significant differences between the fNIRS systems.

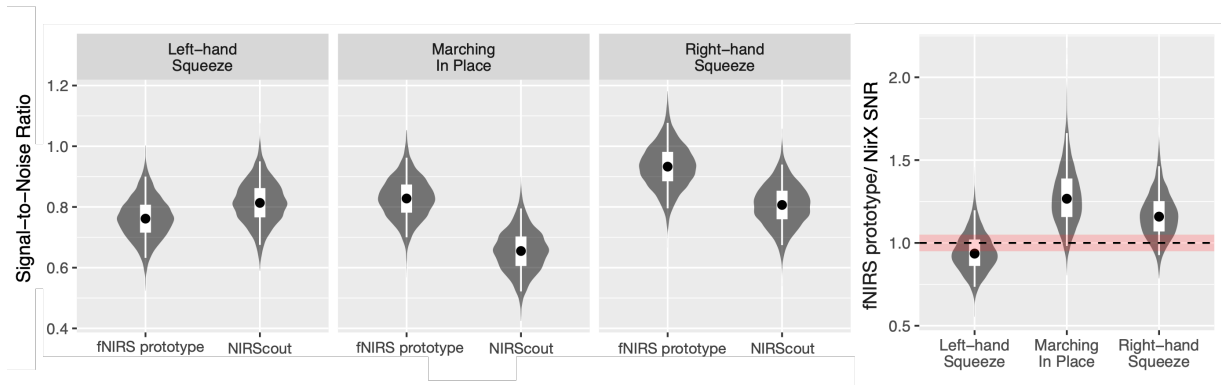


Figure 3-4. Posterior distributions for SNR in each task for each fNIRS system as well as the SNR difference ratio between fNIRS systems (right-most pane)—i.e., the SNR of an fNIRS prototype system divided by the SNR of the NIRScout system (with 1 meaning no differences). Grey violins depict the mirrored density-smoothed distributions, black dots depict the posterior median, thick white rectangles depict the 50% credible interval and thin white lines depict the 95% credible interval. Red bands in the ratio plot depict the range of ratios from 0.95 to 1.05.

### 3.4 DISCUSSION

The present study tested the validity of data collected at the motor cortex during unilateral upper- and bilateral lower-extremity movement from a prototype fNIRS system; it also compared these data to that of an established fNIRS system. The prototype fNIRS system had been designed to enable measurements from sensorimotor regions to be taken independently, employing a novel wire- and fibreless design; thus the present study compares the validity of fNIRS data from such a device with an fNIRS system which utilizes the traditional full headcap form factor. Healthy adults >50 years of age were selected as participants in order to be representative of stroke survivors, given that the final version of this device endeavors to provide at-home sensorimotor BCI feedback during physical rehabilitation. The fact that both fNIRS systems used in this study showed the expected pattern of increased  $\Delta\text{HbO}$  values across the motor cortex in all three tasks (i.e., contra-lateralized increases in the unilateral upper-extremity tasks, primarily medially located increases in the bilateral lower-extremity task) indicate that

data from both fNIRS systems are valid (see Figure 2). Moreover, the 95% credible interval of the ratio comparing SNR values from these two fNIRS systems included a ratio of one (i.e., no difference) for all three motor tasks (see Figure 4); therefore, these data do not permit us to make any claims about the superiority or inferiority of one system compared with another. And finally, results from the participant self-rating about the presence of any discomfort or pain while utilizing the fNIRS prototype indicated this fNIRS prototype is feasible for long periods of continuous use. While preliminary, together these results suggest the novel fNIRS prototype tested herein provides equivalent measurements of activity from the motor cortex during simple upper- and lower-extremity movements compared with an established fNIRS system.

However, there were notable differences in the spatial specificity of the increases in  $\Delta\text{HbO}$  observed between these two fNIRS systems. In the upper-extremity tasks, the prototype fNIRS system had a reliable level of  $\Delta\text{HbO}$  increase (denoted by the presence of an asterisk at that location in Figure 3) across all 20 contra-lateral measurement locations, as well as 5 (in the left-handed task) and 2 (in the right-handed task) at ipsilateral locations; while the NIRScout system only showed this reliable increase in  $\Delta\text{HbO}$  in 4 (right-handed movement) and 5 (left-handed movement) of a total 14 possible contra-lateral measurement locations, with none in the ipsilateral hemisphere. Likewise, in the lower-extremity task, the fNIRS prototype showed a reliable increase at 20 of 40 possible measurement locations, with the NIRScout system showing this reliable  $\Delta\text{HbO}$  increase in just 4 measurement locations. While both fNIRS systems do show responses congruent with our neuroanatomical priors for these tasks (with the largest increases in  $\Delta\text{HbO}$  at the most contra-lateral locations for the upper-extremity task, and at medial locations for the lower-extremity task), these findings suggest the NIRScout system may have greater spatial specificity compared with the prototype fNIRS system. This may be a result of the

NIRScout system's greater reliance on detectors (as opposed to emitters) within its array of optical components; given that this results in a larger ratio of short-path channels to long-path channels, it is possible the pre-processing techniques employed in the present study were more effective in removing extra-cerebral noise from the NIRScout compared with the fNIRS prototype data, though more work needs to be done to confirm this hypothesis.

These findings are notable given the differences between these two fNIRS systems in their inherent design: while the NIRScout employs a traditional headcap system, interfacing with a bundle of fiber optic cables to optimize easy set-up by an experimenter, the fNIRS prototype tested in this study employs a wireless, fibreless design, with light transmitting parts that allow for manipulation by the individual on whom measurements are being taken. While other fNIRS systems have been developed to measure at haired locations on the head without the use of fiber optic cable, these fNIRS systems either still utilize either a headcap form factor<sup>18</sup> or employ the use of light transmission pipes made of high durometer material (e.g., glass<sup>19</sup>), making them of limited use in translation to an fNIRS system meant for independent use. Also of note are the recent developments in small and wearable fNIRS systems which use silicon photomultipliers<sup>20</sup> or avalanche photo diodes<sup>21</sup> as detectors to obtain fibreless measurements at haired locations on the head; while impressive, the fact that these fNIRS systems rely on being tethered to a large unit to provide control and power to its optical components means they are not feasible for applications requiring independent use. Thus the findings that fNIRS data from each of the systems used in this study provide equivalent cerebral hemodynamic measurements of both upper- and lower-extremity movement represents an encouraging step for future development of ergonomic, user-centric fNIRS systems that are built to measure from parts of the head that underly hair.



However, there are several important limitations to this study. Firstly, while the fNIRS prototype tested in the present study was designed to enable wearers of the device to receive sensorimotor BCI feedback independent of a second individual assisting with device set-up, the ability for wearers of the device to set it up independently and take valid measurements was not tested. As this study involved the fNIRS prototype being set up by the experimenter in a similar manner as the NIRScout device, the results only provide a validation of this fNIRS prototype's ability to collect valid data from the motor cortex; it does not provide validation of its ability to allow the wearer of the fNIRS device to take valid fNIRS measurements independently. With that said, the present study provides preliminary support for a 'valid range' of measurement locations within which this fNIRS prototype is capable of taking valid motor cortex measurements (i.e., ranging from one cm posterior to CZ to 2cm anterior to CZ), given that within each sagittal row of measurement locations there were locations (primarily at the lateral measurement locations, as illustrated at Figures 2-3) where an increase in oxyhemoglobin was found. Moreover, the choice to only include participants >50 years old does make the task of taking fNIRS measurements through hair easier (since follicular density is a major factor in the ability to get good fNIRS measurements on haired parts of the head<sup>22</sup>, and this value negatively correlates with age<sup>23</sup>).

In conclusion, while preliminary, these data provide an encouraging indication this fNIRS prototype is indeed capable of taking valid fNIRS measurements during both upper- and lower-extremity movement, to a comparable degree as an established headcap and fiber optic cable based fNIRS system. Given that this ergonomic fNIRS prototype's design may be further adapted to allow for independent fNIRS measurements to be taken, this study represents a

transitory but important step towards the development of a device capable of enabling users to independently take sensorimotor fNIRS measurements.

### 3.5 REFERENCES

1. Cui, X., Bray, S., Bryant, D. M., Glover, G. H. & Reiss, A. L. A quantitative comparison of NIRS and fMRI across multiple cognitive tasks. *NeuroImage* **54**, 2808–2821 (2011).
2. Ayaz, H. *et al.* Continuous monitoring of brain dynamics with functional near infrared spectroscopy as a tool for neuroergonomic research: empirical examples and a technological development. *Front. Hum. Neurosci.* **7**, (2013).
3. Gramann, K., Fairclough, S. H., Zander, T. O. & Ayaz, H. Editorial: Trends in Neuroergonomics. *Front. Hum. Neurosci.* **11**, (2017).
4. Gateau, T., Ayaz, H. & Dehais, F. In silico vs. Over the Clouds: On-the-Fly Mental State Estimation of Aircraft Pilots, Using a Functional Near Infrared Spectroscopy Based Passive-BCI. *Front. Hum. Neurosci.* **12**, (2018).
5. Utilizing functional near-infrared spectroscopy for prediction of cognitive workload in noisy work environments. <https://www.spiedigitallibrary.org/journals/Neurophotonics/volume-4/issue-4/041406/Utilizing-functional-near-infrared-spectroscopy-for-prediction-of-cognitive-workload/10.1117/1.NPh.4.4.041406.full>.
6. Li, L., Liu, Z., Zhu, H., Zhu, L. & Huang, Y. Functional near-infrared spectroscopy in the evaluation of urban rail transit drivers' mental workload under simulated driving conditions. *Ergonomics* **62**, 406–419 (2019).
7. Sibi, S., Ayaz, H., Kuhns, D. P., Sirkin, D. M. & Ju, W. Monitoring driver cognitive load using functional near infrared spectroscopy in partially autonomous cars. in *2016 IEEE Intelligent Vehicles Symposium (IV)* 419–425 (IEEE, 2016). doi:10.1109/IVS.2016.7535420.
8. Piper, S. K. *et al.* A wearable multi-channel fNIRS system for brain imaging in freely moving subjects. *NeuroImage* **85 Pt 1**, 64–71 (2014).

9. Mihara, M. *et al.* Near-infrared Spectroscopy–mediated Neurofeedback Enhances Efficacy of Motor Imagery–based Training in Poststroke Victims. *Stroke* (2013).
10. Oldfield, R. C. The assessment and analysis of handedness: The Edinburgh inventory. *Neuropsychologia* **9**, 97–113 (1971).
11. Sato, T. *et al.* Reduction of global interference of scalp-hemodynamics in functional near-infrared spectroscopy using short distance probes. *NeuroImage* **141**, 120–132 (2016).
12. Fishburn, F. A., Ludlum, R. S., Vaidya, C. J. & Medvedev, A. V. Temporal Derivative Distribution Repair (TDDR): A motion correction method for fNIRS. *NeuroImage* **184**, 171–179 (2019).
13. Baker, W. B. *et al.* Modified Beer-Lambert law for blood flow. *Biomed. Opt. Express* **5**, 4053–4075 (2014).
14. von Lüthmann, A., Li, X., Müller, K.-R., Boas, D. A. & Yücel, M. A. Improved physiological noise regression in fNIRS: A multimodal extension of the General Linear Model using temporally embedded Canonical Correlation Analysis. *NeuroImage* **208**, 116472 (2020).
15. Cui, X., Bray, S. & Reiss, A. L. Functional near infrared spectroscopy (NIRS) signal improvement based on negative correlation between oxygenated and deoxygenated hemoglobin dynamics. *NeuroImage* **49**, 3039–3046 (2010).
16. Gelman, A., Lee, D. & Guo, J. Stan: A Probabilistic Programming Language for Bayesian Inference and Optimization. *J. Educ. Behav. Stat.* **40**, 530–543 (2015).
17. Welvaert, M. & Rosseel, Y. On the Definition of Signal-To-Noise Ratio and Contrast-To-Noise Ratio for fMRI Data. *PLOS ONE* **8**, e77089 (2013).

18. Saikia, M. J., Besio, W. & Mankodiya, K. WearLight: Towards a Wearable, Configurable Functional NIR Spectroscopy System for Noninvasive Neuroimaging. *IEEE Trans. Biomed. Circuits Syst.* 1–1 (2018) doi:10.1109/TBCAS.2018.2876089.
19. Kiguchi, M. *et al.* Note: Wearable near-infrared spectroscopy imager for haired region. *Rev. Sci. Instrum.* **83**, 056101 (2012).
20. Wyser, D. G., Lambercy, O., Scholkmann, F., Wolf, M. & Gassert, R. Wearable and modular functional near-infrared spectroscopy instrument with multidistance measurements at four wavelengths. *Neurophotonics* **4**, 041413 (2017).
21. Funane, T. *et al.* Rearrangeable and exchangeable optical module with system-on-chip for wearable functional near-infrared spectroscopy system. *Neurophotonics* **5**, 011007 (2017).
22. Zhao, H. & Cooper, R. J. Review of recent progress toward a fiberless, whole-scalp diffuse optical tomography system. *Neurophotonics* **5**, 011012 (2017).
23. Kligman, A. M. The comparative histopathology of male-pattern baldness and senescent baldness. *Clin. Dermatol.* **6**, 108–118 (1988).

## Chapter 4 – AXEM HOME FORMATIVE USABILITY

### STUDY

#### 4.0 ABSTRACT

This study investigated the potential usability and utility of a preliminary set of prototypes which together approximate the projected user experience of the Axem Home. Twelve chronic stroke survivors (age:  $m = 62.18$ ,  $sd = 11.77$ ; months since most recent stroke:  $m = 63.27$ ,  $sd = 41.51$ ) participated in a formative usability study either in their homes or at the offices of Axem Neurotechnology. Participants were asked to attempt to don a surface model prototype approximating the form factor of the Axem Home (AP-LL), and subsequently to perform a rehabilitation session using a prototype version of the Axem Home software app while fNIRS measurements were taken with a working Axem Home fNIRS prototype (AP-2). Following these tests participants completed a usability questionnaire and interview to investigate their perception of the usability and utility of the prototypes employed in the present study. Results suggested that all aspects of these Axem Home prototypes were feasible for use, though all still required improvement in order to satisfy the user needs (UN) associated with the Axem Home—placement of the AP-LL was feasible, however the majority of participants failed to place the device within the desired range to optimally achieve motor cortex measurements; participants reported the fNIRS prototype as moderately comfortable during ~30 minutes of use, suggesting its use in this population is feasible though requires improvement; participants reported that use of the prototype software was moderately easy to use, though this tepid response (together with the fact that not all features of the eventual Axem Home product) suggests more work is needed to improve usability; and finally, participants reported that they

would find the Axem Home useful in helping them perform at-home rehabilitation, though the unblinded nature of this study necessitates that these responses only be considered preliminary.

## **4.1 INTRODUCTION**

### **4.1.1 Background**

Prior to having representative users conduct rehabilitation sessions independently with prototypes of the Axem Home, it is important to gain a preliminary understanding of the level of usability of Axem's prototypes while development remains ongoing. The purpose of usability studies, broadly, are to help the developers of products make informed decisions about how they might improve their current prototype in the pursuit of a usable final product. A 'usable' product is one which its intended users are willing to use, and which allows those users to achieve their goals<sup>1</sup>. Formative usability studies are formal experiments conducted on prototypes of products or product features that are still in the design phase; formative usability studies are meant to help the product's developers gain a better understanding of some narrowly defined aspect of its usability. In the development of a medical device, formative usability studies are meant to be followed by a summative usability study, which is meant to verify that a production equivalent prototype (or a product that the designer presupposes to be a final design) meets all relevant usability requirements.<sup>2</sup>

The purpose of this first formative usability study is to identify challenges that must be overcome to initiate a clinical pilot where representative users would be using Axem Home prototypes independently, as well as to determine how feasible the current preliminary fNIRS and software prototypes designed by Axem would be for independent use in a home environment.

### **4.1.2 Axem Home Use Specification**

The use specification of a product refers to a summary of a product's intended use, users, and use environments; it is considered best practice to define the goals and results of a usability study in reference to this specific contextual information<sup>2,3</sup>, and for this reason the Intended Use, Patient User Description, and Use Environment sections of Axem Neurotechnology's design history file (as of the initiation of this study) are included in this section.

#### *4.1.2.1 Intended Use*

The following is a draft of the Intended Use of the Axem Home system, as it has been presented to the regulatory bodies for preliminary evaluation:

*Axem Home is intended to facilitate upper-extremity rehabilitation for adult patients who have experienced a cerebrovascular accident or "stroke".*

*The device is comprised of software and hardware. The software guides patients through health care professional-approved exercises, and the hardware measures a patient's performance and progress via functional near-infrared spectroscopy (fNIRS) monitoring of cortical activation via the cortical hemodynamic response during exercises focused on the injured upper extremity.*

*The Axem Home includes software that allows a health care professional to monitor progress and modify prescribed exercises remotely based on these and other data available to the health care professional. Axem home is intended to be used in a professional healthcare facility and at home when prescribed by a qualified health care professional.*

#### *4.1.2.2 Patient User Description*

Axem Home is targeted for (but not necessarily limited to) survivors of stroke who are left with one-sided movement impairment (i.e., "hemiparesis"). Users can include adult patients (i.e., 18+) deemed by the prescriber to benefit from rehabilitation for movement impairment of



neurological origin (e.g., acquired brain injury). Potentially, though not necessarily, this will include older adults who may be experiencing paralysis, and/or suffering from mild cognitive impairments.

Patients need not be able to don the device themselves or interact with the Axem Home App if used in the presence of a caregiver (family member or otherwise) — however for patients deemed by their prescriber as capable of using the product independently, the device will be designed so that it can be put on with one hand. Patients need the device to be comfortable; at the very least, patients or their caregivers must be able to easily put it on; they need any instructions received from the product to be clear, concise, and simple; and they need any data they are exposed to from the device to be easily understandable (again clear, concise, and simple).

Patient users may be aided by a caretaker; in the case that a patient is cognitively impaired (<24 on the Mini-mental state examination<sup>4</sup>), a caregiver is assumed to be helping the patient user in order for the Axem Home to meet the patient user needs. While the term “patient” may imply that the user is currently under the care of a HCP, Axem is designed to be usable outside the circle of care of such a professional (e.g., without remote monitoring).

#### *4.1.2.3 Use Environment*

The primary environment for use is the patient’s home. The device may also be used in an inpatient or outpatient rehabilitation center or clinic. Such a facility may be part of a larger public or private hospital or a smaller privately-owned establishment (e.g. a physical therapy clinic). In all environments it is expected that users are adequately capable of following instructions for the appropriate placement of the device, including ensuring adequate power and cleaning, and basic operation of the device via the provided software.

### **4.1.3 Research Questions**

The purpose of this first formative usability study is to determine how representative users of the Axem Home perceive the usability of preliminary Axem Home prototypes, to determine whether these users would use the device and/or recommend usage of the device to other representative users, and to gather feedback that will help Axem improve its design in subsequent Axem Home prototypes. The primary questions of this study were:

1. To what degree are users able to successfully don the Axem headset?
2. To what degree are users able to successfully navigate through a session using the Axem app?
3. To what degree do users perceive the product (i.e., the prototypes in their preliminary state) as usable?
4. To what degree do users perceive the product as useful?

These primary questions were posed in order to evaluate prototypes available to Axem Neurotechnology at the time of the study from the perspective of effectiveness (i.e., how well do they accomplish their intended purpose), and usefulness (i.e., how useful do intended users perceive them to be).<sup>1,2</sup> Moreover, each of these primary research questions is directly related to a User Need (as defined in the Axem Home's design history file as of the initiation of this study; see Appendix C for full list of User Needs) that is critical to the core functionality of the Axem Home headband (i.e., to support at-home upper-extremity rehabilitation for stroke survivors), and thus critical to address as soon as possible through preliminary prototypes, since insight into the performance of the most preliminary prototypes may result in substantial changes in design.

#### **4.1.4 Axem Home prototypes used in present study**

The functioning Axem Home hardware prototype available at the time this study took place (AP-2) was not designed for independent use, and thus testing utilized AP-2 (as described in Chapter 2) when participants were testing the Axem Home software (to investigate feasibility associated with donning an active fNIRS device during rehabilitation exercise, as well as to attempt to include and investigate the feasibility of providing brain activity through the prototype software), and while for testing the usability of the Axem Home headband, a model more closely approximating the final form factor of the Axem Home—a ‘looks like’ model for the Axem Home—was used (referred to as AP-LL; see Figure 4.1-A and section 4.1.4.1 for more information).

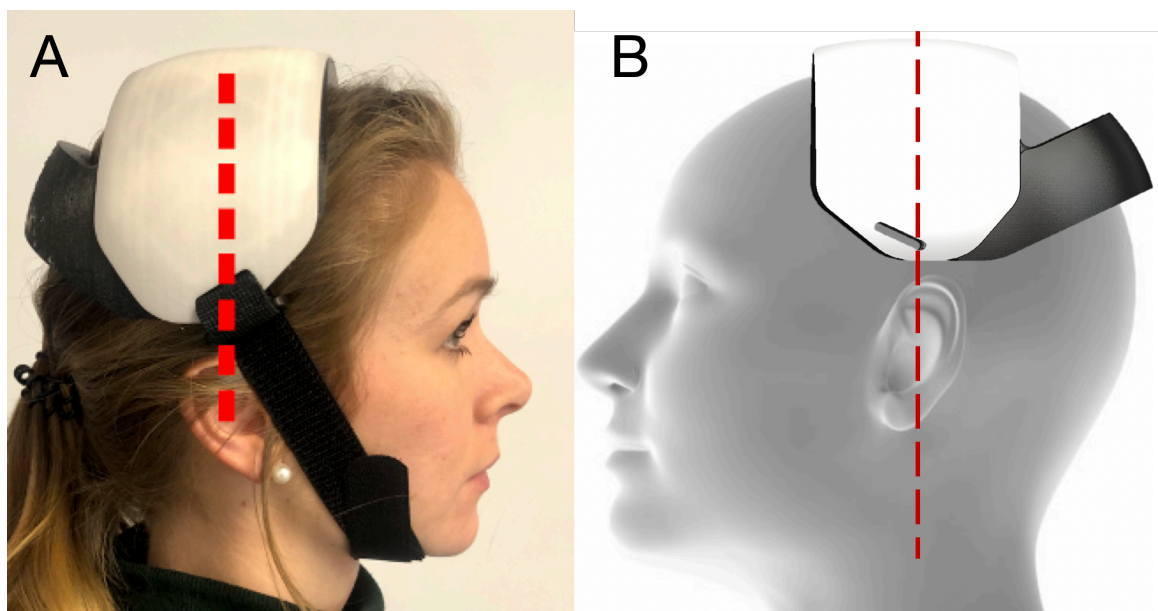


*Figure 4-1. (A) AP-LL prototype used in the present study, together with the visual cue (red line) used as an overlay for the instructions that were presented to participants in the present study. (B) A revised version of the visual used for the instructions for AP-LL placement used for latter participants.*

##### **4.1.4.1 AP-LL**

The design of the AP-LL prototype was meant to approximate the look and feel of the functional prototype that would follow AP-2 in development. Thus, it was the product of several constraints and requirements (many of which are included in the User Needs outlined in Appendix C). Having validated the performance of AP-2 (see Chapter 2), and (in the time since designing AP-2) having decided to focus on measuring cortical activity associated with upper-extremity movements only, AP-LL then needed to be capable of supporting the similar fNIRS measurement capabilities (i.e., providing analogous power to analogous optical components housed in an analogously flexible manner) as per AP-2, with the important exception that it did not need to measure from the medial measurement positions AP-2 was capable of measuring from.

Of particular importance in the present study, AP-LL was designed to order to be donned with one hand (UN-13 in Table 4.1) and placed in the correct place on the head (UN-9 in Table 4.1). While the final product will need to be tolerable to wear for a minimum of 30 minutes (UN-P-4 in Table 4.1), this was not the focus of AP-LL, as it was decided that gaining preliminary validation on its ability to meet UN-13 and UN-9 (see Table 4.1) was of higher priority.

#### *4.1.4.2 AP-2*

As mentioned above, AP-2 (described in Chapter 2) was used in the present study in order to take fNIRS measurements while representative users performed a rehabilitation session using prototype Axem Home software.

#### *4.1.4.3 Axem Prototype Software (AP-S)*

The Axem Prototype Software (AP-S) utilized in the present study was an android app that participants utilized on a 10” Samsung Galaxy Tablet. AP-S allowed participants to select various exercises to complete (Figure 4.2), then guided them through completion of those

exercises through first-person videos that the participants were instructed to follow along with (Figure 4.3), interspersed with rest periods where participants were shown feedback based on the brain activity readings taken from AP-2 (Figure 4.4-A). Given that AP-S was designed for use by stroke survivors (who may be experiencing some level of cognitive impairment and/or aphasia), the user interface design for AP-S endeavoured to convey only what it needed to, opting for minimalism in the pursuit of clarity. It also strived to express all affordances with the least amount of text possible (given the possibility for cognitive overload in stroke survivors with even minor cognitive impairment<sup>5</sup>, as well as linguistic-specific challenges for stroke survivors with aphasia<sup>6</sup>). For example, the exercise selection screen (Figure 4.2) was clean, sparse, and intended to be clear with respect to the affordances available—opting to represent each exercise with a large icon that spanned the length of the tablet’s screen; while this did require a stroke survivor to scroll up and down to browse the exercises, it allowed for all buttons and text to be relatively large. Moreover, the number of exercises available (five: ball squeeze, coin pick up and place, jar lid twist open and close, towel push, and shoulder raise) were chosen to provide a small amount of variety but were limited in order to avoid overwhelming the stroke survivor with a long list of choices to scroll through. Specifically, this screen enabled stroke survivors to scroll through all available exercises, preview an exercise (whereby the video for the exercise would play for ~5 seconds before closing), or select an exercise. The screen also indicated how often during that session the stroke survivor had completed the exercises.

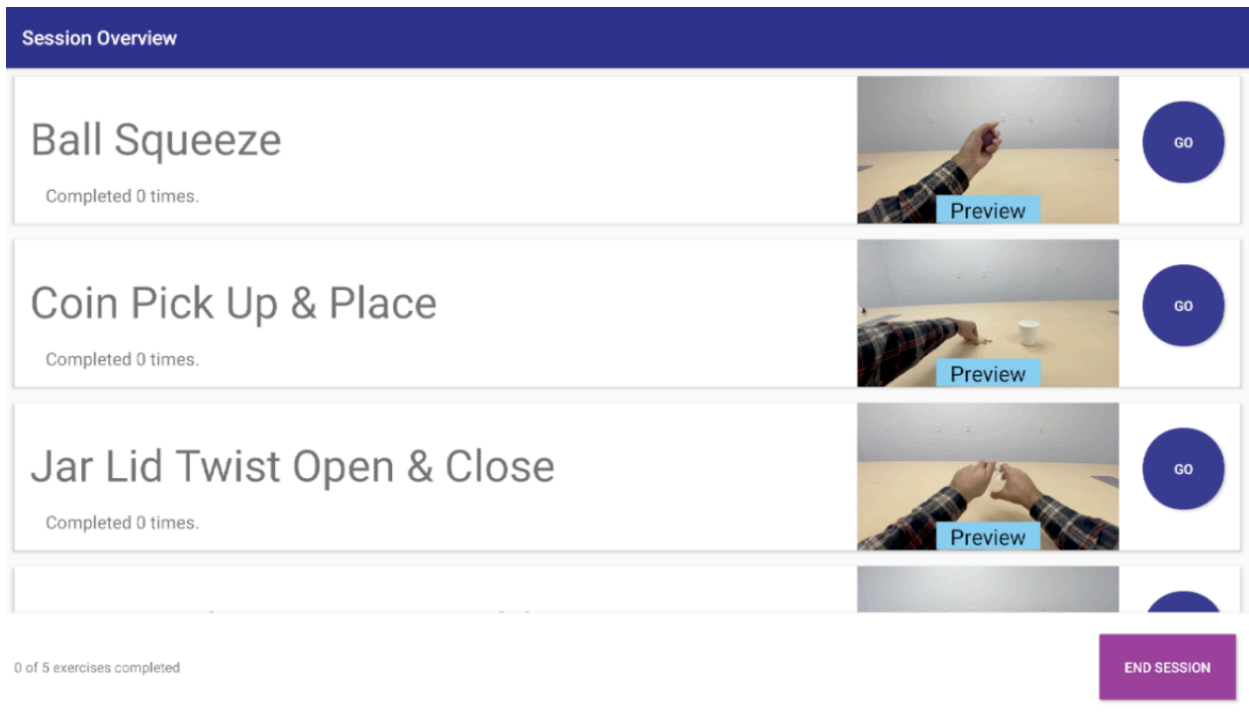


Figure 4-2. Final iteration of the 'exercise select' screen of AP-S.



Figure 4-3. Representative stills from videos that play during rehabilitation exercises. While these videos played participants were instructed to follow along with the movements in the video (or imagine movement if they were not able to approximate the movement at all).

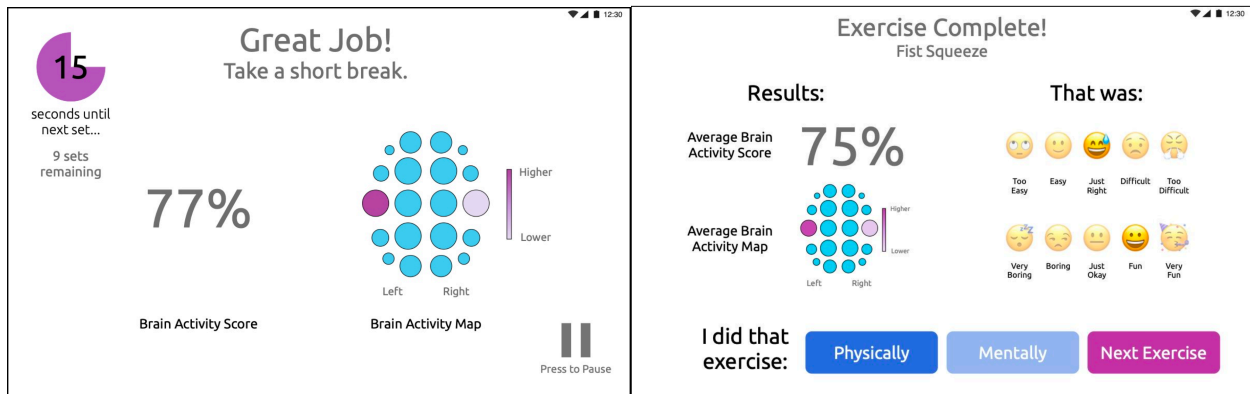


Figure 4-4. **Left pane (A)** - Representative illustration of the ‘rest period’ feedback that would display in between active periods of rehabilitation exercise. A ‘brain activity score’ (see section 4.2.4) was displayed to the participants while a countdown to the next active period counted down. **Right pane (B)** - Representative illustration of the ‘exercise summary’ screen that would display following the completion of all trials for a particular exercise the participant had selected. Participants were also able to rate their perceived challenge and enjoyment associated with that particular exercise, using a visualized Likert scale.

Likewise, the screen during exercises (i.e., when stroke survivors are intended to be performing rehabilitation exercises, either physically or through motor imagery) only showed the first-person video of upper-extremity movement (Figure 4.3), and the screen during rest periods (which was displayed in between exercises) displayed a single brain activity metric as a percentage, as well as an accompanying heatmap overlaid on a simplified glass brain (Figure 4.4, left pane). The screen that displayed at the end of an exercise was the one screen that contained >3 affordances, as it gave stroke survivors the ability to indicate how difficult and enjoyable that exercise was, to indicate whether they’d performed the exercise physically or through imagery, and (required to leave the screen) to decide when to progress back to the exercise select screen (Figure 4.4, right pane); in addition to these affordances, this screen displayed an average of the brain activity scores the stroke survivor had received throughout that exercise (again expressed as a percentage), as well as an accompanying topographical map illustrating this brain activity level overlaid on the simple glass brain.

#### **4.1.4 Study Design Overview and Rationale**

As outlined above, the present formative usability study was completed with preliminary prototypes of the Axem Home that necessitated that the protocol be comprised of two separate simulated user tests—firstly, participants were asked to don AP-LL, and following this, participants were asked to complete a rehabilitation session using AP-S (while fNIRS data was being collected with AP-2, which was set-up by the experimenter). These simulated user tests (further described in sections 4.2.4.1 and 4.2.4.2 below) are examples of ‘task success’-based usability evaluation methods (i.e., evaluating usability based on participant’s ability to complete the tasks provided), which are considered to be the optimal method of assessing questions of effectiveness (see the “Method Evaluated in the Present Study” column of Table 4.1 for more information).<sup>1</sup> Following these two user tests participants were asked to complete a usability questionnaire (see Appendix D) based on the technology acceptance model.<sup>7</sup> This questionnaire was designed to further assess these prototypes’ effectiveness (via questions which closely mirrored those intended to assess “perceived ease of use” in the technology acceptance model<sup>7</sup>), as well as participants’ perception of their usefulness (via questions which closely mirrored those intended to assess “perceived usefulness” in the technology acceptance model<sup>7</sup>). And finally, following this, participants were asked to complete a semi-structured usability interview (see Appendix D) which asked participants their opinion on specific features of the Axem Home prototypes used in the study, and allowed for follow-up on the results of the two simulated user tests, as well as the participant’s responses to the usability questionnaire.



Table 4-1. User Needs addressed in some capacity in the present study.

User Need	Research Question in Present Study	Method Evaluated in Present Study
UN-1 - Patient users need device headband to collect valid fNIRS data from the motor cortex while they perform a reasonably wide variety of seated upper-body movements	n/a	Preliminary evaluation provided through analysis of fNIRS data collected (see Chapter 5).
UN-14 - The Device shall be provided with clear and concise user instructions	n/a	Feasibility of both AP-LL and AP-S testing. Specific questions (asked through the Usability Interview) related to misunderstandings or sub-optimal occurrences in the AP-LL and AP-S testing.
UN- 3 - Patient users needs the device headband to be safe and usable in their home environment.	To what degree are users able to successfully don the Axem headset?	Feasibility of the AP-LL testing Feasibility of AP-2 testing for >30 minutes usability questionnaire question "How comfortable did you find the Axem Home prototype?" <i>How difficult was it to place the Axem Home surface model in the correct position?</i>
UN-4 - Patient users need to tolerate wearing the device headband for at least 30 minutes uninterrupted, and 45 minutes each day.	n/a	Feasibility of AP-2 testing for >30 minutes usability questionnaire question " <i>How comfortable did you find the Axem Home prototype?</i> " Feasibility of the AP-LL testing performed
UN-9 - Patient users need to be able to consistently and correctly place the device headband on their heads. UN-13 - The device will be designed so that it can be donned with one hand	n/a	Feasibility of the AP-LL testing
UN-13 - The device will be designed so that it can be donned with one hand	n/a	Measurement results of AP-LL testing <i>How difficult was it to place the Axem Home surface model in the correct position?</i>
UN-10 (1) - Patient users need to navigate the device app in order to conduct rehabilitation sessions	To what degree are users able to successfully navigate through a session using the Axem app?	Feasibility of AP-S testing

		usability questionnaire question: How difficult was it navigate the Axem Home app? ----- How useful did you find the video provided during movement periods?
UN-11 - Patient users need to understand the feedback they receive during rehabilitation sessions.	To what degree are users able to successfully navigate through a session using the Axem app?	usability questionnaire question: "How did you find the feedback provided during rest periods?" ----- Usability questionnaire question: "How did you find the data presented in the 'Session Review' screen?"
n/a	To what degree do users perceive the product as useful?	Using the Axem Home would cause me to spend more time doing rehabilitation exercises. ----- If you had access to the Axem Home, how often do you think you would use it? ----- Using the Axem Home would help me do rehabilitation exercises better. ----- I would recommend using the Axem Home to another stroke survivor. ----- I would find the Axem Home useful. ----- How useful did you find the feedback provided during movement periods?

**4.2 METHODS**

**4.2.1 Note on COVID-19’s impact on the present study**

It should be noted that the approved research ethics for the present study specified that 30 participants would be included, and that participants might be offered the opportunity to complete subsequent sessions if they were willing and it was deemed feasible and useful for the study sponsor, Axem Neurotechnology. However, due to the public health risk represented by the COVID-19 pandemic, data collection was paused in March of 2020; and while data collection could have technically begun months later, due to uncertainty about the pandemic, as well as the study’s structure being suboptimal for the immediate post-pandemic period (i.e., involving experimenters entering the homes of predominantly elderly individuals) the study’s sponsors decided to discontinue the study. This is the reason only 12 participants were included in the results reported herein. Moreover, during the course of the study, only 2 participants engaged in subsequent sessions (with one participant completing four and another completing

two); as longitudinal data was obtained from a small sample and had a limited number of observations, its inclusion was not warranted.

#### **4.2.2 Participants & Inclusion Criteria**

Twelve self-reported stroke survivors were recruited from the Halifax Regional Municipality and the surrounding area. Participants were recruited via word of mouth and internet advertisements. The study was approved by Veritas IRB.

Participants were required to self-report having previously experienced at least one stroke, and to be currently experiencing hemiparesis of the upper-extremity (e.g., self-reporting unilateral weakness or limited function in the stroke-affected limb). The inclusion criteria for this study was left intentionally broad, to ensure a varied population was represented in this, the first formative usability study for the Axem Home. Inclusion criteria were:

1. *Self-reported stroke survivor.*
2. *Self-reported hemiparesis of the upper extremity.*
3. *>17 years of age*
4. *Score >16 on the Mini mental state examination (MMSE) or (if they do not score >16 on the MMSE and ≤14 on the Language Screen Test (LAST)) >19 on the Cognitive Assessment for Stroke Patients (CASP).*

#### **4.2.3 Measures**

##### *4.2.3.1 Mini mental state examination*

The MMSE contains 30 questions designed to identify whether individuals are experiencing cognitive impairment. The MMSE takes about 10 minutes to complete and was administered by the experimenter. The cut off for participation used in the present study was the level set for administration of the stroke impact scale (SIS; see “6.5 – Stroke Impact Scale”

below) — that is, a score of 16/30 (53%)<sup>8</sup>— to ensure participants are capable of following instructions and providing valid feedback.

#### *4.2.3.2 Cognitive Assessment scale for Stroke Patients*

While the MMSE was utilized due to its clinical ubiquity (particularly in the United States), a low score on the MMSE may be due to aphasia rather than cognitive impairment. Given that Axem may be able to design its software to be usable by stroke survivors living with aphasia, it was not desirable to exclude stroke survivors who were experiencing aphasia symptoms but were otherwise cognitively intact; for this reason, participants with a score  $\leq 16$  on the MMSE, who also scored on the  $\leq 14$  on the LAST, (indicating the presence of significant aphasia symptoms) were then administered the Cognitive Assessment scale for Stroke Patients (CASP), which has been designed to assess cognitive impairment without using language.<sup>9,10</sup> The CASP contains 36 items designed to identify whether individuals are experiencing cognitive impairment. The CASP takes ~10 minutes to complete and was administered by the experimenter. The cut off for participation in this experiment was a CASP score of  $\geq 19$ , a score which has been shown to be equivalent to a score of 16 on the MMSE<sup>11,12</sup>.

#### *4.2.3.4 Demographic Questionnaire*

Participants were given a brief demographic questionnaire that asked them the following questions:

1. What is your age?
2. How many strokes have you had in total?
3. When did your most recent stroke occur?
4. In which arm do you experience weakness, spasticity or paralysis?
5. What was your dominant hand before your stroke?

#### *4.2.3.5 Head Measurements*

In order to characterize the accuracy of the placement of the AP-LL prototype, to ensure the AP-2 prototype was placed in the same position across participants, and to potentially understand the effect of different head shapes and sizes on the performance of these prototypes, the following measurements were recorded: nasion-to-inion distance, tragus-to-tragus distance, and head circumference.

#### *4.2.3.6 Stroke Impact Scale – Hand Domain (SIS-Hand)*

Participants were asked to complete the SIS-Hand, which is comprised of five questions pertaining to their perception of their stroke-affected hand function. The SIS is a well-established stroke specific health status measure that is appropriate for self-report and does not require training to administer.<sup>8</sup>

#### *4.2.3.7 Fugl-Meyer short form upper extremity section*

To provide further context for understanding the results of the usability test, participants had their function characterized using the Fugl-Meyer short form (FM-12) upper extremity section — a series of six standardized tasks that span a wide range of difficulty level for stroke survivors with upper extremity hemiparesis — as it has been shown to adequately assess motor function of stroke patients while subjecting patients to minimal assessment time (< 10 minutes).<sup>13,14</sup> Assessment of FM-12 items was administered using previously established standardized procedures.<sup>15,16</sup>

#### *4.2.3.8 Usability questionnaire and interview*

Participants were asked to complete a usability questionnaire, and the experimenter then followed up with a brief, semi-structured interview about the particulars of the participants use of the Axem Home surface model and/or the Axem Pro app. The usability questionnaire attempted

to further clarify the performance of AP-LL, AP-2, and AP-S to satisfy several fundamental User Needs (see Table 1 for summary of the user needs relevant to the present study and their relation to the study's design, as well as Appendix D for full Usability Questionnaire and Usability Interview) with five- or seven-item Likert scale questions; for example, several questions presented a statement, then asked participants to indicate their level of agreement, with five items anchored by 'strongly agree' and 'strongly disagree'; other questions utilized a 5-item question anchored by 'Very Easy' and 'Very Difficult' in order to ascertain participants' perceptions of the ease of use associated with a particular feature or design element of these prototypes (e.g., the use of AP-LL with a single hand, or a particular user interface element of AP-S). The usability interview consisted of specific questions probing the participants' opinion on specific features of the prototypes used; this interview format allowed for impromptu follow-up questions on the details of the participant's simulated user tests, as well as their responses to the usability questionnaire; questions were constrained to those relevant to observations the experimenter had during the experiment that might have implications for these same user needs. The total time allotted for the usability interview portion of the experiment was limited to 10 minutes maximum.

#### **4.2.4 Experimental Protocol**

All subjects participated in a single usability testing session that took place in their homes.

##### *4.2.4.1 AP-LL Simulated User Testing*

Participants were asked to place the AP-LL with minimal instructions: simply a photo of someone wearing it correctly, together with instructions that the white band should be approximately in-line with their ears (see Figure 4.1 for multiple iterations of the visual

instruction that were given throughout the course of the study). After the participant placed the device on their head and adjusted the strap, the experimenter measured the distance from the nasion to the front of the device; this distance was subsequently compared to the optimal placement of the device (i.e., such that the center of the device lining up with the C level of the international 10-20 system<sup>17</sup>).

#### *4.2.4.2 AP-S Simulated User Testing*

Participants conducted a rehabilitation session using AP-S and AP-2. The experimenter placed AP-2 on the participants head such that the middle of the device in the sagittal plane lined up with the C level of the international 10-20 system<sup>17</sup>, and adjusted the chin strap so that it was snug yet comfortable. The experimenter then powered on the AP-2 device and initiated data collection.

The participant was then prompted to turn their attention to a tablet where the AP-S user interface displayed the ‘exercise select’ screen (see Figure 4.2), which displayed 6 possible exercise activities they could engage in; these exercises were selected in order to cover a wide variety of challenge levels as well as engage all upper-extremity muscles. Participants were instructed to choose any exercise they like, but that they should choose the ‘fist squeezing’ exercise (see Figure 4.3, left pane for a still frame from this video) as their first choice.

All exercise sessions consist of a 30 second rest period followed by ten 40 second trials, where participants were instructed to move according to the guidance of the video for 10 seconds (or imagine moving if they could not), then rest for 30 seconds. During the 10 seconds of movement, a looping first person video of a person performing a unilateral upper extremity movement was played (see Figure 4.3). The side of the upper-extremity being moved corresponded to the side on which the participant self-reported to experience hemi-paresis.

Moreover, while a feedback signal signifying the level of brain activity in the hemisphere contralateral to the hand being moved was displayed during rest periods (Figure 4.4-A), the calculation of this feedback signal was not working as expected throughout this study, and thus participants were instructed of this and told to not become too fixated or concerned by the values they saw.

#### **4.2.5. fNIRS Analysis and Feedback Signal**

Given that the fNIRS data collected in the present study are analyzed in Chapter 5, the fNIRS pre-processing and results will not be described in this chapter.

### **4.3- RESULTS**

#### **4.3.1 – Participant Characteristics**

No participants were excluded due to a score of  $<18$  on the MMSE (26.45; SD = 4.54; see Figure 4.5). Participants averaged 2.57 on the SIS-hand (SD = 1.17) and 8.75 on the FM-12 (SD = 3.02)—see Figure 4.5 for visualization of these scores.

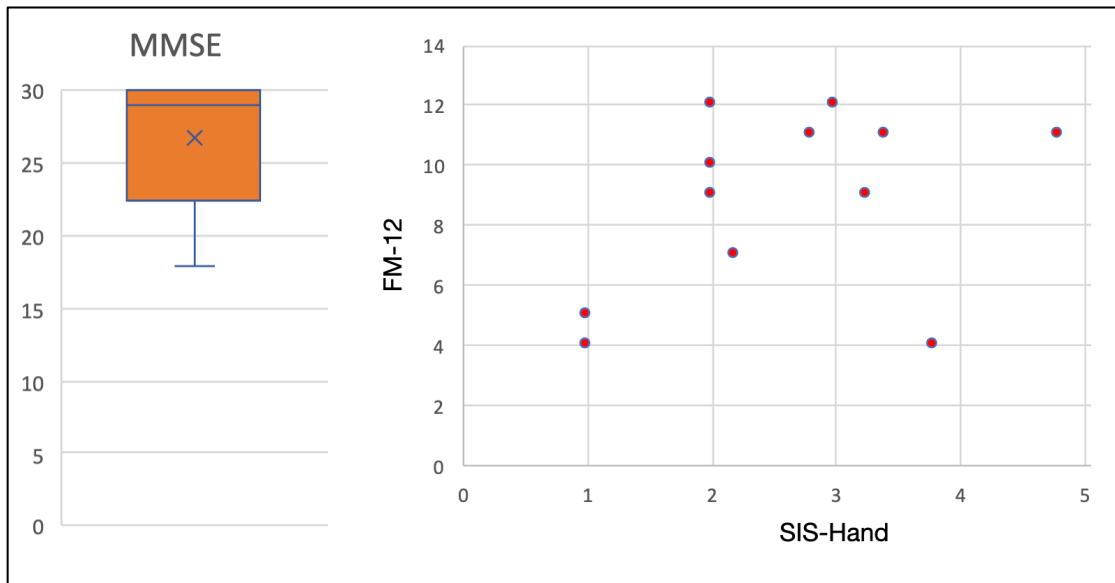


*Figure 4-5.* Left – participants MMSE scores; right – participant scores on the SIS-Hand and FM-12.



### **4.3.2 – General Study Feasibility**

As discussed in section 2.1, the present study was halted prematurely due to the COVID-19 pandemic, and thus only 12 participants were collected. In 11 of these 12 sessions the entire protocol was executed without interruption—while all participants were able to don the AP-LL prototype, one participant did request to prematurely terminate the portion of the session testing AP-2 and AP-S due to discomfort they felt wearing AP-2. However, this was the only deviation from the pre-established protocol due to a usability issue—all other 11 participants were able to complete the protocol, including navigating the AP-S interface in order to conduct several rehabilitation exercises.

### **4.3.3 – AP-LL Testing**

As mentioned in the preceding section, all 12 participants were able to don the AP-LL prototype. However, two of the first seven participants tested initially placed the AP-LL on backwards, and thus required additional instruction to correct its orientation. The instructions used were subsequently updated to better improve the visual clarity of the distinguishing features of AP-LL (see Figure 1-A for the original visual used, and 1-B for the updated visual; also see Appendix E for the full instruction sheets), and this mistake was not repeated by the subsequent participants. Furthermore, in response to the question “How difficult was it to place the model prototype on your head?”, with a Likert scale from -2 (very difficult) to 2 (very easy), participants responded with a mean response of 0.75 (SD = 0.75; see Table 4.3 for full results). However, when examining the placement AP-LL, we see that only five participants placed the device in the range validated by the Data Quality Study (discussed in Chapter 2; see Figure 4.5 for visualization of placement results).

*Table 4-2. Distribution of answers to the question “How difficult was it to place the Axem Home surface model on your head?”*

<i>How difficult was it to place the Axem Home surface model on your head?"</i>	
Very Easy (2)	1
Easy (1)	8
Neutral (0)	2
Difficult (-1)	1
Very Difficult (-2)	0

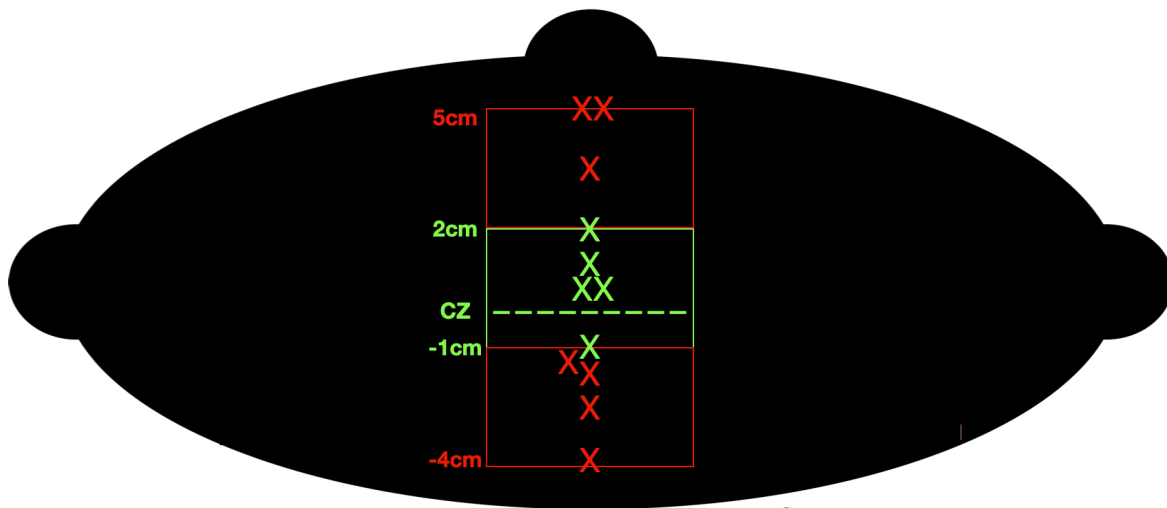


*Figure 4-6.* Locations where individuals placed the AP-LL model in the current study. The location marked represents the position of the center of the AP-LL model in the sagittal plane. The green locations represent those measurement locations verified as valid placement locations in the Data Quality Study (Chapter 2).

#### **4.3.4– AP-S/AP-2 Testing**

As mentioned above, 11 of the 12 participants in the present study were able to successfully complete the entire AP-S/AP-2 testing protocol as intended. The one participant who declined to complete the protocol cited discomfort in wearing the AP-2 prototype, while all other participants wore the AP-2 for the duration of testing with the AP-S (at least 30 minutes). Furthermore, when examining the responses to the question “How comfortable did you find the Axem Home prototype?”, with a Likert scale from -3 (very painful) to 3 (very comfortable) the mean response was 0.92 (SD = 1.3 see Table 4.4 for full results).

Table 4-3. Distribution of answers to the question “How comfortable did you find the Axem Home prototype?”

How comfortable did you find the Axem Home prototype?	
Very Comfortable (-3)	1
Comfortable (-2)	4
Slightly Comfortable (-1)	3
Neither Comfortable or Painful (0)	1
Slightly Painful (1)	3
Painful (2)	0
Very Painful (3)	0

On questions investigating the ease with which participants were able to use the AP-S to complete a rehabilitation session, as well as understand the individual aspects of the AP-S interface, participants answered slightly positively (i.e., more positive than neutral but not strongly positive). For instance, in response to the question “How difficult was it navigate the Axem Home app?”, on a Likert scale from -2 (very difficult) to 2 (very easy) participants’ mean response was 0.58 (SD = 0.40), and answers of a similar valence were given to questions about the usefulness of the videos shown during the movement periods, as well as the feedback provided during the rest periods and upon completing an exercise (see Table 4.5 for full results).

Table 4-4. Distribution of answers to the questions relating to the usability of the AP-S software prototype.

How difficult was it to navigate the Axem Home app?		How useful did you find the video shown during movement periods?	
Very Easy (2)	0	Extremely Useful (2)	2
Easy (1)	9	Considerable Useful (1)	2
Neutral (0)	2	Moderately Useful (0)	8
Difficult (-1)	0	Slightly Useful (-1)	0
Very Difficult (-2)	1	Not Useful at all (-2)	0

How useful did you find the feedback provided during rest periods?		How useful did you find the data presented in the summary screen at the end of each exercise?	
Extremely Useful (2)	1	Extremely Useful (2)	0
Considerable Useful (1)	3	Considerable Useful (1)	2
Moderately Useful (0)	4	Moderately Useful (0)	5
Slightly Useful (-2)	3	Slightly Useful (-1)	2
Not Useful at all (-1)	1	Not Useful at all (-2)	2

#### **4.3.5 – Assessment of Perceived Usefulness**

The usability questionnaire used in the present study also contained five questions assessing the perceived usefulness of the Axem Home system. Four of these questions used 5-item Likert scales, and on all of these questions the mean response from participants lay between the first and second most positive response (see Table 4.6). And moreover, participants response to the 1-to-10-rating question “I would recommend using the Axem Home to another stroke survivor” (with 1 indicating they definitely would not recommend, and 10 indicating they definitely would) averaged 8.25 (SD = 1.48).

*Table 4-5.* Distribution of answers to the questions relating to the perceived usefulness of the Axem Home system.

If you had access to the Axem Home, how often do you think you would use it?		Using the Axem Home would help me do rehabilitation exercises better.	
More than 2 times per week (2)	8	Strongly Agree (2)	7
2 times per week (1)	1	Agree (1)	4
Once per week (0)	3	Neutral (0)	1
1-2 times per month (-1)	0	Disagree (-1)	0
Less than once per month (-2)	0	Strongly Disagree (-2)	0
Using the Axem Home would cause me to spend more time doing rehabilitation exercises.		I would find the Axem Home useful	
Strongly Agree (2)	3	Strongly Agree (2)	3

Agree (1)	8	Agree (1)	8
Neutral (0)	1	Neutral (0)	1
Disagree (-1)	0	Disagree (-1)	0
Strongly Disagree (-2)	0	Strongly Disagree (-2)	0

#### 4.4- DISCUSSION

While it is unfortunate the current study was cut short due to COVID-19, strides were made towards its purpose: to assess the ability of representative users of the Axem Home to utilize it independently in a home environment, and specifically to identify challenges that must be overcome to initiate a clinical pilot where users do in fact use a similar prototype of the Axem Home independently.

For instance, results from the present study suggest that representative users of the Axem Home are able to place a prototype projected to look and feel like the one used in eminent clinical pilots (AP-LL) with minimal instructions. However, two of the first seven participants did place the device in the wrong orientation; and while the subsequent five participants, who used an updated visual to provide instruction on the orientation of the device, did not make this mistake, more work is warranted to ensure instructions are sufficiently expressive and clear. In particular, the second revision of these instructions used were more visually simple, using an artificial representation of a head and the headband, instead of a photograph of a person wearing the device (see Figure 1 for the visualizations used in the original and updated instructions). Moreover, the deficits of the original instructions suggested the text which accompanied the visualization of the optimal placement of the headband were sub optimal; work conducted in parallel with speech language pathologists lead to the revision of these textual instructions as well, with a move away from full sentence explanations and to short, succinct statements captured in individual bullet points (see Appendix E for the full sets of the original and revised

instructions). Another learning was that multiple participants (through the usability interview) mentioned how video instructions would have been preferable to the static instructions provided in the present study. Moreover, results also showed that placement of the device was inconsistent, as only 5 of the 12 participants managed to place the device in what would be considered a valid location on the head (i.e., the 5cm range around the C level of the international 10-20 system<sup>18</sup>, which had been validated by the Data Quality Study, as outlined in Chapter 2, and the NIRScout comparison study, as described in Chapter 3). This suggests that further work is needed on the features facilitating adequate positioning of the headband in the sagittal plane. In particular, these results suggest that the approach of using a single chin strap together with instructional cues may be deficit, and that the user experience should be dictated more so by the design of the headband itself rather than instructional cues—thus a re-thinking of the strapping system is required. For instance, if the device had a strapping system that was sized in the sagittal plane it might allow users to simply tighten the device and get it in the correct position consistently, rather than relying on an adequate understanding of instructions. Such an approach is reflected in the standard approach to risk reduction in medical device development, where inherent safety by design is strongly favoured over the use of instructions to ensure safety. While this focus on headband design is likely the most prudent approach to iterate on the AP-LL design, long-term solutions involving computer vision could also bear fruit—though since these would also place the burden more so on the user than a design solution targeting the design of the headband itself, this should not be considered a focus at the present time.

It should also be noted that measurements and instructions in the present study did not address the symmetry of the headband in the row or yaw planes. Thus, future design and usability studies should contend with these current deficits in the design of AP-LL and its

associated instructions, providing features on the headband and accompanying instruction that might ensure that users are able to correctly achieve and/or assess and correct the placement of the headband in all three planes.

With respect to the comfort of the AP-2 device, it was rated as moderately comfortable on average by the participants in the present study. However, given the small sample size and the fact that one of the participants was unable to complete the protocol with the AP-2 as intended, more work is warranted on improving the comfort, given the significant risk of discouraging repeated use if the Axem Home headband is insufficiently comfortable. While the use of light guides of a lower durometer than those used in the present study would introduce a trade off with a reduction in light transmission, there are other more preliminary steps that might be taken to increase comfort, such as: further optimization of the ‘comfort features’ (Figure 4.6), which are meant to reduce the pressure on the light pipes by the creation of a ‘bed of nails’ effect—these features have not been experimented since the move from AP-1 to AP-2 (as described in Chapter 2 of this dissertation), and thus iterating on the material they are composed of, the placement and orientation within the headband, as well as the geometry of the individual features themselves would be fertile ground for improvements in comfort. And lastly, given that the present study was just a single session, it is unknown whether the completion of sequential sessions, repeatedly over many days, might render the Axem Home headband less comfortable over time; this is another aspect of comfort testing that warrants further testing.

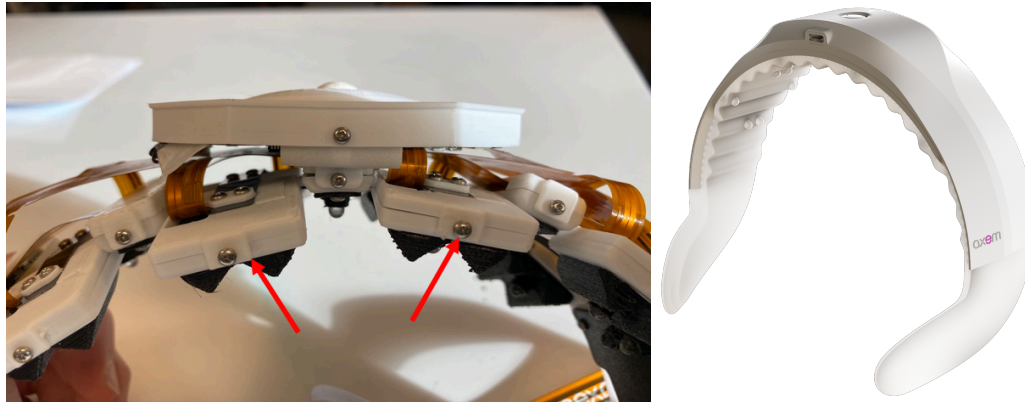


*Figure 4-7.* Images where the ‘comfort features’ (i.e., ridges on the ventral side of the headband, meant to reduce the pressure felt at the tip of the light guide) are illustrated in both the AP-2 (left pane; black bumps on the ventral side of the pods denoted with the red arrows) and in idealized industrial design of the Axem Home (right pane; see the ridge in white lining the ventral portion of the headband).

Similar to the topics of headband user experience and comfort discussed above, while the present study provides a preliminary indication that this prototype version of the usability app (AP-S) is in fact usable by representative users in a home environment, there are several caveats and nuances that remain open questions. Firstly, while all users were capable of completing a session of rehabilitation using AP-S, the average response to “How difficult was it navigate the Axem Home app?” was only modestly positive. This indicates that the app was not altogether easy or simple to use; and given that AP-S did not include all facets of the final user experience, or even all features that would be necessary for a preliminary clinical trial—such as connection to the headband and calibration of the headband—this suggests that improvements in the usability of the app are warranted. In particular, the suggestion provided by participants discussed above, the instructions for placement of the headband might benefit from a video tutorial, may be applicable here as well, as the present study used a static Powerpoint slide-style presentation of introductory information, which may not be ideal. Furthermore, despite the fact that participants answered in the affirmative that the videos provided during movement periods were helpful, the average response was only slightly positive. Moreover, it was observed that



while some participants used the videos in order to imitate their movements exactly, others simply used them as a guide, concentrating their visual attention rather on the upper-extremity being used in the movements; this was not anticipated, and should be factored into the design, either through explicit recognition in the tutorial, or specific guidance towards one method or the other. And finally, unfortunately the brain activity feedback signal presented during rest periods was not working reliably during the present study (and the communication that was made to the participants to this effect) and thus its effectiveness and utility could not be tested. This represents a notable omission from the assessment of the complete software component of the Axem Home system, as while participants were exposed to the brain activity feedback scores during rest periods and exercise summary screens (Figure 4.4) they were instructed to “not place too much consideration or concern” on the precise numbers presented (so as to assuage any worry that something was wrong if the numbers presented were low), as they may not be reliable in the current study. Thus, while the responses participants provided were a valuable initial indication that such feedback signals presented at these points in the user experience might be useful (on average participants rated these feedback signals moderately useful), the optimal manner in which to introduce these feedback signals, as well as the utility of presenting them remain open questions. However, it should be noted, that through the responses of the participants to these feedback signals (both during the AP-2/AP-S testing, as well as during the usability interview) it became clear that presenting these feedback signals as percentages was not optimal: they raise the question of ‘what might they have done differently?’ to gain that explicitly-quantified additional percentage, and in that way have almost a negative or punitive connotation. Based on these preliminary observations, it seems clear that representations of these

feedback signals that are not explicitly quantified (i.e., expressing the level of brain activity through graphical representation alone) might be preferable for this application.

And finally, users provided strongly positive responses to questions assessing the perceived utility of the Axem Home system for use in the independent performance of upper-extremity rehabilitation in the home environment; however, as this is one of the core aspects that upcoming clinical pilots of the Axem Home system are meant to test, no preliminary self-reported positive affirmation of ‘perceived usability’ should be considered a replacement for real user data demonstrating actual utility (in the form of actual data showing compliance with use of the Axem Home system). Moreover, an important limitation of the present study in this regard is that there was no blinding implemented, and the participants were in fact often aware that the experimenters were responsible for the construction of the Axem Home prototypes they were using. This may have led to a bias towards positive responses, and while (as stated above) measures of utility will not be taken as proof of utility, the lack of blinding in the present study may have resulted in false positive feedback, with participants exaggerating the perceived utility of the Axem Home system, and therefore precluding the present study from generating more insightful and actionable insights on perceived usefulness of the Axem Home system.

Another important limitation is sample size; due to the unforeseen termination of the study as a result of COVID-19, the sample size collected represents less than half of the intended number of participants originally intended (i.e., 30); moreover, the sample size of 12 is less than the minimum suggested by various established international guidelines for usability testing<sup>2,3,19</sup>. Another limitation of the present study is the fact that the overall user experience of the Axem Home was artificially broken up into constituent parts: given that the working fNIRS prototype used in the present study could not be independently operated and donned by the participants.

This artificial separation of aspects of the user experience which might be otherwise be seamless limits the ecological validity of the findings surrounding the assessment of the usability of these preliminary Axem Home prototypes<sup>1</sup>. Therefore, in addition to the specific improvements required (discussed in the preceding paragraph), there is a need to blend together all elements of the Axem Home user experience into a seamless whole for preliminary testing with representative users. Moreover, the present study also neglected to incorporate other aspects which will be required in the full user experience, such as turning the headband on/off, connecting the Bluetooth within the app, calibrating the headband in the app, and charging the headband.

With all this said, these results suggest the prototypes used in the present study (AP-LL, AP-2, and AP-S) are usable by representative users. Specifically, these results suggest AP-2 can be used to of take such measurements in a home environment (see Chapter 5 for a discussion of these data specifically), that AP-LL may be usable by stroke survivors with a single hand, and that AP-S is capable of guiding stroke survivors through a rehabilitation session. Therefore, the present study represents a significant stride towards the realization of a novel achievement in neuroergonomics—as despite the expansive literature surrounding the application of brain-computer-interface (BCI) systems to post-stroke physical rehabilitation, no rehabilitative BCI system has ever enabled stroke survivors to operate it independently. While in the present study the complete BCI user experience was artificially segregated into discreet tasks (e.g., placing the headband and operating the software), all core elements of the final Axem Home user experience were tested in the present study, with some level of feasibility validated for each of them. This represents a significant step in and of itself, and more importantly, as outlined, it provides an actionable assessment of where subsequent validation efforts ought to be applied.

## 4.5 REFERENCES

1. Rubin, J. & Chisnell, D. *Handbook of Usability Testing*. (Wiley).
2. IEC/TR 62366-2: Guidance on the application of usability engineering to medical device. (2016).
3. U.S. Department of Health and Human Services Food and Drug Administration. Applying Human Factors and Usability Engineering to Medical Devices. (2011).
4. Folstein, M. F., Folstein, S. E. & McHugh, P. R. "Mini-mental state". *J. Psychiatr. Res.* **12**, 189–198 (1975).
5. Jamieson, M., Cullen, B., Lennon, M., Brewster, S. & Evans, J. Designing ApplTree: usable scheduling software for people with cognitive impairments. *Disabil. Rehabil. Assist. Technol.* 1–11 (2020) doi:10.1080/17483107.2020.1785560.
6. Mobile computing technology and aphasia: An integrated review of accessibility and potential uses: *Aphasiology*: Vol 27, No 4.  
<https://www.tandfonline.com/doi/abs/10.1080/02687038.2013.772293>.
7. Davis, F. D. Perceived Usefulness, Perceived Ease of Use, and User Acceptance of Information Technology. *MIS Q.* **13**, 319–340 (1989).
8. Sullivan, J. E. Measurement Characteristics and Clinical Utility of the Stroke Impact Scale. *Arch. Phys. Med. Rehabil.* **95**, 1799–1800 (2014).
9. Barnay, J.-L. *et al.* Feasibility of the Cognitive Assessment scale for Stroke Patients (CASP) vs. MMSE and MoCA in aphasic left hemispheric stroke patients. *Ann. Phys. Rehabil. Med.* **57**, 422–435 (2014).

10. Benaim, C. *et al.* The Cognitive Assessment scale for Stroke Patients (CASP) vs. MMSE and MoCA in non-aphasic hemispheric stroke patients. *Ann. Phys. Rehabil. Med.* **58**, 78–85 (2015).
11. Crivelli, D. *et al.* When is a novel psychometric measure needed? A preliminary analysis regarding the Cognitive Assessment for Stroke Patients (CASP) battery compared with MMSE and MoCA. *Appl. Neuropsychol. Adult* **25**, 410–416 (2018).
12. Park, K.-H. *et al.* The Korean Version of the Cognitive Assessment Scale for Stroke Patients (K-CASP): A Reliability and Validity Study. *Ann. Rehabil. Med.* **41**, 362–375 (2017).
13. Hsieh, Y.-W. *et al.* Development and validation of a short form of the Fugl-Meyer motor scale in patients with stroke. *Stroke* **38**, 3052–3054 (2007).
14. Chen, K.-L. *et al.* Is the long form of the Fugl-Meyer motor scale more responsive than the short form in patients with stroke? *Arch. Phys. Med. Rehabil.* **95**, 941–949 (2014).
15. Alt Murphy, M., Danielsson, A. & Sunnerhagen, K. S. Letter by Murphy *et al* regarding article, ‘Fugl-Meyer assessment of sensorimotor function after stroke: standardized training procedure for clinical practice and clinical trials’. *Stroke* **42**, e402 (2011).
16. Sullivan, K. J. *et al.* Fugl-Meyer assessment of sensorimotor function after stroke: standardized training procedure for clinical practice and clinical trials. *Stroke* **42**, 427–432 (2011).
17. Klem, G. H., Lüders, H., Jasper, H. H. & Elger, C. The ten-twenty electrode system of the International Federation. The International Federation of Clinical Neurophysiology. *Electroencephalogr. Clin. Neurophysiol. Suppl.* **52**, 3–6 (1958).
18. Homan, R. W. The 10-20 Electrode System and Cerebral Location. *Am. J. EEG Technol.* **28**, 269–279 (1988).

19. Applying Human Factors and Usability Engineering to Medical Devices, Guidance for Industry and Food and Drug Administration Staff. (2016).

## Chapter 5 - MEASUREMENT OF SENSORIMOTOR BRAIN ACTIVITY IN STROKE SURVIVORS DURING AT-HOME UPPER-EXTREMITY REHABILITATION: A MOBILE fNIRS PILOT STUDY

### 5.0 Abstract:

Improved understanding of the relationship between post-stroke rehabilitation interventions and functional motor outcomes could result in improvements in the efficacy of post-stroke physical rehabilitation. The laterality of motor cortex activity during paretic upper-extremity movement has been documented as a useful biomarker of post-stroke motor recovery. However, the expensive, labour intensive and laboratory-based equipment required to take measurements of M1-LAT limit its potential clinical utility in improving post-stroke physical rehabilitation. The present study tested the ability of a mobile fNIRS system (designed to enable independent measurement by stroke survivors) to measure cerebral hemodynamics at the motor cortex in the homes of chronic stroke survivors. Eleven chronic stroke survivors, ranging widely in their level of upper-extremity motor deficit, performed a simple unilateral movement protocol (using their paretic upper-extremity) in their homes while a wireless prototype fNIRS headband took measurements at the motor cortex. Both objective (FM-12) and self-reported (SIS-Hand) measures of participants' upper-extremity function were taken. Participants demonstrated either a typically lateralized response, with an increase in contralateral  $\Delta\text{HbO}$ , or response showing a bilateral pattern of increase in  $\Delta\text{HbO}$  during the motor task. Laterality index (LI) values during the simple unilateral task correlated significantly with both the FM-12 and SIS-Hand scores, indicating that participants with more severe motor deficits had more a more atypical (i.e., bilateral) pattern of lateralization. It is feasible to gain valid LI values from stroke survivors in their homes using fNIRS. These results represent a preliminary step towards the goals of using

ergonomic functional neuroimaging to improve post-stroke rehabilitative care, via the capture neural biomarkers of post-stroke motor recovery, and/or via use as part of an accessible rehabilitation brain-computer-interface.

## 5.1 INTRODUCTION

It has become part of the consensus in clinical research that the investigation of post-stroke motor recovery must include and make use of neural biomarkers of recovery<sup>1</sup>. Fundamentally, this call for the use of biomarkers is an acknowledgement that our imperfect understanding of the mechanisms of post-stroke motor recovery is holding back our ability to optimize post-stroke care, as well as to develop new rehabilitation interventions. Relatedly, it has been shown that clinical trials with a biological rationale outperform those without one<sup>2</sup>. The persisting uncertainty due to our collective lack of understanding is especially impactful considered in light of the high cost of rehabilitation to the health care system currently (in the U.S. alone over \$41 billion is spent on post-stroke physical rehabilitation)<sup>3</sup>, and the disappointing discrepancy between our inability to meet established standards on the amount of rehabilitation volume stroke survivors should receive<sup>4</sup>, and the pre-clinical literature which suggests that the amount of volume prescribed by these standards is in fact likely insufficient, given the high volume of post-stroke rehabilitation required to facilitate cortical re-organization in the motor system<sup>5</sup>. While the collective realization that more post-stroke rehabilitation is better than less has been used to great effect in the Queen Square programme<sup>3</sup>, which produced uniquely strong positive results with very large volumes of rehabilitation in chronic stroke survivors<sup>6</sup>, this mantra alone is not sufficient to significantly improve the standard of care in post-stroke rehabilitation,

---

<sup>3</sup> In this study 268 chronic stroke survivors were enrolled in an extremely intensive (3-week 90 hour) in-person rehabilitation program, resulting in clinically important improvements on measures of both impairment (e.g., Fugl-Meyer Upper Limb) and functional ability (e.g., Action Research Arm Test).



given the complicated trade-off besetting this issue, with high costs and inconsistent effectiveness of rehabilitation interventions on the other side of the ledger.

Indeed, the attempt to increase the volume of rehabilitation patients receive, as demonstrated in the Queen Square programme, as well as the integration of neural biomarkers into stroke recovery research, might both be viewed as an attempt to overcome the proportional recovery rule of post-stroke motor recovery—which controversially posits that survivors of stroke can be expected to gain back ~70% of the difference between their acute post-stroke function (for a given measure) and typical function, regardless of rehabilitation interventions. This model and its implicit implications (i.e., that stroke survivor’s recovery potential operates by some ‘rule’ independent of rehabilitation) challenge the utility of deploying more public health system resources on rehabilitation as an ‘investment’, given rehabilitation’s highly variable return on investment over-and-above the progress that can be expected regardless of intervention. In the context of these challenges, it is not surprising that some studies have found that nearly half of patients fail to significantly benefit from rehabilitation<sup>7</sup>, and that only 12% of patients fully regain use of their upper-extremity<sup>8</sup>.

However, pre-clinical work<sup>9,10</sup> does suggest the proportionate recovery model can be overcome, specifically by better characterizing an individual animal’s rehabilitation by using neural biomarkers (in this case information on the nature of an animal’s lesion). In this work, researchers created a model that predicted the ‘minimum effective dose’ of rehabilitation required for animals given the details of their lesion, and successfully demonstrated that using this dosage prescription algorithm the number of ‘non-responders’ to rehabilitation was decreased. And recent findings in humans suggest such a concept may generalize across species, as through better characterization a stroke survivor’s rehabilitation needs, it has been shown to

be possible to break the proportionate recovery law in humans,<sup>11</sup> and moreover that through the use of neural biomarkers one can also increase the efficiency of rehabilitation (in this case leading to decreased length of stay at an inpatient rehabilitation facility with no decrease in functional outcomes)<sup>12</sup>.

One promising candidate biomarker of motor recovery in stroke is the ratio of activity between the primary motor cortices during movement of one's paretic limb (i.e., M1-LAT). Using fMRI,<sup>13–16</sup> fNIRS,<sup>17,18</sup> or EEG,<sup>19</sup> it has been shown that deviation from a typical contra-lateralized pattern of M1-LAT corresponds to worse upper-extremity movement deficits. Moreover, fNIRS studies have also found that the inverse pattern (i.e., a departure from the typically symmetrical pattern of M1-LAT) corresponds to worse gait abilities<sup>20,21</sup>. A proposed mechanism for this association is the presence of maladaptive IHI, whereby the contralesional sensorimotor system becomes disinhibited and thus more active during paretic limb movement, reducing or reversing the typical contra-lateralized pattern of sensorimotor activity.<sup>22</sup> And while this relationship does not seem to be universal (in particular in that in a subset of stroke survivors with severe deficits, this IHI may be adaptive, as the ipsilesional corticospinal pathway is not capable of regaining a useful role in the actuation of movement<sup>23</sup>) it has been established as a consistent pattern across stroke location, stage, and severity<sup>22,24</sup>. And importantly, studies have also shown that M1-LAT is not only associated with, but predictive of future function as well as one's response to rehabilitation: it has been found to outperform functional status in predicting motor deficits 3 months<sup>25</sup>, 6 months<sup>26</sup> and one year<sup>27</sup> following incidence of stroke, as well as being predictive of a stroke survivor's treatment response to one month of rehabilitation<sup>28</sup>. One might imagine how widespread, longitudinal collection of M1-LAT in stroke survivors could aid in optimizing how rehabilitation resources are deployed, potentially one day contributing

towards the construction of a personalized model of a minimum effective dose, which pre-clinical data suggests may be the level of rehabilitation at which brain-derived neurotropic factor is released to promote greater recovery<sup>29</sup>; and again, this idea is supported by recent findings which show that even chronic stroke patients can reliably benefit from stroke rehabilitation, given that the volume of rehabilitation is sufficiently intensive<sup>6</sup>. M1-LAT has also been used as a part of a brain-computer-interface that was shown to increase the clinical benefits of post-stroke upper-extremity rehabilitation interventions.<sup>30-33</sup>

However, a major barrier in realizing this potential is that at present it is expensive and labor-intensive to take any relevant biomarkers of post-stroke motor recovery. All the studies mentioned above that utilized M1-LAT to characterize and/or predict recovery used either fMRI or laboratory-based fNIRS/EEG equipment to take their M1-LAT measurements. This is why leaders of the research community have acknowledged this is a central challenge to overcome in the use of any potential biomarkers of stroke recovery<sup>1</sup>. Thus, there is a need to develop technology that makes the collection of relevant biomarkers easier. While the majority of the literature on the relationship between M1-LAT and post-stroke physical recovery has been based on fMRI measurements, the high cost, specialized staff, and lengthy set-up time required to take these measurements limits its clinical utility in this domain. Moreover, the fact that wet, head-cap-based EEG systems require a lengthy set-up process by a trained experimenter, as well as the difficulty in gaining spatially specific measurements with dry and/or non-full-headcap based EEG (due to the smearing of electrical activity at the scalp; as discussed in section 1.4.2)<sup>34</sup> limit its clinical utility for this purpose as well. Given that fNIRS has also been shown to be capable of taking measurements of post-stroke motor laterality,<sup>17,18</sup> that its method of measurement lends

itself naturally to the capture of spatially-specific cortical signals,<sup>4</sup> as well as the fact that it can be made portable (as discussed in section 1.4.2), fNIRS may be a viable modality to increase the clinical utility of M1-LAT in post-stroke physical rehabilitation. Specifically, the use of ergonomic fNIRS devices to capture neural biomarkers of post-stroke motor recovery, and/or to be used as a part of more accessible rehabilitation brain-computer-interfaces has the potential to help clinicians better understand and thereby optimize post-stroke rehabilitation, as well as for the development of brain-computer-interface systems designed to enhance post-stroke rehabilitation.

The present study tests the ability of a prototype fNIRS headband to take measurements of M1-LAT (during upper-extremity movements) from chronic stroke survivors in their homes, and moreover examines the relationship between these measures of M1-LAT and measures of upper-extremity function and impairment. Specifically, the study hypothesizes that measures of M1-LAT taken via fNIRS will correlate with measures of upper-extremity impairment and function. The prototype fNIRS headband was designed to measure cerebral hemodynamics from the sensorimotor cortices, and to enable independent placement by a stroke survivor; the headband is synchronized to a tablet app which guides stroke survivor's through upper-extremity rehabilitation exercises while fNIRS measurements are taken. This work contributes to the ultimate goal of demonstrating that neural biomarkers of post-stroke motor recovery can be taken outside the laboratory, with easy-to-use equipment that might one day enable an improvement of the standard of care for post-stroke physical rehabilitation.

---

<sup>4</sup> Shining near-infrared light into the brain at a particular location, and measuring the returning light at an adjacent location, allowing for inference on changes in a blood-oxygen-level-dependent (BOLD) signal at a point equidistant the emission and detection locations (as discussed in section 1.4.2).

## **5.2 METHODS**

### **5.2.1 Participants – inclusion and exclusion criteria**

Twelve chronic stroke survivors (three women; age:  $m = 62.18$ ,  $sd = 11.77$ ; months since most recent stroke:  $m = 63.27$ ,  $sd = 41.51$ ; these participants are also described in Chapter 4) were recruited from the community. The study received ethical approval from Veritas IRB. Inclusion criteria required participants to self-report that they had previously experienced at least one stroke and were currently experiencing some level of hemiparesis as a result; it also required them to score  $\geq 16$  on the MMSE<sup>35</sup> or (if they failed to do so)  $\geq 19$  on the CASP.<sup>36–38</sup> All but three of these participants reported having experienced only a single stroke.

### **5.2.2 – Cognitive Testing**

Participants were first asked to complete the MMSE. The MMSE contains 30 questions designed to identify whether individuals are suffering from serious cognitive impairment. The cut off for participation used in the present study was the level set for administration of the SIS<sup>39</sup> (see 5.2.5 below), to ensure participants are capable of following instructions and providing valid feedback. While the MMSE was utilized due to its clinical ubiquity (particularly in the United States), a low score on the MMSE may be due to aphasia rather than cognitive impairment; thus if a participant scored less than 17 on the MMSE, they were asked to complete the CASP, a cognitive assessment designed for stroke survivors with language impairments.<sup>36,37</sup> The cut off of 19 chosen for the CASP (as discussed in 5.2.1 above) was meant to harmonize to the MMSE cut off of 16 chosen for the present study.<sup>38,40</sup>

### **5.2.3 - Fugl-Meyer short form upper extremity section**

Participants had their hemiparetic upper-extremity function characterized using the FM-12 upper extremity section — a series of six standardized tasks designed to span a wide range of

difficulty levels for stroke survivors with upper extremity hemiparesis — as it has been shown to adequately assess motor function of stroke patients while subjecting patients to minimal assessment time (< 10 minutes).<sup>41,42</sup> Assessment of FM-12 items was administered using previously established standardized procedures.<sup>43,44</sup>

#### **5.2.4 SIS-Hand**

Participants were asked to complete the SIS-Hand, which is comprised of five questions pertaining to their perception of their stroke-affected hand function. The SIS is a well-established stroke specific health status measure that is appropriate for self-report and does not require training to administer.<sup>39</sup>

#### **5.2.5 – Motor Task**

Experimental sessions took place in the homes of the recruited stroke survivors. All participants performed a fist squeezing task on the side they reported experiencing upper-extremity hemiplegia. Participants were instructed to follow along with a first-person video displayed on a tablet on the table in front of them—the video showed a fist squeezing task being performed with an exercise ball, with the ball being squeezed at ~1Hz. Participants were also provided an exercise ball, which some chose to use but some were not able to make use of because of their deficit in hand function. Participants performed 10 trials where they were instructed to squeeze their fist along with the video in this manner for 10 seconds after which they were asked to rest for 40 seconds. Participants were asked to perform this task as best they could, and to utilize motor imagery (i.e., the mental rehearsal of movement<sup>45</sup>) in the event that they are unable to complete the movement physically. While the fist squeezing task was being performed, measurements at the lateral motor cortex were taken with a prototype fNIRS headband (described in 5.2.6 below, see Figure 1).



*Figure 5-1. Illustration of the experimental set up for the present study. Participants wore the fNIRS prototype headband while a movement video played a fist squeezing task on a tablet. Participants were asked to follow along with the movements in the video as best they could.*

### **5.2.6 Prototype fNIRS Headband**

The fNIRS headband prototype used in the present study (AP-2, as described in section 2.2.2.2 of Chapter 2) was powered by a lithium-ion battery attached to a headband of optical components as previously described in Friesen et al.<sup>46</sup>; the headband utilized Bluetooth low energy and supports a 8 x 2 grid of 16 unique cerebral hemodynamic measurement locations (see Figure 2-B)—thus the fNIRS headband was entirely wireless, with no fiber optic cable, data transmission wires, or the need to clip the power supply to the body (as other fNIRS devices that measure through hair have employed<sup>47</sup>) increasing the ease of set-up in uncontrolled environments (in this case in the homes of stroke survivors). The headband is meant to be worn at the apex of the head (i.e., approximately where over-the-ear headphones sit) to enable measurement of the brain’s sensorimotor region, with the lateral measurement locations overlaying C3 and C4 of the international 10-20 System, which have been shown to overlay the portion of the motor cortex associated with upper-extremity movement<sup>48</sup>. The components and

measurement locations enabled by AP-2 are illustrated in Figure 5.2-B. The headband contained both long-path (3cm from the detector; 745 and 850nm), as well as short-path (8mm from the detector; 735 and 850nm)<sup>49</sup>. The long-path LEDs were attached to the headband by individually articulating springs (Figure 5.2-A), allowing the headband to adjust to the shape of users heads in the sagittal plane, while the use of a flexible central band (which contained the detectors and short-path LEDs) allowed for adjustment in the coronal plane. Importantly, all optical components (i.e., LEDs and SPDs) were butt coupled to light pipes which enabled light transmission to and from the scalp. These light pipes were of a relatively low durometer (i.e., are softer) compared to traditional fiber optic cable, which allows them to be “worked through hair” by simply shuffling the headband back and forth on the head, whilst remaining comfortable despite making secure contact with the scalp. All these design features (a flexible, one-size-fits all band, which can be manipulated through hair by the person donning the device) in concert allow for a quick and simple device set up—in the present study it allowed the experimenter to set up the device in ~1 minute.

While the headband was designed with independent use in mind, in the present study the headband was placed by the experimenter, with its center detector (ie., item S1 in Figure 5.2-B) positioned at CZ according to the international 10-20 system<sup>48</sup>.



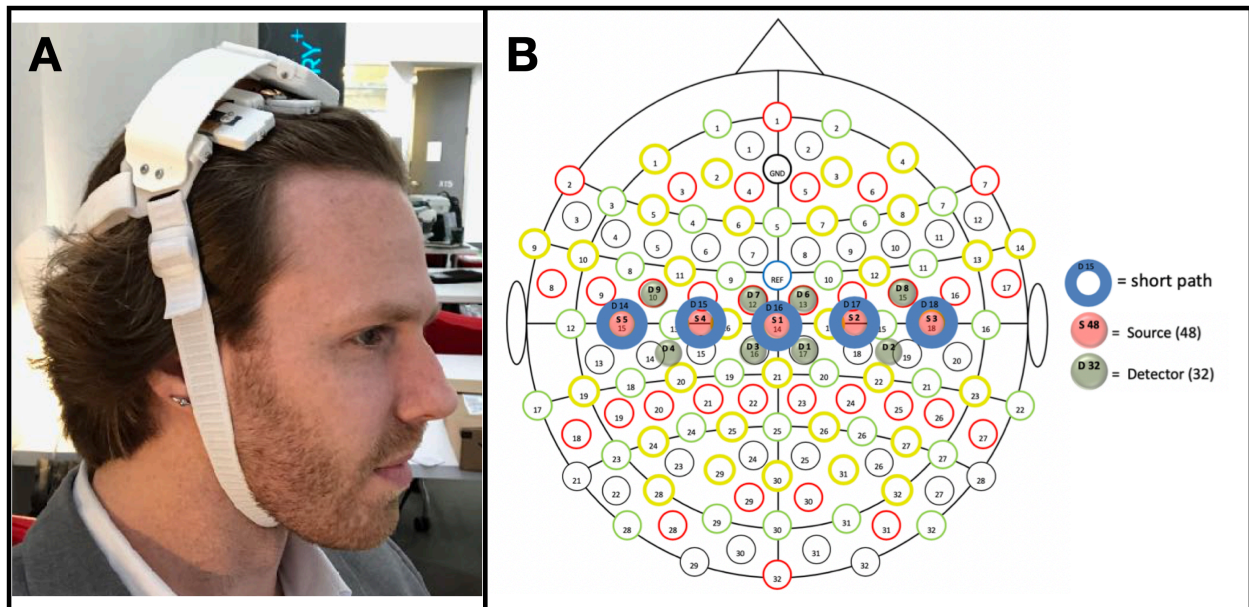


Figure 5-2. (A) Prototype fNIRS headband AP-2 used in the present study. (B) Array of optical components included in the fNIRS prototype. The central three detectors (being 3cm from 4 long-path LEDs) enabled 4 measurement locations each, with the two detectors on either end (being 3cm from 2 long-path LEDs) enabled two, resulting in a total of 16 measurement locations.

### **5.2.7 fNIRS Acquisition and Pre-processing**

The fNIRS prototype used in the present study had a system-wide sample rate of 5.4 Hz. Pre-processing procedures were applied as described in Friesen et al.<sup>46</sup> Briefly, TDDR<sup>50</sup> was applied to all signals. Three sets of inter-channel delays were calculated from 850nm data which had been bandpassed to the cardiac pulse (0.5Hz to 1.5Hz), respiration (0.15Hz to 0.3Hz) and Mayer Wave (0.05Hz to 0.15Hz) bands. All data were then transformed to  $\Delta\text{HbO}$  and  $\Delta\text{Hb}$  using the modified Beer Lambert equations<sup>51</sup>. Data from the short-paths was then submitted to a structural equation model to estimate latent common influences between the short-path channel in four permutations—once using the unfiltered  $\Delta\text{HbO}$  and  $\Delta\text{Hb}$  data, then three more times, using  $\Delta\text{HbO}$  and  $\Delta\text{Hb}$  data filtered to the cardiac pulse, respiration, and Mayer Wave bands respectively; on these new three filtered versions of the  $\Delta\text{HbO}$  and  $\Delta\text{Hb}$  data, the previously estimated delays were removed by interpolation prior to estimation of the latent common signal.

The resulting four latent common signals were then regressed out of all long-path and short-path  $\Delta\text{HbO}$  and  $\Delta\text{Hb}$  channels. Next, information from each long-path channel's associated local short-path was regressed out of the long-path data—this again was conducted both using the unfiltered short-path data, as well as short-path data which had been filtered to the cardiac pulse, respiration, and Mayer Wave bands (which again had had their band-specific delays removed by linear interpolation). And finally, all long-path channels were filtered to the frequency band containing the BOLD response (0.01Hz to 0.1Hz) and Correlation-Based Signal Improvement<sup>52</sup> was used to subtract any residual noise (identified using the  $\Delta\text{Hb}$  data) from the  $\Delta\text{HbO}$  data. Lastly, the resulting  $\Delta\text{HbO}$  data was baseline corrected (to the moment of task onset).

## **5.2.8 fNIRS Analysis**

### *5.2.8.1 fNIRS Generalized Additive Model Analysis*

To visualize a representation related to the average timeseries for each measurement location and each participant, the  $\Delta\text{HbO}$  time series data were collapsed across trials (within each measurement location) to a mean timeseries using a GAM. A GAM was then fit by generalized cross-validation, resulting in a single timeseries for each participant for each measurement location, and the 95% confidence ribbons of a mean time course at each location was preserved (results from this process are visualized in Figure 5.3).

In addition, a posterior distribution for the mean  $\Delta\text{HbO}$  values during the task period were generated using a Bayesian 3-level hierarchical model in which the mean slope for a given subject ( $\mu_{\text{subject}}$ ) was a random normal deviate from a group mean slope ( $\mu_{\text{group}}$ ):  $\mu_{\text{subject}} \sim \text{normal}(\mu_{\text{group}}, \sigma_{\text{subjs}})$ , the slope for a given trial ( $\mu_{\text{trial}}$ ) was a random normal deviate from the participant's mean slope:  $\mu_{\text{trial}} \sim \text{normal}(\mu_{\text{subject}}, \sigma_{\text{trials}})$ , and finally, the observations through time on a given trial were random normal deviates from that expected given the trial slope:  $\text{obs} \sim \text{normal}(\text{time} \times$

$\mu_{\text{trial}}, \sigma_{\text{obs}}$ ). Weakly-informed priors for all parameters were employed such that the gross variability observed in the data (quantified by computing the standard deviation across all datapoints,  $SD_{\text{obs}}$ ) informed on the general scale of the parameters. Specifically,  $\mu_{\text{group}} \sim \text{normal}(0, SD_{\text{obs}})$ ,  $\sigma_{\text{subjs}} \sim \text{weibull}(2, SD_{\text{obs}})$ ,  $\sigma_{\text{trials}} \sim \text{weibull}(2, SD_{\text{obs}})$ ,  $\sigma_{\text{obs}} \sim \text{weibull}(2, SD_{\text{obs}})$ . The model and priors were expressed in Stan<sup>53</sup>, permitting use of the cmdstan MCMC sampler to generate posterior samples reflecting the posterior probability distributions on the model parameters given the model structure, priors and observed data. Diagnostics for all sampling runs were evaluated to ensure that no samples encountered divergent transitions, all chains exhibited convergence ( $\text{rhat} < 1.01$ ) for all parameters, and no parameters exhibited low effective sample size for tail quantities (results from this process are visualized in Figure 5.4).

### **5.2.9 fNIRS M1-LAT Analysis**

After pre-processing, for each movement trial, the average of the  $\Delta\text{HbO}$  values observed during the 10 second task window was computed. The resulting mean values were then collapsed to a mean across locations in each hemisphere, whereupon a ‘lateralization score’ (i.e., the difference between the mean  $\Delta\text{HbO}$  from the ipsilesional hemisphere and the contralesional hemisphere) was computed for each trial.

To evaluate the relationships between M1-LAT and our measures of post-stroke upper-extremity impairment (FM-12) and function (SIS-Hand), we constructed a structural equation model (SEM). SEMs are the more powerful successor to standard regression models, whereby the dependence between outcomes can be evaluated in the presence of both measurement noise and hierarchical structure.<sup>54,55</sup> The model’s latent structure is comprised of the expectation of a latent (i.e. unobserved, but eventually informed/constrained by the data) trait that varies among

participants in a Gaussian-distributed manner,<sup>5</sup> with mean and standard deviation is fixed at values of 0 and 1, respectively.<sup>6</sup> The use of the standard normal<sup>56</sup> distribution in this way is a common means to ensure “identifiability” of the subsequent model. A model is said to be non-identified when two or more parameters end up achieving the same purpose in the model.

Next, we express that this latent trait influences three additional latent traits (i.e., one associated with each outcome: lateralization scores, FM-12, and SIS-Hand), with the magnitude of this influence on each outcome modelled with a proportional loading parameter, reflecting competition between the common latent trait and variance unique to each outcome’s latent trait.<sup>7</sup>

For the lateralization score data, the observed lateralization score values are first scaled (multiplied) by a parameter reflecting the scale of variability of this trait in the population, to which is then added another parameter reflecting the mean of this trait in the population. Finally, the observed lateralization scores from each participant<sup>8</sup> were modelled as samples from a normal distribution, with a mean equal to the (scaled and centered) latent lateralization trait for

---

<sup>5</sup>  $H_p \sim \text{normal}(0,1)$

Take for example a model of the following form:

$$Y \sim \text{normal}(\mu_1 + \mu_2, 1)$$

In this model, Y is modelled as samples from a normal distribution with a mean equal to the sum of parameters  $\mu_1$  and  $\mu_2$ , but without any additional structure,  $\mu_1$  and  $\mu_2$  will cause non-identifiability because the implied mean for Y will be the same in the circumstance that  $\mu_1=0$  &  $\mu_2=0$  as when  $\mu_1=+1$  &  $\mu_2=-1$ .

$$\begin{aligned} \text{Latent\_Lateralization\_p} &\sim H_p * \text{loading\_LL} + \text{unique\_LL} * (1 - \text{loading\_LL}) \\ \text{Latent\_FM\_p} &\sim H_p * \text{loading\_LF} + \text{unique\_LF} * (1 - \text{loading\_LF}) \\ \text{Latent\_SIS\_p} &\sim H_p * \text{loading\_LS} + \text{unique\_LS} * (1 - \text{loading\_LS}) \end{aligned}$$

To achieve identifiability with this additional structure, each of the unique traits are modelled as standard-normally distributed:

$$\begin{aligned} \text{unique\_LL} &\sim \text{normal}(0,1) \\ \text{unique\_LF} &\sim \text{normal}(0,1) \\ \text{unique\_LS} &\sim \text{normal}(0,1) \end{aligned}$$

Additionally, the sign of one loading must be set arbitrarily-but-necessarily to ensure identifiability, so we here chose to restrict the sign of loading LS loading for the SIS measure as positive.

<sup>8</sup> One score from each trial, `t`

that participant, and a standard deviation equal to a value reflecting the magnitude of measurement noise.<sup>9</sup>

Both FM-12 and SIS-Hand were similarly modelled hierarchically, such that the item-by-item score on each was modelled as a cumulative normal ordinal outcome with a mean equal to that participant's latent trait for that scale, and ordinal cutpoints associated with each item.<sup>10</sup>

We then utilized Bayesian estimation on this model structure, to derive what we should believe about the parameters of the model, given both the data and whatever prior information we might have about said parameters. While the model has many parameters (e.g. the value of a given latent trait for a given participant can be considered a parameter), the structure described above constrains the vast majority, leaving us to needing priors on (1) the mean of the latent lateralization, (2) the standard deviation of the latent lateralization traits, (3) the measurement noise for the lateralization data, (4) the cutpoints for each item in the FM-12 and SIS-Hand, and (5) the loadings in the latent SEM. For the first three parameters, as these do not relate directly to our hypothesis about the relationship between latent laterality and upper-extremity

---

<sup>9</sup> A value modelled as common across participants:

Observed\_lateralization\_{p,t} ~ normal( Latent\_lateralization\_p , noise )

<sup>10</sup> observed\_FM\_{p,i} ~ cumulative\_normal\_ordinal( Latent\_FM\_p , cutpoints\_i )  
observed\_SIS\_{p,j} ~ cumulative\_normal\_ordinal( Latent\_SIS\_p , cutpoints\_j )

Unlike the lateralization measurement model, scaling and centering of the latent traits is not necessary for the physical ability measures, and indeed it is necessary for identifiability that they remain on their implied standard normal scales.

impairment/function, and we have weak prior beliefs as to their value, we employ data-driven weakly-informed priors.<sup>11</sup>

For the cutpoints of each item of the FM-12 and SIS-Hand, we employ the “induced Dirichlet” prior.<sup>57</sup> And finally, we employ uninformative uniform priors for each of the loading parameters, reflecting equal credibility of all possible values from -1 to 1 (importantly, including zero, reflecting no influence from the common latent trait).

We expressed this model in Stan,<sup>12</sup> yielding posterior samples for each parameter reflecting the Bayesian solution to the relative credibility of parameter values given the model, priors and data.<sup>13</sup>

---

<sup>11</sup> Mean latent lateralization  $\sim$  normal(  $m$  ,  $t$  )SD latent lateralization  $\sim$  half-normal( 0,  $t$  )  
Measurement noise  $\sim$  weibull(2,  $t$  )

Where  $m$  is the mean lateralization computed from the observed data and  $s$  is the standard deviation of lateralization scores computed from the observed data (n.b. without first collapsing scores to a mean per participant). The use of a normal distribution centered on  $m$  and with a scale of  $s$  achieves a prior on the mean of the latent lateralization traits whereby the empirical mean is considered most credible apriori, but with a relatively broad range of alternate values, informed by the scale of variability observed in raw scores (which, thanks to measurement noise, should have relatively broad range) also considered reasonably credible. The use of a half-normal for the prior on the SD of latent lateralization traits is fairly conventional for this kind of parameter and implicitly achieves a slight regularization of the distribution of latent lateralization traits, shrinking outliers towards the mean. The use of a weibull distribution with a shape of 2 and scale  $s$  yields a prior peaked at approximately  $0.8*t$ , tapering rapidly to the left of this peak such that there is zero credibility for measurement noise values of zero, and tapering more slowly to the right of this peak such that values of even  $2*t$  are relatively credible. To implement these priors more efficiently, the observed lateralization scores were scaled via the operation

$\text{Scaled\_observed\_laterality} = (\text{observed\_laterality} - m) / s$

In the context of data scaled in this way, the above priors are achieved now as:

Mean latent lateralization  $\sim$  normal( 0 , 1 )  
SD latent lateralization  $\sim$  half-normal( 0, 1 )  
Measurement noise  $\sim$  weibull(2, 1)

<sup>12</sup> A probabilistic programming language, and employed the cmdstan and cmdstanr interfaces to a state-of-the-science Dynamic Hamiltonian Monte Carlo sampler to combine the model, priors and data.

<sup>13</sup> We ran 6 independent chains, each for 1000 warmup iterations (during which DHMC learns the topology of the posterior distribution) followed by 1000 sampling iterations. The cmdstanr interface provides a number of diagnostic checks that can flag when the results from such sampling are certainly untrustworthy, but our sampling passed all said checks. Specifically, no post-warmup divergent transitions were encountered, E-BFMI was above .3 for all transitions, Rhat values were below 1.01 for all parameters, and effective sample sizes for both bulk and tail quantities of all parameters were above 1000.

### 5.3 RESULTS

No participants were excluded due to cognitive impairment (MMSE scores:  $M = 26.45$ ;  $SD = 4.54$ ; see Figure 4.5 of chapter 4 for visualization of the distribution), and participants varied greatly in both their levels of upper-extremity impairment (FM-12 scores:  $M = 8.75$ ;  $SD = 3.02$ ; see Figure 4.5 of chapter 4 for visualization of the distribution) and self-reported upper-extremity function (SIS-Hand scores:  $M = 2.57$ ;  $SD = 1.17$ ; see Figure 4.5 of chapter 4 for visualization of the distribution).

Given the hypothesis that the degree of M1-LAT would vary as a function of stroke survivor's level of impairment, we expected the topographical distributions of event-related  $\Delta\text{HbO}$  patterns to vary between individuals (with more contra-lateralized patterns for stroke survivors with lower levels of impairment)—though with strong priors that we would see a task-evoked increase in at least a sub-segment of measurement locations, in at least one hemisphere. In looking at the topographical distribution of mean  $\Delta\text{HbO}$  values as determined by the GAM model, indeed, we generally see a mixture of typically contra-lateralized increases in  $\Delta\text{HbO}$  during the task period (e.g., participants 5, 7, and 11), as well participants with a more bilateral pattern of activation (e.g., participants 3, 8, and 12). As a result, in examining the posterior samples for the group mean slope obtained for the task window, as with the GAM-generated mean time-series, we see a generally bilateral increase in  $\Delta\text{HbO}$  (Figure 4), with a slight contra-lateralization.

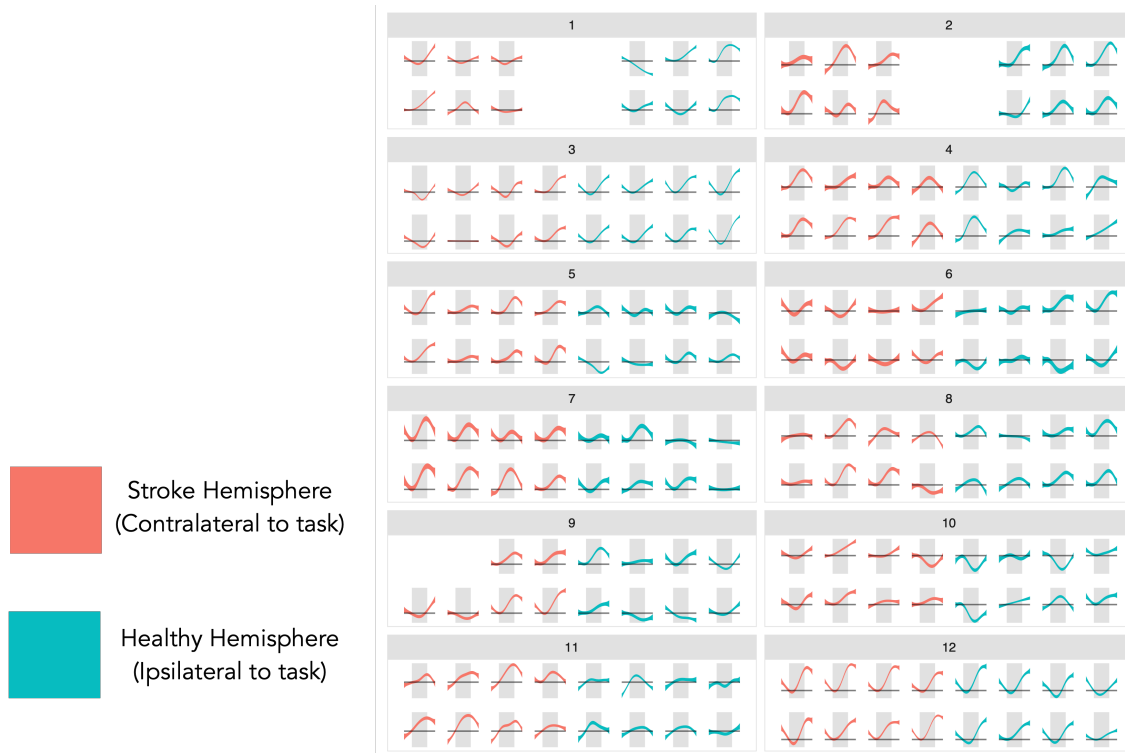


Figure 5-3. Estimated 95% confidence ribbons for  $\Delta\text{HbO}$  timeseries for all participants. Time series windows highlighted in red are contralateral to the hand being used in the task. The portion of the time series shaded in grey represents the 10s block of  $\sim 1\text{Hz}$  fist squeezing or attempted fist squeezing. Visualized ribbons were obtained from a GAM fit separately to each participant and measurement, and specifically represent  $\pm 2$  standard error of the mean, resulting in a 95% confidence interval.

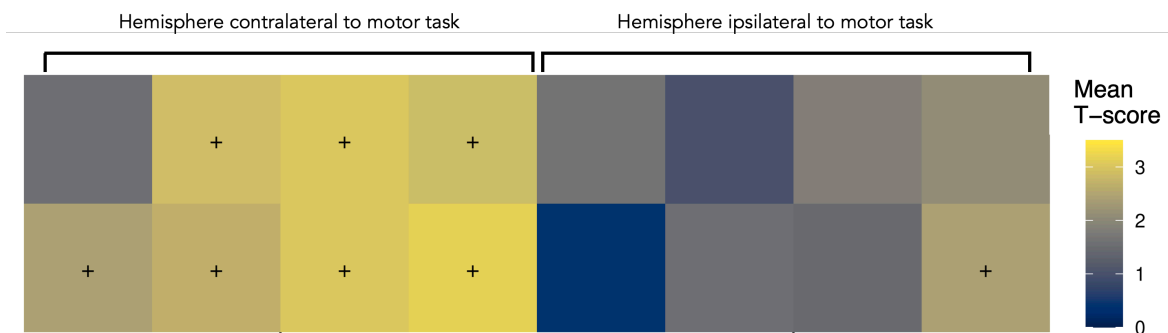


Figure 5-4. Topographic maps (top-down view, with the top row representing the anterior row of measurement locations, and vice versa; locations on the left of the grid representing the left hemisphere, and vice versa) of group mean slope (in units of  $\text{mMol}/\text{mm}^3$ ) during task for AP-2's 16 measurement locations. Because not all participants used the same hand in the task, the hemispheres for some of the participants' data were flipped such that the left side represents the hemisphere contralateral to the participants' paretic hand. Colors indicate posterior median of



*$\Delta\text{HbO}$  values; locations with posterior distributions in which zero falls outside the 95% credible interval are marked with crosses.*

Given that these data indicate that the fNIRS data captured during the motor task had a more contra-lateralized pattern (i.e., greater magnitude of activation in the contralateral or ipsilesional hemisphere) for some participants while this pattern of activation was more bilaterally distributed for others (i.e., activity distributed over both the ipsi-lateral and contra-lateral hemispheres), it is relevant to examine the relationship between the degree of laterality and the upper-extremity ability of each participant. To this end, we can examine both the correlations between each individual measure of upper-extremity ability (FM-12 and SIS-Hand) and M1-LAT (Figure 5), as well as the correlation derived from the Bayesian SEM developed to explore this relationship. Figure 6 shows the relevant marginal posterior distributions for important parameters in the model. As expected, given the scaled data and its data-driven prior, the posterior distribution for the lateralization score measurement noise concentrates at values near-but-below 1 (around .9), reflecting that most, but not all, of the variability observed in the lateralization scores is associated with measurement noise, with the remainder being associated with differences among the participants in their latent lateralization traits. Consistent with this is the observation that the posterior on the variability among participants in latent lateralization scores is concentrated away from zero at values near 0.3, reflecting that the latent scores have a variability that is approximately 30% the magnitude of the variation observed in the raw laterality scores (which include measurement noise). The posterior for the mean latent lateralization remains centered on zero but has narrowed from its prior SD of 1 to approximately 0.5, primarily reflecting increased confidence in values closer to zero as a consequence of seeing scaled data consistent with those values. The loadings on latent FM and latent SIS are both strongly positive, indicating a very strong belief that these measures are credibly interrelated via

their common association with a single latent factor. And finally, the posterior distributions for the loading on latent laterality—reflecting the correlation between post-stroke function and M1-LAT—has a 95% credible interval ranging from 0.03-0.98 (median: 0.63); the fact that this interval does not include zero, reflects a strong belief that M1-LAT is positively correlated with post-stroke upper-extremity impairment and function.<sup>14</sup>

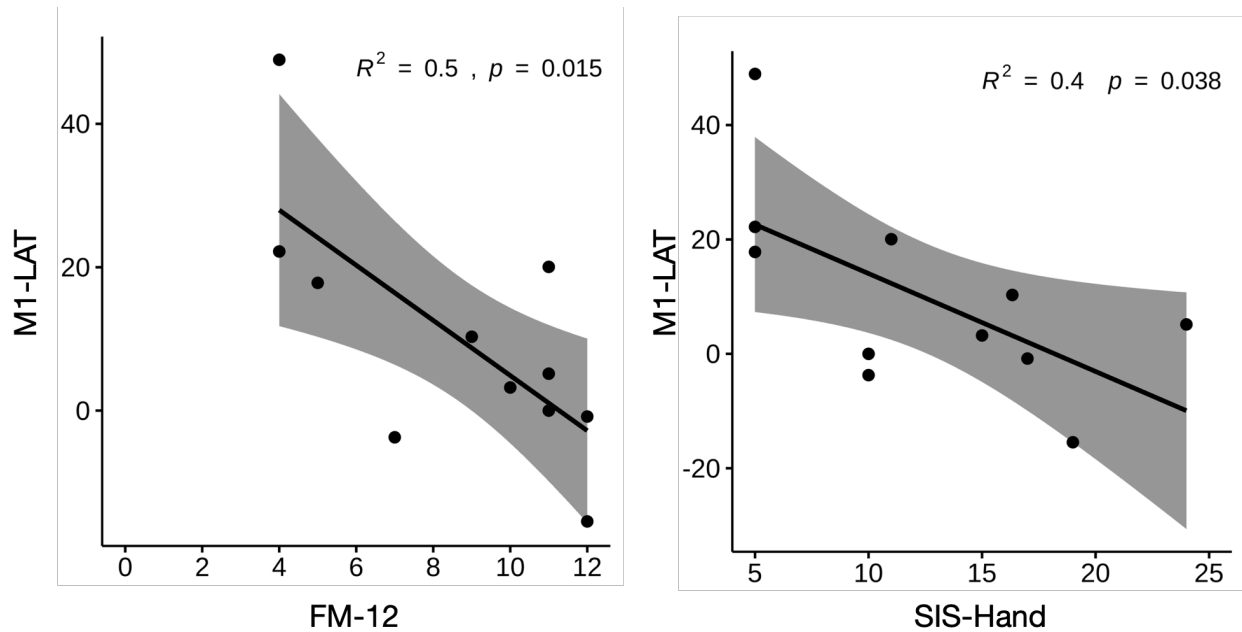


*Figure 5-5. Correlation coefficients (and 95%ile Credible Intervals thereof) between M1-LAT and both FM-12 and SIS-Hand respectively. M1-LAT is calculated such that higher values represents higher  $\Delta$ HbO lateralization towards the contralesional hemisphere (i.e., the hemisphere ipsilateral). These preliminary analyses were conducted using the pre-processing pipeline described in Chapter 2.*

<sup>14</sup> It should be emphasized that this is by no means a guaranteed outcome of the structure of the model; it would be entirely possible, should the data support it, for loading values at or near zero to be considered highly credible for one or more of the traits. While the loading for the latent SIS trait was constrained to be positive for the purposes of identifiability, even this would yield a posterior that would be concentrated at least near zero should the data in fact support the credibility of such values. That we observe credibly non-zero loadings for all traits strongly supports mutual association.

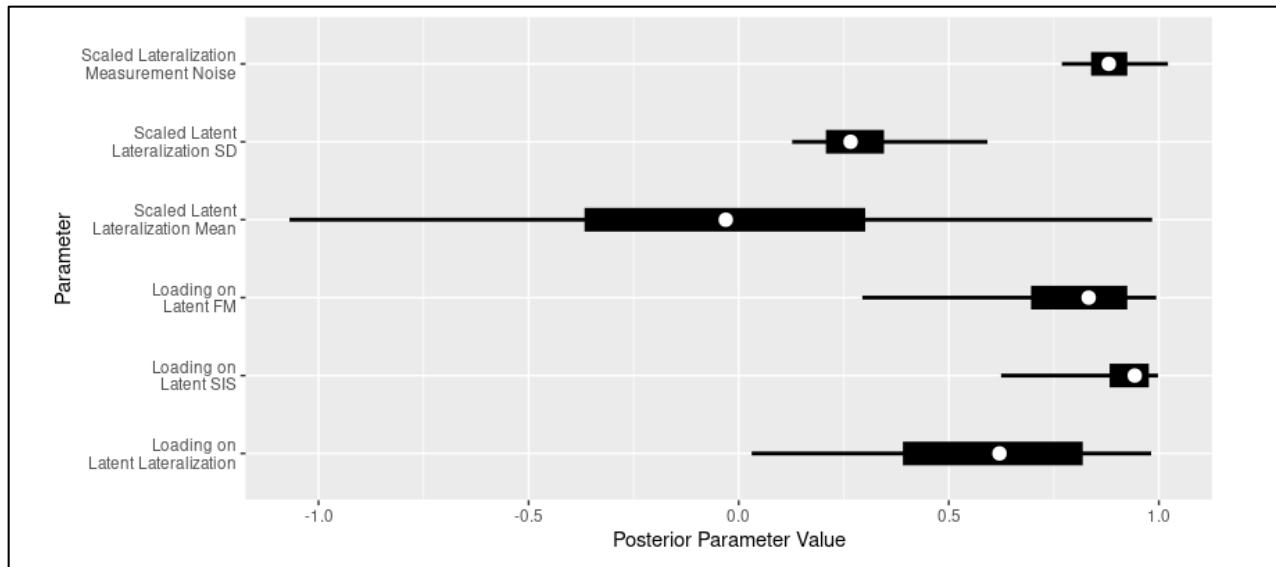


Figure 5-6. Posterior distributions for core model parameters. White dots convey the posterior median while the thick and thin bars convey 50% Credible Intervals (i.e., bounded by the 25%ile and 75%ile) and the 95% Credible Interval (i.e., bounded by the 2.5%ile and 97.5%ile).

## 5.4 DISCUSSION

This study tested the ability of AP-2 (an ergonomic, easy-to-set-up fNIRS headband) to take neurophysiological measurements from the motor cortex of stroke survivors in their homes during a simple unilateral movement; it also examined the relationship between M1-LAT (as measured during these simple unilateral upper-extremity movements) and measures of upper-extremity impairment (FM-12) and function (SIS-Hand). As expected, results showed that all participants demonstrated some event-related increases in  $\Delta\text{HbO}$  across AP-2's measurement grid, with participants broadly either demonstrating a contra-lateralized or bilateral response to paretic upper-extremity movement. Moreover, the present study's results showed that the level of motor cortex lateralization during unilateral movement of the paretic upper-extremity was associated with upper-extremity function and impairment. Thus the data from this mobile system, collected on stroke survivors in their homes, replicates the previously reported

relationship whereby decreased function and increased impairment is associated with a more atypical pattern of M1-LAT during paretic upper-extremity movement.

As discussed in the introduction, M1-LAT measurements have been shown to correlate with both motor function and impairment. The results of this study specifically replicate several other studies that have shown cross-sectionally that a deviation from the typical pattern of M1-LAT (during simple paretic upper-extremity movement) corresponds with worse motor outcomes; this includes an fNIRS study which used a similar hand-grasping task during which to measure M1-LAT, and characterized impairment using Brunnstrom stages,<sup>58</sup> as well as studies using other modalities (e.g., fMRI, EEG and positron emission topography) which have shown that atypical M1-LAT correlates with worse performance on finger tapping<sup>59</sup> and peg-board tasks,<sup>60,61</sup> as well worse self-reported functional abilities (as measured by the motor activity log).<sup>62</sup> And while the ability to gain functional neuroimaging markers of recovery may be of limited clinical utility, other research has shown that these same measures of M1-LAT can be used to also predict functional gains from a rehabilitation intervention,<sup>25-28</sup> meaning these measures could potentially improve clinicians ability to personalize the planned rehabilitation intervention to the needs of individual stroke survivors.

However, to date the literature documenting the relationship of M1-LAT with post-stroke motor recovery relies primarily on studies using fMRI; while fMRI is surely the optimal way to gain non-invasive functional measurements on cerebral activity, the use of MRI comes with significant cost (both upfront and maintenance), a large footprint (meaning stroke survivors must be brought from their site of care in order for these measurements to be gained), and specialized staff required to support data acquisition and analysis; these realities therefore represent a significant barrier to utilizing fMRI for any use case related to post-stroke physical rehabilitation.

In addition to the substantial fMRI literature, there are also studies using headcap-based EEG<sup>63,64</sup> and fNIRS<sup>58,65</sup> systems to measure M1-LAT in stroke survivors. While cheaper and more user-friendly (smaller and less maintenance required) than fMRI, these systems are all laboratory-based, and require the use of a full headcap—they therefore are difficult to utilize in a variety of locations, and time-consuming to set-up. Thus, the present study is novel in that it suggests that it is possible to measure M1-LAT outside the laboratory with a non-headcap-based fNIRS system.

However, with that said there are several limitations to the present study. Firstly, as mentioned above the data collected in the present study was only cross-sectional. And while there is no reason to suspect that the used in this present study wouldn't be capable of capturing longitudinal measurements when it is able to capture these measures cross-sectionally, further work is required to determine if longitudinally captured M1-LAT data from this fNIRS prototype or one similar would be capable of seeing the longitudinal changes over time that have been reported elsewhere<sup>65</sup>. Another notable limitation is that while AP-2 was designed to enable independent use, because of the preliminary nature of this study an experimenter placed the headband on the participants; moreover, while AP-2 was designed to enable quick set-up, the time to set-up the device was not recorded (although this time was ~1 minute)—future work on this or subsequent fNIRS prototypes should include this aspect in their experimental designs, enabling the continual optimization of device setup ease-of-use over time. And finally, again because of the preliminary nature of this study, only fNIRS data from a simple fist-squeezing task was presented; while existing research has shown a similar topographic pattern of increased  $\Delta\text{HbO}$  across an fNIRS measurement array between movements of the hand and shoulder<sup>66,67</sup>, future work with the AP-2 or subsequent fNIRS prototypes ought to utilize movements also involving the shoulder to replicate these results; moreover, more complex upper-extremity tasks,

which might result in a more broad pattern of motor cortex activation (as has been shown via both fNIRS and fMRI) ought to be included in future tests of AP-2 or related fNIRS prototypes, to determine the ability of its measurement array to capture the neurophysiological response at the motor cortex to such tasks.

In conclusion, the present study demonstrated that neurophysiological measurements from the motor cortex could be taken using a mobile fNIRS system in the homes of stroke survivors, and moreover that these measurements replicate the previously described relationship between M1-LAT during paretic arm movement, and levels of function/impairment in stroke survivors. This suggests it may be possible for M1-LAT measurements to be taken on stroke survivors in more convenient and cost-effective ways than the literature to date (primarily fMRI and laboratory-based EEG and fNIRS studies) would suggest. Moreover, given previous studies that have shown that the provision of M1-LAT NFB during various rehabilitation interventions can enhance the efficacy of rehabilitation<sup>30,68</sup>, the present study's findings that a mobile, easy-to-use fNIRS system can take these measurements might also be built on through future development of more accessible rehabilitation brain-computer-interface systems. These findings portend the possibility of using ergonomic fNIRS devices to capture neural biomarkers of post-stroke motor recovery, and/or to be used as a part of more accessible rehabilitation brain-computer-interfaces.

## 5.5 REFERENCES

1. Boyd, L. A. *et al.* Biomarkers of stroke recovery: Consensus-based core recommendations from the Stroke Recovery and Rehabilitation Roundtable. *Int. J. Stroke Off. J. Int. Stroke Soc.* **12**, 480–493 (2017).
2. Borschmann, K. *et al.* Rationale for Intervention and Dose Is Lacking in Stroke Recovery Trials: A Systematic Review. *Stroke Res. Treat.* **2018**, 8087372 (2018).
3. Ovbiagele, B. *et al.* Forecasting the Future of Stroke in the United States: A Policy Statement From the American Heart Association and American Stroke Association. *Stroke* **44**, 2361–2375 (2013).
4. UK Sentinel Stroke National Audit Programme (SSNAP), July-Sept 2015 report.
5. Nudo, R. J. & Milliken, G. W. Reorganization of movement representations in primary motor cortex following focal ischemic infarcts in adult squirrel monkeys. *J. Neurophysiol.* **75**, 2144–2149 (1996).
6. Ward, N. S., Brander, F. & Kelly, K. Intensive upper limb neurorehabilitation in chronic stroke: outcomes from the Queen Square programme. *J. Neurol. Neurosurg. Psychiatry* **90**, 498–506 (2019).
7. A, H., Rh, N., Ac, G. & G, K. Functional recovery of the paretic upper limb after stroke: who regains hand capacity? *Archives of physical medicine and rehabilitation* vol. 94 <https://pubmed.ncbi.nlm.nih.gov/23201317/> (2013).
8. Predicting Activities after Stroke: What is Clinically Relevant? - G. Kwakkel, B. J. Kollen, 2013. <https://journals.sagepub.com/doi/abs/10.1111/j.1747-4949.2012.00967.x>.
9. Vliet, R. van der *et al.* Predicting Upper Limb Motor Impairment Recovery after Stroke: A Mixture Model. *Ann. Neurol.* **87**, 383–393 (2020).

10. Does Stroke Rehabilitation Really Matter? Part B: An Algorithm for Prescribing an Effective Intensity of Rehabilitation. - PubMed - NCBI.  
<https://www.ncbi.nlm.nih.gov/pubmed/29334831>.
11. Senesh, M. R. & Reinkensmeyer, D. J. Breaking Proportional Recovery After Stroke. *Neurorehabil. Neural Repair* **33**, 888–901 (2019).
12. Stinear, C. M., Barber, P. A., Petoe, M., Anwar, S. & Byblow, W. D. The PREP algorithm predicts potential for upper limb recovery after stroke. *Brain J. Neurol.* **135**, 2527–2535 (2012).
13. Daly, J. J., Hrovat, K., Holcomb, J. & Pundik, S. Brain control of functional reach in healthy adults and stroke survivors. *Restor. Neurol. Neurosci.* **32**, 559–573 (2014).
14. The relationship between motor deficit and primary motor cortex hemispheric activation balance after stroke: longitudinal fMRI study | Journal of Neurology, Neurosurgery & Psychiatry. <https://jnnp.bmj.com/content/81/7/788.short>.
15. Marshall, R. S. *et al.* Evolution of Cortical Activation During Recovery From Corticospinal Tract Infarction. *Stroke* **31**, 656–661 (2000).
16. Tombari, D. *et al.* A longitudinal fMRI study: in recovering and then in clinically stable sub-cortical stroke patients. *NeuroImage* **23**, 827–839 (2004).
17. Takeda, K. *et al.* Shift of motor activation areas during recovery from hemiparesis after cerebral infarction: A longitudinal study with near-infrared spectroscopy. *Neurosci. Res.* **59**, 136–144 (2007).
18. Delorme, M., Froger, J., Perrey, S., Vergotte, G. & Laffont, I. Changes in hemodynamic responses during movements of the upper extremities in the acute phase after stroke: A fNIRS study. *Ann. Phys. Rehabil. Med.* **60**, e1 (2017).



19. Relationship Between Electrical Brain Responses to Motor Imagery and Motor Impairment in Stroke | Stroke.  
<https://www.ahajournals.org/doi/full/10.1161/STROKEAHA.112.665489>.
20. Miyai, I., Suzuki, M., Hatakenaka, M. & Kubota, K. Effect of body weight support on cortical activation during gait in patients with stroke. *Exp. Brain Res.* **169**, 85–91 (2006).
21. Miyai, I. *et al.* Longitudinal Optical Imaging Study for Locomotor Recovery After Stroke. *Stroke* **34**, 2866–2870 (2003).
22. Tang, Q. *et al.* Modulation of interhemispheric activation balance in motor-related areas of stroke patients with motor recovery: Systematic review and meta-analysis of fMRI studies. *Neurosci. Biobehav. Rev.* **57**, 392–400 (2015).
23. Frontiers | Role of the Contralesional vs. Ipsilesional Hemisphere in Stroke Recovery | Human Neuroscience.  
<https://www.frontiersin.org/articles/10.3389/fnhum.2017.00469/full?report=reader>.
24. Rehme, A. K., Eickhoff, S. B., Rottschy, C., Fink, G. R. & Grefkes, C. Activation likelihood estimation meta-analysis of motor-related neural activity after stroke. *NeuroImage* **59**, 2771–2782 (2012).
25. Nhan, H. *et al.* Brain Function Early after Stroke in Relation to Subsequent Recovery. *J. Cereb. Blood Flow Metab.* **24**, 756–763 (2004).
26. Rehme, A. K. *et al.* Individual prediction of chronic motor outcome in the acute post-stroke stage: Behavioral parameters versus functional imaging. *Hum. Brain Mapp.* **36**, 4553–4565 (2015).
27. Loubinoux, I. *et al.* Prognostic Value of fMRI in Recovery of Hand Function in Subcortical Stroke Patients. *Cereb. Cortex* **17**, 2980–2987 (2007).

28. Quinlan, E. B. *et al.* Neural function, injury, and stroke subtype predict treatment gains after stroke. *Ann. Neurol.* **77**, 132–145 (2015).
29. MacLellan, C. L. *et al.* A critical threshold of rehabilitation involving brain-derived neurotrophic factor is required for poststroke recovery. *Neurorehabil. Neural Repair* **25**, 740–748 (2011).
30. Mihara, M. *et al.* Near-infrared Spectroscopy–mediated Neurofeedback Enhances Efficacy of Motor Imagery–based Training in Poststroke Victims. *Stroke* (2013).
31. Várkuti, B. *et al.* Resting State Changes in Functional Connectivity Correlate With Movement Recovery for BCI and Robot-Assisted Upper-Extremity Training After Stroke. *Neurorehabil. Neural Repair* **27**, 53–62 (2013).
32. Ono, Y. *et al.* Hand Motor Rehabilitation of Patients with Stroke Using Physiologically Congruent Neurofeedback. in *2018 IEEE International Conference on Systems, Man, and Cybernetics (SMC)* 39–44 (2018). doi:10.1109/SMC.2018.00016.
33. Pichiorri, F. *et al.* Brain–computer interface boosts motor imagery practice during stroke recovery. *Ann. Neurol.* **77**, 851–865 (2015).
34. Müller-Gerking, J., Pfurtscheller, G. & Flyvbjerg, H. Designing optimal spatial filters for single-trial EEG classification in a movement task. *Clin. Neurophysiol.* **110**, 787–798 (1999).
35. Folstein, M. F., Folstein, S. E. & McHugh, P. R. “Mini-mental state”. *J. Psychiatr. Res.* **12**, 189–198 (1975).
36. Barnay, J.-L. *et al.* Feasibility of the Cognitive Assessment scale for Stroke Patients (CASP) vs. MMSE and MoCA in aphasic left hemispheric stroke patients. *Ann. Phys. Rehabil. Med.* **57**, 422–435 (2014).

37. Benaim, C. *et al.* The Cognitive Assessment scale for Stroke Patients (CASP) vs. MMSE and MoCA in non-aphasic hemispheric stroke patients. *Ann. Phys. Rehabil. Med.* **58**, 78–85 (2015).
38. Park, K.-H. *et al.* The Korean Version of the Cognitive Assessment Scale for Stroke Patients (K-CASP): A Reliability and Validity Study. *Ann. Rehabil. Med.* **41**, 362–375 (2017).
39. Sullivan, J. E. Measurement Characteristics and Clinical Utility of the Stroke Impact Scale. *Arch. Phys. Med. Rehabil.* **95**, 1799–1800 (2014).
40. Crivelli, D. *et al.* When is a novel psychometric measure needed? A preliminary analysis regarding the Cognitive Assessment for Stroke Patients (CASP) battery compared with MMSE and MoCA. *Appl. Neuropsychol. Adult* **25**, 410–416 (2018).
41. Hsieh, Y.-W. *et al.* Development and validation of a short form of the Fugl-Meyer motor scale in patients with stroke. *Stroke* **38**, 3052–3054 (2007).
42. Chen, K.-L. *et al.* Is the long form of the Fugl-Meyer motor scale more responsive than the short form in patients with stroke? *Arch. Phys. Med. Rehabil.* **95**, 941–949 (2014).
43. Alt Murphy, M., Danielsson, A. & Sunnerhagen, K. S. Letter by Murphy *et al* regarding article, ‘Fugl-Meyer assessment of sensorimotor function after stroke: standardized training procedure for clinical practice and clinical trials’. *Stroke* **42**, e402 (2011).
44. Sullivan, K. J. *et al.* Fugl-Meyer assessment of sensorimotor function after stroke: standardized training procedure for clinical practice and clinical trials. *Stroke* **42**, 427–432 (2011).
45. Sharma Nikhil, Pomeroy Valerie M., & Baron Jean-Claude. Motor Imagery. *Stroke* **37**, 1941–1952 (2006).

46. Friesen, C. *et al.* Wireless, fibreless, and user-friendly fNIRS headband compared with headcap fNIRS system for sensorimotor measurement of upper- and lower-extremity movement. *Manuscr. Submitt. Publ.* (2020).
47. Piper, S. K. *et al.* A Wearable Multi-Channel fNIRS System for Brain Imaging in Freely Moving Subjects. *NeuroImage* **85**, (2014).
48. Homan, R. W. The 10-20 Electrode System and Cerebral Location. *Am. J. EEG Technol.* **28**, 269–279 (1988).
49. Sato, T. *et al.* Reduction of global interference of scalp-hemodynamics in functional near-infrared spectroscopy using short distance probes. *NeuroImage* **141**, 120–132 (2016).
50. Fishburn, F. A., Ludlum, R. S., Vaidya, C. J. & Medvedev, A. V. Temporal Derivative Distribution Repair (TDDR): A motion correction method for fNIRS. *NeuroImage* **184**, 171–179 (2019).
51. Baker, W. B. *et al.* Modified Beer-Lambert law for blood flow. *Biomed. Opt. Express* **5**, 4053–4075 (2014).
52. Cui, X., Bray, S. & Reiss, A. L. Functional near infrared spectroscopy (NIRS) signal improvement based on negative correlation between oxygenated and deoxygenated hemoglobin dynamics. *NeuroImage* **49**, 3039–3046 (2010).
53. Gelman, A., Lee, D. & Guo, J. Stan: A Probabilistic Programming Language for Bayesian Inference and Optimization. *J. Educ. Behav. Stat.* **40**, 530–543 (2015).
54. Schreiber, J. B., Nora, A., Stage, F. K., Barlow, E. A. & King, J. Reporting Structural Equation Modeling and Confirmatory Factor Analysis Results: A Review. *J. Educ. Res.* **99**, 323–338 (2006).

55. Weston, R. & Gore, P. A. A Brief Guide to Structural Equation Modeling. *Couns. Psychol.* **34**, 719–751 (2006).
56. Weisstein, E. W. Normal Distribution.  
<https://mathworld.wolfram.com/NormalDistribution.html>.
57. Betancourt, M. Case Studies: Ordinal Regression.
58. Kato, H. Near-Infrared Spectroscopy and Motor Lateralization after Stroke: A Case Series Study. *Int. J. Phys. Med. Rehabil.* **02**, (2014).
59. Calautti, C. *et al.* The relationship between motor deficit and hemisphere activation balance after stroke: A 3T fMRI study. *NeuroImage* **34**, 322–331 (2007).
60. Zemke, A. C., Heagerty, P. J., Lee, C. & Cramer, S. C. Motor Cortex Organization After Stroke Is Related to Side of Stroke and Level of Recovery. *Stroke* **34**, (2003).
61. Serrien, D. J., Strens, L. H. A., Cassidy, M. J., Thompson, A. J. & Brown, P. Functional significance of the ipsilateral hemisphere during movement of the affected hand after stroke. *Exp. Neurol.* **190**, 425–432 (2004).
62. Cunningham, D. A. *et al.* Assessment of Inter-Hemispheric Imbalance Using Imaging and Noninvasive Brain Stimulation in Patients With Chronic Stroke. *Arch. Phys. Med. Rehabil.* **96**, S94–S103 (2015).
63. Gandolfi, M. *et al.* Quantification of Upper Limb Motor Recovery and EEG Power Changes after Robot-Assisted Bilateral Arm Training in Chronic Stroke Patients: A Prospective Pilot Study. *Neural Plasticity* vol. 2018 e8105480  
<https://www.hindawi.com/journals/np/2018/8105480/> (2018).
64. Sebastián-Romagosa, M. *et al.* EEG Biomarkers Related With the Functional State of Stroke Patients. *Front. Neurosci.* **14**, (2020).

65. Delorme, M., Vergotte, G., Perrey, S., Froger, J. & Laffont, I. Time course of sensorimotor cortex reorganization during upper extremity task accompanying motor recovery early after stroke: An fNIRS study. *Restor. Neurol. Neurosci.* **37**, 207–218 (2019).
66. Verstynen, T., Diedrichsen, J., Albert, N., Aparicio, P. & Ivry, R. B. Ipsilateral motor cortex activity during unimanual hand movements relates to task complexity. *J. Neurophysiol.* **93**, 1209–1222 (2005).
67. Yang, C.-L., Lim, S. B., Peters, S. & Eng, J. J. Cortical Activation During Shoulder and Finger Movements in Healthy Adults: A Functional Near-Infrared Spectroscopy (fNIRS) Study. *Front. Hum. Neurosci.* **14**, (2020).
68. Tsuchimoto, S. *et al.* Sensorimotor Connectivity after Motor Exercise with Neurofeedback in Post-Stroke Patients with Hemiplegia. *Neuroscience* **416**, 109–125 (2019).

# Chapter 6 - DISCUSSION

## **6.1 – SUMMARY OF FINDINGS BY CHAPTER**

This dissertation documents some steps undertaken in the preliminary development of a fNIRS BCI system meant to take measurements from the M1, both for the purposes of providing neurofeedback during physical rehabilitation, as well as to potentially measure neural biomarkers of recovery to be used to better understand and help optimize stroke rehabilitation more generally. Throughout the time these studies took place, the vision for what this BCI system might be (i.e., how exactly it will be implemented as a product) evolved, however throughout this dissertation it is referred to as the Axem Home (the current product vision for Axem Neurotechnology's first product): a rehabilitation system meant to enable at-home BCI-based rehabilitation. The chapters of this dissertation show a progression from the verification of preliminary fNIRS prototypes, alongside an examination of some of the relevant technical challenges to taking these fNIRS measurements (Chapter 2), to a comparison study comparing an fNIRS prototype to an established fNIRS system (Chapter 3), to an examination of the human factors feasibility of early prototypes (Chapter 5) and the associated fNIRS data collected (Chapter 5). A brief overview of the purpose and conclusions of these chapters are summarized below.

### **6.1.1 Axem Home Prototype Data Quality Study**

This study's purpose was to characterize the ability of preliminary fNIRS headband prototypes (designed to be compatible with future designs that might enable independent use) to measure the M1 response to upper-extremity movement. Thus, this study's design was unique in its iterative nature, which endeavored to assess the performance of preliminary prototypes

through a standardized paradigm, while allowing for iteration (as deemed needed) on those prototypes. This chapter also included an overview of the technical challenges an fNIRS system must overcome to provide valid measurements of M1-related activity, in the hope of providing context for iterations on the fNIRS prototype's design which might be undertaken throughout the course of the study. Testing of an initial, preliminary prototype (AP-1, described in section 2.2.2.1) provided encouraging results as to the feasibility of using this device to take neurophysiological measurements from M1 via fNIRS during a simple upper-extremity task; however, throughout testing it became apparent the device did not perform well on individuals with dense hair, and thus it was determined that changes were warranted to this prototype's design—in particular, changes that would better enable its emitted light to penetrate through densely concentrated follicles of hair. The second fNIRS headband prototype (AP-2, described in section 2.2.2.2) tested had more powerful emitters, more efficient optical transmission, and better flexibility which allowed it to better accommodate for differences in head shape, and in preliminary assessments AP-2 appeared to perform better than AP-1 in gaining neurophysiological measurements from M1 on individuals with dense hair.

### **6.1.2 Portable Wireless and Fibreless fNIRS Headband Compares Favourably to a Stationary Headcap-based system**

This study endeavored to compare the performance of AP-2 to an established fNIRS system (which utilizes a traditional full headcap form factor); specifically, the ability of both systems to measure the M1 response to movement in individuals >50 years of age (i.e., a sample age-matched to representative users of the Axem Home) was evaluated—as measurements from the same participants on both systems, across both an upper- and lower-extremity task were compared. Moreover, the study also asked participants to rate the comfort of the AP-2 system as



experienced in the present paradigm (which involved them wearing it for ~45 minutes). Results suggested that the fNIRS prototype's signal-to-noise ratio for both upper- and lower-extremity tasks was non-inferior to that of the established fNIRS system, and that the comfort of the AP-2 was feasible for extended use in this population.

### **6.1.3 Axem Home Formative Usability Study**

This study investigated the potential usability and utility of preliminary hardware (both AP-2 and a “looks like” Axem Home prototype, or “AP-LL”, the latter of which is described at section 4.1.4.1) and software prototypes that were meant to approximate several core aspects of the user experience of the Axem Home. This formative usability test was conducted with chronic stroke survivors in their homes. While disjointed in comparison to the envisioned complete, final user experience, this study successfully demonstrated the feasibility of several crucial elements of the overall user experience of the Axem Home: including the feasibility of having stroke survivors place a device approximating a final Axem Home headband on their head, having these users wear an fNIRS device throughout the course of an entire rehabilitation session, and to conduct a rehabilitation session through the guidance provided by a simple tablet-based software app. That said, while preliminary feasibility was demonstrated in all these areas, the findings for each begs future work that must be done to improve upon the functioning of these prototypes before pursuing clinical trials. For example, the exact placement of the headband in the majority of stroke survivors was incorrect, the rehabilitation session performed in the present study was relatively short (~30 minutes), suggesting any insights on the comfort of AP-2 in this user group should only be considered preliminary, and the software user experience presented was oversimplified and not inclusive of all crucial steps that would be required to perform a session of

BCI-based rehabilitation independently; as such, several areas for immediate, necessary improvement were identified in this productive, though preliminary, step forward.

#### **6.1.4 Measurement of Sensorimotor Brain Activity in Stroke Survivors during At-home Upper-extremity Rehabilitation: a mobile fNIRS pilot study**

This study examined the fNIRS data collected during the formative usability study outlined (from a human-factors perspective) in Chapter 4. The protocol ensured that all participants collected at least one full exercise of fist squeezing with their paretic hand, and these data were examined in relation to existing literature on the laterality of M1 activation in participants post-stroke as a correlate for upper-extremity motor function. In the event that the Axem Home is able to become successful as a rehabilitation tool, the fNIRS data collected might be subsequently used to better understand the individualized rehabilitation needs of stroke survivors, in an attempt to better optimize system-wide healthcare resources devoted to post-stroke rehabilitation. Thus, an indication that the data collected from AP-2 in this study aligns with the functional neuroimaging literature linking M1 activation during movement to a stroke survivor's level of impairment (FM-12) and function (SIS-Hand) would be a positive preliminary indication that the use of these fNIRS data for this purpose may be feasible. And indeed, a significant correlation between laterality index (i.e., the ratio of M1 activity between each hemisphere of the M1 during movement of the paretic arm) and both assessment-based and self-report-based measures of motor function was found, replicating existing literature that worse upper-extremity motor function is associated with a more atypical pattern of M1 laterality (i.e., less lateralized to the contra-lateral cortex) during paretic limb movement.

Taken together, these studies show the gradual but sure progression from internal verification testing to preliminary research indicating feasibility in a group of representative users. The challenges associated with this progress, as well as a contextualization of these

innovations in bespoke fNIRS design and BCI user experience, as related to the development of the Axem Home, are described below.

## **6.2 – LESSONS LEARNED DURING THE DEVELOPMENT OF AN fNIRS SYSTEM FOR USE BY STROKE SURVIVORS, AND THE FUTURE DIRECTION FOR ERGONOMIC fNIRS**

During the course of development on the Axem Home described in this dissertation, several changes were made to Axem's prototype fNIRS system (see Chapter 2 section 2.2.2.1 for a description of the AP-1 and AP-2 prototypes tested throughout this dissertation) due to the suboptimal performance on individuals with dense hair. While these changes were not made in an entirely controlled manner (due to the slow scale of implementing changes to fNIRS prototypes), there are many conclusions to be drawn from this work, relating to fNIRS technology generally, as well in discussing the directions fNIRS technology may take as increasingly ergonomic and user-friendly fNIRS systems are developed and used. This section describes these learnings within the framework for fNIRS signal quality introduced in Chapter 2 section 2.1.2 (see Figure 1 below, included here for ease of reading; also included in Chapter 2), discusses potential future work to be taken on the Axem Home in particular, as well as provides commentary on the implications of these findings for the field of ergonomic fNIRS in general.

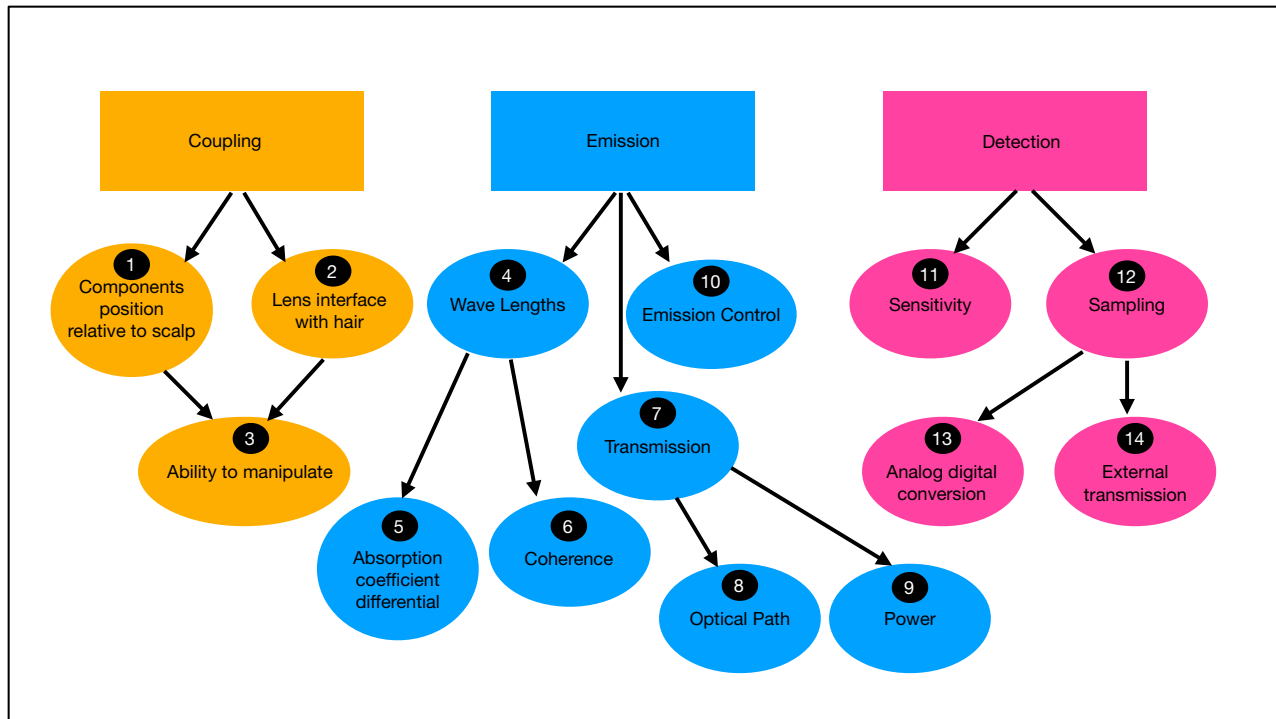


Figure 6-1. Schematic of the major aspects contributing to an fNIRS system's ability to measure cerebral hemodynamics.

## 6.2.1 Coupling

### 6.2.1.1 Progress made and lessons learned

As discussed in Chapter 2 section 2.1.2, the ability to get optical components in the desired position at the scalp is an important aspect of fNIRS system performance. In moving from AP-1 to AP-2, one important addition included in AP-2 was the additional flexibility of long-path emitters in the sagittal plane, which was implemented due to the experimenter's observation<sup>15</sup> (discussed in section 2.3.1) that the AP-1 headband would often appear to be tilting, such that its posterior section was higher off the head, tilting downward; moreover, this 'tilting' of AP-1 caused a substantial detrimental effect<sup>16</sup> on signal quality in ~10% of

<sup>15</sup> In addition to observations from internal testing

<sup>16</sup> These observations were noted in the experimenter's log as a result of the observation that posterior measurement locations appeared to have obviously worse lower signal quality (i.e., less presence of cardiac pulse and Mayer waves), and that the posterior portion of AP-1 was visibly tipped up off of the head.

participants, and was determined to have been in part caused by the lack of flexibility of AP-1 in the sagittal plane: since heads that were more concave, as opposed to more flat would force the AP-1 prototype to become unable to make contact with the scalp with all its optical components. And while no controlled test was performed between two fNIRS prototypes differing only in this manner, no observations of this ‘tipping phenomenon’ and the associated detriment in signal quality in posterior measurement locations were noted in tests conducted with AP-2. These changes were made in conjunction with the change from lower- to higher-power LEDs (see section 6.2.2 below)—as given that these higher-power LEDs required larger circuit boards, there was a need to change the mechanism used to attach the circuit-boards housing these higher-powered LEDs to the medial portion of the headband. Given this reality, these changes were not implemented in a controlled manner (e.g., the new sagittal flexibility was not implemented with lower-powered LEDs first, in order to identify their unique benefit to performance), but rather were implemented simultaneously. While this does limit our ability to isolate the effects of this change to how light guides were coupled to the scalp from AP-1 to AP-2, the fundamental geometry (that an additional degree of freedom in the sagittal plane would allow for a better fit between heads varying in their curve in this plane), together with the observation of reduced ‘tipping’ of the AP-2 headband in the sagittal plane, suggests that this change improved the performance of the Axem Home prototype within the domain of coupling light transmitting parts to the scalp.

Another aspect of fNIRS system design that relates to ‘coupling’ is both the interface between light transmitting parts and any hair which might be present, as well as the ability to manipulate this interface (either by the wearer of the fNIRS system or a research assistant). As described in Chapter 2 (section 2.1.2), the typical research-grade solution to this problem (to

enable a research assistant to manually remove an optode, divert any obscuring hair, and return the optode back to its original position) is incompatible with an fNIRS system meant to be used independently; therefore, the Axem Home would need to ensure another solution was employed. The solution employed by both AP-1 and AP-2 was low-durometer light guides, which are wider than typical fiber optic cable (in this case, with its width matching the lens of the LED it is being butt coupled to), and thus enable a relatively comfortable-feeling concave lens (as a narrower concave lens might have been felt on the scalp more like a needle). This solution allows the wearer of AP-2 to shift the device around on their head themselves in order to improve the penetration of its light guides through the hair, in a way that would not be possible with a device that employs more pointed light guides, and/or light guides made of a higher durometer material (e.g., acrylic). While this design surely can still be improved upon (see next section), in particular to allow for adequate coupling in the presence of voluminous hair, or hair that is styled in tight braids (which were not tested in this work), this solution appeared to work well across a wide range of individuals, and moreover may have been made more effective by the addition of sagittal flexibility in AP-2—since with this sagittal flexibility the user’s ability to ‘work the device through hair’ results in more pressure being applied to the scalp (i.e., resulting from pressure of the band flexing in the coronal plane as well as the pressure from the springs flexing in the sagittal plane) thus making it more likely to improve contact between the scalp and optical components.

#### *6.2.1.2 Limitations and future directions for the Axem Home and ergonomic fNIRS generally*

There are several avenues that would be worth exploring and building on to improve the function of the AP-2 prototype. Firstly, it would be useful to better understand the trade-off between the durometer used in light guides and light transmittance performance (both acutely

and over time). Indeed, previous fNIRS prototypes developed by Axem (not discussed in this dissertation) utilized acrylic light pipes, since acrylic is a commonly used material for light guides in research grade fNIRS systems<sup>17</sup>. While optimal from the perspective of light transmittance, acrylic is a very hard material (with a Shore A durometer >90<sup>1</sup>; with values >80 considered ‘hard’<sup>2</sup>) the design of the light guides used in AP-1 and AP-2 did take this trade-off into consideration—specifically a Shore A durometer of 70 (a value considered to be at the intersection of ‘medium soft’ and ‘medium hard’; or, approximately the hardness of a tire tread) was chosen because it was hypothesized (through the testing of sample materials) that it would be unlikely to deform when in use in AP-2 (established through observational testing with the non-Lumisil pipes, then by testing on the actual Lumisil pipes), to the extent that the light transmittance through it would be negatively impacted, but also that its durometer was not so high that it would be painful and/or uncomfortable to wear during extended sessions of use, and might enable comfortable manipulation by the wearer to attempt to have the light guides better penetrate the hair. Failing to strike the right balance in this trade-off could have dire consequences in either direction: not considering comfort enough could render the device undesirable by users, while allowing the light guides to be too soft would cause them to be deformable,<sup>3</sup> which could then reduce internal reflection back into the light guide, resulting in greater light losses<sup>4</sup> and thereby worse signal quality (causing less light to arrive at the fNIRS system’s detectors, potentially invalidating the fNIRS data and rendering the device incapable of achieving its intended use); or become susceptible to physical damage, resulting in a gradual loss of its light-transmitting ability over time. However, this decision was based on the testing of several sample parts which were not capable of light-transmittance (being made of material other

---

<sup>17</sup> E.g., <http://www.hitachi-medical-systems.eu/products/optical-topography/etg-4100.html>, <https://nirx.net/nirscout>

than Lumisil, the optically-transparent silicon used for the light guides in AP-1 and AP-2), and thus the trade-off between comfort and light transmittance for these light guides was never explicitly explored<sup>18</sup>; doing so might enable parts of lower durometer (which would thus be more comfortable) to be used with little or no reduction in light transmittance.

Another area that might be explored in future work building off the AP-2 is the use of longer light guides that would be capable of protruding from the main headband unit more or less based on the volume of hair—with more protrusion needed for more voluminous hair. Related solutions are employed by some research grade systems, that allow a research assistant to manipulate the tensile properties of springs which control the protrusion of optical components. While there is not an obvious way to translate this technique to an fNIRS system meant to enable independent measurement, related solutions (e.g., it may be possible for the wearer of the device to press a button on the device itself that then initiates an automated mechanical process, whereby the protrusion distance of the light guides are extended until they are either fully extended or it is detected that the springs pushing out the light guides are sufficiently tense) may be worth exploring in order to improve the ability of AP-2 to facilitate contact between its optical components and the scalp even in the presence of very voluminous hair.

### **6.2.2 Notes on Emission**

#### *6.2.2.1 Progress made and lessons learned*

As described in Chapter 2 section 2.1.2, the main two sub-components of emission with respect to fNIRS system design are the wave lengths of light utilized, and the details of light transmittance. Unfortunately, innovating on wave lengths of light utilized in an fNIRS system is

---

<sup>18</sup> Rather, the decision to select Shore A 70 Lumisil was based on the perception that, in preliminary testing, material of this durometer (though no lower) would not visibly deform in response to approximately 3lbs of pressure (with 3 lbs being an upper band on the approximate weight of the Axem Home system)



challenging—given the high cost of the equipment and expertise required to develop novel LED and laser technology (due to the complex chemical processes required to fabricate the semiconductor wafers and grow the epitaxial layers that are required for the construction of dies<sup>5</sup>), the ability to construct truly custom LED and/or laser components is not possible for groups with limited research and development budgets. However, the move from AP-1 to AP-2 involved several innovations with respect to light transmittance. Firstly, the shape of the light guides themselves were changed from AP-1 to AP-2: improvements to the shape of the light guides were made that resulted in a significant improvement in light transmittance. This improved design optimized to collimate the maximum amount of light possible, whereas the light guides used in AP-1 contained features that served mechanical properties (e.g., to make them convenient to hold in place within the headband). Specifically, the pipes used in AP-2 used a tapered section at their base (see Figure 6.2) as the area from which other mechanical parts might hold it in place, as opposed to the hard angled cut-out mid-way up from the base used in the AP-1 design (i.e., the section where an illustrated light ray is exiting the pipe in Figure 6.2). Moving this section to the base of the light guide results in a smaller proportion of light interfacing with this section (since the chance of this occurring increases as you move down towards the distal end of the pipe, due to the scattering pattern of the light); moreover, the change from a rectangular-shaped, 90 degree cut-out to a tapered pattern results in fewer light losses from light interfacing with this area of the pipe, due to the fact that the angle between the tapered surface the shaft of the pipe is decreased, making this tapered angle closer to the critical angle of total internal reflection, and thus causing more light that strikes this portion of the pipe to be reflected back into the light guide.<sup>4</sup>

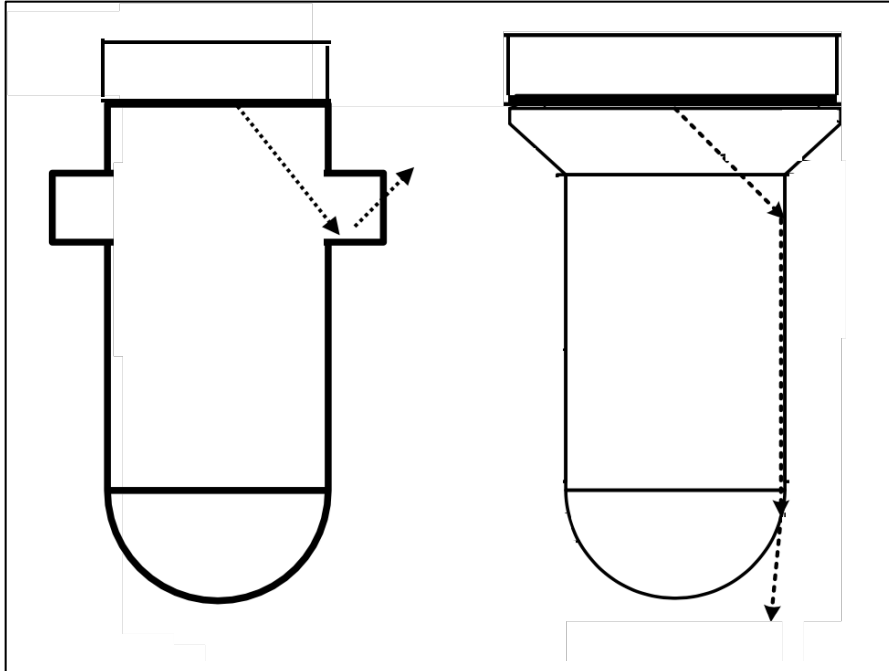


*Figure 6-2. Light guides from AP-1 (left; butt coupled to the light guides used in AP-1) and AP-2 (right; butt coupled to the light guides used in AP-2) fNIRS systems shown; dotted light represents hypothetical light ray emitted from the same location within the LED lens, and at the same angle.*

And secondly, the most significant change from AP-1 to AP-2 that was made was the use of more powerful LEDs in AP-2. While this increase in power provided the most significant increase in number of photons being delivered from the terminus of the light guides, as mentioned in the preceding section, the exact effect of this change compared with other changes that were introduced simultaneous are not isolated in this work. However, it is important to point out the significant trade-offs that increasing the power output of an fNIRS system's emitters introduces: mainly (1) the need for a power supply that has the ability to deliver larger amounts of current and overall greater capacity (i.e., battery life), as well as (2) the need to manage the increase in thermal energy created as a by-product of having an fNIRS system emit more light. In the case of the AP-2, this required the use of a more powerful battery (and thus a modification to the design, wherein which the battery was positioned at the back of the head as opposed to at

the vertex) as well as larger circuit-boards to both house the more expansive supporting circuitry required to control the more powerful LEDs, as well as the larger heat sinks needed to dissipate a larger amount of thermal energy these higher-power LEDs generate when compared with the lower-power LEDs used in the short-path channels of AP-2 (and for all channels in AP-1).

#### *6.2.2.2 Limitations and Future directions for the Axem Home and fNIRS generally*

As discussed above, significant strides were made in light transmittance between AP-1 and AP-2, though those strides associated with increasing the power of emission were accompanied by trade-offs. In particular, the trade-off of increased heat is especially fraught, given the need for the Axem Home device to keep all external parts  $\leq 43$  degrees Celsius.<sup>6</sup> Therefore, future work might endeavor to better mitigate the downside of increased heat by improving the Axem Home's ability to draw heat away from its external parts (i.e., the portions of the headband adjacent the LED, as well as the light guide). Such a method might involve an expansion of the size, a change in heat sink material, and/or a change in the geometry of the heat sinks used (though the limited internal space available makes this challenging and is associated with its own mechanical performance trade-offs). Of course, another way to improve this trade-off would be to determine ways to direct a larger proportion of the light generated by an LED source to the scalp (while maintaining comfort and robustness). One potential method may be though affixing the LEDs to the light guides via an epoxy, which would reduce Fresnel losses<sup>7</sup> associated with having an airgap between the LED lens and the light guide—see Figure 6.3 for an illustration of phenomenon, as well as its interaction with the degree of LED light collimation.<sup>8</sup> And while the work described in the preceding section did include optimizing light collimation (and thereby transmittance) from the point where the light guides butt coupled with the LEDs to the scalp (i.e., optimization of the light guide's geometry), it may also be possible to

take this work further, and to optimize the collimation of the light from the point where it is emitted from the LED lens itself. Such a solution may take the form of a nano-material-film overlaying the case of the LED, which is selectively optimized to collimate light within certain frequencies.<sup>9</sup> A similar concept is currently used in the aviation industry to prevent laser attacks on planes (e.g., by selectively diffusing light when it hits the film on the plane’s windshield),<sup>10</sup> and such solutions may be used in in this case as well to allow an fNIRS system to capture a greater proportion of the light its parts are generating for its purposes of brain measurement.

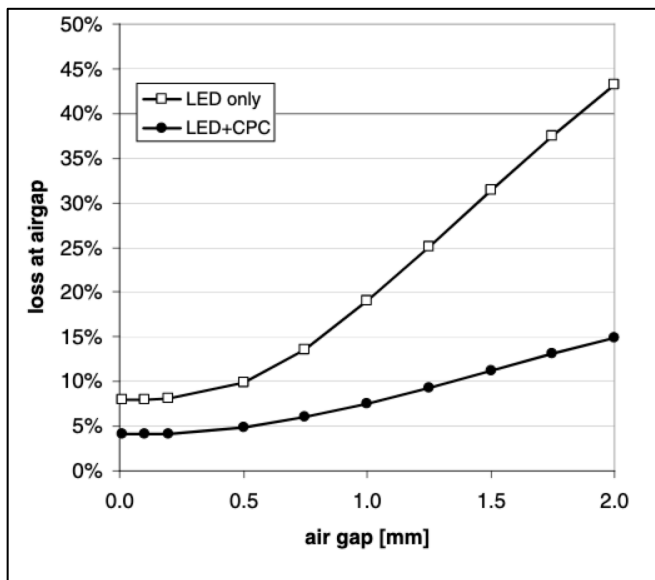


Figure 6-3. Figure 6 from Tessnow et al. (2007).<sup>8</sup> Theoretical Fresnel losses at an air gap, comparing standard surface Lambertian (i.e., flat lensed) LED (LED only) versus a fully collimated source (LED + CPC, or compound parabolic concentrator).

### **6.2.3 Notes on Detection**

#### *6.2.3.1 Progress made and lessons learned*

Unfortunately, innovations in light detection, like innovations in wavelength selection discussed in the preceding section, are challenging to implement. Given the high level of expertise required to innovate on the fundamental process of light detection itself (for similar

reasons as listed above, for the difficulty in fabricating one's own LEDs), an fNIRS manufacturer is left primarily to the choice of which commercially available optical detector to choose, and how to design their system around this detector. The silicon photodiode (SiPD) chosen for AP-1, and also used in AP-2, was determined to be the most sensitive SiPD for the wavelengths being employed for fNIRS measurements, and (as discussed in the next section) while this is fertile ground for future innovation, there was no significant innovation or improvements made on this front in the evolution from AP-1 to AP-2.

#### *6.2.3.2 Limitations and Future directions for the Axem Home and fNIRS generally*

The evolution of fNIRS has in part been a result of the increasing availability of increasingly sensitive detectors. As avalanche photodiodes (APDs) and silicon photomultipliers (SiPMs) gradually become more affordable, we have increasingly seen them used in fNIRS systems. Avalanche photodiodes are a particular type of SiPDs that possess internal gain by means of a high reverse bias voltage (100-500V<sup>11</sup>); this means that the signals APDs pass to an amplifier have already had a gain factor (of 30-200<sup>12</sup>) applied, increasing their sensitivity far beyond that afforded by SiPDs.<sup>13</sup> Whereas SiPMs consists of an array of thousands of single-photon APDs (called 'pixels');<sup>14</sup> this approach means the bias voltage required (given that it is only needed to create internal gain for each single-photon APD, they require only ~30V<sup>15</sup>) is significantly lower than that required by traditional APDs, and that their internal gain generated is orders of magnitude larger than that produced by APDs.<sup>11</sup> While APDs are a popular choice for several non-mobile fNIRS systems (e.g., <https://nirx.net/nirscout>), the use of SiPMs, while proven feasible and highly effective,<sup>16</sup> their use has yet to become widespread, with SiPMs are not currently employed in any commercially available fNIRS systems.

However, at present the use of APDs and SiPMs both present significant challenges for the development of a scalable and ergonomic fNIRS system. Both APDs and SiPMs require very precise temperature monitoring and calibration, since both devices ability to take accurate measurements depend on controlling their internal temperature with great precision;<sup>12,17</sup> moreover, the high bias voltage required by APDs introduces significant safety challenges for their integration with wireless fNIRS devices (see Figure 6.4 for an example of a mobile system utilizing APDs),<sup>18,19</sup> and the large amounts of data generated by the single-photon pixels of SiPDs requires extremely sophisticated custom microprocessor circuitry.<sup>20</sup> And finally, both APDs and SiPMs remain very expensive (>1 order of magnitude) compared with the commodified SiPDs.



*Figure 6-4. Example of a mobile fNIRS system utilizing APDs.* <sup>18</sup>

For these reasons, at present the Axem Home is not a good fit for the use of APDs or SiPMs: even more so than the trade-offs between increasing the power of emission and a corresponding increasing need for additional circuitry and thermal management, using APDs and SPMs necessitate even more significant increases in the complexity of the circuitry required, as well as the need to manage the vastly larger amounts of current that these components require

(which increases the safety risks by orders of magnitude, as opposed to the generally linear increases in safety risks associated with the introduction of increasing the power output of an fNIRS system's emitters). However, this is a rapidly developing area, and one that might be of interest to Axem as it charts its long-term plans to improve upon its fNIRS technology.

### **6.3 – HUMAN FACTORS LESSONS LEARNED AND THOUGHTS ON FUTURE DIRECTIONS: DEVELOPMENT OF AN AT-HOME fNIRS BRAIN-COMPUTER-INTERFACE SYSTEM FOR STROKE REHABILITATION**

#### **6.3.1 – fNIRS Hardware User Experience: Limitations, Lessons Learned, and Future Directions**

While the framework referenced in the preceding section (illustrated in Figure 6.1) adequately captures the major factors dictating the ability of an fNIRS system to gain adequate signal, its focus is narrowly on only the most fundamental elements associated with gaining an fNIRS signal, not considering the types of cerebral signals that are of interest or during which tasks. When considered in light of the specific intended use of the Axem Home fNIRS headband, some key omissions are the requirements that the optodes facilitate comfort over lengthy and repeated uses (given that its purpose is to compel the user to complete large volumes of rehabilitation), while being impervious to a modest level of movement (enough to accommodate seated, upper-extremity rehabilitation tasks in individuals who, unavoidably, may also be performing compensatory movements of the trunk and/or lower body). These inter-related issues relate to items 1-3 and 8-9 on the framework illustrated in Figure 1. The three sub-components of coupling (i.e., items 1-3), as well as light transmission (or item 8, 'optical path') all represent something of a trade-off with comfort, since solutions which optimize for these sub-components alone will be solutions imparting mechanical stress onto the user's scalp, thus potentially causing discomfort. It is for this reason that solutions for comfort must always be considered in light of their deleterious impact on an fNIRS system's ability to achieve adequate light transmission to

the scalp. Likewise, the amount of power used by an fNIRS system (i.e., Figure 1 item 9) also represents a factor wherein optimizing for light delivered to the scalp will result in discomfort, given that emission sources which generate large amounts of power generate greater amounts of heat (although it should be noted that this trade-off is significantly less severe when using lasers as opposed to LEDs, given their superior efficiency; however, lasers are not suitable for portable fNIRS applications due to the substantial supporting circuitry required); internal testing within Axem has revealed that if an fNIRS system is generating sufficient heat to cause discomfort, that this effect is strictly time-dependent—i.e., it scales linearly with the amount of time (within a given session) they use the device; this is distinct from the nonlinear relationship we have observed between mechanical stress and time, whereby discomfort often remains negligible until a threshold is crossed and discomfort increases quickly. This means that an fNIRS system meant to be used for any reasonable length of time (e.g., >10 minutes) should not impart discomfort to a user based on the generation of large amounts of heat. Also, unlike mechanical stress, the process of causing discomfort via heat is more likely to sensitize the skin,<sup>21</sup> making repeated uses of such an fNIRS device problematic.

Another aspect not included in this framework that is highly relevant to the development of the Axem Home headband is the challenge of proper positioning of the optodes. While experimental fNIRS systems can rely on researcher intervention to provide a reliable solution to this problem, in the case of the Axem Home the user of the fNIRS device themselves must be able to independently place the device within a precise range of valid measurement locations that spans only a few centimeters (presently the range of valid measurement locations are estimated to be those validated through the studies in Chapters 2 and 3: a 4cm range spanning 1cm posterior to CZ to 3cm anterior to CZ). These considerations interact with and mirror item 3 in



Figure 1: just as the Axem Home must enable the wearer of the fNIRS device to independently manipulate the coupling interface between the light guides and the scalp, it must also facilitate correct placement on the head. As described in chapter 4, this is an aspect of the Axem Home user experience that is far from refined, with most participants in the present study failing to correctly place the surface model prototype used in that study. As discussed in Chapter 4, this unique challenge may necessitate a re-consideration of the design of the AP-LL going forward, with more emphasis placed on using the design of the device to make its proper placement inevitable. Specifically, it may be necessary to move away from the ‘one size fits all’ vision for the Axem Home headband, and bring in some aspect of custom fit into the design—if not with respect to the main headband unit, then potentially to the strapping system used. Inspiration might be taken from the human factors work that has been done on virtual reality headsets, where it has been learned that the weight distribution of the device must be such that users are compelled towards placing the device in the correct location (since placing it elsewhere feels uncomfortable or makes the device feel unstable), and that multiple degrees of freedom for adjustment to the shape of an individual’s head should be provided in a seamless and easy-to-understand manner.<sup>22</sup> However, to our knowledge, the need to design a device that (1) fits well to a variety of heads, (2) allows for quick independent set-up, and (3) requires precise placement on the head is a unique human factors problem that other head-mounted electronics devices (e.g., virtuality reality headsets), or even other wearer-donning neuroimaging equipment (e.g., Interaxon’s Muse EEG device, which only requires the user to place the device’s sensors on the forehead, with no real import given to the precise plane at which they sit) do not need to contend with on this level. For this reason, there are few precise parallels to this human factor problem, and therefore Axem must simply take the appropriate development time to iterate on solutions to

this problem, and these solutions may in the future be used to inform other regionally-bespoke neuroimaging systems. While the details of implementation are beyond the scope of this dissertation, in the time since the work described herein took place, this approach of adding an element of adjustment to the Axem Home has borne substantial progress, with better legibility of the affordances of the headband (i.e., reduction in the propensity to place it incorrectly) and greater consistency with respect to placement (see Figure 6.5).



*Figure 6-5. Axem Home headband prototype as of January 2021. This prototype includes a one-time adjustable forehead strap that is sized depending on the head size of the wearer (i.e., this strap would only need to be sized by the wearer upon first use), as well as an adjustable band back that allows for a snug fit to be achieved each time they don the device.*

### **6.3.2 – Axem Home Software User Experience: Limitations, Lessons Learned, and Future Directions**

As with the development of the user experience for the Axem Home headband, the development of the Axem Home software app remains a work in progress, with many key issues unresolved with respect to the overall direction of its design. While (as discussed in Chapter 4) the menu systems were perceived as moderately easy to navigate (see Table 4.5), and proved feasible for use by all stroke survivors included in the formative usability study (Chapter 4), it remains to be seen whether the structure of rehabilitation sessions defined by AP-S in Chapter 4 is viable for extended, independent use. Moreover, AP-S did not include several aspects of the

app that will be required in any manifestation of the final product—e.g., there was no requirement to log into the app, connect the headband via Bluetooth, nor to calibrate the headband.

And while the formative usability study presented in Chapter 4 provided a preliminary indication of the usability and perceived usefulness of the prototype holistically (see Table 4.5), any concrete test of product ‘stickiness’ (i.e., the ability for the software to compel the user to use it<sup>23,24</sup>), which is be a pre-requisite to using the Axem Home to enhance compliance to a home rehabilitation program, was beyond the scope of this dissertation. While the use of gamification (used here in the strictest sense of the word, to refer to Skinnerian operant conditioning linking the completion of tasks to otherwise-only-arbitrarily-related rewards<sup>25</sup>) could surely be ‘slapped on’ (i.e., applied in a relatively straightforward, formulaic manner, the same way it might be towards any healthy-behaviour-promoting product<sup>26</sup>) quickly, the integration of any gamification elements with the specific design language of the software would be a nuanced and challenging undertaking<sup>27,28</sup> that will require significant future design iteration to optimize in the case of the Axem Home software.

However, over and above the implementation of gamification, one of the major opportunities for the Axem Home software to drive engagement is making the rehabilitation exercises themselves pleasant to use—in other words, making the rehabilitation exercise itself a type of serious game.<sup>19</sup> On this front, the formative usability study presented in Chapter 4 did make at least some minute progress. While the video presentation of the rehabilitation exercises tested in the study presented in Chapter 4 did prove comprehensible by users (Table 4.1), the

---

<sup>19</sup> Serious game here meaning a game that is not primarily for entertainment, and that is designed with the goal of promoting some utility function that is larger than the elements comprising the game itself (e.g., to promote a healthy behaviour).<sup>29</sup>

lack of interactivity may prove to be an impediment to long-term compliance. Thus, one important aspect to explore in the long-term development of the Axem Home app is embedding legible game mechanics into the very act of performing rehabilitation exercises. The most apparent mechanism for this would be through some type of motion tracking mechanic. The main advantage that rehabilitation software based on motion tracking inputs has is the immediacy with which the user's movements are instantaneously transformed into a meaningful element within a comprehensible, reinforcing game environment. This approach greatly expands the possibility space of game mechanics that might be utilized, and has been shown feasible in enhancing the engagement of both lower-<sup>30,31</sup> and upper-extremity<sup>32-35</sup> stroke rehabilitation.

And while there are surely many game mechanics based on real-time neurofeedback that might be integrated into the performance of rehabilitation exercises, there are not many examples of this in practice.<sup>36</sup> Thus, it should be a future priority for Axem Neurotechnology to investigate the use of camera-based motion tracking technology (potentially utilizing the front-facing camera already present on any tablet that will be used for use of the Axem Home app)<sup>20</sup> into the Axem Home app, given the ability of motion-tracking based feedback to increase the immediacy of the interactivity associated with performing rehabilitation movements.

However, in lieu of these trappings of interactivity, the Axem Home software's immediate direction ought to focus on better understanding the relative strengths and weaknesses of using the video for instructional purposes (i.e., provided to help the user understand the actions to be performed) and imitation purposes (i.e., provided as an evidence-based aid in generating a more effective motor simulation<sup>37</sup>). This pursuit also relates to the use of the Axem Home for the performance of rehabilitation exercises via motor imagery as opposed to motor

---

<sup>20</sup> And/or movement tracking on the tablet itself (e.g., a whack a mole game wherein the user is to tap moles that appear at various areas of the tablet's screen).

execution—with imagery and execution both potentially benefiting from the use of videos for imitation purposes,<sup>21</sup> while also benefiting from the use of videos for strictly instructional purposes (since in some cases during motor execution a user might want to focus on their extremities being moved, while during imagery they may at times prefer to close their eyes to better visualize the movement, or to better block out distractions); a better understanding of this trade off, of when one approach might work versus the other, will be an important aspect of making the user experience of the Axem Home app a rewarding one. Moreover, a better understanding the role of videos presented for instruction versus presented for imitation might also aid in the integration of real-time neurofeedback into the Axem Home app in the future.

On the topic of neurofeedback, the lack of progress on this front in Chapter 4 represents a major deficiency in this dissertation’s attempt to characterize the feasibility and utility of the Axem Home system. As discussed in Chapter 4, due to technical problems with the calculation of the neurofeedback signal in that study (in addition to the study’s premature termination due to COVID-19), that study provided only the most preliminary steps forward for Axem’s understanding of how neurofeedback might function in the Axem Home app. In particular, the one finding that study garnered on this front was the finding that a discrete, quantified neurofeedback signal—in this case a percentage—was frustrating and demotivating. This finding aligns with the majority of other effective neurofeedback systems, that have tended to present feedback to users in an implicitly (versus explicitly) quantified manner (i.e., as a line moving up or down within an implicitly ambiguous 2D space, as opposed to floating point values within explicitly defined range). However, it is possible that it is not the explicit nature of the feedback signal per say, but rather the use of a point estimate specifically which was suboptimal. Support

---

<sup>21</sup> The implementation of neurofeedback based on motor imagery and action observation having been shown to be feasible previously.<sup>38</sup>

for this idea comes from the only M1 neurofeedback study that experimentally compared the effectiveness of real-time versus delayed M1 neurofeedback during MI<sup>39</sup>. This study used a ‘thermostat’ style visualization to represent the level of contralateral M1 activity either in real-time during MI, or during rest blocks following MI blocks (see Figure 6.2). While this thermostat-style visualization does not assign a point estimate value to the neurofeedback score being presented, it does represent neurofeedback scores within an obvious, explicit range of potential values (with an easily legible view of all the possible scores). The hypothesized reason point estimate values are suboptimal (as deduced from notes taken during usability interviews) is that they cause frustration over and above any frustration communicated by non-point-estimate-based neurofeedback score displays (i.e., a low percentage may be perceived as more negative than an empty thermostat, simply because of the user’s prior associations with percentages). This suggests that either (1) the use of a point-estimate neurofeedback score (as opposed to an explicitly defined neurofeedback score) is suboptimal for neurofeedback systems in general, or that (2) the use of a point-estimate value neurofeedback score is uniquely suboptimal for neurofeedback systems designed for stroke survivors. Regardless, it suggests that it is likely best to avoid such neurofeedback displays going forward for the design of the Axem Home app’s neurofeedback scores.

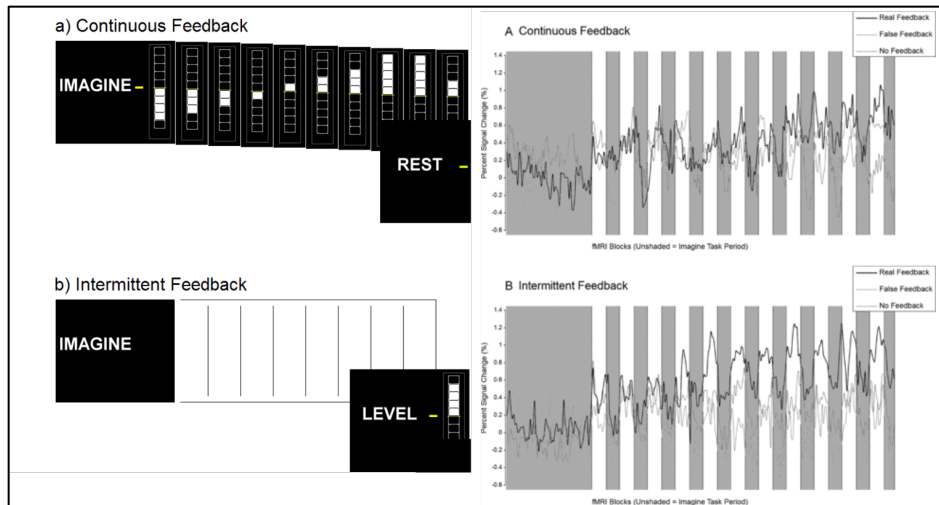


*Figure 6-6. Illustration of both types of neurofeedback used in a study testing the efficacy of intermittent versus 'real-time' motor imagery neurofeedback.*

Another unresolved aspect of the present work is the potential for using real-time neurofeedback (during motor imagery and/or motor execution) in the Axem Home app. While the AP-S system tested in the study presented in Chapter 4 did not have the ability to provide real-time feedback, all fNIRS MI neurofeedback studies to date have utilized real-time (versus intermittent) neurofeedback. For instance, effective fNIRS-based MI neurofeedback systems have utilized line graph representations of relative oxyhemoglobin<sup>40</sup> (see Figure 6.3, left pane, for an example), as well as bar graph<sup>41</sup>, and heatmap representations<sup>42</sup>. All of these methods of presenting neurofeedback scores involve translating a point-estimate (i.e., a 50% score of a possible 100%) to either a colour scale (in the case of the heat map) or spatial (in the case of the line and bar graph) representation. Another method of presenting M1-based neurofeedback that has been utilized<sup>43</sup> with an EEG-based system is the use of a threshold-based neurofeedback signal, whereby during an active period of MI a feedback signal is only presented if the user's level of M1 activation reaches a pre-determined threshold. In this case the feedback presented was a proprioceptive stimulus delivered to a prosthetic hand, but this technique is worth mentioning for its innovative design: not only did it use a unique threshold-neurofeedback-

system, it utilized a digital mirror box-style presentation for the active period via a tablet, a technique which could potentially be used in future Axem Home software (Figure 6.3, right pane).

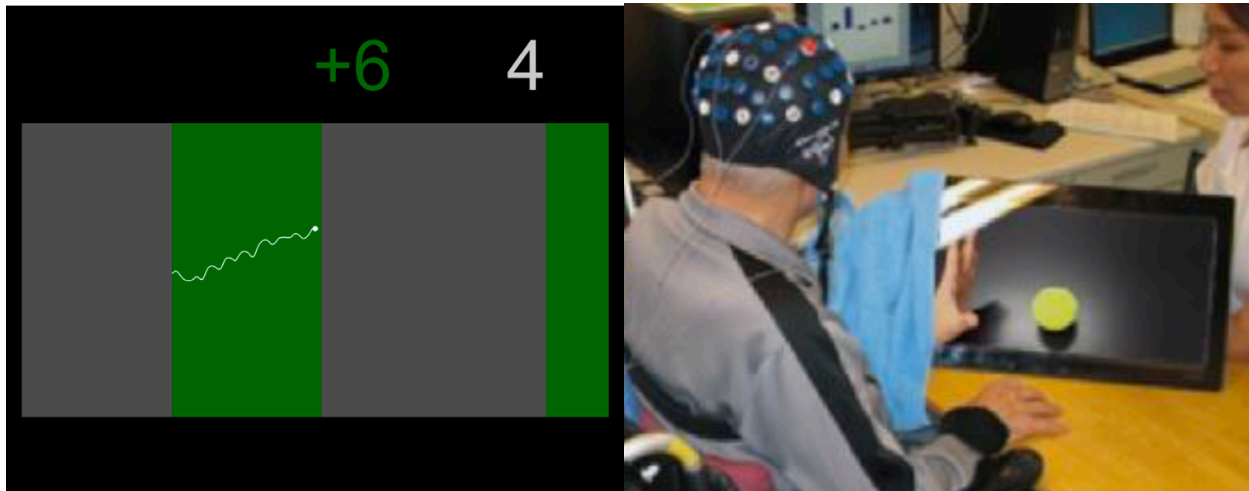


*Figure 6-7. Left pane - Illustration of the neurofeedback score display utilized in Kober et al.<sup>40</sup> Green areas represented task periods while grey areas represented rest periods. The line graph would only display the relative oxyhemoglobin value during task periods, and following each task period the user was given a score based on the slope of the oxyhemoglobin value during that task period (i.e., the “+6” in this screen) which would be added to their cumulative score (i.e., the “4” in this screen). Right pane – illustration of digital mirror box task used in<sup>43</sup>.*

It is clear the future of both the method with which the Axem Home guides rehabilitation sessions and presents neurofeedback both require extensive further development. In the short-term, the role of videos for instructional and/or imitation purposes must be better articulated, and improved intermittent neurofeedback presentations must be tested; while in the longer-term, experiments with integrating motion-tracking into the rehabilitation exercise, as well as bringing in some aspect of real-time neurofeedback warrant exploration. Moreover, other simpler features warrant inclusion in the short-term, such as the addition of a level of gamification (e.g., cumulative points and rewards for completing exercises across rehabilitation sessions). If strides can be made on all these fronts, to the point where the performance of rehabilitation exercises feels seamless and natural, and the neurofeedback presented feels legible, tangible, and the user



feels rewarded for returning to the Axem Home app, the experience may begin to feel meaningful—an achievement that may render the otherwise arduous task of post-stroke rehabilitation slightly more tolerable.

#### **6.4 – THE POTENTIAL OF fNIRS BIOMARKERS IN STROKE RECOVERY: PROGRESS, LIMITATIONS, AND FUTURE DIRECTIONS**

As discussed in Chapter 1 section 1.3.2, the laterality of M1 activity during simple unilateral movements of the paretic upper-extremity (i.e., M1-LAT) in stroke survivors represents an intriguing potential neural biomarker of post-stroke motor recovery. In brief, not only has M1-LAT been shown to correlate with the functional status of the upper-extremities, even when controlling for time since stroke, it has also been shown to be predictive of the response to rehabilitation intervention (see Chapter 1 section 1.3.2). Moreover, as outlined in Chapter 1 section 1.3.3, resting state M1 interhemispheric functional connectivity (i.e., M1-rsFC) has also been shown to both correlate with and predict stroke survivor's functional status (see Chapter 1 section 1.3.3). Thus, in the future, it may be feasible to use M1-LAT measurements throughout stroke survivor's recovery to predict treatment response, in order to advocate that a patient receive more rehabilitation, or to best optimize rehabilitation resources across an entire healthcare provider (e.g., inpatient rehabilitation facility with limited capacity) or payer (e.g., insurance company that desires to generate the best motor outcomes for the lowest expenditures).

In Chapter 5 of this dissertation, the ability of a preliminary Axem Home prototype to measure M1-LAT was demonstrated cross-sectionally in a group of 11 stroke survivors; that study found a positive correlation between M1-LAT and both the upper-extremity Fugl-Meyer Assessment and the hand sub-scale of the Stroke Impact Scale (see Chapter 5, Figure 5). These findings suggest that it may be feasible for stroke survivors to independently take M1-LAT measurements from their own brain activity generated during rehabilitation using a wireless

fNIRS system suitable for use in their homes. In addition to acting as the basis for an accessible neurofeedback system for post-stroke rehabilitation (a topic which was not explored sufficiently in Chapter 5 to warrant additional explanation here), the accessibility of this technology has the potential to greatly expand the scale with which M1-LAT measurements are gathered. However, a limitation of this dissertation is that at no point was any resting state paradigm employed. Given that fNIRS has been shown to be feasible to gain resting state measurements that are analogous to those taken by fMRI,<sup>44</sup> and moreover that fNIRS has been used to document the expected increase in M1-rsFC associated with post-stroke motor recovery,<sup>45</sup> this represents a notable shortcoming. While the focus of this dissertation on preliminary validation aligned better with a focus on event-related designs (in particular the performance of simple motor tasks, which allowed several characterizations of M1-LAT across healthy controls in Chapters 2-3, and chronic stroke survivors in Chapter 5), the absence of any resting state tasks throughout this work represents a notable limitation that should be rectified through the collection of resting state fNIRS data on stroke survivors, from an Axem prototype, in the near-term future.

Moreover, as discussed in Chapter 1, there remains uncertainty about the precise mechanism at play underlying the relevance of M1-LAT to post-stroke motor recovery—with studies both supporting and discounting the hypothesis that a normalization of M1-LAT in stroke survivors reflects a normalization of maladaptive IHI. Supporting this mechanistic explanation are studies showing a normalization of M1-LAT upon inhibition (via TMS) of contra-lesional M1<sup>46-52</sup>; while other work has found that a normalization of M1-LAT was not accompanied by a co-occurring reversion to typical mIHI<sup>53</sup>. This suggests that while mIHI is a cause of atypical M1-LAT, it is not the only cause, as M1-LAT can be normalized in spite of a continuation of mIHI. Other potential underlying pathologies that may cause atypical patterns of M1-LAT

include damage to the CST connecting the ipsi-lesional hemisphere to subcortical regions (leading to diaschisis and therefore hypoactivation of ipsi-lesional M1),<sup>54</sup> or cellular damage to ipsilesional M1 itself.<sup>55</sup>

Another avenue that requires better understanding is the cases in which stroke survivors demonstrate improved motor outcomes with an increasingly atypical M1-LAT pattern<sup>56–62</sup>. This suggests that for a sub-set of stroke survivors, their best chance for optimal recovery lies in the hyper-activation of the contra-lesional M1. Given that this pattern has been shown to occur in individuals with very large lesions<sup>60</sup>, and/or lesions which have caused large amounts of damage to M1 or the corticospinal tract (CST<sup>62</sup>), this might suggest that the viability of the ipsilesional CST pathway is the main determinant of whether M1-LAT might represent a metric which ought to be optimized for normalization or to be made further abnormal. Therefore the use of DTI<sup>63,64</sup> (which are able to provide a quantification of CST damage) may aid in this determination; alternately, given the demonstrated relationship between M1-rsFC and CST damage,<sup>65,66</sup> it may also be feasible to use functional resting state measurements at M1 for this purpose also.

Likewise, (as discussed in Chapter 1 section 1.3.3) while M1-rsFC has consistently been found to be associated with motor recovery from stroke, there are nuances with respect to its variable interpretations in stroke survivor's with and without serious CST damage, as well as to its role at different phases of recovery<sup>66,67</sup>. In order to maximize the utility of its M1-based neurofeedback, as well as the utility of the Axem Home to predict and optimize rehabilitation treatment, future research and development on the Axem Home will need to better resolve this uncertainty; ideally, such work would build towards the capacity to derive answers to these questions, through fNIRS measurements alone, or in combination with other inputs from the Axem Home system or relevant items from patients' electronic health records (e.g., routine

computerized tomography scans). One of the best candidate biomarkers for providing more value to the Axem Home's fNIRS data, in both differentiating stroke survivors who should have their ipsi-lesional M1 activity enhanced or attenuated, as well as in more broadly resolving how to interpret M1-LAT and M1-rsFC for optimal predictive power, could be CST damage as measured by diffusion tensor MRI, which has also shown to be predictive of stroke survivor's motor recovery<sup>64,68,69</sup> and which has been shown to be more predictive when combined with functional measurements from M1<sup>70</sup>. Future research with the Axem Home would significantly benefit from the collection of these data alongside longitudinal fNIRS measurements (another limitation of the work presented in this dissertation).

## **6.5 – CONCLUSION**

The work presented herein chronicles some preliminary steps in the development of a stroke rehabilitation product that endeavours to, in the short-term, provide compelling at-home BCI enabled rehabilitation; and which, in the long term, endeavours to use the scalable functional neuroimaging at its core to help optimize post-stroke rehabilitation—towards the overall goal of helping health systems around the world improve outcomes. The steps presented in this work span from initial validation of a novel functional neuroimaging device, to comparison of a prototype device with an established system, and finally to preliminary testing with representative users. While obviously incomplete, and not completely chronologically organized (aspects of all studies occurred simultaneously), this work, and its description herein, has resulted in many learnings that might be of use to future innovators looking to improve the accessibility of functional neuroimaging, and/or create novel digital-health-based products for the promotion of neurological health.

## 6.6 – REFERENCES

1. Spasojevic, P. *et al.* The Mechanical Properties of a Poly(methyl methacrylate) Denture Base Material Modified with Dimethyl Itaconate and Di-n-butyl Itaconate. *International Journal of Polymer Science* vol. 2015 e561012 <https://www.hindawi.com/journals/ijps/2015/561012/> (2015).
2. Smooth-on. Smooth-on Shore Hardness Scale. <https://www.smooth-on.com/page/durometer-shore-hardness-scale/>.
3. Qi, H. J., Joyce, K. & Boyce, M. C. Durometer Hardness and the Stress-Strain Behavior of Elastomeric Materials. *Rubber Chemistry and Technology* **76**, 419–435 (2003).
4. Sharma, K. K. *Optics: Principles and Applications*. (Elsevier, 2006).
5. howmade.com. How Products are Made - Light-Emitting Diode (LED). <http://www.madehow.com/Volume-1/Light-Emitting-Diode-LED.html>.
6. 14:00-17:00. IEC 60601-1-11:2015. *ISO* <https://www.iso.org/cms/render/live/en/sites/isoorg/contents/data/standard/06/55/65529.html>.
7. Weik, M. H. Fresnel reflection loss. in *Computer Science and Communications Dictionary* (ed. Weik, M. H.) 657–657 (Springer US, 2001). doi:10.1007/1-4020-0613-6\_7725.
8. Application of LED Light Sources with Light Guide Optics. <https://www.sae.org/publications/technical-papers/content/2007-01-1041/>.
9. Abbasi, S., Peerzada, M. H., Nizamuddin, S. & Mubarak, N. M. Chapter 25 - Functionalized nanomaterials for the aerospace, vehicle, and sports industries. in *Handbook of Functionalized Nanomaterials for Industrial Applications* (ed. Mustansar Hussain, C.) 795–825 (Elsevier, 2020). doi:10.1016/B978-0-12-816787-8.00025-9.
10. Laser Glare Protection. *META* <https://metamaterial.com/solutions/laser-glare-protection/>.

11. Schneider, F. Technology. *KETEK GmbH* <https://www.ketek.net/sipm/technology/>.
12. Gain options fulfill application needs. *Laser Focus World*  
<https://www.laserfocusworld.com/detectors-imaging/article/16552458/gain-options-fulfill-application-needs> (2002).
13. Avalanche photodiodes (APDs) | Hamamatsu Photonics.  
<https://www.hamamatsu.com/eu/en/product/optical-sensors/apd/index.html>.
14. Gundacker, S. & Heering, A. The silicon photomultiplier: fundamentals and applications of a modern solid-state photon detector. *Phys. Med. Biol.* **65**, 17TR01 (2020).
15. SensL. An Introduction to the Silicon Photomultiplier.
16. Zimmermann, R. *et al.* Silicon photomultipliers for improved detection of low light levels in miniature near-infrared spectroscopy instruments. *Biomed. Opt. Express*, **BOE 4**, 659–666 (2013).
17. Characterization of a fiber-less, multichannel optical probe for continuous wave functional near-infrared spectroscopy based on silicon photomultipliers detectors: in-vivo assessment of primary sensorimotor response.  
<https://www.spiedigitallibrary.org/journals/Characterization-of-a-fiber-less-multichannel-optical-probe-for-continuous/volume-4/issue-03/035002/Characterization-of-a-fiber-less-multichannel-optical-probe-for-continuous/10.1117/1.NPh.4.3.035002.full?webSyncID=e46e9e6e-c7a4-9dab-6a0c-bad059329ad8&sessionGUID=83c9d902-bc99-93ce-d268-bead49a28531>.
18. Multichannel wearable system dedicated for simultaneous electroencephalography/near-infrared spectroscopy real-time data acquisitions.  
<https://www.spiedigitallibrary.org/journals/journal-of-biomedical-optics/volume-16/issue->

9/096014/Multichannel-wearable-system-dedicated-for-simultaneous-electroencephalography-near-infrared-spectroscopy/10.1117/1.3625575.full.

19. Zhao, H. & Cooper, R. J. Review of recent progress toward a fiberless, whole-scalp diffuse optical tomography system. *NPh* **5**, 011012 (2017).
20. Del Guerra, A. *et al.* Advantages and pitfalls of the silicon photomultiplier (SiPM) as photodetector for the next generation of PET scanners. *Nuclear Instruments and Methods in Physics Research Section A: Accelerators, Spectrometers, Detectors and Associated Equipment* **617**, 223–226 (2010).
21. Fitzgerald, M. & Lynn, B. The sensitization of high threshold mechanoreceptors with myelinated axons by repeated heating. *The Journal of Physiology* **265**, 549–563 (1977).
22. Mariani, C. & Ponsa, P. Improving the Design of Virtual Reality Devices Applying an Ergonomics Guideline. in *Advances in Ergonomics in Design* (eds. Rebelo, F. & Soares, M.) vol. 588 16–25 (Springer International Publishing, 2018).
23. Furner, C. P., Racherla, P. & Babb, J. S. Mobile app stickiness (MASS) and mobile interactivity: A conceptual model. *The Marketing Review* **14**, 163–188 (2014).
24. Development of hierarchical structure and analytical model of key factors for mobile app stickiness - ScienceDirect.  
<https://www.sciencedirect.com/science/article/pii/S2444569X19300204>.
25. Bogost, I., Walz, S. P. & Deterding, S. Gamification is Bullshit. in *The Gameful World: Approaches, Issues, Applications* 65–78 (MIT Press, 2014).
26. Lewis, Z. H., Swartz, M. C. & Lyons, E. J. What's the Point?: A Review of Reward Systems Implemented in Gamification Interventions. *Games for Health Journal* **5**, 93–99 (2016).

27. Deterding, S., Dixon, D., Khaled, R. & Nacke, L. From game design elements to gamefulness: defining 'gamification'. in *Proceedings of the 15th International Academic MindTrek Conference: Envisioning Future Media Environments* 9–15 (Association for Computing Machinery, 2011). doi:10.1145/2181037.2181040.
28. Developing a Theory of Gamified Learning: Linking Serious Games and Gamification of Learning - Richard N. Landers, 2014.  
<https://journals.sagepub.com/doi/abs/10.1177/1046878114563660>.
29. Ávila-Pesántez, D., Rivera, L. A. & Alban, M. S. Approaches for Serious Game Design: A Systematic Literature Review. **8**, 11 (2017).
30. Fung, J., Richards, C. L., Malouin, F., McFadyen, B. J. & Lamontagne, A. A Treadmill and Motion Coupled Virtual Reality System for Gait Training Post-Stroke. *CyberPsychology & Behavior* **9**, 157–162 (2006).
31. Richards, C. L. *et al.* Gait Training after Stroke on a Self-Paced Treadmill with and without Virtual Environment Scenarios: A Proof-of-Principle Study. *Physiother Can* **70**, 221–230 (2018).
32. Lee, H.-S., Lim, J.-H., Jeon, B.-H. & Song, C.-S. Non-immersive Virtual Reality Rehabilitation Applied to a Task-oriented Approach for Stroke Patients: A Randomized Controlled Trial. *Restorative Neurology and Neuroscience* **38**, 165–172 (2020).
33. Norouzi-Gheidari, N., Archambault, P. S. & Fung, J. Robot-Assisted Reaching Performance of Chronic Stroke and Healthy Individuals in a Virtual Versus a Physical Environment: A Pilot Study. *IEEE Transactions on Neural Systems and Rehabilitation Engineering* **27**, 1273–1281 (2019).



34. Perez, C., Kaizer, F., Archambault, P. & Fung, J. A novel approach to integrate VR exergames for stroke rehabilitation: Evaluating the implementation of a ‘games room’. in *2017 International Conference on Virtual Rehabilitation (ICVR)* 1–7 (IEEE, 2017).  
doi:10.1109/ICVR.2017.8007538.
35. Ikbali Afsar, S., Mirzayev, I., Umit Yemisci, O. & Cosar Saracgil, S. N. Virtual Reality in Upper Extremity Rehabilitation of Stroke Patients: A Randomized Controlled Trial. *Journal of Stroke and Cerebrovascular Diseases* **27**, 3473–3478 (2018).
36. Development of a neuro-feedback game based on motor imagery EEG | SpringerLink.  
<https://link.springer.com/article/10.1007/s11042-017-5168-x>.
37. Borges, L. R., Fernandes, A. B., Melo, L. P., Guerra, R. O. & Campos, T. F. Action observation for upper limb rehabilitation after stroke. *Cochrane Database Syst Rev* **10**, CD011887 (2018).
38. Friesen, C. L., Bardouille, T., Neyedli, H. F. & Boe, S. G. Combined Action Observation and Motor Imagery Neurofeedback for Modulation of Brain Activity. *Front. Hum. Neurosci.* **10**, (2017).
39. Johnson, K. A. *et al.* Intermittent “Real-time” fMRI Feedback Is Superior to Continuous Presentation for a Motor Imagery Task: A Pilot Study. *Journal of Neuroimaging* **22**, 58–66 (2012).
40. Kober, S. E. *et al.* Near-infrared spectroscopy based neurofeedback training increases specific motor imagery related cortical activation compared to sham feedback. *Biological Psychology* **95**, 21–30 (2014).
41. Mihara, M. *et al.* Near-infrared Spectroscopy–mediated Neurofeedback Enhances Efficacy of Motor Imagery–based Training in Poststroke Victims. *Stroke* (2013).

42. Lapborisuth, P., Zhang, X., Noah, A. & Hirsch, J. Neurofeedback-based functional near-infrared spectroscopy upregulates motor cortex activity in imagined motor tasks. *NPh* **4**, 021107 (2017).
43. Ono, Y. *et al.* Hand Motor Rehabilitation of Patients with Stroke Using Physiologically Congruent Neurofeedback. in *2018 IEEE International Conference on Systems, Man, and Cybernetics (SMC)* 39–44 (2018). doi:10.1109/SMC.2018.00016.
44. Duan, L., Zhang, Y.-J. & Zhu, C.-Z. Quantitative comparison of resting-state functional connectivity derived from fNIRS and fMRI: A simultaneous recording study. *NeuroImage* **60**, 2008–2018 (2012).
45. Arun, K. M., Smitha, K. A., Sylaja, P. N. & Kesavadas, C. Identifying Resting-State Functional Connectivity Changes in the Motor Cortex Using fNIRS During Recovery from Stroke. *Brain Topogr* (2020) doi:10.1007/s10548-020-00785-2.
46. Tang, Q. *et al.* Modulation of interhemispheric activation balance in motor-related areas of stroke patients with motor recovery: Systematic review and meta-analysis of fMRI studies. *Neuroscience & Biobehavioral Reviews* **57**, 392–400 (2015).
47. Bütefisch, C. M., Weßling, M., Netz, J., Seitz, R. J. & Hömberg, V. Relationship Between Interhemispheric Inhibition and Motor Cortex Excitability in Subacute Stroke Patients. *Neurorehabil Neural Repair* **22**, 4–21 (2008).
48. Murase, N., Duque, J., Mazzocchio, R. & Cohen, L. G. Influence of interhemispheric interactions on motor function in chronic stroke. *Annals of Neurology* **55**, 400–409 (2004).
49. Chollet, F. *et al.* The functional anatomy of motor recovery after stroke in humans: A study with positron emission tomography. *Annals of Neurology* **29**, 63–71 (1991).

50. Weiller, C., Chollet, F., Friston, K. J., Wise, R. J. S. & Frackowiak, R. S. J. Functional reorganization of the brain in recovery from striatocapsular infarction in man. *Annals of Neurology* **31**, 463–472 (1992).
51. Shimizu, T. *et al.* Motor cortical disinhibition in the unaffected hemisphere after unilateral cortical stroke. *Brain* **125**, 1896–1907 (2002).
52. Bütefisch, C. M., Netz, J., Weßling, M., Seitz, R. J. & Hömberg, V. Remote changes in cortical excitability after stroke. *Brain* **126**, 470–481 (2003).
53. Stinear, C. M., Petoe, M. A. & Byblow, W. D. Primary Motor Cortex Excitability During Recovery After Stroke: Implications for Neuromodulation. *Brain Stimulation* **8**, 1183–1190 (2015).
54. The Role of Diaschisis in Stroke Recovery | Stroke.  
<https://www.ahajournals.org/doi/full/10.1161/01.STR.30.9.1844>.
55. Jaillard, A., Martin, C. D., Garambois, K., Lebas, J. F. & Hommel, M. Vicarious function within the human primary motor cortex?: A longitudinal fMRI stroke study. *Brain* **128**, 1122–1138 (2005).
56. Schaechter, J. D. & Perdue, K. L. Enhanced Cortical Activation in the Contralesional Hemisphere of Chronic Stroke Patients in Response to Motor Skill Challenge. *Cereb Cortex* **18**, 638–647 (2008).
57. Bütefisch, C. M. *et al.* Recruitment of contralesional motor cortex in stroke patients with recovery of hand function. *Neruology* **64**, 1067–1069 (2005).
58. Lotze, M. *et al.* The Role of Multiple Contralesional Motor Areas for Complex Hand Movements after Internal Capsular Lesion. *J. Neurosci.* **26**, 6096–6102 (2006).

59. Riecker, A. *et al.* The role of the unaffected hemisphere in motor recovery after stroke. *Human Brain Mapping* **31**, 1017–1029 (2010).
60. The Effect of Lesion Size on the Organization of the Ipsilesional and Contralesional Motor Cortex - Boris Touvykine, Babak K. Mansoori, Loyda Jean-Charles, Joan Deffeyes, Stephan Quessy, Numa Dancause, 2016.  
<https://journals.sagepub.com/doi/abs/10.1177/1545968315585356>.
61. Schaechter, J. D. *et al.* Motor Recovery and Cortical Reorganization after Constraint-Induced Movement Therapy in Stroke Patients: A Preliminary Study. *Neurorehabil Neural Repair* **16**, 326–338 (2002).
62. Park, W., Kwon, G. H., Kim, Y.-H., Lee, J.-H. & Kim, L. EEG response varies with lesion location in patients with chronic stroke. *Journal of NeuroEngineering and Rehabilitation* **13**, 21 (2016).
63. Park, C., Kou, N., Boudrias, M.-H., Playford, E. D. & Ward, N. S. Assessing a standardised approach to measuring corticospinal integrity after stroke with DTI. *NeuroImage: Clinical* **2**, 521–533 (2013).
64. Lin, D. J. *et al.* Corticospinal Tract Injury Estimated From Acute Stroke Imaging Predicts Upper Extremity Motor Recovery After Stroke. *Stroke* **50**, 3569–3577 (2019).
65. Resting State Functional Connectivity Is Associated With Motor Pathway Integrity and Upper-Limb Behavior in Chronic Stroke - Brenton Hordacre, Mitchell R. Goldsworthy, Ellana Welsby, Lynton Graetz, Sophie Ballinger, Susan Hillier, 2020.  
<https://journals.sagepub.com/doi/abs/10.1177/1545968320921824>.
66. Carter, A. R. *et al.* Upstream dysfunction of somatomotor functional connectivity after corticospinal damage in stroke. *Neurorehabil Neural Repair* **26**, 7–19 (2012).

67. Lam, T. K. *et al.* Variability in stroke motor outcome is explained by structural and functional integrity of the motor system. *Sci Rep* **8**, 9480 (2018).
68. Proportional recovery after stroke depends on corticomotor integrity - Byblow - 2015 - *Annals of Neurology* - Wiley Online Library.  
<https://onlinelibrary.wiley.com/doi/abs/10.1002/ana.24472>.
69. Corticospinal tract lesion load: An imaging biomarker for stroke motor outcomes - Feng - 2015 - *Annals of Neurology* - Wiley Online Library.  
<https://onlinelibrary.wiley.com/doi/abs/10.1002/ana.24510>.
70. Quinlan, E. B. *et al.* Neural function, injury, and stroke subtype predict treatment gains after stroke. *Annals of Neurology* **77**, 132–145 (2015).

## APPENDIX A – CHAPTER 2 SUPPLEMENTAL MATERIAL

*Table below outlines the measurement locations (as per Figure 2.5) that were not working (as a result of electronics failure on the AP-1 prototype) for subjects of the study outlined in Chapter 2.*

Subject	Measurement Locations
1	7,8,9,10
5	3,4
13	1

# APPENDIX B – CHAPTER 2 SUPPLEMENTAL PRELIMINARY ANALYSES

## Subject classifications for results (used in following histograms):

The following classifications were used to determine the level of functioning of the Axem Pro prototype. It takes into account (1) the expectation that the expected evoked motor response is one of preferential contralateral brain activity (i.e., more activity on the left hand side of the brain for a right-handed task and vice versa), as well as (2) a measure of variability, operating under the assumption that the increase in oxyhemoglobin during the task period, at a region involved in the evoked response, should have the lower bound of its confidence interval be  $>0$  (i.e., no change) for at least 2 seconds of the task window.

**Worked satisfactorily** - For both motor tasks (i.e., right- and left-handed stress ball squeezing), the measurement location with the highest change in oxygenated hemoglobin during the task window was in the contralateral hemisphere (e.g., the right hemisphere for a left-handed fist squeeze), and lower bound of the 95% confidence interval for the change in oxygenated hemoglobin values was  $>0$  for at least 2 consecutive seconds of the task window.

**Worked but not satisfactorily** = The above was true but only for one of the two motor tasks.

**Did not work** = The above was not true for either motor task.

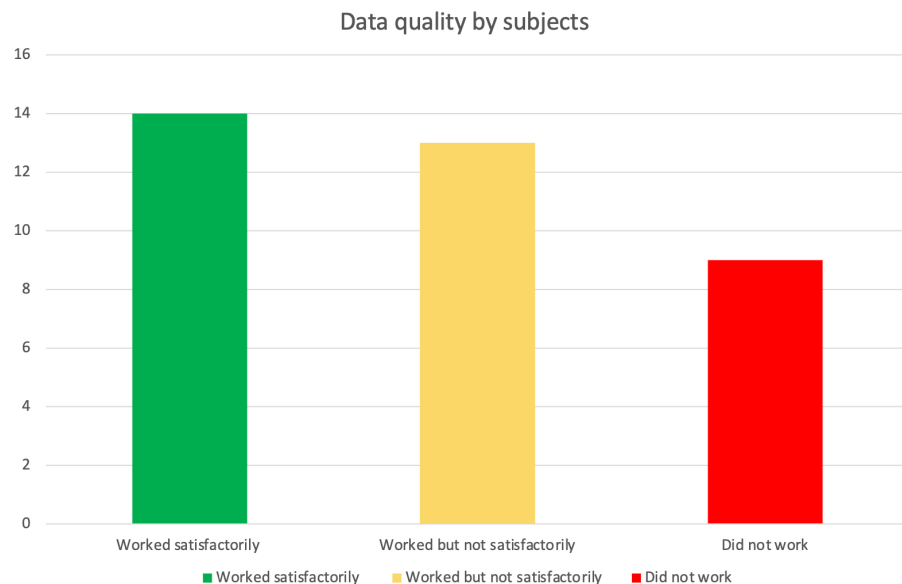
## Data Quality Study – Summary

As of Jan 16/19...

N = 36

Mean age = 39.33

Sex = F:12 M:24



## Subjects >50 years of age

N = 10

Mean age = 60.8

Sex = F:5 M:5

Notes: The “worked but not satisfactorily” participant clearly did not have good contact of headset — this has informed mechanical design for next version currently in development. The “Did not work” participant yawned throughout — movement artefact reduction was not implemented in this data but is currently in development.

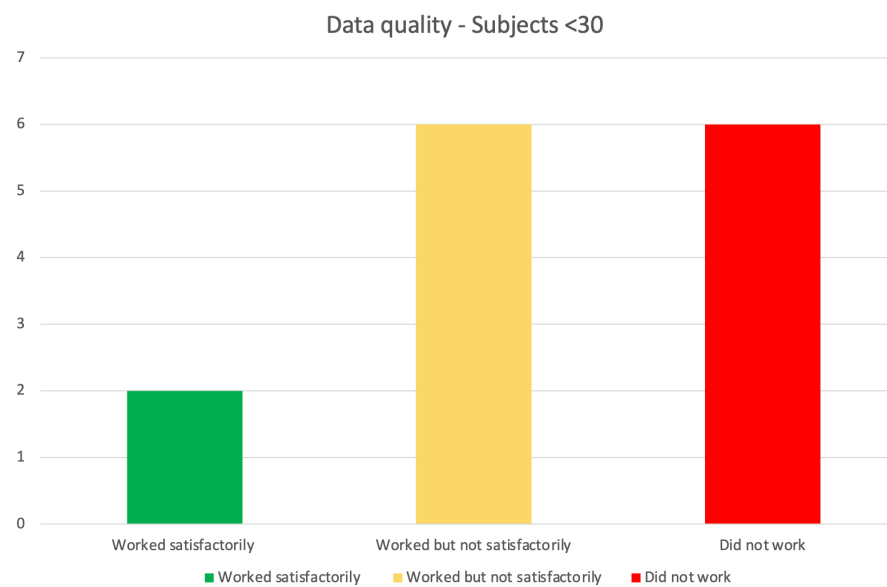


## Subjects <30

N = 14

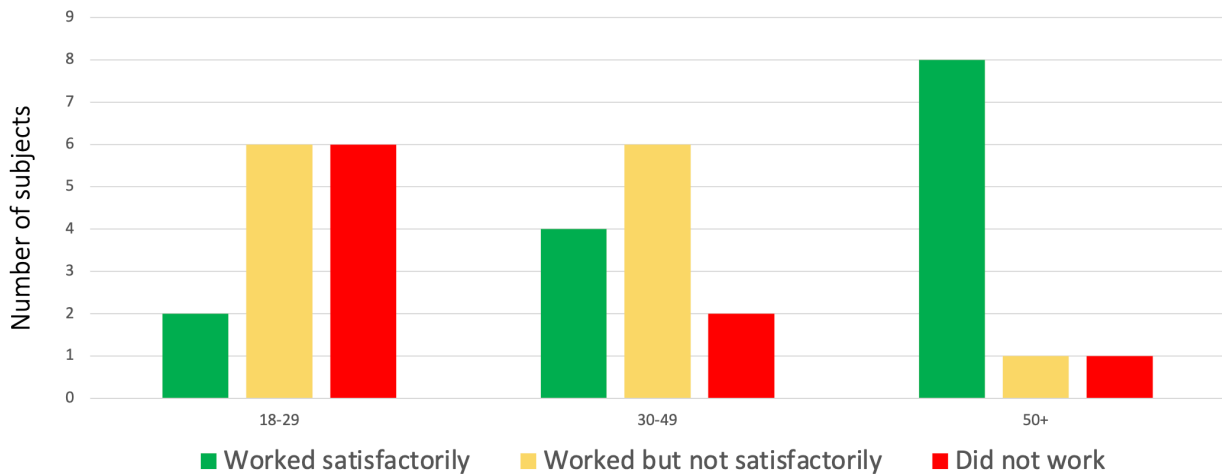
Mean age = 25.9

Sex = F:5 M:9





# Data quality by age



## Summary of Interim Results

Conclusions drawn from first 36 subjects:

1. Current Axem Pro prototype works well on individuals >50 years of age, likely due to decreased hair density as well as decreased hair pigmentation.
2. Current Axem Pro prototype does not work satisfactorily on individuals <50 years of age.
3. Data from individuals with dark skin did not seem to differ in quality significantly from their hair-group- matched caucasian counterparts. However more subjects with darker skin should be collected to further validate this.
4. The level of light being detected at the photodetector varied considerably between- and within-subjects, even controlling for the effect of hair. Meaning the optical components were not making consistent coupling between- and within-heads of various sizes.

Decisions made based on study results:

1. The use of more effective optical components in the Axem Pro final product is warranted given these results.
2. Further iteration on the mechanical design of the prototype (i.e., in particular making the position of the LEDs and photodiodes more flexible to perform better on a larger range of head sizes) is warranted.

Alternate classification for results (used in the following histogram):

We believe the classification used in the previous histograms (using simple but quantitative decision rules) is the optimal way to determine the level of functioning of the Axem Pro prototype.

However, an alternative approach is to use a simple classifier (i.e., an algorithm that seeks to categorize unlabeled data as belonging to one of two categories). We used dynamic time warping classification (a simple method of classification that is not deep or recurrent) to attempt to classify data during task performance (i.e., stress ball squeezing) from rest data.

In the following histogram we categorized subjects' data as such:

**Worked satisfactorily** - For both motor tasks (i.e., right- and left-handed stress ball squeezing), there was a measurement location in the contralateral hemisphere that produced a classification accuracy >80%.

**Worked but not satisfactorily** = The above was true but only for one of the two motor tasks. **Did not work** = The above was not true for either motor task.

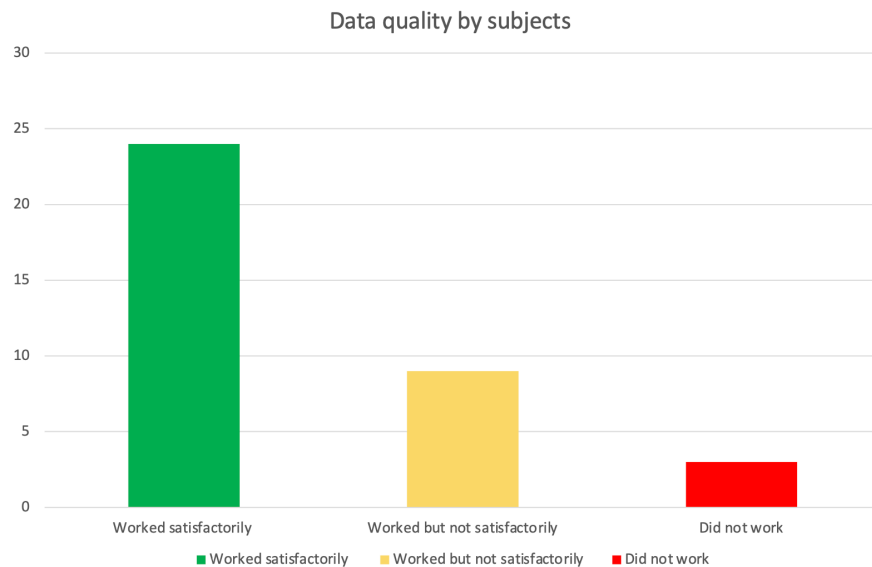
## Classification using Dynamic Time Warping

As of Jan 16/19...

N = 36

Mean age = 39.33

Sex = F:12 M:24



# APPENDIX C – AXEM HOME USER NEEDS

## User Needs

The following section describes the user needs requirements for the Axem Home.

## Patient User Needs

- UN-P-1. Patient users need device headband to collect valid fNIRS data from the motor cortex while they perform a reasonably wide variety of seated upper-body movements (and/or safe attempts and/or motor imagery<sup>22</sup> and/or action observation<sup>23</sup> of those movements).
- UN-P-2. Patient users need to transport the device headband.
- UN-P-3. Patient users need the device headband to be safe and usable in their home environment.
- UN-P-4. Patient users need to tolerate wearing the device headband for at least 30 minutes uninterrupted, and 45 minutes each day.
- UN-P-5. Patient users need to recharge the device headband.
- UN-P-6. Patient users need to clean the device headband and to receive instructions on how often they should clean the device.
- UN-P-7. Patient users need the device headband battery to enable 45 minutes of data collection time prior to recharging.
- UN-P-8. Patient users need the device headband to refrain from turning on its LEDs when it is not on someone's head and device must disable LEDs if headset is removed.
- UN-P-9. Patient users need to be able to consistently and correctly place the device headband on their heads.
- UN-P-10. Patient users need to navigate the device app in order to (1) conduct rehabilitation sessions and (2) view results/usage related to past rehabilitation sessions.
- UN-P-11. Patient users need to understand the feedback they receive during rehabilitation sessions.
- UN-P-12. Patient users need their data to be securely transmitted from the device app to their HCP.
- UN-P-13. The device will be designed so that it can be donned with one hand.
- UN-P-14. The Device shall be provided with clear and concise user instructions.
- UN-P-15. Labeling must be kept in line with the submissions to the regulatory body governing the country of sale, including User Instructions and product labeling.
- UN-P-16. The Device must be functional at the time of unboxing.

---

<sup>22</sup> Motor imagery is the mental rehearsal of a movement, whereby one imagines themselves performing the movement, typically involving visualization of the movement from the first person perspective but with an emphasis on how it would feel to physically perform the movement.

<sup>23</sup> Action observation refers to the perception of movement.

- UN-P-17. The Device Labelling shall be UDI compliant.
- UN-P-18. The Device shall be Restriction of Hazardous Substances (RoHS) directive compliant.
- UN-P-19. The Device can be re-used.
- UN-P-20. The Device shall be compatible with System Accessories.
- UN-P-21. Device must not produce sensitivity or allergic reaction with patient.
- UN-P-22. Patient users need to turn device power on and off.
- UN-P-23. Patient users need to be aware of the power and connectivity status of the device headband.

# APPENDIX D – USABILITY QUESTIONNAIRE AND INTERVIEW

## Usability Questionnaire

- How comfortable did you find the Axem Home prototype?
  - Very comfortable (3)
  - Comfortable (2)
  - Slightly comfortable (1)
  - Neither comfortable or painful (0)
  - Slightly painful (-1)
  - Painful (-2)
  - Very painful (-3)
- How difficult was it to place the Axem Home surface model in the correct position?
  - Very difficult (-2)
  - Difficult (-1)
  - Neutral (0)
  - Easy (1)
  - Very easy (2)
- How difficult was it navigate the Axem Home app?
  - Very difficult (-2)
  - Difficult (-1)
  - Neutral (0)
  - Easy (1)
  - Very easy (2)
- How useful did you find the feedback provided during movement periods?
  - Not useful at all (-2)
  - Slightly useful (-1)
  - Moderately useful (0)
  - Considerably useful (1)
  - Extremely useful (2)
- How did you find the feedback provided during rest periods?
  - Not useful at all (-2)
  - Slightly useful (-1)
  - Moderately useful (0)
  - Considerably useful (1)
  - Extremely useful (2)
- How did you find the data presented in the ‘Session Review’ screen?
  - Not useful at all, (-2)
  - slightly useful, (-1)
  - moderately useful, (0)
  - considerably useful, (1)
  - extremely useful (2)
- How often do you typically perform rehabilitation exercises?

- Less than once per month (-2)
- 1-2 times per month (-1)
- Once per week (0)
- 2 times per week (1)
- More than 2 times per week (2)
- Using the Axem Home would cause me to spend more time doing rehabilitation exercises.
  - Strongly agree (2)
  - Agree (1)
  - Neutral (0)
  - Disagree (-1)
  - Strongly disagree (-2)
- If you had access to the Axem Home, how often do you think you would use it?
  - Less than once per month (-2)
  - 1-2 times per month (-1)
  - Once per week (0)
  - 2 times per week (1)
  - More than 2 times per week (2)
- Using the Axem Home would help me do rehabilitation exercises better.
  - Strongly agree (2)
  - Agree (1)
  - Neutral (0)
  - Disagree (-1)
  - Strongly disagree (-2)
- I would recommend using the Axem Home to another stroke survivor.
  - 1-10 rating
- I would find the Axem Home useful.
  - Strongly agree (2)
  - Agree (1)
  - Neutral (0)
  - Disagree (-1)
  - Strongly disagree (-2)

Items scored such that favourable responses (e.g., very comfortable, or very easy) have a larger positive number, and unfavourable responses have a larger negative number, with the exception of the question: “I would recommend using the Axem Home to another stroke survivor” which is scored 1 to 10 with 10 representing greater likelihood of recommending.

## Usability Interview Guide

- Ask about any specific action/behaviour during the test
- Follow up on all questionnaire items where they answered unfavorably
- *How do you feel about the system of following along with videos?*
- *Were there some videos you thought this worked better or worse for?*
- *Can you think of any ways that we could improve this video system?*
- Follow up on their answer to “Using the Axem Home would cause me to spend more time doing rehabilitation exercises.”
- How did you feel about the ratings you were asked to give after each exercise? Did you understand what was being asked in each question
- Ask about the strap; why they chose that technique and what their thoughts are on how it’s currently designed
- On a scale of 1-5 (where 1 is comfortable and 5 is unbearably painful) how did you feel about the Axem Home prototype you used

## APPENDIX E – AP-LL PLACEMENT INSTRUCTIONS

### *Original Headband Placement Instructions:*

Please attempt to place the headband in a similar position as you see it in the picture below (so that the band approximately lines up with your ears). Once you have the headband on, please tighten its strap just so much that it is touching your jaw (snug but not tight).

*See picture below for an example...*

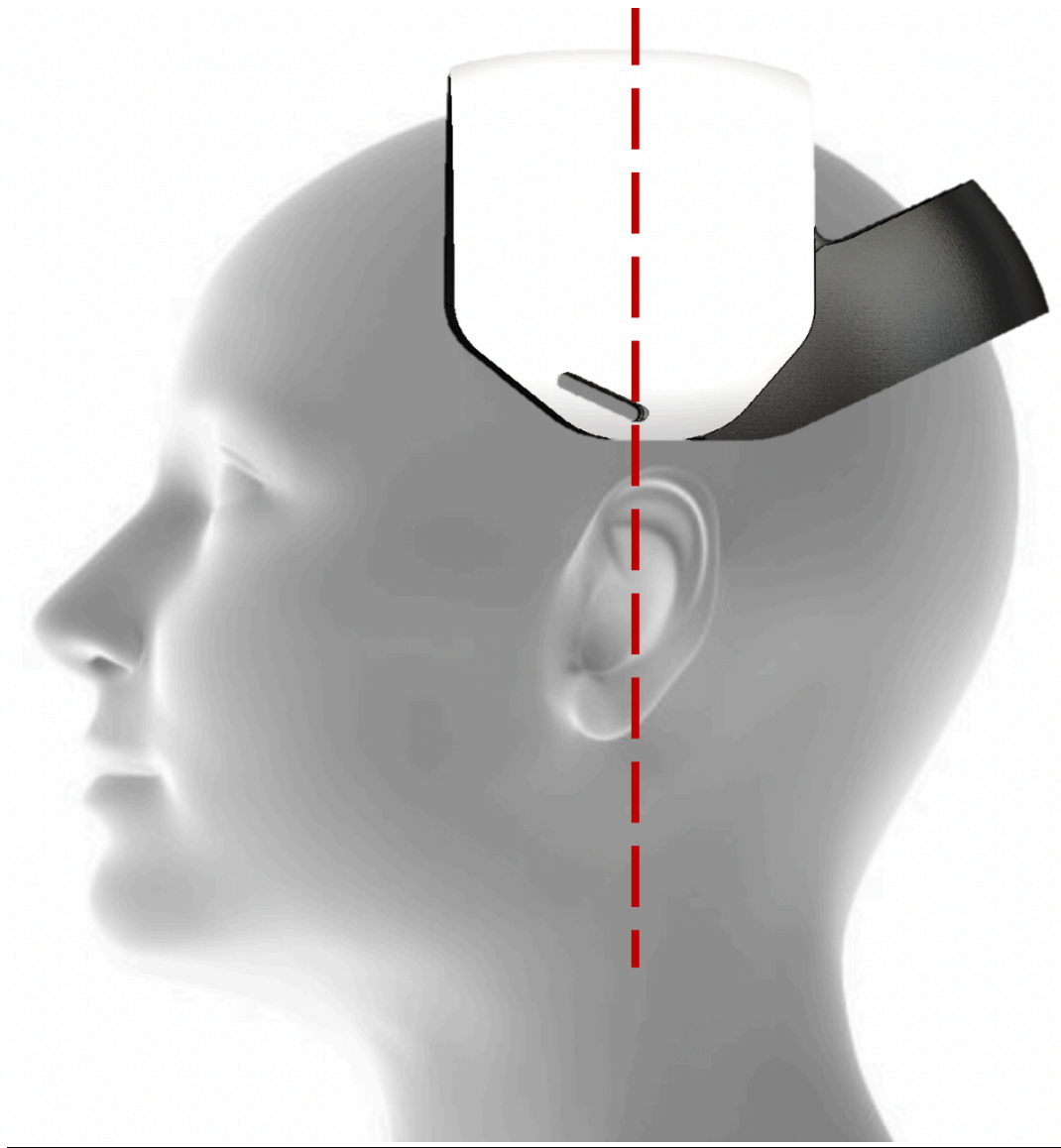




*Revised Headband Placement Instructions:*

- Please attempt to place the headband as you see it below
- Note that the **white band** is meant to approximately **line up with your ears**
- Once you have the headband on, please tighten its strap just so much that it is touching your jaw (snug but not tight).

**See picture below for an example...**



## APPENDIX F - DECLARATION OF INTERESTS

Christopher Friesen is a co-founder of and has stock ownership in Axem Neurotechnology. Moreover, Michael Lawrence and Tony Ingram are all co-founders of and have stock ownership in Axem Neurotechnology, while Megan Smith and Eric Hamilton are full time employees of Axem Neurotechnology (see Section 1.6 – Contributions to Study Chapters).

## BIBLIOGRAPHY

- 14:00-17:00. (n.d.). *IEC 60601-1-11:2015*. ISO. Retrieved January 21, 2021, from <https://www.iso.org/cms/render/live/en/sites/isoorg/contents/data/standard/06/55/65529.html>
- 2019 Report on Heart, Stroke and Vascular Cognitive Impairment*. (2019). Heart and Stroke Foundation. <https://www.heartandstroke.ca/-/media/pdf-files/canada/2019-report/heartandstrokereport2019.ashx>
- A, H., Rh, N., Ac, G., & G, K. (2013, May). *Functional recovery of the paretic upper limb after stroke: Who regains hand capacity?* *Archives of Physical Medicine and Rehabilitation; Arch Phys Med Rehabil*. <https://doi.org/10.1016/j.apmr.2012.11.031>
- A Randomized Controlled Trial of EEG-Based Motor Imagery Brain-Computer Interface Robotic Rehabilitation for Stroke—Kai Keng Ang, Karen Sui Geok Chua, Kok Soon Phua, Chuanchu Wang, Zheng Yang Chin, Christopher Wee Keong Kuah, Wilson Low, Cuntai Guan, 2015*. (n.d.). Retrieved May 15, 2020, from <https://journals.sagepub.com/doi/10.1177/1550059414522229>
- Abbasi, S., Peerzada, M. H., Nizamuddin, S., & Mubarak, N. M. (2020). Chapter 25—Functionalized nanomaterials for the aerospace, vehicle, and sports industries. In C. Mustansar Hussain (Ed.), *Handbook of Functionalized Nanomaterials for Industrial Applications* (pp. 795–825). Elsevier. <https://doi.org/10.1016/B978-0-12-816787-8.00025-9>
- Activation of Cortical and Cerebellar Motor Areas during Executed and Imagined Hand Movements: An fMRI Study | Journal of Cognitive Neuroscience | MIT Press Journals*. (n.d.). Retrieved January 30, 2019, from <https://www.mitpressjournals.org/doi/abs/10.1162/089892999563553>

- Adamson, J., Beswick, A., & Ebrahim, S. (2004). Is stroke the most common cause of disability? *Journal of Stroke and Cerebrovascular Diseases: The Official Journal of National Stroke Association*, 13(4), 171–177. <https://doi.org/10.1016/j.jstrokecerebrovasdis.2004.06.003>
- Allred, R. P., Maldonado, M. A., Hsu and, J. E., & Jones, T. A. (2005). Training the “less-affected” forelimb after unilateral cortical infarcts interferes with functional recovery of the impaired forelimb in rats. *Restorative Neurology and Neuroscience*, 23(5,6), 297–302.
- Allred, Rachel P., Cappellini, C. H., & Jones, T. A. (2010). The “good” limb makes the “bad” limb worse: Experience-dependent interhemispheric disruption of functional outcome after cortical infarcts in rats. *Behavioral Neuroscience*, 124(1), 124–132. <https://doi.org/10.1037/a0018457>
- Allred, Rachel P., & Jones, T. A. (2008). Maladaptive effects of learning with the less-affected forelimb after focal cortical infarcts in rats. *Experimental Neurology*, 210(1), 172–181. <https://doi.org/10.1016/j.expneurol.2007.10.010>
- Allred, Rachel P., Kim, S. Y., & Jones, T. A. (2014). Use it and/or lose it—Experience effects on brain remodeling across time after stroke. *Frontiers in Human Neuroscience*, 8. <https://doi.org/10.3389/fnhum.2014.00379>
- Alt Murphy, M., Danielsson, A., & Sunnerhagen, K. S. (2011). Letter by Murphy et al regarding article, “Fugl-Meyer assessment of sensorimotor function after stroke: Standardized training procedure for clinical practice and clinical trials.” *Stroke*, 42(6), e402. <https://doi.org/10.1161/STROKEAHA.111.619304>
- Application of LED Light Sources with Light Guide Optics*. (n.d.). Retrieved January 21, 2021, from <https://www.sae.org/publications/technical-papers/content/2007-01-1041/>

*Applying Human Factors and Usability Engineering to Medical Devices, Guidance for Industry and Food and Drug Administration Staff.* (2016). Food and Drug Administration.

Arun, K. M., Smitha, K. A., Sylaja, P. N., & Kesavadas, C. (2020). Identifying Resting-State Functional Connectivity Changes in the Motor Cortex Using fNIRS During Recovery from Stroke. *Brain Topography*. <https://doi.org/10.1007/s10548-020-00785-2>

*Avalanche photodiodes (APDs) | Hamamatsu Photonics.* (n.d.). Retrieved January 21, 2021, from <https://www.hamamatsu.com/eu/en/product/optical-sensors/apd/index.html>

Ávila-Pesántez, D., Rivera, L. A., & Alban, M. S. (2017). *Approaches for Serious Game Design: A Systematic Literature Review*. 8(3), 11.

Ayala, C., Fang, J., Luncheon, C., King, S. C., Chang, T., Ritchey, M., & Loustalot, F. (2018). Use of Outpatient Rehabilitation Among Adult Stroke Survivors—20 States and the District of Columbia, 2013, and Four States, 2015. *Morbidity and Mortality Weekly Report*, 67(20), 575–578. <https://doi.org/10.15585/mmwr.mm6720a2>

Ayaz, H., Onaral, B., Izzetoglu, K., Shewokis, P. A., McKendrick, R., & Parasuraman, R. (2013). Continuous monitoring of brain dynamics with functional near infrared spectroscopy as a tool for neuroergonomic research: Empirical examples and a technological development. *Frontiers in Human Neuroscience*, 7. <https://doi.org/10.3389/fnhum.2013.00871>

Baker, W. B., Parthasarathy, A. B., Busch, D. R., Mesquita, R. C., Greenberg, J. H., & Yodh, A. G. (2014). Modified Beer-Lambert law for blood flow. *Biomedical Optics Express*, 5(11), 4053–4075. <https://doi.org/10.1364/BOE.5.004053>

Baldassarre, A., Ramsey, L., Rengachary, J., Zinn, K., Siegel, J. S., Metcalf, N. V., Strube, M. J., Snyder, A. Z., Corbetta, M., & Shulman, G. L. (2016). Dissociated functional connectivity

- profiles for motor and attention deficits in acute right-hemisphere stroke. *Brain*, 139(7), 2024–2038. <https://doi.org/10.1093/brain/aww107>
- Barnay, J.-L., Wauquiez, G., Bonnin-Koang, H. Y., Anquetil, C., Pérennou, D., Piscicelli, C., Lucas-Pineau, B., Muja, L., le Stunff, E., de Boissezon, X., Terracol, C., Rousseaux, M., Bejot, Y., Binquet, C., Antoine, D., Devilliers, H., & Benaim, C. (2014). Feasibility of the Cognitive Assessment scale for Stroke Patients (CASP) vs. MMSE and MoCA in aphasic left hemispheric stroke patients. *Annals of Physical and Rehabilitation Medicine*, 57(6), 422–435. <https://doi.org/10.1016/j.rehab.2014.05.010>
- Baron, J.-C., Yamauchi, H., Fujioka, M., & Endres, M. (2014). Selective Neuronal Loss in Ischemic Stroke and Cerebrovascular Disease. *Journal of Cerebral Blood Flow & Metabolism*, 34(1), 2–18. <https://doi.org/10.1038/jcbfm.2013.188>
- Beaulé, V., Tremblay, S., & Théoret, H. (2012). Interhemispheric Control of Unilateral Movement. *Neural Plasticity*, 2012, 1–11. <https://doi.org/10.1155/2012/627816>
- Bellinger, J. D., Zhimin, C., Glover, S., Jones, K., Bennett, K., & Probst, J. (n.d.). Post-discharge Rehabilitation Care Delivery for Rural Medicare Beneficiaries with Stroke. *South Carolina Rural Health Research Center*.
- Benaim, C., Barnay, J. L., Wauquiez, G., Bonnin-Koang, H. Y., Anquetil, C., Pérennou, D., Piscicelli, C., Lucas-Pineau, B., Muja, L., le Stunff, E., de Boissezon, X., Terracol, C., Rousseaux, M., Bejot, Y., Antoine, D., Binquet, C., & Devilliers, H. (2015). The Cognitive Assessment scale for Stroke Patients (CASP) vs. MMSE and MoCA in non-aphasic hemispheric stroke patients. *Annals of Physical and Rehabilitation Medicine*, 58(2), 78–85. <https://doi.org/10.1016/j.rehab.2014.12.001>

- Bernhardt Julie, Dewey Helen, Thrift Amanda, & Donnan Geoffrey. (2004). Inactive and Alone. *Stroke*, 35(4), 1005–1009. <https://doi.org/10.1161/01.STR.0000120727.40792.40>
- Betancourt, M. (n.d.). *Case Studies: Ordinal Regression*. Retrieved January 21, 2021, from [https://betanalpha.github.io/assets/case\\_studies/ordinal\\_regression.html](https://betanalpha.github.io/assets/case_studies/ordinal_regression.html)
- Birch, M. P., Messenger, J. F., & Messenger, A. G. (2001). Hair density, hair diameter and the prevalence of female pattern hair loss. *British Journal of Dermatology*, 144(2), 297–304. <https://doi.org/10.1046/j.1365-2133.2001.04018.x>
- Boe, S., Gionfriddo, A., Kraeutner, S., Tremblay, A., Little, G., & Bardouille, T. (2014). Laterality of brain activity during motor imagery is modulated by the provision of source level neurofeedback. *NeuroImage*, 101, 159–167. <https://doi.org/10.1016/j.neuroimage.2014.06.066>
- Bogost, I., Walz, S. P., & Deterding, S. (2014). Gamification is Bullshit. In *The Gameful World: Approaches, Issues, Applications* (pp. 65–78). MIT Press.
- Bonkhoff, A. K., Hope, T., Bzdok, D., Guggisberg, A. G., Hawe, R. L., Dukelow, S. P., Rehme, A. K., Fink, G. R., Grefkes, C., & Bowman, H. (2020). Bringing proportional recovery into proportion: Bayesian modelling of post-stroke motor impairment. *Brain*, 143(7), 2189–2206. <https://doi.org/10.1093/brain/awaa146>
- Borges, L. R., Fernandes, A. B., Melo, L. P., Guerra, R. O., & Campos, T. F. (2018). Action observation for upper limb rehabilitation after stroke. *The Cochrane Database of Systematic Reviews*, 10, CD011887. <https://doi.org/10.1002/14651858.CD011887.pub2>
- Borschmann, K., Hayward, K. S., Raffelt, A., Churilov, L., Kramer, S., & Bernhardt, J. (2018). Rationale for Intervention and Dose Is Lacking in Stroke Recovery Trials: A Systematic Review. *Stroke Research and Treatment*, 2018, 8087372. <https://doi.org/10.1155/2018/8087372>

Boyd, L. A., Hayward, K. S., Ward, N. S., Stinear, C. M., Rosso, C., Fisher, R. J., Carter, A. R., Leff, A. P., Copland, D. A., Carey, L. M., Cohen, L. G., Basso, D. M., Maguire, J. M., & Cramer, S. C. (2017a). Biomarkers of stroke recovery: Consensus-based core recommendations from the Stroke Recovery and Rehabilitation Roundtable. *International Journal of Stroke: Official Journal of the International Stroke Society*, 12(5), 480–493. <https://doi.org/10.1177/1747493017714176>

Boyd, L. A., Hayward, K. S., Ward, N. S., Stinear, C. M., Rosso, C., Fisher, R. J., Carter, A. R., Leff, A. P., Copland, D. A., Carey, L. M., Cohen, L. G., Basso, D. M., Maguire, J. M., & Cramer, S. C. (2017b). Biomarkers of stroke recovery: Consensus-based core recommendations from the Stroke Recovery and Rehabilitation Roundtable. *International Journal of Stroke: Official Journal of the International Stroke Society*, 12(5), 480–493. <https://doi.org/10.1177/1747493017714176>

*Brain-Derived Neurotrophic Factor Contributes to Recovery of Skilled Reaching After Focal Ischemia in Rats* | *Stroke*. (n.d.). Retrieved November 20, 2020, from <https://www.ahajournals.org/doi/full/10.1161/STROKEAHA.108.531806>

Brigadoi, S., & Cooper, R. J. (2015). How short is short? Optimum source–detector distance for short-separation channels in functional near-infrared spectroscopy. *Neurophotonics*, 2(2), 025005. <https://doi.org/10.1117/1.NPh.2.2.025005>

Bundy David T., Souders Lauren, Baranyai Kelly, Leonard Laura, Schalk Gerwin, Coker Robert, Moran Daniel W., Huskey Thy, & Leuthardt Eric C. (2017). Contralesional Brain–Computer Interface Control of a Powered Exoskeleton for Motor Recovery in Chronic Stroke Survivors. *Stroke*, 48(7), 1908–1915. <https://doi.org/10.1161/STROKEAHA.116.016304>



- Buntin, M. B. (2007). Access to Postacute Rehabilitation. *Archives of Physical Medicine and Rehabilitation*, 88(11), 1488–1493. <https://doi.org/10.1016/j.apmr.2007.07.023>
- Bütefisch, Cathrin M., Netz, J., Weßling, M., Seitz, R. J., & Hömberg, V. (2003). Remote changes in cortical excitability after stroke. *Brain*, 126(2), 470–481. <https://doi.org/10.1093/brain/awg044>
- Bütefisch, Cathrin M., Weßling, M., Netz, J., Seitz, R. J., & Hömberg, V. (2008). Relationship Between Interhemispheric Inhibition and Motor Cortex Excitability in Subacute Stroke Patients. *Neurorehabilitation and Neural Repair*, 22(1), 4–21. <https://doi.org/10.1177/1545968307301769>
- Bütefisch, C.M., Kleiser, R., Müller, K., Wittsack, H. J., Hömberg, V., & Seitz, R. J. (2005). Recruitment of contralesional motor cortex in stroke patients with recovery of hand function. *Neurology*, 64(6), 1067–1069. <https://doi.org/10.1212/01.WNL.0000154603.48446.36>
- Byblow, W. D., Stinear, C. M., Barber, P. A., Petoe, M. A., & Ackerley, S. J. (2015). Proportional recovery after stroke depends on corticomotor integrity. *Annals of Neurology*, 78(6), 848–859. <https://doi.org/10.1002/ana.24472>
- Calautti, C., Naccarato, M., Jones, P. S., Sharma, N., Day, D. D., Carpenter, A. T., Bullmore, E. T., Warburton, E. A., & Baron, J.-C. (2007). The relationship between motor deficit and hemisphere activation balance after stroke: A 3T fMRI study. *NeuroImage*, 34(1), 322–331. <https://doi.org/10.1016/j.neuroimage.2006.08.026>
- Carey, J. R., Kimberley, T. J., Lewis, S. M., Auerbach, E. J., Dorsey, L., Rundquist, P., & Ugurbil, K. (2002). Analysis of fMRI and finger tracking training in subjects with chronic stroke. *Brain*, 125(4), 773–788. <https://doi.org/10.1093/brain/awf091>

- Carter, A. R., Astafiev, S. V., Lang, C. E., Connor, L. T., Rengachary, J., Strube, M. J., Pope, D. L. W., Shulman, G. L., & Corbetta, M. (2010). Resting Inter-hemispheric fMRI Connectivity Predicts Performance after Stroke. *Annals of Neurology*, *67*(3), 365–375.  
<https://doi.org/10.1002/ana.21905>
- Carter, A. R., Patel, K. R., Astafiev, S. V., Snyder, A. Z., Rengachary, J., Strube, M. J., Pope, A., Shimony, J. S., Lang, C. E., Shulman, G. L., & Corbetta, M. (2012). Upstream dysfunction of somatomotor functional connectivity after corticospinal damage in stroke. *Neurorehabilitation and Neural Repair*, *26*(1), 7–19. <https://doi.org/10.1177/1545968311411054>
- Chapter 2 Comparative anatomy and physiology of the corticospinal system. - Abstract—Europe PMC.* (n.d.). Retrieved January 28, 2019, from <https://europepmc.org/abstract/med/18808887>
- Characterization of a fiber-less, multichannel optical probe for continuous wave functional near-infrared spectroscopy based on silicon photomultipliers detectors: In-vivo assessment of primary sensorimotor response.* (n.d.). Retrieved January 21, 2021, from <https://www.spiedigitallibrary.org/journals/Characterization-of-a-fiber-less-multichannel-optical-probe-for-continuous/volume-4/issue-03/035002/Characterization-of-a-fiber-less-multichannel-optical-probe-for-continuous/10.1117/1.NPh.4.3.035002.full?webSyncID=e46e9e6e-c7a4-9dab-6a0c-bad059329ad8&sessionGUID=83c9d902-bc99-93ce-d268-bead49a28531>
- Chen, J. L., & Schlaug, G. (2013). Resting State Interhemispheric Motor Connectivity and White Matter Integrity Correlate with Motor Impairment in Chronic Stroke. *Frontiers in Neurology*, *4*. <https://doi.org/10.3389/fneur.2013.00178>
- Chen, K.-L., Chen, C.-T., Chou, Y.-T., Shih, C.-L., Koh, C.-L., & Hsieh, C.-L. (2014). Is the long form of the Fugl-Meyer motor scale more responsive than the short form in patients with

stroke? *Archives of Physical Medicine and Rehabilitation*, 95(5), 941–949.

<https://doi.org/10.1016/j.apmr.2014.01.014>

Cho, S.-H., Shin, H.-K., Kwon, Y.-H., Lee, M. Y., Lee, Y.-H., Lee, C.-H., Yang, D. S., & Jang, S.-H. (2007). Cortical activation changes induced by visual biofeedback tracking training in chronic stroke patients. *NeuroRehabilitation*, 22(2), 77–84.

Chollet, F., Dipiero, V., Wise, R. J. S., Brooks, D. J., Dolan, R. J., & Frackowiak, R. S. J. (1991). The functional anatomy of motor recovery after stroke in humans: A study with positron emission tomography. *Annals of Neurology*, 29(1), 63–71.

<https://doi.org/10.1002/ana.410290112>

Christensen, H., Derex, L., Pialat, J.-B., Wiart, M., Nighoghossian, N., Hermier, M., Szabo, K., Achtnichts, L., Grips, E., Binder, J., Gerigk, L., Hennerici, M., Gass, A., Soltanian-Zadeh, H., Daley, S., Hearshen, D., Ewing, J. R., Patel, S. C., Chopp, M., ... Lewandowski, C. (2004). Neuroimaging in Stroke Recovery: A Position Paper from the First International Workshop on Neuroimaging and Stroke Recovery. *Cerebrovascular Diseases*, 18(3), 260–267.

<https://doi.org/10.1159/000080293>

*Collimator.jpg*. (n.d.). <https://commons.wikimedia.org/w/index.php?curid=46413806>

*Combining energy and Laplacian regularization to accurately retrieve the depth of brain activity of diffuse optical tomographic data*. (n.d.). Retrieved September 23, 2020, from <https://www.spiedigitallibrary.org/journals/journal-of-biomedical-optics/volume-21/issue-3/036008/Combining-energy-and-Laplacian-regularization-to-accurately-retrieve-the-depth/10.1117/1.JBO.21.3.036008.full>

Conroy, B. E., DeJong, G., & Horn, S. D. (2009). Hospital-Based Stroke Rehabilitation in the United States. *Topics in Stroke Rehabilitation*, 16(1), 34–43. <https://doi.org/10.1310/tsr1601-34>

*Contribution of the Resting-State Functional Connectivity of the Contralateral Primary Sensorimotor Cortex to Motor Recovery after Subcortical Stroke.* (n.d.). Retrieved January 30, 2019, from <https://journals.plos.org/plosone/article?id=10.1371/journal.pone.0084729>

*Corticospinal tract lesion load: An imaging biomarker for stroke motor outcomes—Feng—2015—Annals of Neurology—Wiley Online Library.* (n.d.). Retrieved November 20, 2020, from <https://onlinelibrary.wiley.com/doi/abs/10.1002/ana.24510>

Courtois, M., Loussouarn, G., Hourseau, C., & Grollier, J. F. (1995). Ageing and hair cycles. *British Journal of Dermatology*, 132(1), 86–93. <https://doi.org/10.1111/j.1365-2133.1995.tb08630.x>

Cramer, S. C., & Riley, J. D. (2008). Neuroplasticity and brain repair after stroke. *Current Opinion in Neurology*, 21(1), 76–82. <https://doi.org/10.1097/WCO.0b013e3282f36cb6>

Crivelli, D., Angelillo, M. T., Grippa, E., Colucci, A., Nardulli, R., & Balconi, M. (2018). When is a novel psychometric measure needed? A preliminary analysis regarding the Cognitive Assessment for Stroke Patients (CASP) battery compared with MMSE and MoCA. *Applied Neuropsychology: Adult*, 25(5), 410–416. <https://doi.org/10.1080/23279095.2017.1320556>

Cui, X., Bray, S., Bryant, D. M., Glover, G. H., & Reiss, A. L. (2011). A quantitative comparison of NIRS and fMRI across multiple cognitive tasks. *NeuroImage*, 54(4), 2808–2821. <https://doi.org/10.1016/j.neuroimage.2010.10.069>

Cui, X., Bray, S., & Reiss, A. L. (2010). Functional near infrared spectroscopy (NIRS) signal improvement based on negative correlation between oxygenated and deoxygenated

hemoglobin dynamics. *NeuroImage*, 49(4), 3039–3046.

<https://doi.org/10.1016/j.neuroimage.2009.11.050>

Cunningham, D. A., Machado, A., Janini, D., Varnerin, N., Bonnett, C., Yue, G., Jones, S., Lowe, M., Beall, E., Sakaie, K., & Plow, E. B. (2015). Assessment of Inter-Hemispheric Imbalance Using Imaging and Noninvasive Brain Stimulation in Patients With Chronic Stroke. *Archives of Physical Medicine and Rehabilitation*, 96(4), S94–S103.

<https://doi.org/10.1016/j.apmr.2014.07.419>

Daly, J. J., Hrovat, K., Holcomb, J., & Pundik, S. (2014). Brain control of functional reach in healthy adults and stroke survivors. *Restorative Neurology and Neuroscience*, 32(5), 559–573.

<https://doi.org/10.3233/RNN-130361>

Davis, F. D. (1989). Perceived Usefulness, Perceived Ease of Use, and User Acceptance of Information Technology. *MIS Quarterly*, 13(3), 319–340. JSTOR.

<https://doi.org/10.2307/249008>

*Deep learning for time series classification: A review* | SpringerLink. (n.d.). Retrieved January 9, 2021, from <https://link.springer.com/article/10.1007/s10618-019-00619-1>

Del Guerra, A., Belcari, N., Giuseppina, M., LLosà, G., Marcatili, S., Ambrosi, G., Corsi, F., Marzocca, C., Dalla Betta, G.-F., & Piemonte, C. (2010). Advantages and pitfalls of the silicon photomultiplier (SiPM) as photodetector for the next generation of PET scanners.

*Nuclear Instruments and Methods in Physics Research Section A: Accelerators,*

*Spectrometers, Detectors and Associated Equipment*, 617, 223–226.

<https://doi.org/10.1016/j.nima.2009.09.121>

Delorme, M., Froger, J., Perrey, S., Vergotte, G., & Laffont, I. (2017). Changes in hemodynamic responses during movements of the upper extremities in the acute phase after stroke: A fNIRS

study. *Annals of Physical and Rehabilitation Medicine*, 60, e1.

<https://doi.org/10.1016/j.rehab.2017.07.016>

Delorme, M., Vergotte, G., Perrey, S., Froger, J., & Laffont, I. (2019). Time course of sensorimotor cortex reorganization during upper extremity task accompanying motor recovery early after stroke: An fNIRS study. *Restorative Neurology and Neuroscience*, 37(3), 207–218. <https://doi.org/10.3233/RNN-180877>

Delpy, D. T., Cope, M., Zee, P. van der, Arridge, S., Wray, S., & Wyatt, J. (1988). Estimation of optical pathlength through tissue from direct time of flight measurement. *Physics in Medicine and Biology*, 33(12), 1433–1442. <https://doi.org/10.1088/0031-9155/33/12/008>

Deterding, S., Dixon, D., Khaled, R., & Nacke, L. (2011). From game design elements to gamefulness: Defining “gamification.” *Proceedings of the 15th International Academic MindTrek Conference: Envisioning Future Media Environments*, 9–15. <https://doi.org/10.1145/2181037.2181040>

*Developing a Theory of Gamified Learning: Linking Serious Games and Gamification of Learning—Richard N. Landers, 2014.* (n.d.). Retrieved January 21, 2021, from <https://journals.sagepub.com/doi/abs/10.1177/1046878114563660>

*Development of a neuro-feedback game based on motor imagery EEG | SpringerLink.* (n.d.). Retrieved January 21, 2021, from <https://link.springer.com/article/10.1007/s11042-017-5168->

x

*Development of hierarchical structure and analytical model of key factors for mobile app stickiness—ScienceDirect.* (n.d.). Retrieved January 21, 2021, from <https://www.sciencedirect.com/science/article/pii/S2444569X19300204>

Di Lazzaro, V., Oliviero, A., Profice, P., Insola, A., Mazzone, P., Tonali, P., & Rothwell, J. C. (1999). Direct demonstration of interhemispheric inhibition of the human motor cortex produced by transcranial magnetic stimulation. *Experimental Brain Research*, *124*(4), 520–524. <https://doi.org/10.1007/s002210050648>

*Different Brain Connectivity between Responders and Nonresponders to Dual-Mode Noninvasive Brain Stimulation over Bilateral Primary Motor Cortices in Stroke Patients.* (n.d.). Retrieved September 22, 2020, from <https://www.hindawi.com/journals/np/2019/3826495/>

*Does Stroke Rehabilitation Really Matter? Part B: An Algorithm for Prescribing an Effective Intensity of Rehabilitation.* - PubMed—NCBI. (n.d.). Retrieved May 14, 2020, from <https://www.ncbi.nlm.nih.gov/pubmed/29334831>

Dong Yun, Dobkin Bruce H., Cen Steven Y., Wu Allan D., & Winstein Carolee J. (2006). Motor Cortex Activation During Treatment May Predict Therapeutic Gains in Paretic Hand Function After Stroke. *Stroke*, *37*(6), 1552–1555. <https://doi.org/10.1161/01.STR.0000221281.69373.4e>

Doyle, K. P., Simon, R. P., & Stenzel-Poore, M. P. (2008). Mechanisms of ischemic brain damage. *Neuropharmacology*, *55*(3), 310–318. <https://doi.org/10.1016/j.neuropharm.2008.01.005>

Duan, L., Zhang, Y.-J., & Zhu, C.-Z. (2012). Quantitative comparison of resting-state functional connectivity derived from fNIRS and fMRI: A simultaneous recording study. *NeuroImage*, *60*(4), 2008–2018. <https://doi.org/10.1016/j.neuroimage.2012.02.014>

Dubovik, S., Ptak, R., Aboulafia, T., Magnin, C., Gillibert, N., Allet, L., Pignat, J.-M., Schnider, A., & Guggisberg, A. G. (2013). EEG Alpha Band Synchrony Predicts Cognitive and Motor

Performance in Patients with Ischemic Stroke. *Behavioural Neurology*, 26(3), 187–189.

<https://doi.org/10.1155/2013/109764>

*Effect of Brain-Derived Neurotrophic Factor Treatment and Forced Arm Use on Functional*

*Motor Recovery After Small Cortical Ischemia | Stroke*. (n.d.). Retrieved November 20, 2020,

from <https://www.ahajournals.org/doi/full/10.1161/01.STR.0000119754.85848.0D>

*Effects of Neurofeedback Training with an Electroencephalogram-Ba...: Ingenta Connect*. (n.d.).

Retrieved November 21, 2020, from

<https://www.ingentaconnect.com/content/mjl/sreh/2011/00000043/00000010/art00012>

Emmert, K., Kopel, R., Koush, Y., Maire, R., Senn, P., Van De Ville, D., & Haller, S. (2017).

Continuous vs. Intermittent neurofeedback to regulate auditory cortex activity of tinnitus patients using real-time fMRI - A pilot study. *NeuroImage: Clinical*, 14, 97–104.

<https://doi.org/10.1016/j.nicl.2016.12.023>

“Ergonomic”; *adjective*. (n.d.). Harpercollins. Retrieved January 19, 2021, from

<https://www.dictionary.com/browse/ergonomic>

*Estimating the spatial resolution of fNIRS sensors for BCI purposes*. (n.d.). Retrieved February

2, 2019, from [https://www.spiedigitallibrary.org/conference-proceedings-of-](https://www.spiedigitallibrary.org/conference-proceedings-of-spie/8945/894504/Estimating-the-spatial-resolution-of-fNIRS-sensors-for-BCI-purposes/10.1117/12.2037351.short?SSO=1)

[spie/8945/894504/Estimating-the-spatial-resolution-of-fNIRS-sensors-for-BCI-](https://www.spiedigitallibrary.org/conference-proceedings-of-spie/8945/894504/Estimating-the-spatial-resolution-of-fNIRS-sensors-for-BCI-purposes/10.1117/12.2037351.short?SSO=1)

[purposes/10.1117/12.2037351.short?SSO=1](https://www.spiedigitallibrary.org/conference-proceedings-of-spie/8945/894504/Estimating-the-spatial-resolution-of-fNIRS-sensors-for-BCI-purposes/10.1117/12.2037351.short?SSO=1)

Fan, Y., Wu, C., Liu, H., Lin, K., Wai, Y., & Chen, Y. (2015). Neuroplastic changes in resting-

state functional connectivity after stroke rehabilitation. *Frontiers in Human Neuroscience*, 9.

<https://doi.org/10.3389/fnhum.2015.00546>

Feigin, V. L., Forouzanfar, M. H., Krishnamurthi, R., Mensah, G. A., Connor, M., Bennett, D.

A., Moran, A. E., Sacco, R. L., Anderson, L., Truelsen, T., O'Donnell, M.,



- Venketasubramanian, N., Barker-Collo, S., Lawes, C. M. M., Wang, W., Shinohara, Y., Witt, E., Ezzati, M., Naghavi, M., ... Global Burden of Diseases, Injuries, and Risk Factors Study 2010 (GBD 2010) and the GBD Stroke Experts Group. (2014). Global and regional burden of stroke during 1990-2010: Findings from the Global Burden of Disease Study 2010. *Lancet (London, England)*, 383(9913), 245–254. [https://doi.org/10.1016/s0140-6736\(13\)61953-4](https://doi.org/10.1016/s0140-6736(13)61953-4)
- Ferbert, A., Priori, A., Rothwell, J. C., Day, B. L., Colebatch, J. G., & Marsden, C. D. (1992). Interhemispheric inhibition of the human motor cortex. *The Journal of Physiology*, 453(1), 525–546. <https://doi.org/10.1113/jphysiol.1992.sp019243>
- Feydy, A., Carlier, R., Roby-Brami, A., Bussel, B., Cazalis, F., Pierot, L., Burnod, Y., & Maier, M. A. (2002). Longitudinal Study of Motor Recovery After Stroke: Recruitment and Focusing of Brain Activation. *Stroke*, 33(6), 1610–1617. <https://doi.org/10.1161/01.STR.0000017100.68294.52>
- Fishburn, F. A., Ludlum, R. S., Vaidya, C. J., & Medvedev, A. V. (2019). Temporal Derivative Distribution Repair (TDDR): A motion correction method for fNIRS. *NeuroImage*, 184, 171–179. <https://doi.org/10.1016/j.neuroimage.2018.09.025>
- Fitzgerald, M., & Lynn, B. (1977). The sensitization of high threshold mechanoreceptors with myelinated axons by repeated heating. *The Journal of Physiology*, 265(2), 549–563. <https://doi.org/10.1113/jphysiol.1977.sp011730>
- Folgado, D., Barandas, M., Matias, R., Martins, R., Carvalho, M., & Gamboa, H. (2018). Time Alignment Measurement for Time Series. *Pattern Recognition*, 81, 268–279. <https://doi.org/10.1016/j.patcog.2018.04.003>
- Folstein, M. F., Folstein, S. E., & McHugh, P. R. (1975). “Mini-mental state.” *Journal of Psychiatric Research*, 12(3), 189–198. [https://doi.org/10.1016/0022-3956\(75\)90026-6](https://doi.org/10.1016/0022-3956(75)90026-6)

- French, B., Thomas, L. H., Coupe, J., McMahon, N. E., Connell, L., Harrison, J., Sutton, C. J., Tishkovskaya, S., & Watkins, C. L. (2016). Repetitive task training for improving functional ability after stroke. *The Cochrane Database of Systematic Reviews*, *11*, CD006073.  
<https://doi.org/10.1002/14651858.CD006073.pub3>
- Friesen, C. L., Bardouille, T., Neyedli, H. F., & Boe, S. G. (2017). Combined Action Observation and Motor Imagery Neurofeedback for Modulation of Brain Activity. *Frontiers in Human Neuroscience*, *10*. <https://doi.org/10.3389/fnhum.2016.00692>
- Friesen, C., Lawrence, M., Ingram, T., Smith, M., Hamilton, E., Holland, C., Neyedli, H., & Boe, S. (2020). Wireless, fibreless, and user-friendly fNIRS headband compared with headcap fNIRS system for sensorimotor measurement of upper- and lower-extremity movement. *Manuscript Submitted for Publication*.
- Frolov, A. A., Mokienko, O., Lyukmanov, R., Biryukova, E., Kotov, S., Turbina, L., Nadareyshvily, G., & Bushkova, Y. (2017). Post-stroke Rehabilitation Training with a Motor-Imagery-Based Brain-Computer Interface (BCI)-Controlled Hand Exoskeleton: A Randomized Controlled Multicenter Trial. *Frontiers in Neuroscience*, *11*.  
<https://doi.org/10.3389/fnins.2017.00400>
- Frontiers | A Review of Transcranial Magnetic Stimulation and Multimodal Neuroimaging to Characterize Post-Stroke Neuroplasticity | Neurology*. (n.d.). Retrieved February 2, 2019, from <https://www.frontiersin.org/articles/10.3389/fneur.2015.00226/full>
- Frontiers | Role of the Contralesional Hemisphere in Post-Stroke Recovery of Upper Extremity Motor Function | Neurology*. (n.d.). Retrieved January 25, 2020, from <https://www.frontiersin.org/articles/10.3389/fneur.2015.00214/full>

- Frontiers | Role of the Contralesional vs. Ipsilesional Hemisphere in Stroke Recovery | Human Neuroscience*. (n.d.). Retrieved October 21, 2020, from <https://www.frontiersin.org/articles/10.3389/fnhum.2017.00469/full?report=reader>
- Funane, T., Atsumori, H., Katura, T., Obata, A. N., Sato, H., Tanikawa, Y., Okada, E., & Kiguchi, M. (2014). Quantitative evaluation of deep and shallow tissue layers' contribution to fNIRS signal using multi-distance optodes and independent component analysis. *NeuroImage*, 85, 150–165. <https://doi.org/10.1016/j.neuroimage.2013.02.026>
- Funane, T., Numata, T., Sato, H., Hiraizumi, S., Hasegawa, Y., Kuwabara, H., Hasegawa, K., & Kiguchi, M. (2017). Rearrangeable and exchangeable optical module with system-on-chip for wearable functional near-infrared spectroscopy system. *Neurophotonics*, 5(1), 011007. <https://doi.org/10.1117/1.NPh.5.1.011007>
- Funane, T., Sato, H., Yahata, N., Takizawa, R., Nishimura, Y., Kinoshita, A., Katura, T., Atsumori, H., Fukuda, M., Kasai, K., Koizumi, H., & Kiguchi, M. (2015). Concurrent fNIRS-fMRI measurement to validate a method for separating deep and shallow fNIRS signals by using multidistance optodes. *Neurophotonics*, 2(1), 015003. <https://doi.org/10.1117/1.NPh.2.1.015003>
- Fung, J., Richards, C. L., Malouin, F., McFadyen, B. J., & Lamontagne, A. (2006). A Treadmill and Motion Coupled Virtual Reality System for Gait Training Post-Stroke. *CyberPsychology & Behavior*, 9(2), 157–162. <https://doi.org/10.1089/cpb.2006.9.157>
- Furner, C. P., Racherla, P., & Babb, J. S. (2014). Mobile app stickiness (MASS) and mobile interactivity: A conceptual model. *The Marketing Review*, 14(2), 163–188. <https://doi.org/10.1362/146934714X14024778816913>

*Gain options fulfill application needs.* (2002, April 1). Laser Focus World.

<https://www.laserfocusworld.com/detectors-imaging/article/16552458/gain-options-fulfill-application-needs>

Gandolfi, M., Formaggio, E., Geroin, C., Storti, S. F., Boscolo Galazzo, I., Bortolami, M.,

Saltuari, L., Picelli, A., Waldner, A., Manganotti, P., & Smania, N. (2018, March 26).

*Quantification of Upper Limb Motor Recovery and EEG Power Changes after Robot-Assisted*

*Bilateral Arm Training in Chronic Stroke Patients: A Prospective Pilot Study* [Research

Article]. *Neural Plasticity*; Hindawi. <https://doi.org/10.1155/2018/8105480>

Gateau, T., Ayaz, H., & Dehais, F. (2018). In silico vs. Over the Clouds: On-the-Fly Mental

State Estimation of Aircraft Pilots, Using a Functional Near Infrared Spectroscopy Based

Passive-BCI. *Frontiers in Human Neuroscience*, *12*.

<https://doi.org/10.3389/fnhum.2018.00187>

Gelman, A., Lee, D., & Guo, J. (2015). Stan: A Probabilistic Programming Language for

Bayesian Inference and Optimization. *Journal of Educational and Behavioral Statistics*,

*40*(5), 530–543. <https://doi.org/10.3102/1076998615606113>

Germon, T. J., Evans, P. D., Manara, A. R., Barnett, N. J., Wall, P., & Nelson, R. J. (1998).

Sensitivity of Near Infrared Spectroscopy to Cerebral and Extra-Cerebral Oxygenation

Changes is Determined by Emitter-Detector Separation. *Journal of Clinical Monitoring and*

*Computing*, *14*(5), 353–360. <https://doi.org/10.1023/A:1009957032554>

Giorgino, T. (2009). Computing and Visualizing Dynamic Time Warping Alignments in R: The

**dtw** Package. *Journal of Statistical Software*, *31*(7). <https://doi.org/10.18637/jss.v031.i07>

- Golestani, A.-M., Tymchuk, S., Demchuk, A., & Goodyear, B. G. (2013). Longitudinal Evaluation of Resting-State fMRI After Acute Stroke With Hemiparesis. *Neurorehabilitation and Neural Repair*, 27(2), 153–163. <https://doi.org/10.1177/1545968312457827>
- Gramann, K., Fairclough, S. H., Zander, T. O., & Ayaz, H. (2017). Editorial: Trends in Neuroergonomics. *Frontiers in Human Neuroscience*, 11. <https://doi.org/10.3389/fnhum.2017.00165>
- Gundacker, S., & Heering, A. (2020). The silicon photomultiplier: Fundamentals and applications of a modern solid-state photon detector. *Physics in Medicine & Biology*, 65(17), 17TR01. <https://doi.org/10.1088/1361-6560/ab7b2d>
- Heiss, W.-D. (2012). The ischemic penumbra: How does tissue injury evolve? *Annals of the New York Academy of Sciences*, 1268(1), 26–34. <https://doi.org/10.1111/j.1749-6632.2012.06668.x>
- Hellrung, L., Dietrich, A., Hollmann, M., Pleger, B., Kalberlah, C., Roggenhofer, E., Villringer, A., & Horstmann, A. (2018). Intermittent compared to continuous real-time fMRI neurofeedback boosts control over amygdala activation. *NeuroImage*, 166, 198–208. <https://doi.org/10.1016/j.neuroimage.2017.10.031>
- Hermann, D. M., Buga, A.-M., & Popa-Wagner, A. (2015). Neurovascular remodeling in the aged ischemic brain. *Journal of Neural Transmission*, 122(1), 25–33. <https://doi.org/10.1007/s00702-013-1148-0>
- Hinman, J. D. (2014). The back and forth of axonal injury and repair after stroke. *Current Opinion in Neurology*, 27(6), 615–623. <https://doi.org/10.1097/WCO.0000000000000149>
- Holper, L., Biallas, M., & Wolf, M. (2009). Task complexity relates to activation of cortical motor areas during uni- and bimanual performance: A functional NIRS study. *NeuroImage*, 46(4), 1105–1113. <https://doi.org/10.1016/j.neuroimage.2009.03.027>

- Homan, R. W. (1988). The 10-20 Electrode System and Cerebral Location. *American Journal of EEG Technology*, 28(4), 269–279. <https://doi.org/10.1080/00029238.1988.11080272>
- Homan, R. W., Herman, J., & Purdy, P. (1987). Cerebral location of international 10–20 system electrode placement. *Electroencephalography and Clinical Neurophysiology*, 66(4), 376–382. [https://doi.org/10.1016/0013-4694\(87\)90206-9](https://doi.org/10.1016/0013-4694(87)90206-9)
- Hong, I., Goodwin, J. S., Reistetter, T. A., Kuo, Y.-F., Mallinson, T., Karmarkar, A., Lin, Y.-L., & Ottenbacher, K. J. (2019). Comparison of Functional Status Improvements Among Patients With Stroke Receiving Postacute Care in Inpatient Rehabilitation vs Skilled Nursing Facilities. *JAMA Network Open*, 2(12), e1916646–e1916646. <https://doi.org/10.1001/jamanetworkopen.2019.16646>
- Hope, T. M. H., Friston, K., Price, C. J., Leff, A. P., Rotshtein, P., & Bowman, H. (2019). Recovery after stroke: Not so proportional after all? *Brain: A Journal of Neurology*, 142(1), 15–22. <https://doi.org/10.1093/brain/awy302>
- howmade.com. (n.d.). *How Products are Made—Light-Emitting Diode (LED)*. Retrieved January 20, 2021, from <http://www.madehow.com/Volume-1/Light-Emitting-Diode-LED.html>
- Hsieh, Y.-W., Hsueh, I.-P., Chou, Y.-T., Sheu, C.-F., Hsieh, C.-L., & Kwakkel, G. (2007). Development and validation of a short form of the Fugl-Meyer motor scale in patients with stroke. *Stroke*, 38(11), 3052–3054. <https://doi.org/10.1161/STROKEAHA.107.490730>
- Hu, J., Li, C., Hua, Y., Zhang, B., Gao, B.-Y., Liu, P.-L., Sun, L.-M., Lu, R.-R., Wang, Y.-Y., & Bai, Y.-L. (2019). Constrained-induced movement therapy promotes motor function recovery by enhancing the remodeling of ipsilesional corticospinal tract in rats after stroke. *Brain Research*, 1708, 27–35. <https://doi.org/10.1016/j.brainres.2018.11.011>

- Hübers, A., Orekhov, Y., & Ziemann, U. (2008). Interhemispheric motor inhibition: Its role in controlling electromyographic mirror activity. *European Journal of Neuroscience*, 28(2), 364–371. <https://doi.org/10.1111/j.1460-9568.2008.06335.x>
- IEC/TR 62366-2: Guidance on the application of usability engineering to medical device.* (2016). International Electrotechnical Commission.
- Ikbali Afsar, S., Mirzayev, I., Umit Yemisci, O., & Cosar Saracgil, S. N. (2018). Virtual Reality in Upper Extremity Rehabilitation of Stroke Patients: A Randomized Controlled Trial. *Journal of Stroke and Cerebrovascular Diseases*, 27(12), 3473–3478. <https://doi.org/10.1016/j.jstrokecerebrovasdis.2018.08.007>
- Increasing Patient Engagement in Rehabilitation Exercises Using Computer-Based Citizen Science.* (n.d.). Retrieved January 30, 2019, from <https://journals.plos.org/plosone/article?id=10.1371/journal.pone.0117013>
- Individual prediction of chronic motor outcome in the acute post-stroke stage: Behavioral parameters versus functional imaging—Rehme—2015—Human Brain Mapping—Wiley Online Library.* (n.d.). Retrieved January 30, 2019, from <https://onlinelibrary.wiley.com/doi/abs/10.1002/hbm.22936>
- Inhibitory influence of the ipsilateral motor cortex on responses to stimulation of the human cortex and pyramidal tract—Gerloff—1998—The Journal of Physiology—Wiley Online Library.* (n.d.). Retrieved January 25, 2020, from <https://physoc.onlinelibrary.wiley.com/doi/full/10.1111/j.1469-7793.1998.249bz.x>
- Institute for Clinical Evaluative Services. (n.d.). *Ontario Stroke Evaluation Report 2012*. Ontario Stroke Network & Canadian Stroke Network.

- Ishida, A., Misumi, S., Ueda, Y., Shimizu, Y., Cha-Gyun, J., Tamakoshi, K., Ishida, K., & Hida, H. (2015). Early constraint-induced movement therapy promotes functional recovery and neuronal plasticity in a subcortical hemorrhage model rat. *Behavioural Brain Research*, *284*, 158–166. <https://doi.org/10.1016/j.bbr.2015.02.022>
- Jaillard, A., Martin, C. D., Garambois, K., Lebas, J. F., & Hommel, M. (2005). Vicarious function within the human primary motor cortex?: A longitudinal fMRI stroke study. *Brain*, *128*(5), 1122–1138. <https://doi.org/10.1093/brain/awh456>
- Jamieson, M., Cullen, B., Lennon, M., Brewster, S., & Evans, J. (2020). Designing ApplTree: Usable scheduling software for people with cognitive impairments. *Disability and Rehabilitation: Assistive Technology*, 1–11. <https://doi.org/10.1080/17483107.2020.1785560>
- Jeffers, M. S., Karthikeyan, S., Gomez-Smith, M., Gasinzigwa, S., Achenbach, J., Feiten, A., & Corbett, D. (2018). Does Stroke Rehabilitation Really Matter? Part B: An Algorithm for Prescribing an Effective Intensity of Rehabilitation. *Neurorehabilitation and Neural Repair*, *32*(1), 73–83. <https://doi.org/10.1177/1545968317753074>
- Jia, H., Cowper, D. C., Tang, Y., Litt, E., & Wilson, L. (2012). Postacute stroke rehabilitation utilization: Are there differences between rural-urban patients and taxonomies? *The Journal of Rural Health: Official Journal of the American Rural Health Association and the National Rural Health Care Association*, *28*(3), 242–247. <https://doi.org/10.1111/j.1748-0361.2011.00397.x>
- Johansen-Berg, H., Rushworth, M. F. S., Bogdanovic, M. D., Kischka, U., Wimalaratna, S., & Matthews, P. M. (2002). The role of ipsilateral premotor cortex in hand movement after stroke. *Proceedings of the National Academy of Sciences*, *99*(22), 14518–14523. <https://doi.org/10.1073/pnas.222536799>



- Johnson, K. A., Hartwell, K., LeMatty, T., Borckardt, J., Morgan, P. S., Govindarajan, K., Brady, K., & George, M. S. (2012). Intermittent “Real-time” fMRI Feedback Is Superior to Continuous Presentation for a Motor Imagery Task: A Pilot Study. *Journal of Neuroimaging*, 22(1), 58–66. <https://doi.org/10.1111/j.1552-6569.2010.00529.x>
- Joint Stroke Strategy Working Group. (2000). *Towards an Integrated Stroke Strategy for Ontario: Report*. Ministry of Health & Long-Term Care. <http://www.health.gov.on.ca/en/common/ministry/publications/reports/stroke/strokereport.pdf>
- Jones, T. A., Allred, R. P., Adkins, D. L., Hsu, J. E., O’Bryant, A., & Maldonado, M. A. (2009). Remodeling the Brain With Behavioral Experience After Stroke. *Stroke*, 40(3, Supplement 1), S136–S138. <https://doi.org/10.1161/STROKEAHA.108.533653>
- Kaas, J. H. (2004). Evolution of somatosensory and motor cortex in primates. *The Anatomical Record Part A: Discoveries in Molecular, Cellular, and Evolutionary Biology*, 281A(1), 1148–1156. <https://doi.org/10.1002/ar.a.20120>
- Kassab, A., Lan, J. L., Vannasing, P., & Sawan, M. (2015). Functional near-infrared spectroscopy caps for brain activity monitoring: A review. *Applied Optics*, 54(3), 576–586. <https://doi.org/10.1364/AO.54.000576>
- Kato, H. (2014). Near-Infrared Spectroscopy and Motor Lateralization after Stroke: A Case Series Study. *International Journal of Physical Medicine & Rehabilitation*, 02(03). <https://doi.org/10.4172/2329-9096.1000192>
- Khan, B., Wildey, C., Francis, R., Tian, F., Delgado, M. R., Liu, H., MacFarlane, D., & Alexandrakis, G. (2012). Improving optical contact for functional near-infrared brain spectroscopy and imaging with brush optodes. *Biomedical Optics Express*, 3(5), 878. <https://doi.org/10.1364/BOE.3.000878>

- Kiguchi, M., Atsumori, H., Fukasaku, I., Kumagai, Y., Funane, T., Maki, A., Kasai, Y., & Ninomiya, A. (2012). Note: Wearable near-infrared spectroscopy imager for haired region. *Review of Scientific Instruments*, *83*(5), 056101. <https://doi.org/10.1063/1.4704456>
- Kim, Y. H., & Jang, S. H. (n.d.). Longitudinal fMRI study for locomotor recovery in patients with stroke. *Neurology*, *67*(2).
- Klem, G. H., Lüders, H., Jasper, H. H., & Elger, C. (1958). The ten-twenty electrode system of the International Federation. The International Federation of Clinical Neurophysiology. *Electroencephalography and Clinical Neurophysiology. Supplement*, *52*, 3–6.
- Kligman, A. M. (1988). The comparative histopathology of male-pattern baldness and senescent baldness. *Clinics in Dermatology*, *6*(4), 108–118. [https://doi.org/10.1016/0738-081X\(88\)90074-0](https://doi.org/10.1016/0738-081X(88)90074-0)
- Kober, S. E., Wood, G., Kurzmann, J., Friedrich, E. V. C., Stangl, M., Wippel, T., Väljamäe, A., & Neuper, C. (2014). Near-infrared spectroscopy based neurofeedback training increases specific motor imagery related cortical activation compared to sham feedback. *Biological Psychology*, *95*, 21–30. <https://doi.org/10.1016/j.biopsycho.2013.05.005>
- Krigolson, O. E., Williams, C. C., Norton, A., Hassall, C. D., & Colino, F. L. (2017). Choosing MUSE: Validation of a Low-Cost, Portable EEG System for ERP Research. *Frontiers in Neuroscience*, *11*. <https://doi.org/10.3389/fnins.2017.00109>
- Lam, T. K., Binns, M. A., Honjo, K., Dawson, D. R., Ross, B., Stuss, D. T., Black, S. E., Chen, J. J., Fujioka, T., & Chen, J. L. (2018). Variability in stroke motor outcome is explained by structural and functional integrity of the motor system. *Scientific Reports*, *8*(1), 9480. <https://doi.org/10.1038/s41598-018-27541-8>

- Lang, C. E., Lohse, K. R., & Birkenmeier, R. L. (2015). Dose and timing in neurorehabilitation: Prescribing motor therapy after stroke. *Current Opinion in Neurology*, 28(6), 549–555. <https://doi.org/10.1097/WCO.0000000000000256>
- Lang, C. E., Strube, M. J., Bland, M. D., Waddell, K. J., Cherry-Allen, K. M., Nudo, R. J., Dromerick, A. W., & Birkenmeier, R. L. (2016). Dose-response of task-specific upper limb training in people at least 6 months post stroke: A Phase II, single-blind, randomized, controlled trial. *Annals of Neurology*, 80(3), 342–354. <https://doi.org/10.1002/ana.24734>
- Langhorne, P., Baylan, S., & Early Supported Discharge Trialists. (2017). Early supported discharge services for people with acute stroke. *The Cochrane Database of Systematic Reviews*, 7, CD000443. <https://doi.org/10.1002/14651858.CD000443.pub4>
- Lapborisuth, P., Zhang, X., Noah, A., & Hirsch, J. (2017). Neurofeedback-based functional near-infrared spectroscopy upregulates motor cortex activity in imagined motor tasks. *Neurophotonics*, 4(2), 021107. <https://doi.org/10.1117/1.NPh.4.2.021107>
- Laser Glare Protection*. (n.d.). META. Retrieved January 21, 2021, from <https://metamaterial.com/solutions/laser-glare-protection/>
- Lawrence, E. S., Coshall, C., Dundas, R., Stewart, J., Rudd, A. G., Howard, R., & Wolfe, C. D. A. (2001). Estimates of the Prevalence of Acute Stroke Impairments and Disability in a Multiethnic Population. *Stroke*. <https://www.ahajournals.org/doi/abs/10.1161/01.STR.32.6.1279>
- Lee, H.-S., Lim, J.-H., Jeon, B.-H., & Song, C.-S. (2020). Non-immersive Virtual Reality Rehabilitation Applied to a Task-oriented Approach for Stroke Patients: A Randomized Controlled Trial. *Restorative Neurology and Neuroscience*, 38(2), 165–172. <https://doi.org/10.3233/RNN-190975>

- Lewis, Z. H., Swartz, M. C., & Lyons, E. J. (2016). What's the Point?: A Review of Reward Systems Implemented in Gamification Interventions. *Games for Health Journal*, 5(2), 93–99. <https://doi.org/10.1089/g4h.2015.0078>
- Li, L., Liu, Z., Zhu, H., Zhu, L., & Huang, Y. (2019). Functional near-infrared spectroscopy in the evaluation of urban rail transit drivers' mental workload under simulated driving conditions. *Ergonomics*, 62(3), 406–419. <https://doi.org/10.1080/00140139.2018.1535093>
- Li, S., Nie, E. H., Yin, Y., Benowitz, L. I., Tung, S., Vinters, H. V., Bahjat, F. R., Stenzel-Poore, M. P., Kawaguchi, R., Coppola, G., & Carmichael, S. T. (2015). GDF10 is a signal for axonal sprouting and functional recovery after stroke. *Nature Neuroscience*, 18(12), 1737–1745. <https://doi.org/10.1038/nn.4146>
- Lin, D. J., Cloutier, A. M., Erler, K. S., Cassidy, J. M., Snider, S. B., Ranford, J., Parlman, K., Giatsidis, F., Burke, J. F., Schwamm, L. H., Finklestein, S. P., Hochberg, L. R., & Cramer, S. C. (2019). Corticospinal Tract Injury Estimated From Acute Stroke Imaging Predicts Upper Extremity Motor Recovery After Stroke. *Stroke*, 50(12), 3569–3577. <https://doi.org/10.1161/STROKEAHA.119.025898>
- Lisboa, P. J., & Taktak, A. F. G. (2006). The use of artificial neural networks in decision support in cancer: A systematic review. *Neural Networks*, 19(4), 408–415. <https://doi.org/10.1016/j.neunet.2005.10.007>
- Lkozma, L. K. (n.d.). *K Nearest Neighbors algorithm (kNN)*. 33.
- Lohse Keith R., Lang Catherine E., & Boyd Lara A. (2014). Is More Better? Using Metadata to Explore Dose–Response Relationships in Stroke Rehabilitation. *Stroke*, 45(7), 2053–2058. <https://doi.org/10.1161/STROKEAHA.114.004695>

- Lotze, M., Markert, J., Sauseng, P., Hoppe, J., Plewnia, C., & Gerloff, C. (2006). The Role of Multiple Contralesional Motor Areas for Complex Hand Movements after Internal Capsular Lesion. *Journal of Neuroscience*, *26*(22), 6096–6102.  
<https://doi.org/10.1523/JNEUROSCI.4564-05.2006>
- Loubinoux, I., Carel, C., Pariente, J., Dechaumont, S., Albucher, J.-F., Marque, P., Manelfe, C., & Chollet, F. (2003). Correlation between cerebral reorganization and motor recovery after subcortical infarcts. *NeuroImage*, *20*(4), 2166–2180.  
<https://doi.org/10.1016/j.neuroimage.2003.08.017>
- Loubinoux, I., Dechaumont-Palacin, S., Castel-Lacanal, E., De Boissezon, X., Marque, P., Pariente, J., Albucher, J.-F., Berry, I., & Chollet, F. (2007). Prognostic Value of fMRI in Recovery of Hand Function in Subcortical Stroke Patients. *Cerebral Cortex*, *17*(12), 2980–2987. <https://doi.org/10.1093/cercor/bhm023>
- Ma, V. Y., Chan, L., & Carruthers, K. J. (2014). Incidence, prevalence, costs, and impact on disability of common conditions requiring rehabilitation in the United States: Stroke, spinal cord injury, traumatic brain injury, multiple sclerosis, osteoarthritis, rheumatoid arthritis, limb loss, and back pain. *Archives of Physical Medicine and Rehabilitation*, *95*(5), 986-995.e1.  
<https://doi.org/10.1016/j.apmr.2013.10.032>
- MacLellan, C. L., Keough, M. B., Granter-Button, S., Chernenko, G. A., Butt, S., & Corbett, D. (2011). A critical threshold of rehabilitation involving brain-derived neurotrophic factor is required for poststroke recovery. *Neurorehabilitation and Neural Repair*, *25*(8), 740–748.  
<https://doi.org/10.1177/1545968311407517>

- Malmivuo, J. (2012). Comparison of the Properties of EEG and MEG in Detecting the Electric Activity of the Brain. *Brain Topography*, 25(1), 1–19. <https://doi.org/10.1007/s10548-011-0202-1>
- Mariani, C., & Ponsa, P. (2018). Improving the Design of Virtual Reality Devices Applying an Ergonomics Guideline. In F. Rebelo & M. Soares (Eds.), *Advances in Ergonomics in Design* (Vol. 588, pp. 16–25). Springer International Publishing. [https://doi.org/10.1007/978-3-319-60582-1\\_2](https://doi.org/10.1007/978-3-319-60582-1_2)
- Marshall, R. S., Perera, G. M., Lazar, R. M., Krakauer, J. W., Constantine, R. C., & DeLaPaz, R. L. (2000). Evolution of Cortical Activation During Recovery From Corticospinal Tract Infarction. *Stroke*, 31(3), 656–661. <https://doi.org/10.1161/01.STR.31.3.656>
- Mascaro, A. L. A., Cesare, P., Sacconi, L., Grasselli, G., Mandolesi, G., Maco, B., Knott, G. W., Huang, L., Paola, V. D., Strata, P., & Pavone, F. S. (2013). In vivo single branch axotomy induces GAP-43–dependent sprouting and synaptic remodeling in cerebellar cortex. *Proceedings of the National Academy of Sciences*, 110(26), 10824–10829. <https://doi.org/10.1073/pnas.1219256110>
- McFarland, D. J., Miner, L. A., Vaughan, T. M., & Wolpaw, J. R. (2000). Mu and Beta Rhythm Topographies During Motor Imagery and Actual Movements. *Brain Topography*, 12(3), 177–186. <https://doi.org/10.1023/A:1023437823106>
- Messenger, A. G. (2011). Hair through the female life cycle. *British Journal of Dermatology*, 165(s3), 2–6. <https://doi.org/10.1111/j.1365-2133.2011.10628.x>
- Meyer, B.-U., Rörich, S., von Einsiedel, H. G., Kruggel, F., & Weindl, A. (1995). Inhibitory and excitatory interhemispheric transfers between motor cortical areas in normal humans and

- patients with abnormalities of the corpus callosum. *Brain*, 118(2), 429–440.  
<https://doi.org/10.1093/brain/118.2.429>
- Michel, C. M., & Murray, M. M. (2012). Towards the utilization of EEG as a brain imaging tool. *NeuroImage*, 61(2), 371–385. <https://doi.org/10.1016/j.neuroimage.2011.12.039>
- Mihara, M., Hattori, N., Hatakenaka, M., Yagura, H., Kawano, T., Hino, T., & Miyai, I. (2013). Near-infrared Spectroscopy-mediated Neurofeedback Enhances Efficacy of Motor Imagery-based Training in Poststroke Victims. *Stroke*.  
<https://www.ahajournals.org/doi/abs/10.1161/STROKEAHA.111.674507>
- Mihara, M., Miyai, I., Hattori, N., Hatakenaka, M., Yagura, H., Kawano, T., Okibayashi, M., Danjo, N., Ishikawa, A., Inoue, Y., & Kubota, K. (2012). Neurofeedback Using Real-Time Near-Infrared Spectroscopy Enhances Motor Imagery Related Cortical Activation. *PLOS ONE*, 7(3), e32234. <https://doi.org/10.1371/journal.pone.0032234>
- Miller, K. K., Porter, R. E., DeBaun-Sprague, E., Van Puymbroeck, M., & Schmid, A. A. (2017). Exercise after Stroke: Patient Adherence and Beliefs after Discharge from Rehabilitation. *Topics in Stroke Rehabilitation*, 24(2), 142–148.  
<https://doi.org/10.1080/10749357.2016.1200292>
- Mirbagheri, M., Hakimi, N., Ebrahimzadeh, E., Pourrezaei, K., & Setarehdan, S. K. (2019). Enhancement of optical penetration depth of LED-based NIRS systems by comparing different beam profiles. *Biomedical Physics & Engineering Express*, 5(6), 065004.  
<https://doi.org/10.1088/2057-1976/ab42d9>
- Miyai, I., Suzuki, M., Hatakenaka, M., & Kubota, K. (2006). Effect of body weight support on cortical activation during gait in patients with stroke. *Experimental Brain Research*, 169(1), 85–91. <https://doi.org/10.1007/s00221-005-0123-x>

Miyai, I., Yagura, H., Hatakenaka, M., Oda, I., Konishi, I., & Kubota, K. (2003). Longitudinal Optical Imaging Study for Locomotor Recovery After Stroke. *Stroke*, *34*(12), 2866–2870.

<https://doi.org/10.1161/01.STR.0000100166.81077.8A>

*Mobile computing technology and aphasia: An integrated review of accessibility and potential uses: Aphasiology: Vol 27, No 4.* (n.d.). Retrieved January 20, 2021, from

<https://www.tandfonline.com/doi/abs/10.1080/02687038.2013.772293>

Mottaz, A., Corbet, T., Doganci, N., Magnin, C., Nicolo, P., Schnider, A., & Guggisberg, A. G. (2018). Modulating functional connectivity after stroke with neurofeedback: Effect on motor deficits in a controlled cross-over study. *NeuroImage: Clinical*, *20*, 336–346.

<https://doi.org/10.1016/j.nicl.2018.07.029>

Müller-Gerking, J., Pfurtscheller, G., & Flyvbjerg, H. (1999). Designing optimal spatial filters for single-trial EEG classification in a movement task. *Clinical Neurophysiology*, *110*(5),

787–798. [https://doi.org/10.1016/S1388-2457\(98\)00038-8](https://doi.org/10.1016/S1388-2457(98)00038-8)

*Multichannel wearable system dedicated for simultaneous electroencephalography/near-infrared spectroscopy real-time data acquisitions.* (n.d.). Retrieved January 21, 2021, from

[https://www.spiedigitallibrary.org/journals/journal-of-biomedical-optics/volume-16/issue-](https://www.spiedigitallibrary.org/journals/journal-of-biomedical-optics/volume-16/issue-9/096014/Multichannel-wearable-system-dedicated-for-simultaneous-)

[9/096014/Multichannel-wearable-system-dedicated-for-simultaneous-](https://www.spiedigitallibrary.org/journals/journal-of-biomedical-optics/volume-16/issue-9/096014/Multichannel-wearable-system-dedicated-for-simultaneous-)

[electroencephalography-near-infrared-spectroscopy/10.1117/1.3625575.full](https://www.spiedigitallibrary.org/journals/journal-of-biomedical-optics/volume-16/issue-9/096014/Multichannel-wearable-system-dedicated-for-simultaneous-)

Murase, N., Duque, J., Mazzocchio, R., & Cohen, L. G. (2004). Influence of interhemispheric interactions on motor function in chronic stroke. *Annals of Neurology*, *55*(3), 400–409.

<https://doi.org/10.1002/ana.10848>



- Nathan, P. W., Smith, M. C., & Deacon, P. (1990). THE CORTICOSPINAL TRACTS IN MANCOURSE AND LOCATION OF FIBRES AT DIFFERENT SEGMENTAL LEVELS. *Brain*, *113*(2), 303–324. <https://doi.org/10.1093/brain/113.2.303>
- NCHS Data Brief No. 95, May 2012. (2012). *95*, 8.
- Newman, A. (2019). *Research methods for cognitive neuroscience*. Sage.
- Nhan, H., Barquist, K., Bell, K., Esselman, P., Odderson, I. R., & Cramer, S. C. (2004). Brain Function Early after Stroke in Relation to Subsequent Recovery. *Journal of Cerebral Blood Flow & Metabolism*, *24*(7), 756–763. <https://doi.org/10.1097/01.WCB.0000122744.72175.9C>
- Niimi, M., Hashimoto, K., Kakuda, W., Miyano, S., Momosaki, R., Ishima, T., & Abo, M. (2016). Role of Brain-Derived Neurotrophic Factor in Beneficial Effects of Repetitive Transcranial Magnetic Stimulation for Upper Limb Hemiparesis after Stroke. *PLOS ONE*, *11*(3), e0152241. <https://doi.org/10.1371/journal.pone.0152241>
- No evidence for motor recovery-related cortical reorganization after stroke using resting-state fMRI | *bioRxiv*. (n.d.). Retrieved September 22, 2020, from <https://www.biorxiv.org/content/10.1101/681320v1.abstract>
- Norouzi-Gheidari, N., Archambault, P. S., & Fung, J. (2019). Robot-Assisted Reaching Performance of Chronic Stroke and Healthy Individuals in a Virtual Versus a Physical Environment: A Pilot Study. *IEEE Transactions on Neural Systems and Rehabilitation Engineering*, *27*(6), 1273–1281. <https://doi.org/10.1109/TNSRE.2019.2914015>
- Nowak, D. A., Grefkes, C., Ameli, M., & Fink, G. R. (2009). Interhemispheric Competition After Stroke: Brain Stimulation to Enhance Recovery of Function of the Affected Hand. *Neurorehabilitation and Neural Repair*, *23*(7), 641–656. <https://doi.org/10.1177/1545968309336661>

- Nudo, R. J., & Milliken, G. W. (1996). Reorganization of movement representations in primary motor cortex following focal ischemic infarcts in adult squirrel monkeys. *Journal of Neurophysiology*, 75(5), 2144–2149. <https://doi.org/10.1152/jn.1996.75.5.2144>
- Oldfield, R. C. (1971). The assessment and analysis of handedness: The Edinburgh inventory. *Neuropsychologia*, 9(1), 97–113. [https://doi.org/10.1016/0028-3932\(71\)90067-4](https://doi.org/10.1016/0028-3932(71)90067-4)
- Ono, Y., Wada, K., Seki, N., Ito, M., Minakuchi, M., Kono, M., & Tominaga, T. (2018). Hand Motor Rehabilitation of Patients with Stroke Using Physiologically Congruent Neurofeedback. *2018 IEEE International Conference on Systems, Man, and Cybernetics (SMC)*, 39–44. <https://doi.org/10.1109/SMC.2018.00016>
- OSA | *A wide field-of-view, modular, high-density diffuse optical tomography system for minimally constrained three-dimensional functional neuroimaging*. (n.d.). Retrieved January 9, 2021, from <https://www.osapublishing.org/boe/fulltext.cfm?uri=boe-11-8-4110&id=433351>
- Ott, M., & Aerospace, S. (n.d.). *Capabilites and Reliability of LEDs and Laser Diodes*. 7.
- Ovbiagele, B., Goldstein, L. B., Higashida, R. T., Howard, V. J., Johnston, S. C., Khavjou, O. A., Lackland, D. T., Lichtman, J. H., Mohl, S., Sacco, R. L., Saver, J. L., Trogon, J. G., & on behalf of the American Heart Association Advocacy Coordinating Committee and Stroke Council. (2013). Forecasting the Future of Stroke in the United States: A Policy Statement From the American Heart Association and American Stroke Association. *Stroke*, 44(8), 2361–2375. <https://doi.org/10.1161/STR.0b013e31829734f2>
- Overman, J. J., Clarkson, A. N., Wanner, I. B., Overman, W. T., Eckstein, I., Maguire, J. L., Dinov, I. D., Toga, A. W., & Carmichael, S. T. (2012). A role for ephrin-A5 in axonal

- sprouting, recovery, and activity-dependent plasticity after stroke. *Proceedings of the National Academy of Sciences*, 109(33), E2230–E2239. <https://doi.org/10.1073/pnas.1204386109>
- Park, C., Kou, N., Boudrias, M.-H., Playford, E. D., & Ward, N. S. (2013). Assessing a standardised approach to measuring corticospinal integrity after stroke with DTI. *NeuroImage: Clinical*, 2, 521–533. <https://doi.org/10.1016/j.nicl.2013.04.002>
- Park, K.-H., Lee, H.-W., Park, K.-B., Lee, J.-Y., Cho, A.-R., Oh, H.-M., & Park, J. H. (2017). The Korean Version of the Cognitive Assessment Scale for Stroke Patients (K-CASP): A Reliability and Validity Study. *Annals of Rehabilitation Medicine*, 41(3), 362–375. <https://doi.org/10.5535/arm.2017.41.3.362>
- Park, W., Kwon, G. H., Kim, Y.-H., Lee, J.-H., & Kim, L. (2016). EEG response varies with lesion location in patients with chronic stroke. *Journal of NeuroEngineering and Rehabilitation*, 13(1), 21. <https://doi.org/10.1186/s12984-016-0120-2>
- Passalent, L. A., Landry, M. D., & Cott, C. A. (2009). Wait Times for Publicly Funded Outpatient and Community Physiotherapy and Occupational Therapy Services: Implications for the Increasing Number of Persons with Chronic Conditions in Ontario, Canada. *Physiotherapy Canada*, 61(1), 5–14. <https://doi.org/10.3138/physio.61.1.5>
- Perederiy, J. V., & Westbrook, G. L. (2013). Structural plasticity in the dentate gyrus- revisiting a classic injury model. *Frontiers in Neural Circuits*, 7. <https://doi.org/10.3389/fncir.2013.00017>
- Perez, C., Kaizer, F., Archambault, P., & Fung, J. (2017). A novel approach to integrate VR exer-games for stroke rehabilitation: Evaluating the implementation of a ‘games room.’ 2017 *International Conference on Virtual Rehabilitation (ICVR)*, 1–7. <https://doi.org/10.1109/ICVR.2017.8007538>

- Phillips, L. L., Chan, J. L., Doperalski, A. E., & Reeves, T. M. (2014). Time dependent integration of matrix metalloproteinases and their targeted substrates directs axonal sprouting and synaptogenesis following central nervous system injury. *Neural Regeneration Research*, 9(4), 362–376. <https://doi.org/10.4103/1673-5374.128237>
- Pichiorri, F., Morone, G., Petti, M., Toppi, J., Pisotta, I., Molinari, M., Paolucci, S., Inghilleri, M., Astolfi, L., Cincotti, F., & Mattia, D. (2015). Brain–computer interface boosts motor imagery practice during stroke recovery. *Annals of Neurology*, 77(5), 851–865. <https://doi.org/10.1002/ana.24390>
- Pinti, P., Tachtsidis, I., Hamilton, A., Hirsch, J., Aichelburg, C., Gilbert, S., & Burgess, P. W. (n.d.). The present and future use of functional near-infrared spectroscopy (fNIRS) for cognitive neuroscience. *Annals of the New York Academy of Sciences*, 0(0). <https://doi.org/10.1111/nyas.13948>
- Piper, S. K., Krueger, A., Koch, S. P., Mehnert, J., Habermehl, C., Steinbrink, J., Obrig, H., & Schmitz, C. H. (2014a). A wearable multi-channel fNIRS system for brain imaging in freely moving subjects. *NeuroImage*, 85 Pt 1, 64–71. <https://doi.org/10.1016/j.neuroimage.2013.06.062>
- Piper, S. K., Krueger, A., Koch, S. P., Mehnert, J., Habermehl, C., Steinbrink, J., Obrig, H., & Schmitz, C. H. (2014b). A Wearable Multi-Channel fNIRS System for Brain Imaging in Freely Moving Subjects. *NeuroImage*, 85(0 1). <https://doi.org/10.1016/j.neuroimage.2013.06.062>
- Plasticity in the Injured Brain: More than Molecules Matter—Justine J. Overman, S. Thomas Carmichael, 2014.* (n.d.). Retrieved January 28, 2019, from <https://journals.sagepub.com/doi/abs/10.1177/1073858413491146>

Plautz, E. J., Barbay, S., Frost, S. B., Friel, K. M., Dancause, N., Zoubina, E. V., Stowe, A. M., Quaney, B. M., & Nudo, R. J. (2003). Post-infarct cortical plasticity and behavioral recovery using concurrent cortical stimulation and rehabilitative training: A feasibility study in primates. *Neurological Research*, 25(8), 801–810.

<https://doi.org/10.1179/016164103771953880>

*Predicting Activities after Stroke: What is Clinically Relevant? - G. Kwakkel, B. J. Kollen, 2013.* (n.d.). Retrieved October 21, 2020, from <https://journals.sagepub.com/doi/abs/10.1111/j.1747-4949.2012.00967.x>

*Predicting efficacy of robot-aided rehabilitation in chronic stroke patients using an MRI-compatible robotic device—IEEE Conference Publication.* (n.d.). Retrieved January 30, 2019, from <https://ieeexplore.ieee.org/abstract/document/6091843>

*Prognostic Value of fMRI in Recovery of Hand Function in Subcortical Stroke Patients | Cerebral Cortex | Oxford Academic.* (n.d.). Retrieved January 30, 2019, from <https://academic.oup.com/cercor/article/17/12/2980/383649>

*Proportional recovery after stroke depends on corticomotor integrity—Byblow—2015—Annals of Neurology—Wiley Online Library.* (n.d.). Retrieved September 20, 2020, from <https://onlinelibrary.wiley.com/doi/abs/10.1002/ana.24472>

Qi, H. J., Joyce, K., & Boyce, M. C. (2003). Durometer Hardness and the Stress-Strain Behavior of Elastomeric Materials. *Rubber Chemistry and Technology*, 76(2), 419–435.

<https://doi.org/10.5254/1.3547752>

Quinlan, E. B., Dodakian, L., See, J., McKenzie, A., Le, V., Wojnowicz, M., Shahbaba, B., & Cramer, S. C. (2015a). Neural function, injury, and stroke subtype predict treatment gains after stroke. *Annals of Neurology*, 77(1), 132–145. <https://doi.org/10.1002/ana.24309>

- Quinlan, E. B., Dodakian, L., See, J., McKenzie, A., Le, V., Wojnowicz, M., Shahbaba, B., & Cramer, S. C. (2015b). Neural function, injury, and stroke subtype predict treatment gains after stroke. *Annals of Neurology*, *77*(1), 132–145. <https://doi.org/10.1002/ana.24309>
- Ramos-Murguialday, A., Broetz, D., Rea, M., Läer, L., Yilmaz, Ö., Brasil, F. L., Liberati, G., Curado, M. R., Garcia-Cossio, E., Vyziotis, A., Cho, W., Agostini, M., Soares, E., Soekadar, S., Caria, A., Cohen, L. G., & Birbaumer, N. (2013). Brain–machine interface in chronic stroke rehabilitation: A controlled study. *Annals of Neurology*, *74*(1), 100–108. <https://doi.org/10.1002/ana.23879>
- Rehme, A. K., Eickhoff, S. B., Rottschy, C., Fink, G. R., & Grefkes, C. (2012). Activation likelihood estimation meta-analysis of motor-related neural activity after stroke. *NeuroImage*, *59*(3), 2771–2782. <https://doi.org/10.1016/j.neuroimage.2011.10.023>
- Rehme, A. K., Volz, L. J., Feis, D.-L., Eickhoff, S. B., Fink, G. R., & Grefkes, C. (2015). Individual prediction of chronic motor outcome in the acute post-stroke stage: Behavioral parameters versus functional imaging. *Human Brain Mapping*, *36*(11), 4553–4565. <https://doi.org/10.1002/hbm.22936>
- Relationship Between Electrical Brain Responses to Motor Imagery and Motor Impairment in Stroke* | *Stroke*. (n.d.). Retrieved October 21, 2020, from <https://www.ahajournals.org/doi/full/10.1161/STROKEAHA.112.665489>
- Resting State Functional Connectivity Is Associated With Motor Pathway Integrity and Upper-Limb Behavior in Chronic Stroke*—Brenton Hordacre, Mitchell R. Goldsworthy, Ellana Welsby, Lynton Graetz, Sophie Ballinger, Susan Hillier, 2020. (n.d.). Retrieved January 21, 2021, from <https://journals.sagepub.com/doi/abs/10.1177/1545968320921824>

- Resting-State Functional Connectivity and Its Association With Multiple Domains of Upper-Extremity Function in Chronic Stroke*—M. A. Urbin, Xin Hong, Catherine E. Lang, Alex R. Carter, 2014. (n.d.). Retrieved January 30, 2019, from <https://journals.sagepub.com/doi/abs/10.1177/1545968314522349>
- Rethinking interhemispheric imbalance as a target for stroke neurorehabilitation*—Xu—2019—*Annals of Neurology*—Wiley Online Library. (n.d.). Retrieved January 25, 2020, from <https://onlinelibrary.wiley.com/doi/abs/10.1002/ana.25452>
- Richards, C. L., Malouin, F., Lamontagne, A., McFadyen, B. J., Dumas, F., Comeau, F., Robitaille, N.-M., & Fung, J. (2018). Gait Training after Stroke on a Self-Paced Treadmill with and without Virtual Environment Scenarios: A Proof-of-Principle Study. *Physiotherapy Canada, 70*(3), 221–230. <https://doi.org/10.3138/ptc.2016-97>
- Riecker, A., Gröschel, K., Ackermann, H., Schnaudigel, S., Kassubek, J., & Kastrup, A. (2010). The role of the unaffected hemisphere in motor recovery after stroke. *Human Brain Mapping, 31*(7), 1017–1029. <https://doi.org/10.1002/hbm.20914>
- Rieke, J. D., Matarasso, A. K., Yusufali, M. M., Ravindran, A., Alcantara, J., White, K. D., & Daly, J. J. (2020). Development of a combined, sequential real-time fMRI and fNIRS neurofeedback system to enhance motor learning after stroke. *Journal of Neuroscience Methods, 341*, 108719. <https://doi.org/10.1016/j.jneumeth.2020.108719>
- Rising Stroke Incidence in Young Adults: More Epidemiological Evidence, More Questions to Be Answered* | *Journal of the American Heart Association*. (n.d.). Retrieved January 25, 2020, from <https://www.ahajournals.org/doi/full/10.1161/jaha.116.003661>
- Rizzolatti, G., & Luppino, G. (2001). The Cortical Motor System. *Neuron, 31*(6), 889–901. [https://doi.org/10.1016/S0896-6273\(01\)00423-8](https://doi.org/10.1016/S0896-6273(01)00423-8)

- Rossi, V. M. (n.d.). *Digital Fourier Holographic Microscopy and Potential Applications Towards the Design of Photodynamic Therapy of Osteosarcoma*.
- Rubin, J., & Chisnell, D. (n.d.). *Handbook of Usability Testing* (Second Edition). Wiley.
- Saikia, M. J., Besio, W., & Mankodiya, K. (2018). WearLight: Towards a Wearable, Configurable Functional NIR Spectroscopy System for Noninvasive Neuroimaging. *IEEE Transactions on Biomedical Circuits and Systems*, 1–1.  
<https://doi.org/10.1109/TBCAS.2018.2876089>
- Sato, T., Nambu, I., Takeda, K., Aihara, T., Yamashita, O., Isogaya, Y., Inoue, Y., Otaka, Y., Wada, Y., Kawato, M., Sato, M., & Osu, R. (2016). Reduction of global interference of scalp-hemodynamics in functional near-infrared spectroscopy using short distance probes. *NeuroImage*, 141, 120–132. <https://doi.org/10.1016/j.neuroimage.2016.06.054>
- Schaechter, J. D., Kraft, E., Hilliard, T. S., Dijkhuizen, R. M., Benner, T., Finklestein, S. P., Rosen, B. R., & Cramer, S. C. (2002). Motor Recovery and Cortical Reorganization after Constraint-Induced Movement Therapy in Stroke Patients: A Preliminary Study. *Neurorehabilitation and Neural Repair*, 16(4), 326–338.  
<https://doi.org/10.1177/154596830201600403>
- Schaechter, J. D., & Perdue, K. L. (2008). Enhanced Cortical Activation in the Contralesional Hemisphere of Chronic Stroke Patients in Response to Motor Skill Challenge. *Cerebral Cortex*, 18(3), 638–647. <https://doi.org/10.1093/cercor/bhm096>
- Schneider, F. (n.d.). *Technology*. KETEK GmbH. Retrieved January 21, 2021, from <https://www.ketek.net/sipm/technology/>
- Scholkmann, F., Kleiser, S., Metz, A. J., Zimmermann, R., Mata Pavia, J., Wolf, U., & Wolf, M. (2014). A review on continuous wave functional near-infrared spectroscopy and imaging



instrumentation and methodology. *NeuroImage*, 85, 6–27.

<https://doi.org/10.1016/j.neuroimage.2013.05.004>

Schreiber, J. B., Nora, A., Stage, F. K., Barlow, E. A., & King, J. (2006). Reporting Structural Equation Modeling and Confirmatory Factor Analysis Results: A Review. *The Journal of Educational Research*, 99(6), 323–338. <https://doi.org/10.3200/JOER.99.6.323-338>

Sebastián-Romagosa, M., Udina, E., Ortner, R., Dinarès-Ferran, J., Cho, W., Murovec, N., Matencio-Peralba, C., Sieghartsleitner, S., Allison, B. Z., & Guger, C. (2020). EEG Biomarkers Related With the Functional State of Stroke Patients. *Frontiers in Neuroscience*, 14. <https://doi.org/10.3389/fnins.2020.00582>

Senesh, M. R., & Reinkensmeyer, D. J. (2019). Breaking Proportional Recovery After Stroke. *Neurorehabilitation and Neural Repair*, 33(11), 888–901.

<https://doi.org/10.1177/1545968319868718>

SensL. (n.d.). *An Introduction to the Silicon Photomultiplier*. Retrieved January 21, 2021, from <https://www.sensl.com/downloads/ds/TN%20-%20Intro%20to%20SPM%20Tech.pdf>

Serrien, D. J., Strens, L. H. A., Cassidy, M. J., Thompson, A. J., & Brown, P. (2004). Functional significance of the ipsilateral hemisphere during movement of the affected hand after stroke. *Experimental Neurology*, 190(2), 425–432. <https://doi.org/10.1016/j.expneurol.2004.08.004>

Sharma, K. K. (2006). *Optics: Principles and Applications*. Elsevier.

Sharma Nikhil, Pomeroy Valerie M., & Baron Jean-Claude. (2006). Motor Imagery. *Stroke*, 37(7), 1941–1952. <https://doi.org/10.1161/01.STR.0000226902.43357.fc>

Shimizu, T., Hosaki, A., Hino, T., Sato, M., Komori, T., Hirai, S., & Rossini, P. M. (2002). Motor cortical disinhibition in the unaffected hemisphere after unilateral cortical stroke. *Brain*, 125(8), 1896–1907. <https://doi.org/10.1093/brain/awf183>

- Shiner, C. T., Pierce, K. D., Thompson-Butel, A. G., Trinh, T., Schofield, P. R., & McNulty, P. A. (2016). BDNF Genotype Interacts with Motor Function to Influence Rehabilitation Responsiveness Poststroke. *Frontiers in Neurology, 7*.  
<https://doi.org/10.3389/fneur.2016.00069>
- Shrestha, A., & Mahmood, A. (2019). Review of Deep Learning Algorithms and Architectures. *IEEE Access, 7*, 53040–53065. <https://doi.org/10.1109/ACCESS.2019.2912200>
- Sibi, S., Ayaz, H., Kuhns, D. P., Sirkin, D. M., & Ju, W. (2016). Monitoring driver cognitive load using functional near infrared spectroscopy in partially autonomous cars. *2016 IEEE Intelligent Vehicles Symposium (IV)*, 419–425. <https://doi.org/10.1109/IVS.2016.7535420>
- Sitaram, R., Ros, T., Stoeckel, L., Haller, S., Scharnowski, F., Lewis-Peacock, J., Weiskopf, N., Blefari, M. L., Rana, M., Oblak, E., Birbaumer, N., & Sulzer, J. (2017). Closed-loop brain training: The science of neurofeedback. *Nature Reviews Neuroscience, 18*(2), 86–100.  
<https://doi.org/10.1038/nrn.2016.164>
- Smooth-on. (n.d.). *Smooth-on Shore Hardness Scale*. Retrieved January 20, 2021, from <https://www.smooth-on.com/page/durometer-shore-hardness-scale/>
- Spasojevic, P., Zrilic, M., Panic, V., Stamenkovic, D., Seslija, S., & Velickovic, S. (2015, June 4). *The Mechanical Properties of a Poly(methyl methacrylate) Denture Base Material Modified with Dimethyl Itaconate and Di-n-butyl Itaconate* [Research Article]. *International Journal of Polymer Science*; Hindawi. <https://doi.org/10.1155/2015/561012>
- Stinear, C. M., Barber, P. A., Petoe, M., Anwar, S., & Byblow, W. D. (2012). The PREP algorithm predicts potential for upper limb recovery after stroke. *Brain: A Journal of Neurology, 135*(Pt 8), 2527–2535. <https://doi.org/10.1093/brain/aws146>

- Stinear, C. M., Byblow, W. D., Ackerley, S. J., Barber, P. A., & Smith, M.-C. (2017). Predicting Recovery Potential for Individual Stroke Patients Increases Rehabilitation Efficiency. *Stroke*, 48(4), 1011–1019. <https://doi.org/10.1161/STROKEAHA.116.015790>
- Stinear, C. M., Petoe, M. A., & Byblow, W. D. (2015). Primary Motor Cortex Excitability During Recovery After Stroke: Implications for Neuromodulation. *Brain Stimulation*, 8(6), 1183–1190. <https://doi.org/10.1016/j.brs.2015.06.015>
- Stippich, C., Freitag, P., Kassubek, J., Sörös, P., Kamada, K., Kober, H., Scheffler, K., Hopfengärtner, R., Bilecen, D., Radü, E.-W., & Vieth, J.-B. (1998). Motor, somatosensory and auditory cortex localization by fMRI and MEG. *NeuroReport*, 9(9), 1953.
- Sullivan, J. E. (2014). Measurement Characteristics and Clinical Utility of the Stroke Impact Scale. *Archives of Physical Medicine and Rehabilitation*, 95(9), 1799–1800. <https://doi.org/10.1016/j.apmr.2014.02.011>
- Sullivan, K. J., Tilson, J. K., Cen, S. Y., Rose, D. K., Hershberg, J., Correa, A., Gallichio, J., McLeod, M., Moore, C., Wu, S. S., & Duncan, P. W. (2011). Fugl-Meyer assessment of sensorimotor function after stroke: Standardized training procedure for clinical practice and clinical trials. *Stroke*, 42(2), 427–432. <https://doi.org/10.1161/STROKEAHA.110.592766>
- Sun, J., Ke, Z., Yip, S. P., Hu, X., Zheng, X., & Tong, K. (2014, June 19). *Gradually Increased Training Intensity Benefits Rehabilitation Outcome after Stroke by BDNF Upregulation and Stress Suppression* [Research Article]. BioMed Research International; Hindawi. <https://doi.org/10.1155/2014/925762>
- Takeda, K., Gomi, Y., Imai, I., Shimoda, N., Hiwatari, M., & Kato, H. (2007). Shift of motor activation areas during recovery from hemiparesis after cerebral infarction: A longitudinal

study with near-infrared spectroscopy. *Neuroscience Research*, 59(2), 136–144.

<https://doi.org/10.1016/j.neures.2007.06.1466>

Tang, Q., Li, G., Liu, T., Wang, A., Feng, S., Liao, X., Jin, Y., Guo, Z., He, B., McClure, M. A., Xing, G., & Mu, Q. (2015). Modulation of interhemispheric activation balance in motor-related areas of stroke patients with motor recovery: Systematic review and meta-analysis of fMRI studies. *Neuroscience & Biobehavioral Reviews*, 57, 392–400.

<https://doi.org/10.1016/j.neubiorev.2015.09.003>

Tanno, R., Worrall, D., Kaden, E., Ghosh, A., Grussu, F., Bizzi, A., Sotiropoulos, S. N., Criminisi, A., & Alexander, D. C. (2019). Uncertainty Quantification in Deep Learning for Safer Neuroimage Enhancement. *ArXiv:1907.13418 [Cs, Eess, Stat]*.

<http://arxiv.org/abs/1907.13418>

Teasell, R., Meyer, M. J., Foley, N., Salter, K., & Willems, D. (2009). Stroke Rehabilitation in Canada: A Work in Progress. *Topics in Stroke Rehabilitation*, 16(1), 11–19.

<https://doi.org/10.1310/tsr1601-11>

*The Effect of Lesion Size on the Organization of the Ipsilesional and Contralesional Motor*

*Cortex*—Boris Touvykine, Babak K. Mansoori, Loyda Jean-Charles, Joan Deffeyes, Stephan Quessy, Numa Dancause, 2016. (n.d.). Retrieved January 30, 2019, from

<https://journals.sagepub.com/doi/abs/10.1177/1545968315585356>

*The plasticity of intrinsic functional connectivity patterns associated with rehabilitation*

*intervention in chronic stroke patients* | SpringerLink. (n.d.). Retrieved January 30, 2019,

from <https://link.springer.com/article/10.1007/s00234-016-1647-4>

*The proportional recovery rule for stroke revisited—Krakauer—2015—Annals of Neurology—*

*Wiley Online Library.* (n.d.). Retrieved November 20, 2020, from

<https://onlinelibrary.wiley.com/doi/abs/10.1002/ana.24537>

*The relationship between motor deficit and primary motor cortex hemispheric activation balance*

*after stroke: Longitudinal fMRI study | Journal of Neurology, Neurosurgery & Psychiatry.*

(n.d.). Retrieved January 30, 2019, from <https://jnnp.bmj.com/content/81/7/788.short>

*The Role of Diaschisis in Stroke Recovery | Stroke.* (n.d.). Retrieved January 21, 2021, from

<https://www.ahajournals.org/doi/full/10.1161/01.STR.30.9.1844>

Thulborn, K. R., Chang, S. Y., Shen, G. X., & Voyvodic, J. T. (1997). High-resolution echo-

planar fMRI of human visual cortex at 3.0 tesla. *NMR in Biomedicine*, *10*(4–5), 183–190.

[https://doi.org/10.1002/\(SICI\)1099-1492\(199706/08\)10:4/5<183::AID-NBM469>3.0.CO;2-W](https://doi.org/10.1002/(SICI)1099-1492(199706/08)10:4/5<183::AID-NBM469>3.0.CO;2-W)

Tombari, D., Loubinoux, I., Pariente, J., Gerdelat, A., Albucher, J.-F., Tardy, J., Cassol, E., &

Chollet, F. (2004). A longitudinal fMRI study: In recovering and then in clinically stable sub-cortical stroke patients. *NeuroImage*, *23*(3), 827–839.

<https://doi.org/10.1016/j.neuroimage.2004.07.058>

Tsuchimoto, S., Shindo, K., Hotta, F., Hanakawa, T., Liu, M., & Ushiba, J. (2019). Sensorimotor

Connectivity after Motor Exercise with Neurofeedback in Post-Stroke Patients with

Hemiplegia. *Neuroscience*, *416*, 109–125. <https://doi.org/10.1016/j.neuroscience.2019.07.037>

Turton, A., Wroe, S., Trepte, N., Fraser, C., & Lemon, R. N. (1996). Contralateral and ipsilateral

EMG responses to transcranial magnetic stimulation during recovery of arm and hand

function after stroke. *Electroencephalography and Clinical*

*Neurophysiology/Electromyography and Motor Control*, *101*(4), 316–328.

[https://doi.org/10.1016/0924-980X\(96\)95560-5](https://doi.org/10.1016/0924-980X(96)95560-5)

Ueda, R., Yamada, N., Abo, M., Ruwan, P. W., & Senoo, A. (2020). MRI evaluation of motor function recovery by rTMS and intensive occupational therapy and changes in the activity of motor cortex. *International Journal of Neuroscience*, *130*(3), 309–317.

<https://doi.org/10.1080/00207454.2019.1680553>

*UK Sentinel Stroke National Audit Programme (SSNAP), July-Sept 2015 report.* (n.d.). accessed on <https://www.strokeaudit.org/results/Clinical-audit/National-Results.aspx>

*Upstream Dysfunction of Somatomotor Functional Connectivity After Corticospinal Damage in Stroke—Alex R. Carter, Kevin R. Patel, Serguei V. Astafiev, Abraham Z. Snyder, Jennifer Rengachary, Michael J. Strube, Anna Pope, Joshua S. Shimony, Catherine E. Lang, Gordon L. Shulman, Maurizio Corbetta, 2012.* (n.d.). Retrieved January 30, 2019, from

<https://journals.sagepub.com/doi/abs/10.1177/1545968311411054>

U.S. Department of Health and Human Services Food and Drug Administration. (2011).

*Applying Human Factors and Usability Engineering to Medical Devices.* Center for Devices and Radiological Health Office of Device Evaluation.

<https://www.fda.gov/media/80481/download>

*Utilizing functional near-infrared spectroscopy for prediction of cognitive workload in noisy work environments.* (n.d.). Retrieved June 10, 2020, from

[https://www.spiedigitallibrary.org/journals/Neurophotonics/volume-4/issue-](https://www.spiedigitallibrary.org/journals/Neurophotonics/volume-4/issue-4/041406/Utilizing-functional-near-infrared-spectroscopy-for-prediction-of-cognitive-workload/10.1117/1.NPh.4.4.041406.full)

[4/041406/Utilizing-functional-near-infrared-spectroscopy-for-prediction-of-cognitive-workload/10.1117/1.NPh.4.4.041406.full](https://www.spiedigitallibrary.org/journals/Neurophotonics/volume-4/issue-4/041406/Utilizing-functional-near-infrared-spectroscopy-for-prediction-of-cognitive-workload/10.1117/1.NPh.4.4.041406.full)

Várkuti, B., Guan, C., Pan, Y., Phua, K. S., Ang, K. K., Kuah, C. W. K., Chua, K., Ang, B. T., Birbaumer, N., & Sitaram, R. (2013a). Resting State Changes in Functional Connectivity Correlate With Movement Recovery for BCI and Robot-Assisted Upper-Extremity Training

After Stroke. *Neurorehabilitation and Neural Repair*, 27(1), 53–62.

<https://doi.org/10.1177/1545968312445910>

Várkuti, B., Guan, C., Pan, Y., Phua, K. S., Ang, K. K., Kuah, C. W. K., Chua, K., Ang, B. T., Birbaumer, N., & Sitaram, R. (2013b). Resting State Changes in Functional Connectivity Correlate With Movement Recovery for BCI and Robot-Assisted Upper-Extremity Training After Stroke. *Neurorehabilitation and Neural Repair*, 27(1), 53–62.

<https://doi.org/10.1177/1545968312445910>

Verstynen, T., Diedrichsen, J., Albert, N., Aparicio, P., & Ivry, R. B. (2005). Ipsilateral motor cortex activity during unimanual hand movements relates to task complexity. *Journal of Neurophysiology*, 93(3), 1209–1222. <https://doi.org/10.1152/jn.00720.2004>

Vliet, R. van der, Selles, R. W., Andrinopoulou, E.-R., Nijland, R., Ribbers, G. M., Frens, M. A., Meskers, C., & Kwakkel, G. (2020). Predicting Upper Limb Motor Impairment Recovery after Stroke: A Mixture Model. *Annals of Neurology*, 87(3), 383–393.

<https://doi.org/10.1002/ana.25679>

von Lüthmann, A., Li, X., Müller, K.-R., Boas, D. A., & Yücel, M. A. (2020). Improved physiological noise regression in fNIRS: A multimodal extension of the General Linear Model using temporally embedded Canonical Correlation Analysis. *NeuroImage*, 208, 116472.

<https://doi.org/10.1016/j.neuroimage.2019.116472>

Wada, K., Ono, Y., Kurata, M., Ito, M. (Imanishi), Minakuchi, M. (Tani), Kono, M., & Tominaga, T. (2019). Development of a Brain-machine Interface for Stroke Rehabilitation Using Event-related Desynchronization and Proprioceptive Feedback. *Advanced Biomedical Engineering*, 8, 53–59. <https://doi.org/10.14326/abe.8.53>

Wang, L. V., & Wu, H. (2012). *Biomedical Optics: Principles and Imaging*. John Wiley & Sons.

- Ward, N. S., Brown, M. M., Thompson, A. J., & Frackowiak, R. S. J. (2003). Neural correlates of motor recovery after stroke: A longitudinal fMRI study. *Brain*, *126*(11), 2476–2496. <https://doi.org/10.1093/brain/awg245>
- Ward, Nick S., Brander, F., & Kelly, K. (2019). Intensive upper limb neurorehabilitation in chronic stroke: Outcomes from the Queen Square programme. *Journal of Neurology, Neurosurgery, and Psychiatry*, *90*(5), 498–506. <https://doi.org/10.1136/jnnp-2018-319954>
- Weik, M. H. (2001). Fresnel reflection loss. In M. H. Weik (Ed.), *Computer Science and Communications Dictionary* (pp. 657–657). Springer US. [https://doi.org/10.1007/1-4020-0613-6\\_7725](https://doi.org/10.1007/1-4020-0613-6_7725)
- Weiller, C., Chollet, F., Friston, K. J., Wise, R. J. S., & Frackowiak, R. S. J. (1992). Functional reorganization of the brain in recovery from striatocapsular infarction in man. *Annals of Neurology*, *31*(5), 463–472. <https://doi.org/10.1002/ana.410310502>
- Weisstein, E. W. (n.d.). *Normal Distribution* [Text]. Wolfram Research, Inc. Retrieved January 21, 2021, from <https://mathworld.wolfram.com/NormalDistribution.html>
- Welniarz, Q., Dusart, I., & Roze, E. (2017). The corticospinal tract: Evolution, development, and human disorders: Corticospinal Tract Human Disorders. *Developmental Neurobiology*, *77*(7), 810–829. <https://doi.org/10.1002/dneu.22455>
- Welvaert, M., & Rosseel, Y. (2013). On the Definition of Signal-To-Noise Ratio and Contrast-To-Noise Ratio for fMRI Data. *PLOS ONE*, *8*(11), e77089. <https://doi.org/10.1371/journal.pone.0077089>
- Westlake, K. P., & Nagarajan, S. S. (2011). Functional Connectivity in Relation to Motor Performance and Recovery After Stroke. *Frontiers in Systems Neuroscience*, *5*. <https://doi.org/10.3389/fnsys.2011.00008>



- Weston, R., & Gore, P. A. (2006). A Brief Guide to Structural Equation Modeling. *The Counseling Psychologist*, *34*(5), 719–751. <https://doi.org/10.1177/0011000006286345>
- Wijekumar, S., Huppert, T. J., Magnotta, V. A., Buss, A. T., & Spencer, J. P. (2017). Validating an image-based fNIRS approach with fMRI and a working memory task. *NeuroImage*, *147*, 204–218. <https://doi.org/10.1016/j.neuroimage.2016.12.007>
- Winstein, C. J., Stein, J., Arena, R., Bates, B., Cherney, L. R., Cramer, S. C., Deruyter, F., Eng, J. J., Fisher, B., Harvey, R. L., Lang, C. E., MacKay-Lyons, M., Ottenbacher, K. J., Pugh, S., Reeves, M. J., Richards, L. G., Stiers, W., Zorowitz, R. D., & American Heart Association Stroke Council, Council on Cardiovascular and Stroke Nursing, Council on Clinical Cardiology, and Council on Quality of Care and Outcomes Research. (2016). Guidelines for Adult Stroke Rehabilitation and Recovery: A Guideline for Healthcare Professionals From the American Heart Association/American Stroke Association. *Stroke*, *47*(6), e98–e169. <https://doi.org/10.1161/STR.0000000000000098>
- Wyser, D. G., Lamercy, O., Scholkmann, F., Wolf, M., & Gassert, R. (2017). Wearable and modular functional near-infrared spectroscopy instrument with multidistance measurements at four wavelengths. *Neurophotonics*, *4*(4), 041413. <https://doi.org/10.1117/1.NPh.4.4.041413>
- Yamada, T., Ohashi, M., & Umeyama, S. (2015). Development of a fiber-less fNIRS system and its application to hair-covered head. *Optical Techniques in Neurosurgery, Neurophotonics, and Optogenetics*, 8928, 89280R. <https://doi.org/10.1117/12.2036155>
- Yang, C.-L., Lim, S. B., Peters, S., & Eng, J. J. (2020). Cortical Activation During Shoulder and Finger Movements in Healthy Adults: A Functional Near-Infrared Spectroscopy (fNIRS) Study. *Frontiers in Human Neuroscience*, *14*. <https://doi.org/10.3389/fnhum.2020.00260>

- Young, B. M., Nigogosyan, Z., Walton, L. M., Song, J., Nair, V. A., Grogan, S. W., Tyler, M. E., Edwards, D. F., Caldera, K., Sattin, J. A., Williams, J. C., & Prabhakaran, V. (2014). Changes in functional brain organization and behavioral correlations after rehabilitative therapy using a brain-computer interface. *Frontiers in Neuroengineering*, 7.  
<https://doi.org/10.3389/fneng.2014.00026>
- Zemke, A. C., Heagerty, P. J., Lee, C., & Cramer, S. C. (2003). Motor Cortex Organization After Stroke Is Related to Side of Stroke and Level of Recovery. *Stroke*, 34(5).  
<https://doi.org/10.1161/01.STR.0000065827.35634.5E>
- Zhang, Y., & Pardridge, W. M. (2006). Blood–brain barrier targeting of BDNF improves motor function in rats with middle cerebral artery occlusion. *Brain Research*, 1111(1), 227–229.  
<https://doi.org/10.1016/j.brainres.2006.07.005>
- Zhao, H., & Cooper, R. J. (2017). Review of recent progress toward a fiberless, whole-scalp diffuse optical tomography system. *Neurophotonics*, 5(1), 011012.  
<https://doi.org/10.1117/1.NPh.5.1.011012>
- Zimmermann, R., Braun, F., Achtnich, T., Lamercy, O., Gassert, R., & Wolf, M. (2013). Silicon photomultipliers for improved detection of low light levels in miniature near-infrared spectroscopy instruments. *Biomedical Optics Express*, 4(5), 659–666.  
<https://doi.org/10.1364/BOE.4.000659>
- 齊田和哉. (2018). *Biofeedback Effect of Hybrid Assistive Limb in Stroke Rehabilitation: A Proof of Concept Study Using Functional Near Infrared Spectroscopy* [PhD Thesis]. 福岡大学.